University of Alberta

Examining FinOP control of F plasmid conjugation

by

Michael John Gubbins ©

A thesis submitted to the Faculty of Graduate Studies and Research in partial fulfillment
of the requirements for the degree of Doctor of Philosophy

in

Microbiology and Biotechnology

Department of Biological Sciences

Edmonton, Alberta

Spring 2003

National Library
of Canada

Bibliothèque nationale
du Canada

Acquisitions and
Bibliographic Services

Acquisisitons et
services bibliographiques

395 Wellington Street
Ottawa ON K1A 0N4
Canada

395, rue Wellington
Ottawa ON K1A 0N4
Canada

The author has granted a non-exclusive licence allowing the National Library of Canada to reproduce, loan, distribute or sell copies of this thesis in microform, paper or electronic formats.

L'auteur a accordé une licence non exclusive permettant à la Bibliothèque nationale du Canada de reproduire, prêter, distribuer ou vendre des copies de cette thèse sous la forme de microfiche/film, de reproduction sur papier ou sur format électronique.

The author retains ownership of the copyright in this thesis. Neither the thesis nor substantial extracts from it may be printed or otherwise reproduced without the author's permission.

L'auteur conserve la propriété du droit d'auteur qui protège cette thèse. Ni la thèse ni des extraits substantiels de celle-ci ne doivent être imprimés ou aturement reproduits sans son autorisation.

Canada

University of Alberta

Library Release Form

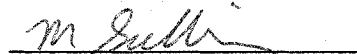**Name of Author:** Michael John Gubbins

Title of Thesis: Examining FinOP Control of F plasmid conjugation

Degree: Doctor of Philosophy

Year this degree granted: 2003

Permission is hereby granted to the University of Alberta Library to reproduce single copies of this thesis and to lend or sell such copies for private, scholarly or scientific research purposes only.

The author reserves all other publication and other rights in association with the copyright in the thesis, and except as herein provided, neither the thesis nor any substantial portion thereof may be printed or otherwise reproduced in any material form whatever without the author's prior written permission.
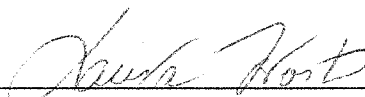
Unit 108, 10208 120th Street
Edmonton, Alberta
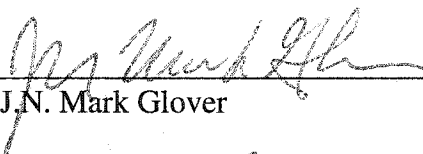T5K 2W2

Dated: December 16, 2002

University of Alberta
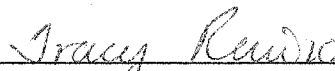
Faculty of Graduate Studies and Research

The undersigned certify that they have read, and recommend to the Faculty of Graduate Studies and Research for acceptance, a thesis entitled **Examining FinOP Control of F Plasmid Conjugation** submitted by **Michael John Gubbins** in partial fulfillment of the requirements for the degree of **Doctor of Philosophy**, in **Microbiology and Biotechnology**.
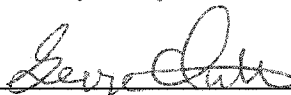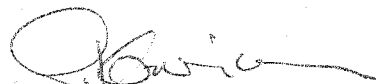
Dr. Laura S. Frost (Supervisor)

Dr. J.N. Mark Glover

Dr. Tracy L. Raivio

Dr. George W. Owttrim

Dr. Brenda K. Leskiw

Dr. Günther Koraimann (External Examiner)

Date: Nov 21, 2002

Abstract

Expression of the *tra* genes of F and F-like plasmids is required for conjugative plasmid transfer. Expression of the positive regulatory protein, TraJ, promotes efficient transcription from the main promoter of the *tra* operon, P_Y. Control of expression of TraJ is regulated by the FinOP (fertility inhibition) system, composed of the antisense RNA, FinP, and FinO, an RNA binding protein. FinP/*traJ* mRNA duplex formation is thought to occlude the ribosome binding site on *traJ* mRNA, preventing TraJ accumulation.

Multiple FinO deletion proteins were tested for FinP binding *in vitro*. Two distinct binding domains were identified in the protein. The first is located within the highly alpha-helical N-terminal region of FinO, and the second extends into the C-terminus of FinO. The highest affinity binding was achieved when both domains were present in the protein.

A well-defined N-terminal region of FinO possesses a double-stranded RNA unwinding capability. This region of FinO also promotes FinP/*traJ* mRNA duplex formation *in vitro*. Analyses of various FinO mutants suggests that the ability of FinO to unwind double-stranded RNA, protect FinP from RNase E-mediated degradation, and promote RNA/RNA duplex formation are critical to the function of the FinOP system.

The RNA structural features that contribute to FinP/*traJ* mRNA duplex formation were analyzed *in vitro*. The amount of single-stranded RNA available in each molecule for intermolecular base pairing, and the intramolecular stability of each RNA, appear to be critical factors in FinP/*traJ* mRNA duplex formation. *In vivo* analyses suggest that interaction between the ribosome binding site in stem-loop Ic of *traJ* mRNA and the complementary anti-ribosome binding site in stem-loop I of FinP is crucial for FinP

function. Evidence is presented that suggests FinO does not require its RNA targets to have perfect complementarity in order to catalyze their formation into a duplex.

Upon activation of the Cpx two-component signal transduction system by the detection of cell envelope perturbations, *tra* gene expression and plasmid transfer are inhibited. The results presented in this work suggest that both constitutive activation of the Cpx regulon, and natural induction of the Cpx regulon, cause a posttrancriptional reduction in the accumulation of TraJ.

Acknowledgements

Many people have helped me in my endeavor to complete my research over the past five-odd years. First and foremost, I must thank my supervisor, Dr. Laura Frost. Laura not only provided me with a lab in which to do my research, but also constant support throughout my time here. For this and more, my thanks and appreciation are extended to Laura.

Several people in our lab really set the groundwork for understanding the FinOP system of F. Dr. Lori Jerome, Dr. Tim van Biesen, and Jim Sandercock all answered many questions about this system, and provided me with an excellent basis on which to work and continue research into this often incredibly frustrating antisense RNA system.

My supervisory committee has been very supportive for the past few years. Drs. Tracy Raivio, Mark Glover, and George Owttrim always had excellent feedback for me, and provided me with many ideas to aid my research. Much of my work on FinOP and the Cpx systems would not have been completed without help and input from Mark and Tracy.

Dr. Alexandru Ghetu was a member of Mark's lab, and we both started on our projects at about the same time. I collaborated with Alex on the FinOP system from the beginning, and I owe a great debt of gratitude to him. Alex determined the crystal structure of FinO, and provided me with all the purified FinO proteins I could handle, which really allowed me to accomplish my work in a timely fashion. Dave Arthur is a current member of Mark's lab, and I must thank him as well. Dave learned an incredible amount about the FinOP system in a very short time, and has proven to be an excellent researcher and a great help to me.

The people in the Frost lab I work with daily have also helped me considerably. Jan Manchak is without question the best technician I have had the pleasure of working with. She has kept the lab working smoothly the entire time I have been here, ensuring that everyone in our lab could work productively. Drs. Richard Fekete and William "Big Billy" Klimke had a hand in teaching me the ropes when I first started. Ryan "Boomer" Will, Jun Lu, Isabella Lau, Trevor Elton, Dr. Perrin Beatty, and numerous project and summer students throughout the years have all been a pleasure to work with. All of them have had to put up with my unique (twisted) sense of humor, and only rarely complained about it. They deserve thanks for that, and for making my work environment much more lighthearted and enjoyable.

I must also thank my family. My parents John and Stephanie always pushed their children to strive to achieve their goals. Without their encouragement, I don't think I would have come this far in my education. My brother Kevin and my sister Kathleen set a high standard with respect to post-secondary education. They pushed me to continue with my studies, and showed me I could achieve whatever goal I tried to reach. I can't thank my family enough for their support, and I dedicate this thesis to them.

Last, but certainly not least, I must thank my girlfriend, Kelly Lehman. Kelly has put up with my long hours in the lab for two years. Luckily for me, she is very understanding. Kelly has made life infinitely more bearable, and has helped me through more than one rough patch on my way to completing this thesis.

Table of Contents

Chapter 5: Analysis of FinO-mediated duplex formation

Chapter 6: TraJ is destabilized in a *cpxA101** background

List of Tables

List of Figures

Chapter 3

Chapter 4

Chapter 5

Chapter 6

Chapter 7

List of Abbreviations

α	alpha
A_{260}	absorbance at 260 nm
A_{420}	absorbance at 420 nm
Amp/Ap	ampicillin
ATP	adenosine triphosphate
β	beta
bp	base pair
BSA	bovine serum albumin
cAMP	cyclic adenosine monophosphate
Cm	chloramphenicol
cpm	counts per minute
Cpx	conjugative plasmid expression
CRP	cAMP repressor protein
CTP	cytosine triphosphate
Δ	deletion, change
ΔG	change in free energy of unfolding
DEPC	diethyl-pyrocarbonate
DNA	deoxyribonucleic acid
DNase	deoxyribonuclease
dNTP(s)	deoxyribonucleoside triphosphate(s)
DTT	dithiothreitol
EDTA	ethylenediaminetetraacetic acid
EMSA	electrophoretic mobility shift assay
F	F plasmid
Fin	fertility inhibition
γ	gamma
GST	glutathione S-transferase
GTP	guanosine triphosphate
HRP	horseradish peroxidase
IHF	integration host factor
Inc	incompatibility
IS	insertion sequence
K_a	equilibrium association constant
k_{app}	apparent equilibrium association constant
Kan/Km	kanamycin

kb	kilobase
kDa	kilo Dalton
λ	bacteriophage lambda
LB	Luria-Bertani
μ	micro
mRNA	messenger RNA
M.U.	Miller Units
Nal	nalidixic acid
OD_{600}	optical density at 600 nm
ONPG	*o*-nitrophenyl β-D-galactopyranoside
ORF	open reading frame
oriT	origin of transfer
P	promoter
PAGE	polyacrylamide gel electrophoresis
PNK	polynucleotide kinase
PVDF	polyvinylidene difluoride
R	resistance factor
RBS	ribosome binding site
RNA	ribonucleic acid
RNase	ribonuclease
rNTP(s)	ribonucleoside triphosphate(s)
rpm	revolutions per minute
s	second(s)
SDS	sodium dodecyl sulphate
SL	stem-loop
Spec/Spc	spectinomycin
Strep/Str	streptomycin
Tet/Tc	tetracycline
tra	transfer
tRNA	transfer RNA
TSB	trypticase soy broth
UTP	uridine triphosphate
UTR	untranslated region
v/v	volume/volume
w/v	weight/volume

Chapter 1: General Introduction

The ability of bacteria to sense and respond to changes in the environment is a key factor in their ability to survive, adapt, and thrive under a wide variety of conditions. The horizontal transfer of genetic material between bacteria is one of the primary methods by which bacteria can acquire new genes, allowing them to quickly adapt to changing environments. The transfer of genes for catabolism of various compounds, resistance to heavy metals, and resistance to antibiotics, among others, illustrates the wide variety of the types of genetic information that can be transferred among bacteria. Of particular importance is the transfer of antibiotic resistance genes. A growing number of medically important bacteria are becoming resistant to a host of antibiotics, demonstrating the importance of understanding the processes involved in the transfer of genes between bacteria.

Horizontal transfer of genes occurs by three common mechanisms. The first, and most basic, mechanism is natural *transformation* by the uptake of "naked" DNA from the environment. The second mechanism is *transduction*, whereby genes from one bacterium are transferred to the chromosome of another by a bacteriophage. The third mechanism, and the one which is the focus of this thesis, is *conjugation*, a process by which plasmids are transferred from one bacterium to another through "sexual" transfer.

1.1 A brief historical perspective on bacterial conjugation.

The discovery of horizontal gene transfer between bacteria can be attributed to the work of Lederberg and Tatum, who discovered that different strains of *Escherichia coli* K-12 could be phenotypically altered when mixed together (Lederberg and Tatum, 1946). A series of experiments led to the conclusion that direct contact between bacteria was required in order for genetic material to be transferred between cultures of bacteria

(Davis, 1950). This transfer was further determined to occur in one direction, from donor to recipient cells, by a mechanism contained within the donor cells (Hayes, 1952). By 1953, it had been determined that the donor cells in fact contained a separate genetic element which could be transferred to recipient cells lacking this element, and it was termed the F (fertility) sex factor (Lederberg et al., 1952; Hayes, 1953).

Subsequent analysis of the F sex factor confirmed that it was an independent genetic element, and that its transfer required the elaboration of an extracytoplasmic protein appendage, the pilus, to initiate contact between donor and recipient cells (Marmur et al., 1961; Brinton et al., 1964). Further work identified another transmissible mobile genetic element that encoded multiple drug resistance genes, suggesting that conjugative transfer of genes between bacteria was in fact a common occurrence (Watanabe, 1963). Transfer of this R (resistance) factor plasmid between antibiotic resistant Shigella spp. was determined to be widespread (Watanabe, 1963; 1966). Since that time, interspecies and interkingdom transfer of plasmids has been determined to occur relatively commonly (Mazodier and Davies, 1991; Davison, 1999), further reinforcing the need to understand the processes by which plasmid transfer occurs.

1.2 The conjugative cycle of the F plasmid.

Much work has been performed on the mechanism of F transfer since the mid 1950s. Multiple subgroups of F-like plasmids are known, and each is separated into one of seven incompatibility (Inc) groups (Ippen-Ihler and Skurray, 1993). These groups are designated IncFI (F and R386), IncFII (ColB2, R1, R6-5, and R100), IncFIII (pSU306), IncFIV (R124), IncFV (pED208), IncFVI (pSU212), and IncFVII (pSU233). These incompatibility groups are defined by the sharing of replication and partitioning systems,

and the inability of plasmids belonging to the same group to stably co-reside in the same cell (Datta, 1975). The F plasmid is considered to be the paradigm for transfer of plasmids belonging to the IncF group of plasmids (Frost *et al.*, 1994).

Detailed reviews of the processes involved in F-like conjugative transfer have recently been assembled (Frost *et al.*, 1994; Firth *et al.*, 1996), and the past two decades have seen an enormous increase in the understanding of the sophisticated processes involved. This introduction will only present a small part of what is currently known about F plasmid transfer, presenting only the salient points that will provide a basic review of the process of F transfer.

The circular F plasmid is approximately 100 kb in length, and encodes most of the genes required for conjugative transfer (Figure 1.1; Frost *et al.*, 1994). Most F-like plasmids are naturally repressed for transfer, meaning that expression of the genes required for transfer are normally maintained in an "off" state by a fertility inhibition (*fin*) system. During the life cycle of an F$^+$ bacterium, sporadic derepression of transfer may occur, allowing expression of the genes required for transfer and subsequent conjugative transfer of the plasmid (Frost *et al.*, 1994). The fertility inhibition system of F is composed of two components, the antisense RNA FinP, and the RNA binding protein, FinO (discussed in detail in subsequent sections; reviewed in Frost *et al.*, 1994).

The process of conjugation is outlined schematically in Figure 1.2. One of the first steps in conjugation is the elaboration of an extracytoplasmic protein appendage, the F-pilus, on the surface of the donor cell. Contact between the pilus and a suitable F$^-$ recipient cell leads to close contact between the cells via depolymerization of the pilus

Figure 1.1 Physical map of the F plasmid. Coordinates are marked in the interior of the diagram, in kilobases. The actual size of the plasmid is 99,159 base pairs. The *Hind*III sites represent the portion of the F plasmid that is present in the F-derivative plasmid pOX38-Km, extending approximately form coordinates 45 to 100 (Table 2.2). The three separate replication (RepF) regions are indicated. The IS*3* insertion in *finO* is marked, as are IS insertions in the distal portion of the plasmid. A Tn*1000* transposon insertion in RepFIC is indicated as well. The origin of transfer (*oriT*) and the direction of transfer are indicated by a black arrow. The transfer (*tra*) region and the leading region of transfer are indicated on the left portion of the diagram.
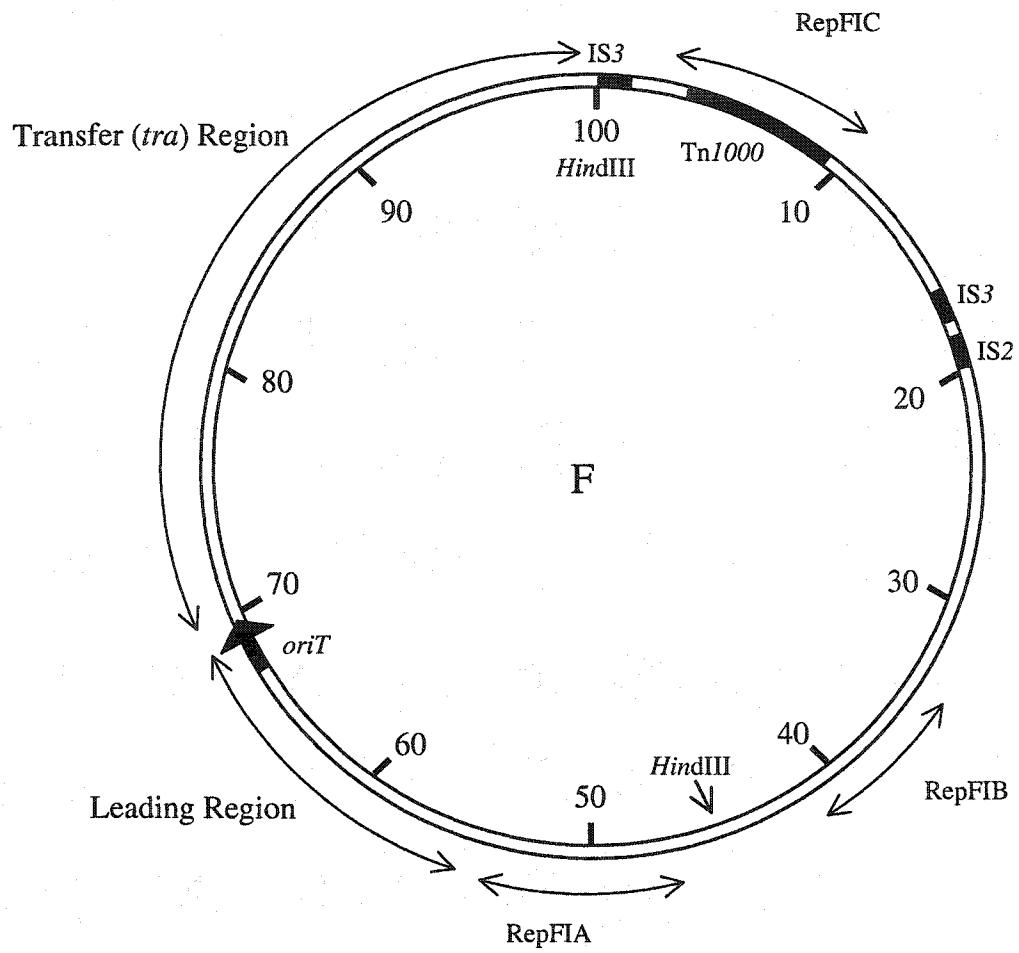
Figure 1.2 Schematic representation of the F mating cycle. Donor cells containing the F plasmid are rectangular, with the pilus represented as a straight line extending from the upper right corner. The plasmid is represented by the double-stranded circle. An F⁻ recipient cell is represented by an oval. The abbreviated steps involved in the process are indicated by numbers as follows: 1. The F^+ cell produces a pilus. 2. The recipient cell is contacted by the F pilus. 3. Close contact and mating stabilization occurs after pilus retraction. 3. The plasmid is nicked at *oriT*, and a single strand of DNA begins to enter the recipient cell. 4. Transfer continues concomitant with synthesis of the second strand of DNA in both cells, followed by disaggregation of the cells. 5. Expression of the *tra* operon occurs in both donor cells, and the process can begin again.

F+ cell expressing a pilus
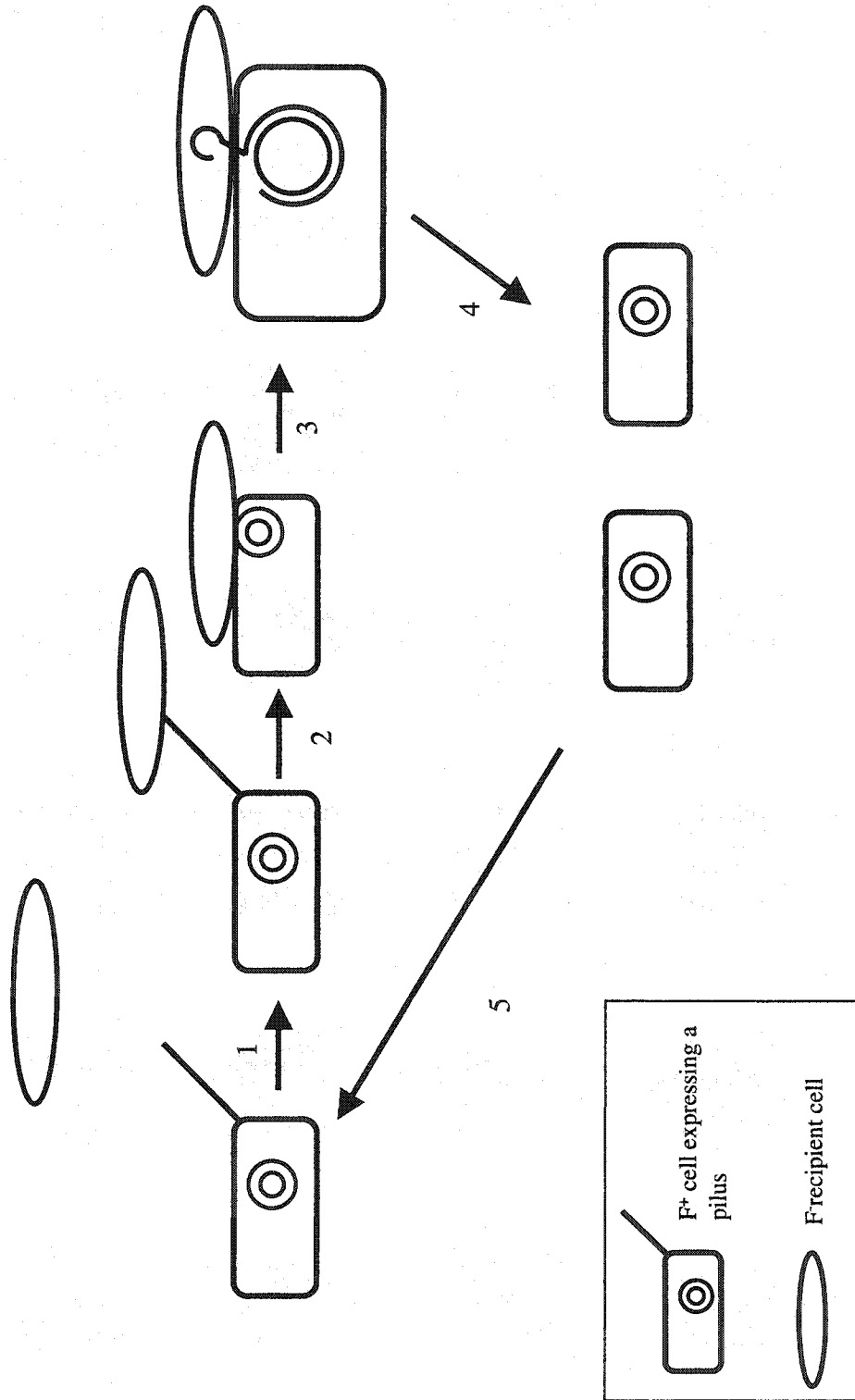
F- recipient cell

(Novotny and Fives-Taylor, 1974; Frost *et al.*, 1994). Once the cells have made contact, mating pair stabilization (MPS) occurs, mediated by the TraN and TraG proteins expressed by F, and OmpA and lipopolysaccharide moieties in the recipient cell (Manning *et al.*, 1981; Frost *et al.*, 1994; Klimke and Frost, 1998). Stabilization of the mating pair is required for high efficiency transfer of F from the donor to the recipient (Klimke and Frost, 1998). Once MPS has been established, an unknown mating signal leads to nicking of one strand of the DNA at the *nic* site located in the origin of transfer (*oriT*), located immediately upstream of the F *traM* gene (Frost *et al.*, 1994). Nicking of the DNA is mediated by the dual function TraI relaxase/helicase, which covalently attaches to the 5' end of the nicked DNA, along with several other proteins, in a complex known as the relaxosome (Zechner *et al.*, 2000). Using its helicase activity, TraI unwinds the DNA, leading to the transfer of the nicked strand into the recipient cell in a 5' to 3' direction (Ihler and Rupp, 1969; Traxler and Minkley, 1988; Matson *et al.*, 1993). The function of TraI is dependent upon host-encoded IHF (integration host factor), as well as plasmid-encoded TraY (Howard *et al.*, 1995; Nelson *et al.*, 1995). Host-encoded proteins synthesize complementary DNA strands in both the donor and recipient at the same time the DNA is transferred. Therefore, once strand transfer is complete, both the donor and the transconjugant cells have a complete copy of the F plasmid. The entire process of transfer of the plasmid and concomitant synthesis of complementary DNA strands is completed within approximately five minutes under ideal conditions at 37°C (Frost *et al.*, 1994). Once the original donor and the newly transformed F+ cell have a complete copy of the plasmid, the cells detach, resulting in two F+ cells capable of repeating the mating process. In the new donor cell, synthesis of plasmid proteins to inhibit mating with other

F$^+$ cells occurs almost immediately. This process, termed surface exclusion (*sfx*) is mediated by the F TraS and TraT proteins (Kingsman and Willetts, 1978; Sukupolvi and O'Connor, 1990).

1.3 The transfer (*tra*) region of the F plasmid.

Most of the genes required for F plasmid transfer are encoded in the 33.3 kb transfer (*tra*) region (Figure 1.3; Frost *et al.*, 1994). Since *oriT* is located immediately upstream of the *tra* region, this region is the last to be transferred into a recipient cell. Thirty-six open reading frames (ORFs) are encoded by the *tra* operon, as well as the regulatory antisense RNA, FinP (Frost *et al.*, 1994). *traM* and *traJ*, which encode regulatory proteins, are transcribed from their own promoters, however most of the *tra* genes are transcribed as a single operon from the major *tra* promoter, P$_Y$ (Mullineaux and Willetts, 1985). It is believed that *finO* may be transcribed from its own promoter, however it is unknown at this time whether this is in fact the case (van Biesen and Frost, 1992; Frost *et al.*, 1994). The genes encoded in the *tra* operon have been classified into five basic subgroups according to their general functions: regulation, pilus synthesis and assembly, aggregate stability, surface exclusion, and DNA processing/transfer (Figure 1.3; Frost *et al.*, 1994). Examination of the regulation of expression of P$_Y$, mediated by the products of the *finP*, *traJ*, and *finO* genes, will form the major part of the work presented in this thesis.

1.4 Regulation of *tra* operon expression.

The regulatory circuit controlling F *tra* operon expression is shown schematically in Figure 1.4. TraJ is a positive activator of transcription from P$_Y$, and it is required for maximum levels of transcription (Willetts, 1977; Mullineaux and Willetts, 1985). This

Figure 1.3 Organization of the conjugative transfer (*tra*) genes of the F plasmid. The figure is not drawn exactly to scale. The 33.3 kb *tra* region is represented, starting with *oriT* and ending with the *finO* gene at the distal end of the operon. The IS*3* insertion element in *finO* is indicated above the gene. *tra* genes are indicated by capital letters, while *trb* genes are denoted by lower case letters. An arrow above the figure on the left side indicates the site of the major promoter of the operon, P_Y, and the direction of transcription of the operon. Direction of transcription of *finP* and *artA* is in the opposite direction of transcription from P_Y, as indicated by the arrows below the figure. The *tra* genes are organized according to their general function, as annotated in the bottom portion of the figure. Adapted from Frost *et al.* (1994).
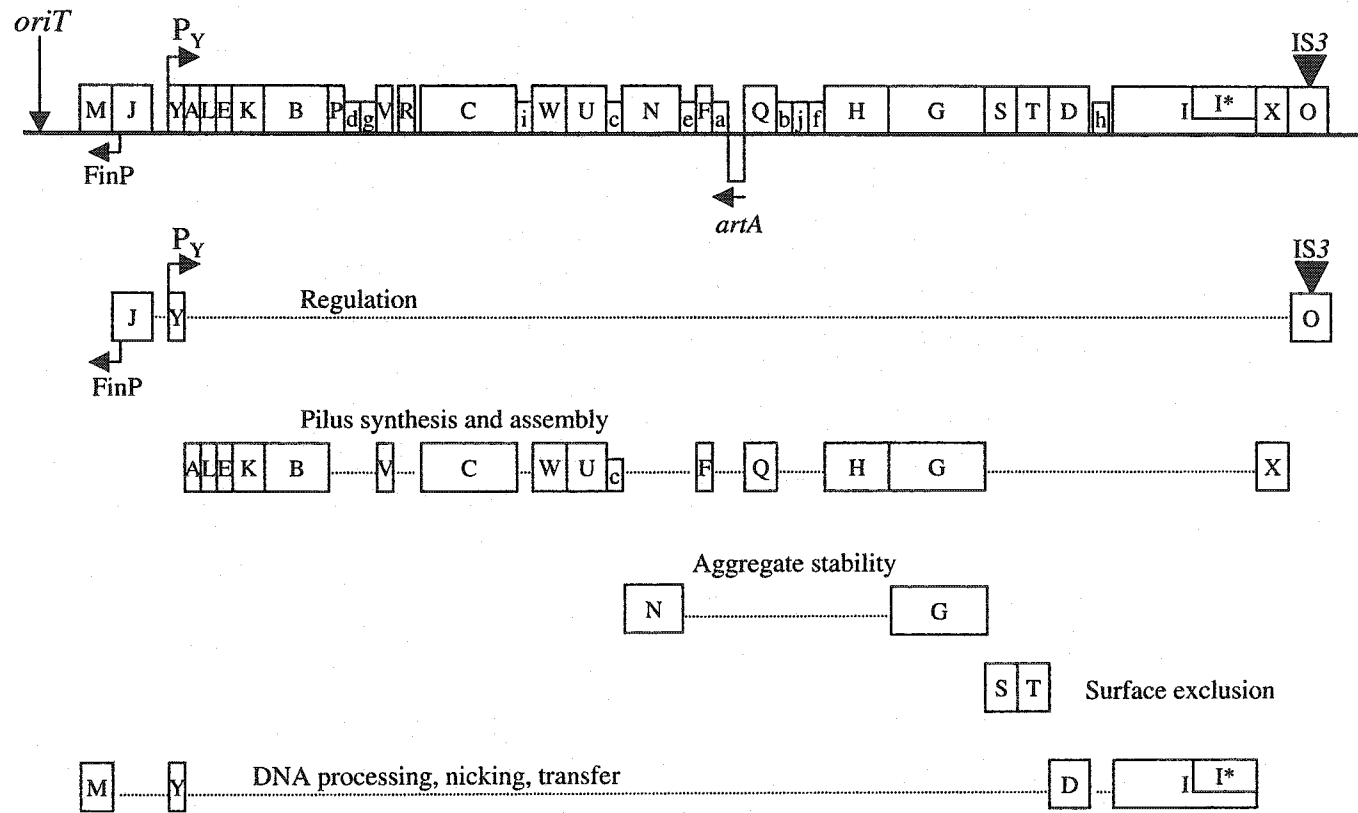
Figure 1.4 Control of *tra* operon expression. An abbreviated schematic representation of the control circuit responsible for regulating *tra* operon expression is presented. The grey line represents *tra* operon DNA. Arrows immediately above the grey line indicate the position and direction of expression from the major promoter of the *tra* operon, P_Y, and promoters for *traJ* (P_J) and *traM* (P_M). The promoter for *finP* (P_{FinP}) and the direction of transcription of *finP* is indicated below the grey line by an arrow. Plasmid encoded factors are represented by normal text, host-encoded factors are represented in bold text. Arrows indicate positive effects, while black bars indicate negative effects. The figure is not drawn to scale.
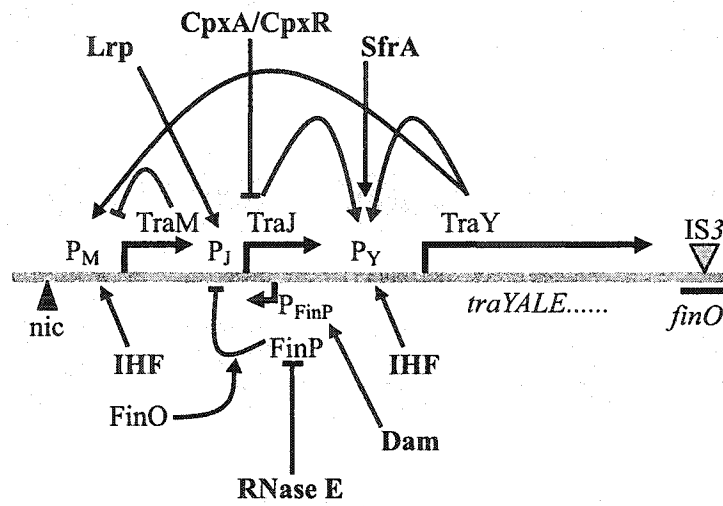
27 kDa cytoplasmic protein contains a helix-turn-helix DNA binding motif, however the exact mechanism of how TraJ stimulates transcription from P_Y is currently unknown (Takeda *et al.*, 1983; Frost *et al.*, 1994). The FinOP system of F-like plasmids (discussed in detail in a later section) consists of two separate components, the antisense RNA, FinP, and the RNA binding protein, FinO. Regulation of TraJ expression by the FinOP system comprises one of the primary plasmid-encoded control mechanisms of F transfer.

Along with TraJ, and by default, FinOP, several other plasmid-encoded factors influence *tra* operon transcription. TraY binds to three distinct sites in the F *tra* region, one near the P_Y promoter, and two upstream of P_Y near *oriT* (Nelson *et al.*, 1993). TraY may function to aid in the TraI-mediated nicking reaction at *oriT*, possibly by bending the DNA in that region (Luo *et al.*, 1994). TraY is believed to regulate its own synthesis, as well as the expression of F *traM* (Penfold *et al.*, 1996; Stockwell and Dempsey, 1997). TraM is essential for F transfer, and it is believed to function at a point after nicking of *oriT* occurs (Kingsman and Willetts, 1978; Manning *et al.*, 1981; Di Laurenzio *et al.*, 1992). TraM binds to three sites in the *oriT* region, which affects TraM autoregulation and relaxosome formation (Di Laurenzio *et al.*, 1992; Penfold *et al.*, 1996; Zechner *et al.*, 2000; Fekete and Frost, 2002). The current model for the role of TraM in F transfer is that it functions along with F TraD to ensure that the relaxosome complex is ideally placed for transfer into a recipient cell (Disque-Kochem and Dreiseikelmann, 1997; Zechner *et al.*, 2000; Fekete and Frost, 2002).

A number of host-encoded factors aid in the regulation of expression from P_Y. ArcA (SfrA) is part of a two-component signal transduction system that senses and responds to the redox state of the cell, and it is required for maximal transcription from

P_Y (Silverman *et al.*, 1991a, 1991c; Lynch and Lin 1996). Direct activation of transcription from P_Y of the F-like plasmid R1 by ArcA has been demonstrated, and presence of TraJ is required for this activity (Strohmaier *et al.*, 1998). *tra* operon expression is also affected by the host-encoded protein IHF (integration host factor), which has been shown to bind to the *oriT* region of F (Tsai *et al.*, 1990), and it likely affects transcription by altering the local superhelical density at P_Y (Silverman *et al.*, 1991a, 1991b; Gaudin and Silverman, 1993). Another two-component signal transduction system, the CpxAR stress response system, has been implicated in the control of accumulation of the TraJ protein (Silverman *et al.*, 1993), which will be discussed in detail in a later section.

Host-encoded pathways that sense and respond to nutrient availability also affect *tra* operon expression. The presence of a putative consensus binding sequence for CRP (cAMP repressor protein) overlapping the initiation site for *traJ* transcription has led to the theory that cAMP-CRP directly influences *tra* operon expression (Kumar and Srivastava, 1983; Paranchych *et al.*, 1986). Indeed, a lack of cyclic AMP has been shown to influence piliation of cells carrying various F-like plasmids (Harwood and Maynell, 1975). At this time, the exact mechanism of cAMP-CRP regulation of *tra* operon expression is unclear (Firth *et al.*, 1996). Recently, the global regulatory protein Lrp (leucine-responsive regulatory protein) has been shown to upregulate directly expression of P_{traJ} of the F-like plasmid pSLT of *Salmonella typhimurium* (Camacho and Casadesús, 2002). Lrp influences expression of a variety of operons involved in responding to changes in nutrient availability. Lrp was shown to bind *in vitro* to a consensus sequence upstream of the *traJ* promoter, and plasmid transfer was reduced by approximately 50-

fold in a *lrp* host (Camacho and Casadesús, 2002). Similarities between pSLT and other F-like plasmids has led these authors to propose that Lrp expression likely influences *tra* expression in multiple F-like plasmids via direct upregulation of P$_{traJ}$. Expression of the *tra* operon is therefore sensitive to numerous environmental cues, including the metabolic and nutritional state of the host cell, as well as physiological changes induced in the host cell imparted by the environmental growth conditions.

1.5 The FinOP fertility inhibition system of F and F-like plasmids.

The primary mechanism for inhibiting expression of the *tra* operon and F plasmid transfer is the FinOP fertility inhibition system. Figure 1.5 presents a schematic summary of the mechanistic pathway employed by the FinOP system to inhibit *tra* operon expression. This system mediates repression of *tra* operon expression by inhibiting expression of the main activator of P$_Y$, the TraJ regulatory protein. Using this method, *tra* operon expression can be rapidly and efficiently shut down using only a small number of plasmid-encoded components (Willetts, 1977). FinOP is a two-component system, consisting of a regulatory antisense RNA, FinP, and a RNA chaperone, the FinO protein (Finnegan and Willetts, 1971; Mullineaux and Willetts, 1985). FinO is absolutely required to mediate repression of F-like plasmid transfer, and in F, an IS*3* insertion in the *finO* gene renders the plasmid derepressed for transfer (Yoshioka *et al.*, 1987) leading to constitutive (de-regulated) transfer of the plasmid (Frost *et al.*, 1994). An examination of each component of the FinOP system is presented in the next two sections.

1.5.1 FinP, a regulatory antisense RNA.

The *traJ* transcript of F contains a 105 nucleotide 5' untranslated region (UTR), which folds into a complex secondary structure consisting of three stem loops (SL) and

Figure 1.5 FinOP regulation of *tra* operon expression. Only a small portion of the operon is shown, and only the promoters for *traJ*, *traY*, and *finP* are represented, as indicated by arrows. All components are represented schematically, and are not meant to resemble the exact structures of each molecule. The upper portion of the figure represents interactions that occur in the absence of FinO. RNase E-mediated degradation of FinP reduces its steady-state concentration. This allows transcription of *traJ* mRNA, which is subsequently translated, allowing TraJ to activate transcription from P_Y. The lower portion of the figure represents events that occur when FinO is supplied. FinO can bind to FinP, preventing its degradation, allowing its steady-state intracellular concentration to increase. FinO can then facilitate FinP/*traJ* mRNA duplex formation, inhibiting TraJ accumulation by preventing translation of the mRNA. The FinP/*traJ* mRNA duplex also becomes susceptible to RNase III-mediated degradation. No TraJ accumulates, and transcription form P_Y is inhibited.

FinP

RNase E cleavage

- FinP is degraded.
- TraJ is translated.
- P_Y is activated.

TraJ

$+$

No FinO

P_J

P_Y

traJ

traY

$+$ FinO

P_{FinP}

FinO

FinP

- FinP is protected by FinO.
- FinP forms a duplex with *traJ* mRNA.
- TraJ is not translated.
- *traJ* mRNA is degraded.
- No activation of P_Y.

traJ mRNA
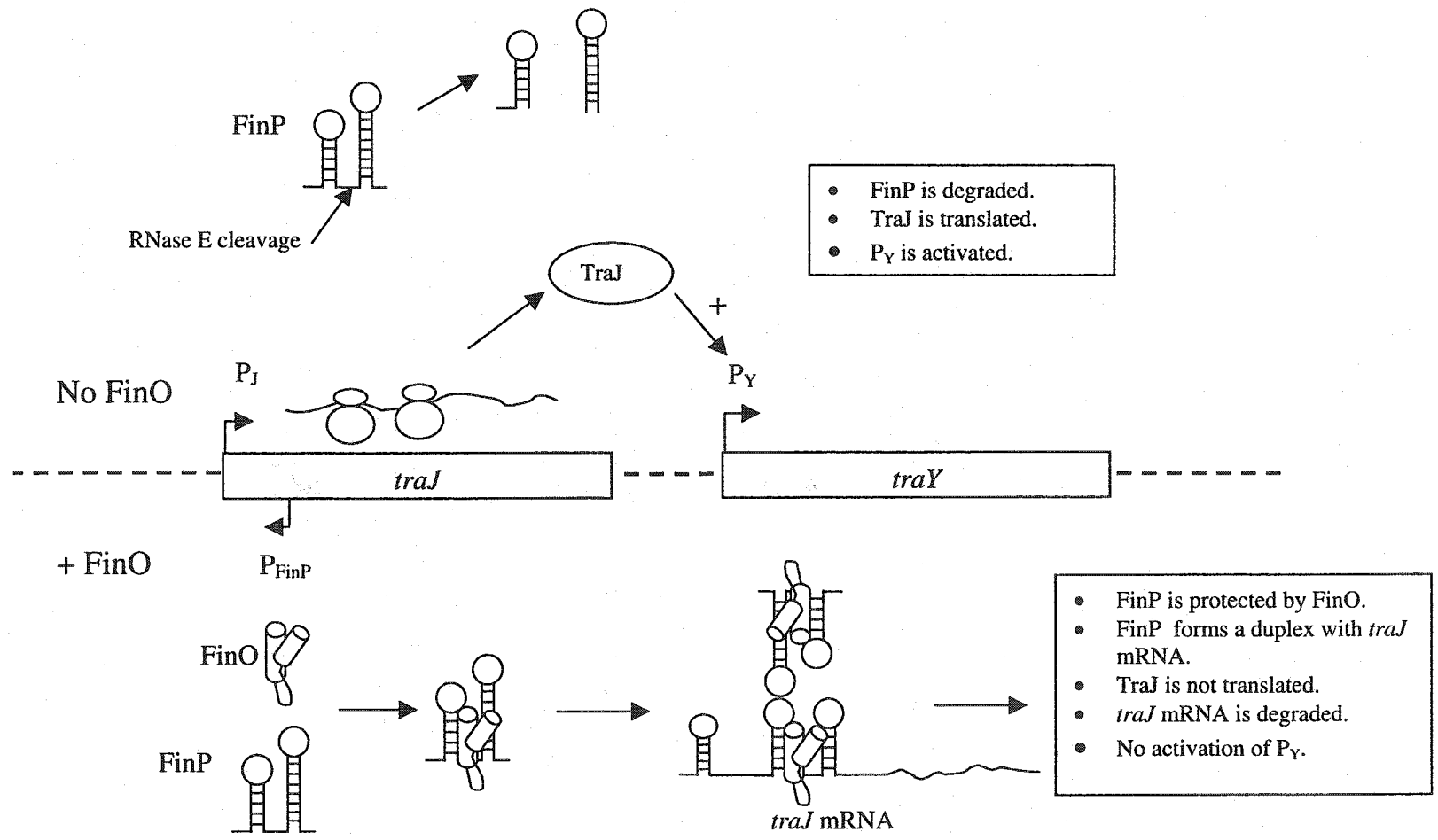
an extended single-stranded region in its 5′ proximal end (Figure 1.6; van Biesen *et al.*, 1993). The three SL regions are designated SL-Ic, SL-IIc, and SL-III. The ribosome binding site (RBS) of the transcript extends from the 3′ side of the loop of SL-Ic into the top portion of the stem of SL-Ic, and the AUG start codon is situated at the bottom of the 3′ side of the stem of SL-Ic, within a double-stranded region of RNA (Figure 1.6). FinP is encoded within the 5′ UTR of *traJ* mRNA, however it is transcribed in the opposite direction, from its own weak constitutive promoter, resulting in a 79 nucleotide antisense RNA molecule with complete complementarity to a portion of the *traJ* transcript (Figure 1.6; Mullineaux and Willetts, 1985). FinP folds into two SL domains, designated SL-I and SL-II, separated by a four-nucleotide single-stranded spacer. SL-I is flanked on its 5′ side by a four nucleotide single-stranded tail, while SL-II is flanked on its 3′ side by a six nucleotide single-stranded tail (Figure 1.6; van Biesen *et al.*, 1993).

FinP SL-I and SL-II are perfectly complementary to *traJ* SL-Ic and SL-IIc, and the FinP SL-I contains a stretch of bases, termed the anti-RBS, which can interact with a portion of the RBS of *traJ* mRNA. Half of the bases of the anti-RBS are located in the upper portion of the stem (bases C13-U15; Figure 1.6), while the rest of the bases that make up the anti-RBS are found in the 5′ portion of the loop (C16-U18; Figure 1.6). Bases C17 and U18 are also part of a common motif, 5′-YUNR-3′ (Y=C or U; N=any base; R=A or G), which forms a particular structural conformation that is important in promoting loop-loop interactions in a variety of sense:antisense pairing reactions (Franch *et al.*, 1999). The formation of a duplex between FinP and *traJ* mRNA, mediated by an initial loop-loop kissing interaction, is thought to sequester the RBS of *traJ* mRNA via pairing of the RBS with the anti-RBS of FinP, preventing translation of the message by

Figure 1.6 The secondary structure of FinP antisense RNA and the 5′ UTR of *traJ184* mRNA. Every tenth base is indicated, starting from the 5′ end of each molecule. The stem-loops composing each molecule are indicated above each loop region. The RBS of *traJ* and the anti-RBS of FinP are indicated by black lines. The AUG start codon of the *traJ* mRNA is labeled in italics. The secondary structure of each molecule was experimentally determined (van Biesen *et al.*, 1993).

SL-II

```
                              A
                          C  ^  C
      SL-I                U     G
                          U     U
              C A 20      G C 60
           U     C        A U
           C      A    50 G C
           C   A  A       G C
            U A           G C
           C G            A U
           C G            C G
         A     A          G C
          A U             G C
       10 G·U             U A
          G C 30          A U
          A U             G C 70
          U A             C G
          A U          40 U·G
          C G           G C
  5'-GAUA    GACA         GAUUUU-3'
```

FinP

SL-IIc

SL-Ic

traJ184 mRNA

```
                               U
                           G       G
                         C           A
                        A   A          G  U G
                         G C 60     90 U      A
                         A U          U        G
                      50 G C            U A   G
                         G C            C G
  SL-III                 G C            C G
         10              A U          U     U 100
      A A                C G            A U
    U   U                G C           A    C
    U   G                U A           G C
    G C                  A U           A U
    G C               40 G C 70     80 U A
    U A                  C G           A U
    G C                                C G
    C G    20       30                 C G
 5'-G    UUAAAAUUUGAAAUUGAAAAUCGC    ACUGUC    UAUC........3'
                              40                    110
```
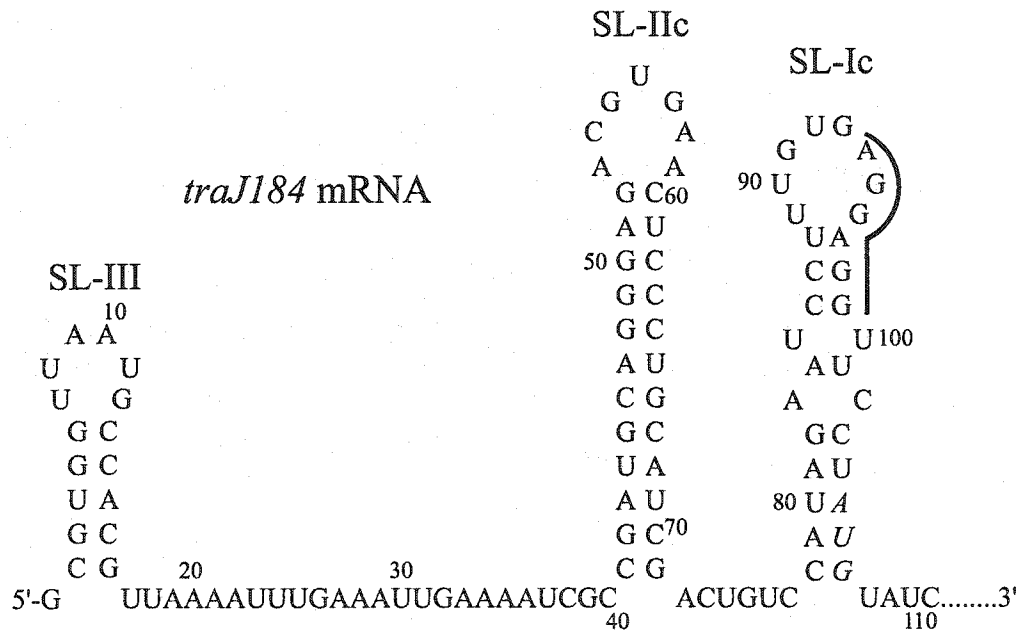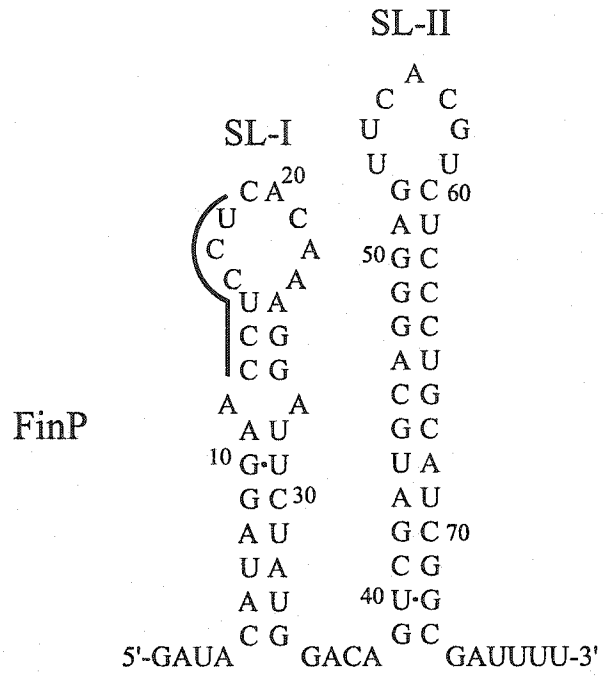
inhibiting ribosome loading. Formation of a FinP/*traJ* mRNA duplex has been demonstrated *in vitro* (van Biesen *et al.*, 1993; Sandercock and Frost, 1998; Ghetu *et al.*, 2000). Preliminary evidence shows that such a duplex also forms *in vivo*, creating a substrate which is a target for degradation by RNase III (van Biesen *et al.*, 1993; Jerome *et al.*, 1999). Efficient and rapid formation of FinP/*traJ* mRNA duplexes *in vitro* and *in vivo* requires the activity of the FinO protein (discussed in section 1.5.2). FinP-mediated reduction of TraJ accumulation is therefore probably controlled by two separate and distinct mechanisms: prevention of translation by sequestration of the RBS, and creation of a double-stranded RNA substrate that is degraded by RNase III.

Eight different alleles of FinP have been described, and all display a high degree of conservation in the stem and single-stranded tail regions, but less conservation in the loop sequences (Figure 1.7; Finlay *et al.*, 1986). The loop differences are therefore thought to provide allelic specificity to FinP antisense RNA encoded by a variety of F-like plasmids (Koraimann *et al.*, 1991, 1996). Mutational analysis of the loops of SL-I and SL-II of FinP encoded by the F-like plasmid R1 determined that complementarity between the loops of FinP and *traJ* mRNA is critical for the ability of FinP to repress both expression of *traJ* and conjugative transfer of the plasmid (Koraimann *et al.*, 1996). Mutational analysis of the stem regions of F and R1 FinP has determined that sequences in these regions have little to no effect on the ability of FinP to repress plasmid transfer or form a duplex with *traJ* mRNA *in vitro* (van Biesen, 1994; Koraimann *et al.*, 1996). These results suggest that initial loop-loop interactions may be an important first step in the interaction of FinP and *traJ* mRNA during the process of fertility inhibition,

Figure 1.7 The sequences of eight different alleles of FinP. The plasmid of origin is indicated to the left of each sequence. The 5' and 3' single-stranded tails, single-stranded spacer region, and loops are indicated above the figure. Bases composing the stems of the stem-loop regions are underlined. Positions marked by an asterisk are identical. Colons mark positions exhibiting two possibilities, while those that exhibit three possibilities are marked with periods. Dashes indicate gaps in the alignment. Adapted from Frost et al. (1994).

| | 5′ tail | Loop I | Spacer | Loop II | 3′ tail |

```
        5′ tail            Loop I                    Spacer                 Loop II              3′ tail
F      GAUACAUAGGAACCUCCUCACAAAGGAUUCUAUGGACAGUCGAUGCAGGGAGUUCACGUCUCCCUGCAUCGGCGAUUUU 79
ColB2   AUACAUAGGAACCUCCUCACAAAGGAUUCUAUGGACAGUCGAUGCAGGGAGUUCACGUCUCCCUGCAUCGGCGAUUUU 78
R1-19   ACACAUAGGAACCUC--CGUUAAGGAUUCUAUGGACAGUCGAUGCAGGGAGUUCAGACCUCCCUGCAUCGGCGAUUUU 76
R100-1  AUACAUAGGAACCUCCUCUCAAAGGAUUCUAUGGACAGUCGAUGCGGGGAGGUCGC-UCUCCCUGCAUCGGCGAUUUU 77
ColB4   ACACAUAGGAACCUC---CGUUAAGGAUUCUAUGGACAGUCGAUGCAGGGAGGUCUGAACUCCCUGCAUCGGCGAUUUU 76
SU233   ACACAUAGGAACCUC---CUCAAAGGAUUCUAUGGACAGUCGAUGCAGGGAGGGACAAGCUCCCUGCAUCGGCGAUUUU 76
SU316   ACACAUAGGAACCUCCUACCAAAGGAUUCUAUGGACAGUCGAUGCAGGGAGCAGCCA-CUCCCUGCAUCGGCGAUUUU 76
P307    ACACAUAGGAACCUC---CUCUAAGGAUUCUAUGGACAGUCGAUGCAGGGAGCAGCCA-CUCCCUGCAUCGGCGAUUUU 76

        * :* * ** ** * * * * * :: : .:  : * ** ** * * * ** * * * * ** *:* * * **: ::.:. . * ** ** ** ** * ** * * *
```

25

and may in fact be sufficient to repress translation of *traJ* mRNA and TraJ accumulation (Koraimann *et al.*, 1996).

The intracellular concentration of FinP is a key factor in determining the ability of the FinOP system to effect its control over TraJ expression. Previous work has demonstrated that in the presence of FinO, the steady-state concentration of FinP increases substantially, and the half-life of the RNA can be significantly extended (Frost *et al.*, 1989; Lee *et al.*, 1992; Jerome *et al.*, 1999). In the absence of FinO, FinP is a target for degradation by RNase E, which cleaves the RNA within the single-stranded spacer region located between SL-I and SL-II (Figure 1.5; Jerome *et al.*, 1999). The intracellular concentration of FinP is therefore critical for its function *in vivo*. Indeed, Koraimann *et al.* (1996) employed *traJ-lacZ* reporter constructs and mating inhibition assays to demonstrate that R1 FinP provided *in trans* at an elevated copy number was able to exert a negative effect on *traJ* expression in the absence of FinO. This observation reveals that the regulatory effect of FinP is highly gene dosage and concentration dependent (Koraimann *et al.*, 1996).

Although FinP is transcribed from its own weak constitutive promoter, its expression is influenced by cellular factors. The presence of a GATC site in the promoter region of FinP prompted an investigation into the influence of Dam methylation on FinP expression and F-like plasmid transfer. Using *finP-lacZ* reporter constructs, Torreblanca *et al.* (1999) demonstrated that FinP promoter activity was significantly reduced in a *dam*⁻ *E. coli* background. As a consequence, F plasmid transfer was elevated, suggesting that FinP expression and F plasmid transfer are sensitive to the methylation state of the plasmid DNA (Torreblanca *et al.*, 1999). These authors suggest that the methylation state

of the plasmid may be a mechanism used to couple plasmid replication with FinP expression and control of *tra* operon expression. It has been proposed that immediately after plasmid replication, the hemi-methylated state of the plasmid DNA might allow for a temporary reduction in FinP expression, thus allowing a short period of *tra* operon derepression and plasmid transfer immediately after the completion of replication (Torreblanca *et al.*, 1999). However, considering that F transfer is derepressed, the benefit of such a mechanism should be of no consequence. Such a control mechanism may in fact operate in other F-like plasmids, however further work is required to determine whether this is the case. Regardless of the potential purpose of controlling FinP expression via *dam* methylation, the evidence suggests that the concentration of FinP antisense RNA is a critical factor in determining the efficacy of repression of *tra* operon expression, and that cellular factors influence FinOP-mediated plasmid transfer inhibition.

1.5.2 FinO, an RNA chaperone.

As mentioned briefly in the previous section, FinO is absolutely required for the repression of F and F-like plasmid transfer. F is derepressed for transfer due to an IS*3* insertion in *finO*, while R100-1 is derepressed due to the insertion of a single nucleotide in *finO*. Both of these mutations cause premature termination of the *finO* transcript (Cheah and Skurray, 1986; Yoshioka *et al.*, 1987). *finO* is encoded at the distal end of the *tra* operon in most F-like plasmids (Frost *et al.*, 1994), and it is currently unknown whether FinO is expressed from its own promoter, or as part of a multicistronic transcript expressed from P_Y. Two alleles of *finO* have been identified, and are defined based upon their level of repression of transfer (Willetts and Maule, 1986). Type I alleles (R100, R6-

5) are characterized by their ability to repress transfer by approximately 100- to 1000-fold, and by the presence of an open reading frame, *orf286*, immediately upstream of the coding region. Type II alleles (ColB2) repress mating by 20- to 50-fold, and lack the upstream *orf286*. The presence of *orf286* appears to stabilize the *finO* transcript, leading to a higher intracellular concentration of FinO, and thus greater repression of plasmid transfer (van Biesen and Frost, 1992). As discussed in section 1.5.1, FinP exhibits allelic specificity among the F-like plasmids, however FinO from one plasmid can function to repress transfer among a wide variety of different F-like plasmids (Finnegan and Willetts, 1973). This observation suggests that FinO functions in a manner which is completely independent of the sequence of both FinP antisense RNA and *traJ* mRNA.

FinO is a 21.2 kDa cytoplasmic RNA binding protein, consisting of 186 amino acids (McIntyre and Dempsey, 1987; Yoshioka *et al.*, 1987). Analysis of the primary amino acid sequence of FinO reveals that the protein has an overall basic character (Figure 1.8a). Initial analysis of the amino acid sequence suggested that the protein was largely alpha-helical in structure (Sandercock and Frost, 1998). The high-resolution three-dimensional structure of FinO has recently been solved by X-ray diffraction studies, which have confirmed that FinO contains a large predominance of alpha-helices (Figure 1.8b and 1.8c Ghetu *et al.*, 2000). The overall structure of FinO can be likened to a closed left-handed fist with an extended index finger and thumb (Figure 1.8a; Ghetu *et al.*, 2000). The N-terminal portion of FinO forms a long solvent-exposed alpha-helix, which is represented by an extended index finger. The central domain of FinO is composed of four short regions of β-sheet structure, interspersed with four short alpha helices (Figure 1.8a and 1.8b). This region forms a solvent-exposed positively charged

Figure 1.8a Primary sequence and secondary structure of plasmid R6-5FinO. The primary amino acid sequence of FinO is represented by standard single letter amino acid code. The three-dimensional structure of the protein is annotated below the amino acid sequence, with alpha helical regions represented by cylinders, random coil structure represented by black lines, and β-sheet regions denoted by arrows.

Figure 1.8b Ribbon diagram of plasmid R6-5 FinO. The three-dimensional structure of FinO was determined by high-resolution X-ray diffraction studies by Dr. Alexandru Ghetu (Ghetu *et al.*, 2000). The N- and C-termini are labeled accordingly. Only the region extending from Thr-32 to Gln-186 at the extreme C-terminus is represented.

Figure 1.8c Surface charge representation of plasmid R6-5 FinO. Blue regions are positively charged, while red regions are negatively charged. The diagram on the left is in the same orientation as the ribbon diagram in Figure 1.8b. The diagram on the right has been rotated by 180 degrees to the right in the plane of the paper. Adapted from Ghetu *et al.* (2000).

a.

```
            10        20        30        40        50        60        70
MTEQKRPVLTLKRKTEGETPTRSRKTIINVTTPPKWKVKKQKLAEKAAREAELTAKKAQARQALSIYLNL

            80        90       100       110       120       130       140
PTLDEAVNTLKPWWPGLFDGDTPRLLACGIRDVLLEDVAQRNIPLSHKKLRRALKAITRSESYLCAMKAG

           150       160       170       180
ACRYDTEGYVTEHISQEEEVYAAERLDKIRRQNRIKAELQAVLDEQ
```

b.

c.
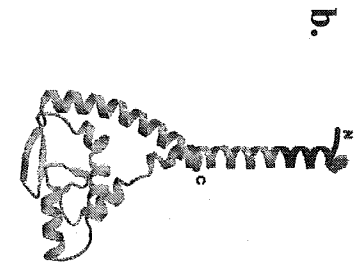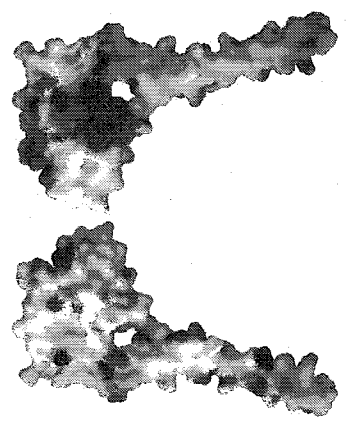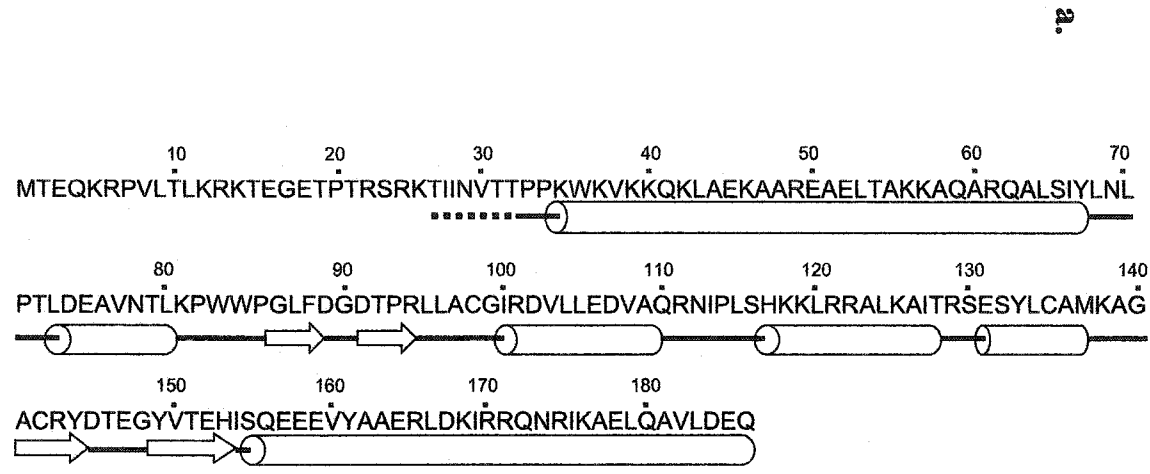
face, and can be likened to the palm of the closed fist (Figure 1.8c). The C-terminal portion of FinO is also composed of a shorter alpha-helix, which can be likened to an extended thumb. This region extends upwards from the central domain of the protein, and the distal end of the helix packs against the base of the long N-terminal alpha-helix (Figure 1.8b). Neither the primary amino acid sequence nor the three-dimensional structure of the protein resemble any of the characterized RNA binding proteins examined to date (Mattaj, 1993; Ghetu *et al.*, 2000).

As mentioned briefly in section 1.5.1, FinO has been shown to increase the steady-state intracellular concentration of FinP antisense RNA. This effect is not mediated by an increase of expression of FinP (Mullineaux and Willetts, 1985). Rather, FinO leads to an increase in the concentration of FinP by directly preventing its degradation by RNase E (Frost *et al.*, 1989; Lee *et al.*, 1992; van Biesen and Frost, 1994 Jerome *et al.*, 1999). van Biesen and Frost (1994) demonstrated that a GST:FinO fusion could bind specifically to both FinP antisense RNA and *traJ* mRNA *in vitro*. Further work determined that the acidic C-terminal region of FinO was required to mediate protection of FinP from RNase E degradation (Sandercock and Frost, 1998). It was hypothesized that binding of FinO to FinP placed this region is in close proximity to the single-stranded spacer located between SL-I and SL-II, sterically inhibiting RNase E-mediated cleavage of the RNA (Sandercock and Frost, 1998; Jerome and Frost, 1999).

Extensive examination of FinP/GST:FinO binding *in vitro* suggested that the N-terminal and central regions of FinO were required for high-affinity RNA binding (Sandercock and Frost, 1998). A detailed analysis of the structural features of FinP and *traJ* mRNA recognized by FinO also provided insight into how this RNA/protein

interaction occurs. Using *in vitro* transcribed RNAs and purified GST:FinO protein, the minimal RNA binding target for FinO was determined to be FinP SL-II (Jerome and Frost, 1999). Binding of FinO to this target was enhanced by the presence of single-stranded tails on either side of the stem-loop. Furthermore, the length, but not the sequence, of these single-stranded tails had a major influence on the affinity of FinO for the RNA (Jerome and Frost, 1999). The finding that both of these single-stranded tails were required for high-affinity binding strengthened the argument that FinO binding to this region of FinP protected the single-stranded spacer region from degradation by RNase E. Although FinP SL-II provided a minimal target for FinO binding, SL-I was also bound by FinO *in vitro*, albeit with a lower affinity (Jerome and Frost, 1999). Interestingly, FinO could also bind to the analogous stem-loop structure of *traJ* mRNA, leading to the conclusion that FinO binds its RNA targets in a structure-dependent manner, and that the sequence of the target had no influence on the binding interaction (van Biesen and Frost, 1994; Jerome and Frost, 1999). This finding provides a clear explanation for why FinO exhibits no plasmid specificity. Recent work has determined that when FinO binds to FinP, significant structural changes may occur to the RNA (Ghetu *et al.*, 2002 RNA). A detailed analysis of the mechanisms of FinO/FinP binding is presented in Chapters 3 and 4.

The observation that FinO increased the intracellular concentration of FinP by approximately two-fold, and increased the half-life of the RNA from two minutes to over forty minutes, could not account for the previously observed 10- to 1000-fold repression of F-like plasmid transfer (Lee *et al.*, 1992; Koraimann *et al.*, 1996). It was hypothesized that FinO may act to increase the rate of FinP/*traJ* mRNA duplex formation. Work by

van Biesen and Frost (1994) clearly demonstrated that *in vitro*, a purified GST:FinO fusion protein could increase the rate of FinP/*traJ* mRNA duplex formation by approximately five-fold. Examination of the ability of several GST:FinO deletion proteins to mediate FinP/*traJ* mRNA duplex formation *in vitro* provided clues as to which portions of FinO mediate this catalytic activity. An N-terminal fragment of FinO containing the first 73 amino acids of the protein was determined to be the minimal region of the protein that was able to promote FinP/*traJ* mRNA duplex formation *in vitro* (Sandercock and Frost, 1998). Surprisingly, removal of a distal portion of the acidic C-terminal domain of FinO resulted in a small but significant increase in the rate of *in vitro* duplex formation compared to wild-type GST:FinO (Sandercock and Frost, 1998). These authors proposed that electrostatic repulsion between this region of FinO and FinP antisense RNA may facilitate the proper alignment of FinO with its target during RNA binding, but inhibit RNA/RNA interaction during duplex formation. The acidic C-terminal alpha-helices of the ColE1 Rom homodimer aid in aligning the protein with its RNA target during binding, a mechanism which could also be employed by FinO during catalysis of FinP/*traJ* mRNA duplex formation (Predki *et al.*, 1995).

An analysis of the data collected to date suggests that FinO appears to have a two-fold function in promoting fertility inhibition of F-like plasmids. Its first effect is to increase the intracellular steady-state concentration of FinP by protecting it from degradation by RNase E. This process would allow FinP to accumulate to a level that would enable it to begin exerting negative repression of TraJ accumulation. The second effect of FinO is to increase the formation of a FinP/*traJ* mRNA duplex, a process which itself has a two-fold effect on repression. The first effect is to directly prevent translation

of the message by sequestering the RBS of *traJ* mRNA within an intermolecular complex, thus directly preventing accumulation of TraJ. The second effect is to promote the formation of a full FinP/*traJ* mRNA duplex, which becomes susceptible to RNase III degradation. Together, these functions may lead to the observed 10- to 1000-fold repression of transfer of F-like plasmids. In Chapter 4, evidence is presented which shows that both of these functions of FinO are required to mediate full repression of conjugative F transfer. In the next section, several antisense RNA systems are examined, providing a comparison of the fertility inhibition mechanisms used by F-like plasmids to antisense RNA systems found in other plasmids.

1.6 Other antisense RNA systems.

The past two decades have seen a large increase in the number of antisense RNA systems that have been discovered and characterized in a host of organisms, ranging from bacteria to higher eukaryotes (reviewed in Brantl, 2002). Bacterial antisense RNA systems were among the first to be discovered and analyzed, and have been the most widely studied systems to date. Antisense RNA systems involved in controlling replication of the plasmids ColE1 and R1 were the first naturally occurring systems discovered, and since that time much work has been accomplished to provide an excellent understanding of the mechanisms employed by these systems (Stougaard *et al.*, 1981; Tomizawa and Itoh, 1981).

While the functions and specific mechanism of antisense RNA systems vary considerably, several common features have emerged over the course of the past few years. Antisense RNAs are generally small, 35 to 105 nucleotides long, and fold into compact but complex secondary structures composed of one or more stem-loop domains.

Loops are generally GC-rich, and five to eight nucleotides in length (Hjalt and Wagner, 1992; reviewed in Brantl, 2002). Stability of antisense RNAs varies considerably, from 2 to 14 minutes for F plasmid FinP (Lee *et al.*, 1992) to more than sixty minutes for RNA-OUT, an antisense RNA expressed by the IS*10* transposon (Case *et al.*, 1989). Most antisense RNAs promote negative regulation of expression of a specific gene, although positive activation of gene expression has been identified (Majdalani *et al.*, 1998)

Studies of the kinetics of several antisense/sense RNA pairing reactions have revealed that inhibition mediated by a given antisense RNA depends on the initial rate of binding, regardless of the overall mechanism employed to achieve negative regulation. The apparent association rate constants (k_{app}) for most systems ranges from 10^5 $M^{-1}s^{-1}$ to 10^6 $M^{-1}s^{-1}$ (Brantl and Wagner, 1994; reviewed in Brantl, 2002). This finding suggests that antisense RNA systems have evolved in a similar fashion, and have developed similar kinetic mechanisms to ensure that their regulatory functions are fast and efficient. The next section provides a summary of two of the best-studied antisense RNA plasmid replication control systems, RNA I/RNA II of ColE1, and CopA/CopT of plasmid R1.

1.6.1 Control of replication of plasmid ColE1.

The replication control system of plasmid ColE1 was one of the first naturally occurring antisense RNA control systems discovered and characterized (Lacatena and Cesarini, 1981; Tomizawa *et al.*, 1981). ColE1 and related plasmids are present in *E. coli* at a medium copy number of approximately ten to thirty copies per chromosome, and their replication by host-encoded proteins is tightly regulated (Conrad and Campbell, 1979). Replication of ColE1 requires the synthesis of an RNA primer, RNA II, whose transcription initiates 555 nucleotides upstream of the origin of replication (Figure 1.9a;

Figure 1.9a Organization of the *ori* region of plasmid ColE1. Only a small portion of the entire region is shown. The origin of replication (*ori*) is shown in gray and labeled below the diagram. The start of transcription of the RNA II preprimer is labeled by a triangle, at a position 555 nucleotides upstream of *ori*. The direction of transcription is labeled by an arrow. The transcription start site for antisense RNA I is marked by a triangle at a position 445 nucleotides upstream of *ori*, and it is transcribed in the opposite direction of RNA II, as indicated by the arrow. *rom* is also shown downstream of *ori*. The diagram is not to scale. Adapted from Wagner and Simons (1994).

Figure 1.9b Control of primer formation at *ori*. Transcription of RNA II extends into the *ori* region. In the absence of RNA I, the RNA II preprimer forms a persistent hybrid with one strand of the DNA at *ori*. RNA II is then cleaved by RNase H, leaving a mature primer that allows for DNA replication by DNA polymerase I. In the presence of RNA I, RNA I/RNA II duplex formation occurs, a process that is enhanced by the Rom protein. Formation of this RNA/RNA duplex prevents the formation of a persistent RNA II/DNA hybrid at the origin of replication, preventing primer maturation and DNA replication. Adapted from Wagner and Simons (1994).

a.

RNA I

RNA II

-555

ori

rom

-445

b.

Elongation of RNA II transcription

No binding by RNA I

Binding by RNA I

Persistent hybrid forms at *ori*

RNA I

Rom

RNA I/RNA II kissing complex

RNAse H cleavage

RNA I/RNA II duplex forms

Initiation of leading strand synthesis

No persistent hybrid forms at *ori*.
No primer maturation.
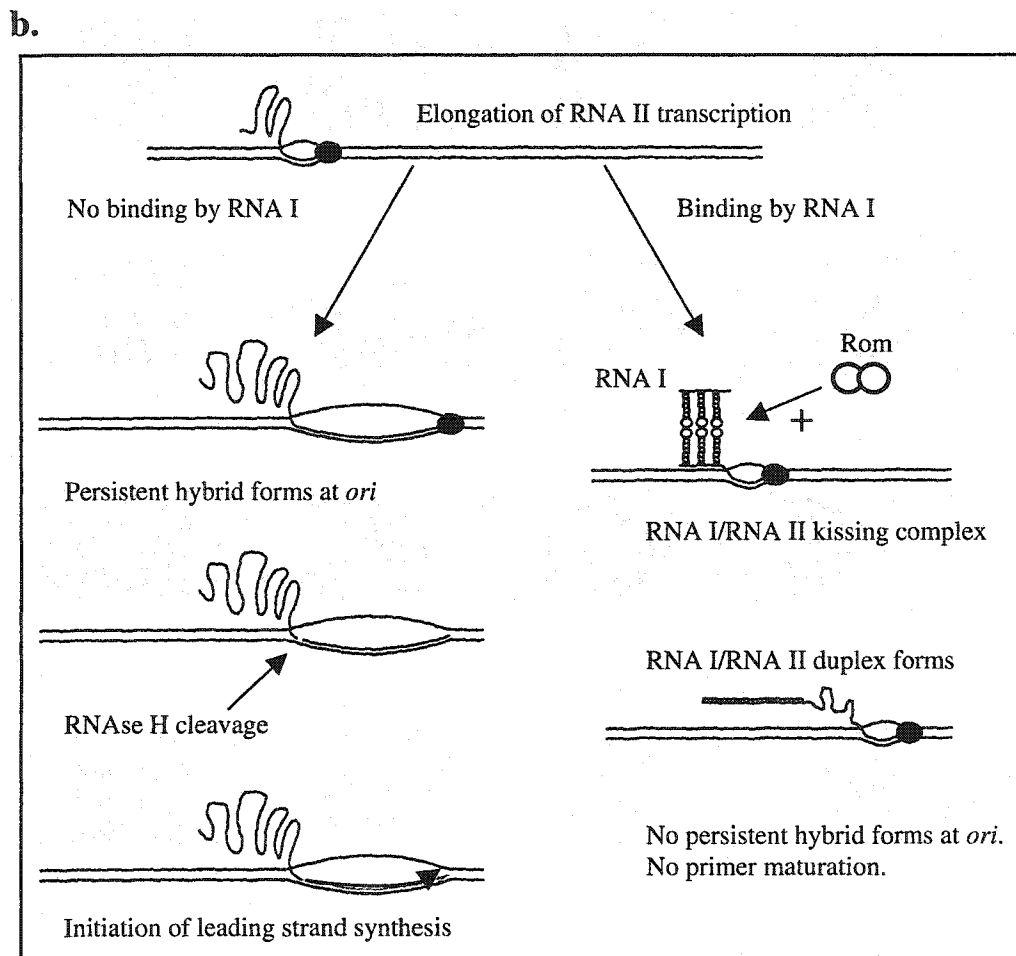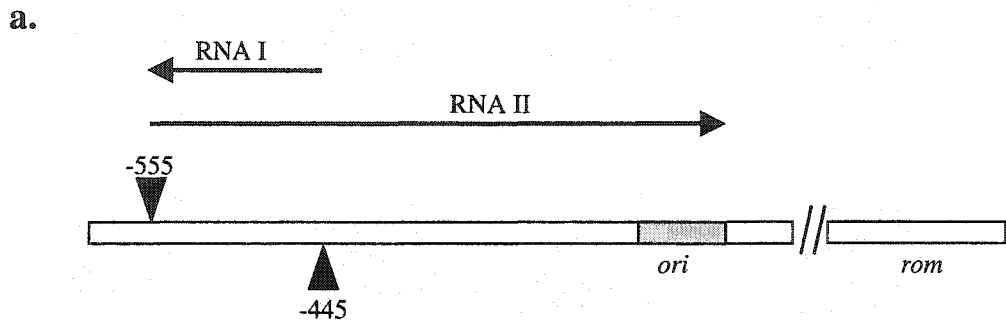
Itoh and Tomizawa, 1980). During plasmid replication, RNA II forms a stable, persistent hybrid with the DNA at the origin of replication. Once this hybrid is formed, RNase H cleaves the RNA, leaving a segment of RNA II hybridized to the DNA. This process provides a mature RNA primer with a free 3' end for replication of the DNA by DNA polymerase I (Figure 1.9b; Itoh and Tomizawa, 1980; Masukata and Tomizawa, 1984).

Control of stable RNA II primer maturation is mediated by an antisense RNA, termed RNA I. Initiation of RNA I synthesis begins 445 nucleotides upstream of the origin of replication, in the opposite direction of RNA II (Figure 1.9a). Insertion mutations in the sequence of RNA I resulted in an increase in copy number of the plasmid, which suggested that RNA I was a regulatory RNA (Conrad and Campbell, 1979). This hypothesis was confirmed by the finding that RNA I could inhibit RNase H-mediated cleavage of the RNA II/DNA hybrid, preventing primer maturation (Tomizawa and Itoh, 1981). RNA I was determined to be a 108 nucleotide antisense RNA, which folds into a relatively stable molecule containing three stem-loops and a 5' single-stranded tail (Figure 1.10; Tamm and Polisky, 1985). Binding of RNA I to the complementary region of RNA II prevents folding of RNA II into the correct conformation required for the formation of a persistent RNA II/DNA hybrid at the replication origin (Masukata and Tomizawa, 1986; Tomizawa, 1985, 1986). Thus, RNA I/RNA II duplex formation prevents RNA II primer maturation, leading to an inhibition of plasmid replication. This interaction is very time sensitive, because RNA I/RNA II pairing must occur when RNA II is between 100 and 360 nucleotides in length. If RNA II reaches a length of more than 360 nucleotides, it folds into a conformation that irreversibly commits it to form a stable hybrid with the replication origin, leading to

Figure 1.10 Duplex formation between antisense RNA I and the RNA II preprimer of ColE1. Loop:loop kissing between nucleotides in the loops of both molecules leads to the formation of an unstable kissing complex, which is a reversible interaction. This complex then proceeds to more stable "deep-kissing" intermediates, which can still dissociate at a reduced rate. Progression of the deep-kissing complex to a stable complete duplex occurs via progression of intermolecular base pairing between the single-stranded 5' leader region of RNA I with a complementary single-stranded region in RNA II. Once the stable full duplex has formed, it cannot dissociate. Adapted from Wagner and Simons (1994).

Deep kissing complex (C**)

Kissing complex (C*)

RNA I/RNA II Duplex (C^F)
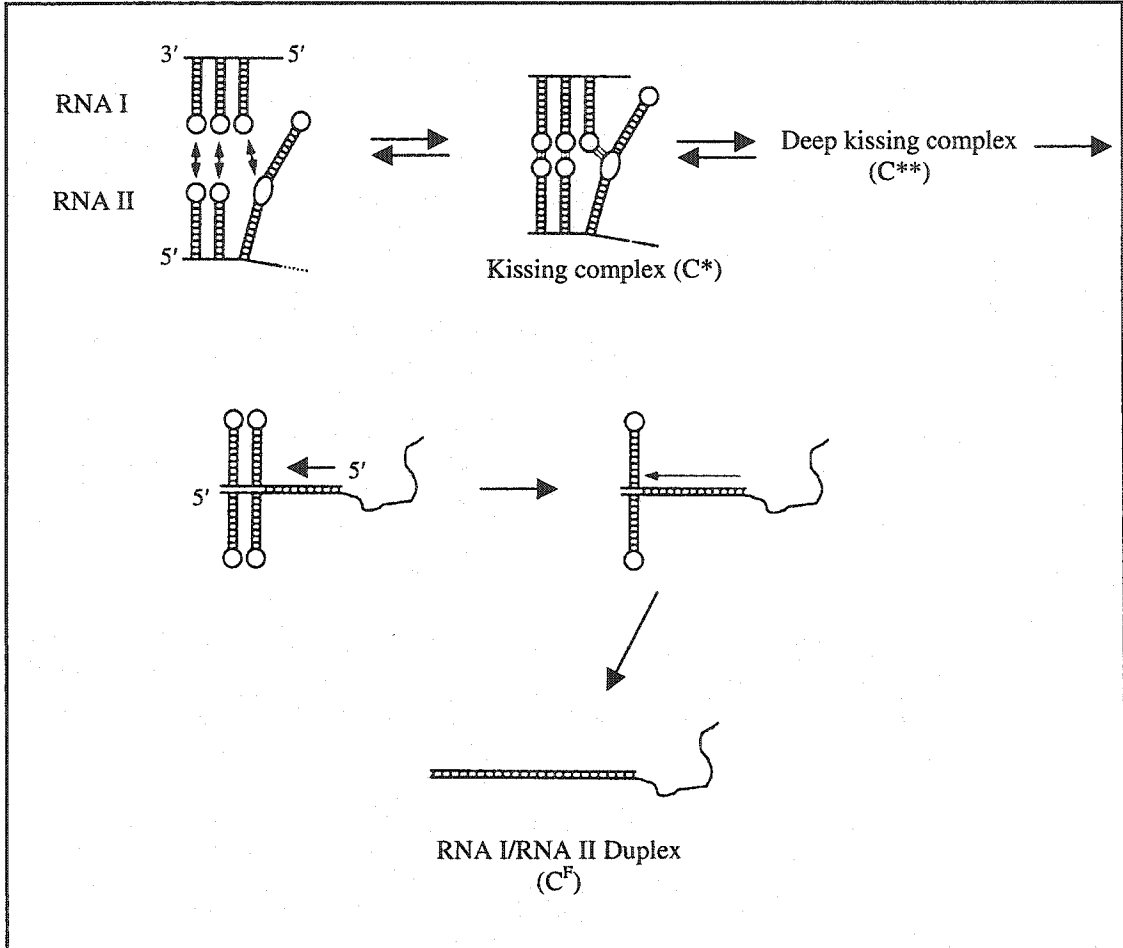
primer maturation by RNase H cleavage of the hybrid (Figure 1.9b; Tomizawa, 1986). Interaction of RNA I with RNA II depends on complementary loop-loop kissing, as well as the presence of the single-stranded region on the 5' side of RNA I (Tomizawa, 1984; Masukata and Tomizawa, 1986).

The kinetics of RNA I/RNA II duplex formation has been extensively examined. Pairing of the RNAs is dependent upon the concentration of both RNA molecules, suggesting the interaction is a second-order reaction. The apparent association rate constant for RNA I/RNA II duplex formation was determined to be 7.1×10^5 $M^{-1}s^{-1}$ (Tomizawa, 1984). Based upon extensive kinetic studies, a multi-step pairing pathway has been determined for RNA I/RNA II interaction (Figure 1.10; Tomizawa, 1984, 1990a). The first step in the process is the formation of a reversible kissing interaction, mediated by base-pairing between nucleotides in all three loops of both RNAs (C* in Figure 1.10; Tomizawa, 1985, 1990b; Eguchi et al., 1991; Gregorian and Crothers, 1995). This initial interaction probably aligns the 5' single-stranded region of RNA I with its complementary region in RNA II, allowing these regions to begin to base pair, promoting the formation of a "deep kissing" intermediate (C** in Figure 1.10; Eguchi and Tomizawa, 1990a, 1991). These initial interactions are sufficient to inhibit RNA II primer maturation (Tomizawa, 1984). Deep kissing can then proceed to the formation of a stable full duplex (C^F in Figure 1.10), a process that is essentially irreversible (Masukata and Tomizawa, 1986). The reaction can be represented as follows:

$$\text{RNA I} + \text{RNA II} \underset{k_{-1}}{\overset{k_1}{\Longleftrightarrow}} C^* \underset{k_{-2}}{\overset{k_2}{\Longleftrightarrow}} C^{**} \overset{k_3}{\Longrightarrow} C^F$$
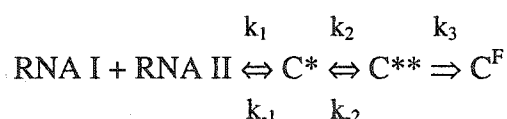
The rate limiting step in this interaction is the formation of the initial kissing intermediate, C*, which may also be sufficient to mediate inhibition of primer maturation (Tomizawa, 1985; Lin-Chao and Cohen, 1991).

A third component of this system is the Rom (RNA one modulator) protein, a sixty-three amino acid protein encoded by the plasmid. Rom is a dimeric protein, consisting of two anti-parallel coiled-coils arranged into four strands in its dimeric form (Banner et al., 1987). Rom is acidic in nature, but the dimer does contain numerous basic amino acids located within a concave binding face of the protein complex (Predki et al., 1995). Alanine scanning mutagenesis has revealed that these amino acids are critical for the RNA binding function of the protein. A negatively charged region in the protein has been proposed to shift the RNA via electrostatic interactions towards the basic binding face of the protein during the binding process (Predki et al., 1995; Sandercock and Frost, 1998). Rom does not bind RNA I or RNA II alone, rather it binds as a single dimer to the interacting loops of both molecules once they have formed the initial kissing intermediate (Tomizawa, 1990b; Eguchi and Tomizawa, 1991).

The solution structure of a model of a kissing loop complex derived from constructs similar to RNA I and RNA II has been determined (Lee and Crothers, 1998). Analysis reveals that all seven of the loop residues in the model hairpin duplexes tested base pair with their partners in the complementary loop. This interaction results in a stable structure which exhibits continuous helix stacking, from the stem of one RNA, through the helix formed by the loop-loop kissing structure, and into the second RNA stem. The structure thus overall resembles a continuous stretch of A-form RNA, containing a pronounced bend towards the major groove in the loop-loop helix, which

narrows the major groove in this region (Lee and Crothers, 1998). Binding of Rom to the structure results in an enhancement of the bend in the RNA (Marino, *et al.*, 1995). It is likely that Rom recognizes several features of the structure formed by the kissing complex, including the sharp bend in the structure towards the narrowed major groove. Cross-strand stacking between G residues in the stems immediately below the loops, and a cluster of phosphate residues which flank the major groove of the loop-loop helix, also likely provide structure-specific features which are recognized by Rom (Lee and Crothers, 1998). The binding of Rom to the kissing complex inhibits dissociation of the unstable kissing intermediate, promoting the formation of more stable intermediates. The interaction of RNA I, RNA II, and Rom can be represented as follows:

$$\text{RNA I+RNA II + Rom} \underset{k_{-1}}{\overset{k_1}{\Leftrightarrow}} C^* + \text{Rom} \underset{k_{-2}}{\overset{k_2}{\Leftrightarrow}} C^m \overset{k_3}{\Rightarrow} C^F$$
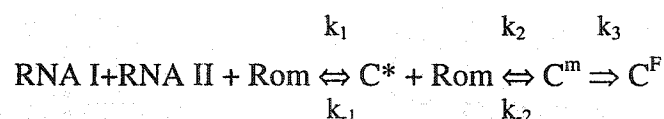
C^* represents the initial unstable kissing intermediate, while C^m represents a more stable intermediate resulting from the binding of a Rom dimer. Rom binding essentially reduces the dissociation constant, k_{-1}, resulting in the formation of a more stable complex, C^m, driving the reaction depicted above to the right, leading to stable duplex formation more efficiently than in the absence of Rom (Tomizawa, 1990b; Eguchi and Tomizawa, 1990). Since Rom does not directly affect formation of the initial kissing complex or catalyze any of the subsequent steps in dimerization, its effect on duplex formation is moderate. The presence of Rom only results in an approximate doubling of the k_{app} from 7.1×10^5 $M^{-1}s^{-1}$ to 1.0×10^6 $M^{-1}s^{-1}$ (Tomizawa and Som, 1984). Therefore, unlike the interaction of FinP antisense RNA and *traJ* mRNA, which absolutely requires the

presence of the FinO RNA chaperone protein *in vivo*, RNA I/RNA II duplex formation occurs in the absence of an accessory protein. Indeed, deletion of the Rom protein from ColE1 only results in an approximate doubling of the copy number of the plasmid.

1.6.2 Control of replication of plasmid R1.

R1 is a member of the IncFII group of F-like plasmids, and its replication requires the plasmid-encoded RepA protein (Masai *et al.*, 1983). Synthesis and accumulation of RepA is in turn regulated by the antisense RNA, CopA (Nordström *et al.*, 1984). CopT is the transcript that encodes RepA, as well as a small 7 kDa protein, Tap (translational activator peptide) (Wagner *et al.*, 1987). Translation of Tap results in the ability of ribosomes to load onto the RBS sequence of *rep*, which is otherwise sequestered within a stem-loop in the CopT transcript. This process results in translation of *rep* and RepA accumulation (Figure 1.11; Wu *et al.*, 1992). RepA expression, and therefore plasmid replication, is thus dependent upon coupling of Tap and RepA translation (Figure 1.11).

CopA is an approximately 90 nucleotide antisense RNA that is transcribed in the opposite direction from CopT, and it folds into two stem-loops separated by an eleven nucleotide single-stranded region and flanked on its 3′ side by a single-stranded tail (Figure 1.11). CopA is therefore perfectly complementary to a portion of the CopT leader located approximately eighty nucleotides upstream of the RepA start codon. This region of CopT was determined to fold into a structure analogous to CopA (Figure 1.11; Nordström *et al.*, 1984; Wagner and Nordström, 1986; Öhman and Wagner, 1989). Binding of CopA antisense RNA to the analogous stem-loop region of CopT occludes the *tap* RBS in the CopT transcript, preventing Tap translation by sterically inhibiting ribosome loading, leading to uncoupling of Tap/RepA translation (Figure 1.11; Blomberg

Figure 1.11 Regulation of synthesis of RepA of plasmid R1. CopT mRNA encodes the 7 kDa peptide Tap, as well as the RepA protein, which is required for replication of the plasmid. The *repA* RBS is sequestered within a small 3' stem-loop in CopT as indicated in the figure. CopA is an antisense RNA that is transcribed in the opposite direction of CopT, and the SL-II region of the antisense RNA is complementary to the analogous region in the CopT message. In the absence of CopA/CopT binding, ribosomes can load onto the *tap* RBS and translate the Tap peptide. This opens the CopT stem-loop, which contains the *repA* RBS, allowing ribosomes to load onto the CopT RBS, translationally coupling Tap and RepA synthesis. When CopA antisense RNA binds to CopT, the *tap* RBS is blocked, preventing translational coupling of Tap and RepA, and causing the *rep* RBS to remain sequestered within the 3' stem-loop. This process results in inhibition of RepA synthesis and plasmid replication. Adapted from Wagner and Simons (1994).
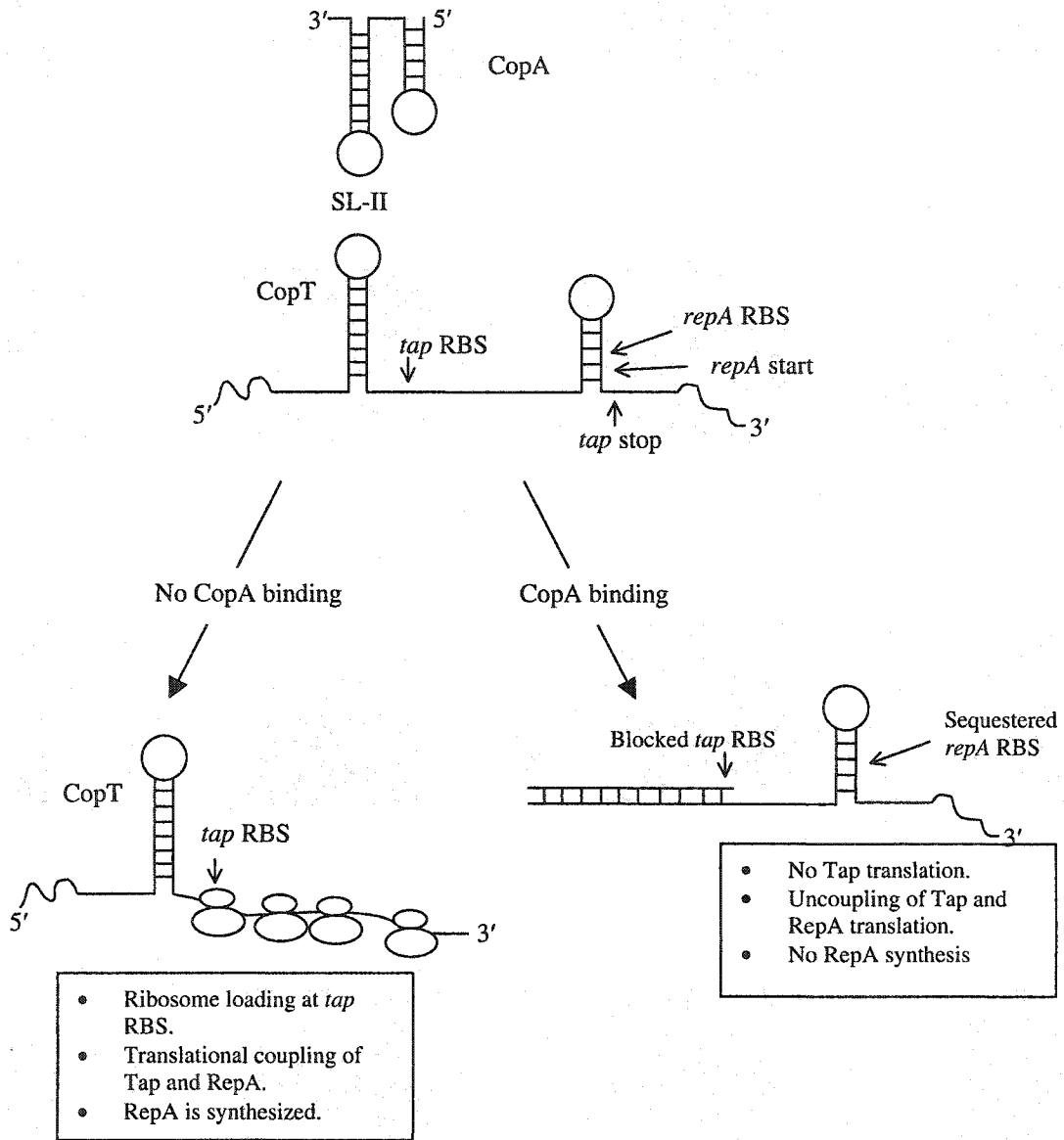
et al., 1990, 1992; Malmgren *et al.*, 1996). Similar to RNA I/RNA II interaction discussed in the previous section, formation of a CopA/CopT complex has been found to progress via a multi-step binding pathway, leading to the formation of RNA/RNA complexes with increasing stability, shown schematically in Figure 1.12a. Formation of this duplex has been found to progress via the breaking of intramolecular bonds of both RNAs, and the formation of new intermolecular interactions, rather than melting of the secondary structures of the RNAs prior to duplex formation (Persson *et al.*, 1990a, 1990b; Malmgren *et al.*, 1997).

Mutational analysis of both CopA and CopT has determined that the structure of both RNAs is critical for efficient RNA/RNA duplex formation and plasmid replication control (Wagner and Simons, 1994). Kinetic analyses have determined that the k_{app} for CopA/CopT duplex formation is approximately 1×10^6 $M^{-1}s^{-1}$, similar to the k_{app} for ColE1 RNA I/RNA II duplex formation (Persson *et al.*, 1988). The initial step of duplex formation is the creation of an unstable loop-loop kissing intermediate, involving interactions between loop nucleotides of CopA SL-II and the loop nucleotides in the complementary stem-loop of CopT (Figure 1.12a; Persson *et al.*, 1990a). Removal of CopA SL-I and the single-stranded region between SL-I and SL-II resulted in a truncated RNA construct that could compete with full-length CopA for binding to CopT *in vitro*, however it was unable to form a stable duplex (Persson *et al.*, 1990b). Such truncated CopA molecules also exhibited a severely reduced ability to inhibit RepA synthesis and accumulation *in vivo* (Wagner *et al.*, 1992). Further analysis determined that truncated CopA missing SL-I and the single-stranded region between SL-I and SL-II could not prevent ribosome loading to the *tap* RBS sequence (Kolb *et al.*, 2001a). This single-

Figure 1.12a Step-wise pairing of R1 CopA and CopT. The initial interaction between CopA and CopT occurs via a reversible kissing interaction between loop nucleotides in both molecules (A.). This initial interaction undergoes a rearrangement to allow an asymmetric extended kissing intermediate to form (B.). This complex is still reversible at this point. Intermolecular base pairing between complementary single-stranded regions in each molecule then occurs (C.) leading to the rapid progression of the stable extended kissing complex in an essentially irreversible reaction (D.). Progression to a full duplex (E.) can then proceed, albeit at a very slow rate. Adapted from Malmgren *et al.* (1997).

Figure 1.12b The extended four-way junction formed by CopA/CopT interaction. This is a schematic representation of the four-way junction that forms as an extended kissing complex of CopA and CopT proceeds towards full duplex formation (complex D. in Figure 1.12a). A black line represents CopT, while a gray line represents CopA. The complex is formed by a side-by-side alignment of both molecules, creating an X-shaped junction. Helix B and B′ are intermolecular helices formed by progression of the kissing complex via intermolecular base pairing between CopA and CopT. Helix C is the stabilizer helix, which is formed as the 5′ single-stranded region of CopA pairs with CopT. Continuing intermolecular helix formation proceeds to its full extent, leading to a full CopA/CopT duplex (complex E. in Figure 1.12a). Adapted from Kolb *et al.* (2000a).

a.
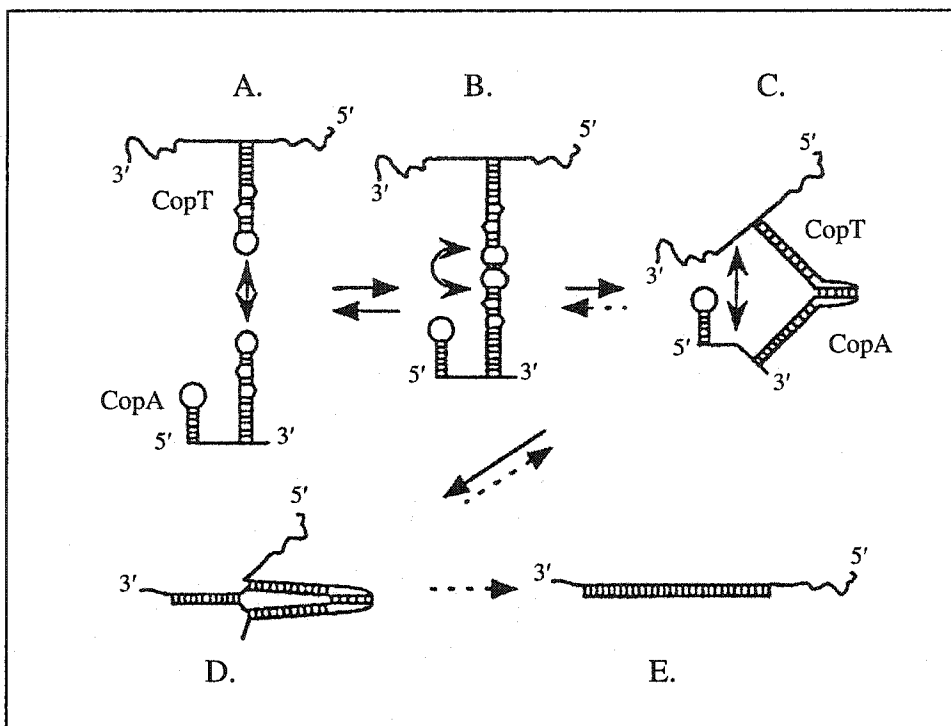
b.
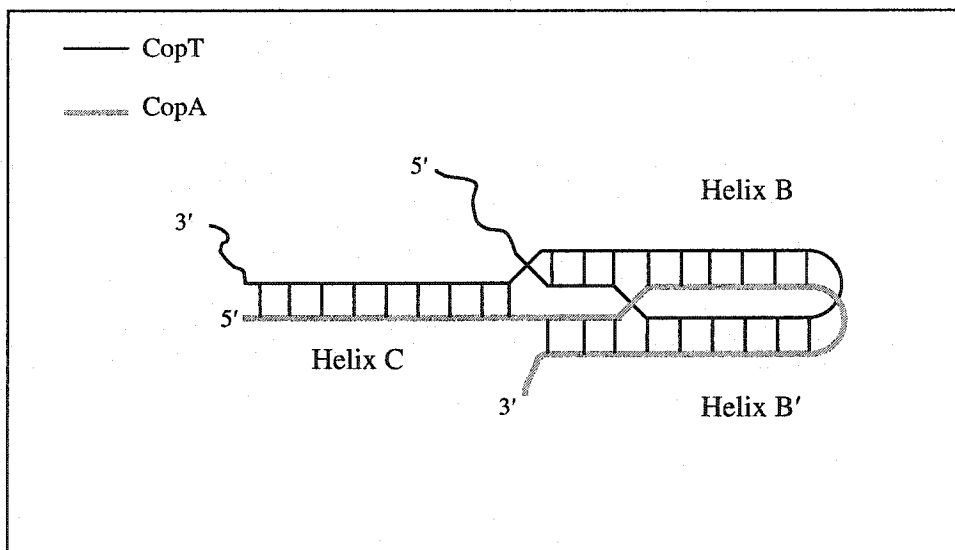
stranded region is therefore critical for the function of CopA antisense RNA. Indeed, Malmgren *et al.* (1997) determined that the thirty nucleotides 5' to SL-II, including SL-I and the eleven nucleotide single-stranded region, pairs with its complementary region in CopT, stabilizing the kissing intermediate formed between the CopA and CopT SL-II regions (Figure 1.12a). This process creates an extended kissing intermediate, which is able to inhibit ribosome binding to the RBS region of *tap*. These results suggested that full duplex formation between CopA and CopT is not required for inhibition of RepA synthesis, and that formation of a full CopA/CopT duplex may therefore be biologically irrelevant (Malmgren *et al.*, 1996, 1997; Wagner and Brantl, 1998).

Recent studies have provided new insights into the processes involved in duplex formation between CopA and CopT. As described above, an extended kissing intermediate formed by interaction of the loop regions of SL-II of both CopA and CopT, coupled with pairing between single-stranded regions of each RNA, are sufficient to inhibit RepA expression. Studies have revealed that once an extended kissing complex has formed, the complex progresses to form a four-way junction, composed of two intramolecular helices coaxially stacked with two intermolecular helices (Figure 1.12b; Kolb *et al.*, 2000b). Structural analysis has shown that this complex assumes an asymmetrical X-shaped junction, forming a side-by-side alignment of the two relatively long intramolecular helices of CopA and CopT RNAs. This alignment promotes the formation of a third intermolecular stabilizer helix, formed by base-pairing interactions between complementary single-stranded regions of the CopA and CopT molecules, which significantly stabilizes the CopA/CopT inhibitory complex (Figure 1.12b; Kolb *et al.*, 2000a). Formation of this four-way junction is critical for the inhibitory action of

CopA RNA, and it must form in order to prevent ribosome loading at the *tap* RBS (Kolb *et al.*, 2000a, 2001a).

Extensive mutational and structural analyses have determined that several factors influence the ability of the initial stable kissing intermediate to progress to the four-way junction. Loop-loop complementarity between CopA and CopT is critical for the formation of the initial complex, and progression of intermolecular helix formation occurs unidirectionally into the upper stems of both CopA and CopT. The direction of helix propagation proceeds in a 5' direction, down the 5' side of the loop of SL-II of CopA, and by default in a 3' direction relative to the complementary loop of SL-II of CopT (Kolb *et al.*, 2000a). The ability of helix propagation to proceed in this direction is critical for the inhibitory function of CopA antisense RNA.

The presence of bulged residues in the upper stems of SL-II of CopA and CopT was predicted to influence melting of the upper stems of both molecules, to facilitate formation of the duplex (Persson *et al.*, 1990a; Hjalt and Wagner, 1995). Removal of the bulged nucleotides in the upper stem of CopA SL-II resulted in an RNA that could still form an initial kissing intermediate. However, such CopA mutant RNAs could not lead to the progression of the initial kissing intermediate to the more stable four-way junction which is required to prevent ribosome loading at the *tap* RBS (Kolb *et al.*, 2001a). The authors confirmed the original hypothesis put forth by Persson *et al.* (1990a), showing that the presence of bulged nucleotides leads to breathing of the CopA and CopT SL-II upper stem regions, which promotes intermolecular helix propagation after the kissing intermediate has formed. Analysis of duplex formation between the Inc antisense RNA and its target *repZ* mRNA encoded by the plasmid Col1b-P9 has shown that a very

similar duplex formation event occurs between these RNAs. A four-way junction formed by Inc and *repZ* mRNA, and the overall binding pathway undertaken by both RNAs, bear a striking resemblance to the four-way junction and step-wise binding pathway involved in CopA/CopT duplex formation (Kolb *et al.*, 2001b). These authors propose that formation of this highly structured four-way junction may in fact be a common feature of antisense-sense RNA pairing reactions of a wide variety of plasmids.

1.7 RNA binding proteins.

Many RNA binding proteins have been characterized over the past several years. RNA binding proteins are structurally diverse, as are their RNA targets (reviewed in Caprara and Nilsen, 2000). Similarly, the mechanisms employed by such proteins to bind their targets with high affinity and specificity vary to a large extent (reviewed in Draper, 1995). Binding of a protein to its target may also alter the structure of the RNA itself, which occurs when the HIV Tat protein binds its RNA target, TAR RNA (Zacharias and Hagerman, 1995; Dayie *et al.*, 2002). Conversely, a conformational change in the RNA binding domain of the protein may result when binding occurs (Tan and Frankel, 1994; Wilkinson *et al.*, 2000). As more RNA binding proteins are characterized, it is becoming increasingly clear that a general characterization of their properties is difficult to achieve.

RNA presents a structurally diverse target for binding by proteins. A-form RNA helices have a major groove that is deep and narrow, while the minor groove is shallow and wide. Interactions with both grooves of RNA helices have been characterized (reviewed in Steitz, 1993). RNA binding proteins can recognize RNA targets in a sequence- or structure-dependent manner. *E. coli* phage MS2 expresses a coat protein that targets and binds a specific sequence within a conserved nineteen nucleotide stem-

loop in the viral genome (Carey *et al.*, 1983; Lowary and Uhlenbeck, 1987; Grahn *et al.*, 2001). The eukaryotic histone mRNA stem-loop binding protein (SLBP) likewise depends on a specific loop sequence in its target, as well as the overall structure of the RNA (William and Marzluff, 1995; Dejong *et al.*, 2002; Zanier *et al.*, 2002). The HIV Rev protein binds its RNA target in a structure-dependent manner, with the sequence of the RNA having little effect on its binding affinity (Heaphy *et al.*, 1991; Wilkinson *et al.*, 2000). The ColE1 Rom protein recognizes a specific structure formed by a loop-loop kissing complex formed by derivatives of RNA I and RNA II, however it can also bind to a kissing loop complex composed of HIV Tar RNA and its complement (Predki *et al.*, 1995; Chang and Tinoco, 1997). Therefore, RNA binding proteins clearly exhibit a wide variety of RNA target requirements for high affinity binding. The next two sections provide a detailed analysis of two diverse RNA binding proteins to provide a sample of the interactions involved when proteins bind RNA.

1.7.1 The lambda phage N protein.

Expression of early genes of the *E. coli* phage lambda (λ) is a critical step in the life cycle of the virus. Transcription of these early genes occurs from two opposing promoters, P_L and P_R, and requires the phage-encoded protein N, and the host-encoded protein factors NusA, NusB, NusG, and ribosomal protein S10. Interaction of all of these protein elements with an RNA enhancer element on the early phage nascent transcript forms a ribonucleoprotein complex that alters *E. coli* RNA polymerase (RNAP) processivity. Once this complex forms, RNAP can transcribe through intrinsic terminators encoded on the early λ transcript, a process called antitermination (Das, 1993; Greenblatt *et al.*, 1993; Friedman and Court, 1995).

N-mediated antitermination relies on the *cis*-acting enhancer element *nut* (N̲-utilization), encoded by the λ DNA template between the early promoter P_L and P_R, and the first intrinsic terminators of each operon (Friedman and Court, 1995). The *nut* site on the transcript is composed of a single-stranded RNA element, *boxA*, followed by a single-stranded spacer region and a fifteen-nucleotide hairpin, *boxB*. The hairpin, in turn, is composed of a five base pair stem topped by a five nucleotide loop (Figure 1.13a; Franklin, 1985a; Whalen *et al.*, 1988; Legault *et al.*, 1998). *boxA* is conserved amongst most lambdoid phages, however the *boxB* sequence varies considerably, providing specificity for N and its cognate binding sequence among these bacteriophages (Franklin 1985a, 1985b; Lazinski *et al.*, 1989). Single nucleotide substitutions in the *boxB* loop can significantly reduce the binding affinity of N, and the ability of N to promote antitermination (Whalen *et al.*, 1988; Doelling and Franklin, 1989; Chattopadhyay *et al.*, 1995; Tan and Frankel, 1995). At elevated levels, N can promote antitermination without any accessory proteins, suggesting that NusA, NusB, NusG, and S10 increase the processivity of the complex during antitermination (Whalen and Das, 1990; Rees *et al.*, 1996; Mogridge *et al.*, 1998). The current model for N function is that binding of N to *boxB* causes the nascent transcript to loop out, bringing the antiterminator complex into close proximity to RNAP and promoting a direct N:RNAP interaction (Nodwell and Greenblatt, 1991). The precise mechanism of antitermination is still not well understood.

N is a 107 amino acid, highly basic protein, and the N-terminal 22 amino acids have been shown to bind *boxB* RNA with the same affinity and specificity as the full-length protein. The N-terminal 22 amino acids of this minimal RNA binding domain

Figure 1.13a The phage λ *nutR* site. The *boxA* region is outlined by a black rectangle, and the single-stranded spacer and *boxB* hairpin are labeled accordingly. Only bases in the *boxB* hairpin are labeled for clarity, starting from G1 on the 5' side at the base of the stem, and continuing to its complementary base C15 at the 3' end of the stem. Adapted from Zhou *et al.* (2001)

Figure 1.13b Schematic diagram of the *nutL boxB* GNRNA pentaloop and the GNRA tetraloop, as indicated to the right of the figure. The closing U5:A11 base pair at the top of the *boxB* stem is indicated. All of the loop nucleotides are labeled according to their position relative to the first base at the 5' end of the stem, as indicated in the legend for Figure 1.13a. Base rings are denoted by rectangles, ribose sugar moieties by white circles, and phosphate moieties by gray circles. Black bars denote base-stacking interactions. The sheared G6:A10 and Watson-Crick U5:A11 base pairs are indicated by dashed lines. Adapted from Legault *et al.* (1998).

Figure 1.13c The primary amino acid sequence of the ARM of the λ N protein RNA binding domain. Residues 1-22 are indicated by standard single letter amino acid code, with every fifth amino acid labeled starting from the N-terminus. Arg residues are in bold text, with Arg-11, around which a 120° bend in the protein centers, underlined. Adapted from Legault *et al.* (1998) and Schärpf *et al.* (2000).

a.

nutR

```
              A
          A   A
       G      A¹⁰
      ⁵U A             boxB hairpin
       C G             loop
       C G
       C G
   ¹G C¹⁵
```

boxA   Spacer

5'-CGCUCUUA|CACAUUCCA

b.

nutL boxB GNRNA pentaloop

Consensus GNRA tetraloop

c.

```
  1       5      10      15      20
MDAQTRRRERRAEKQAQWKAAN
```
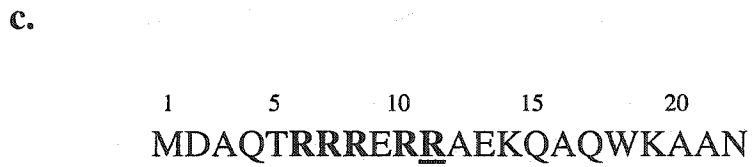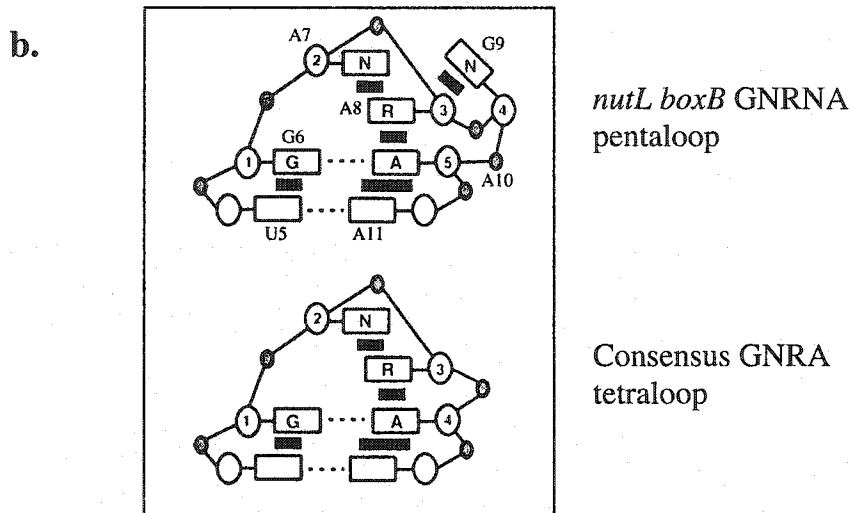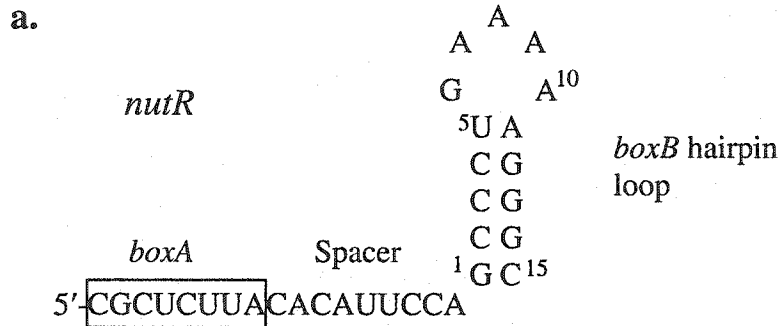
contain an arginine-rich motif (ARM) within the region extending between Gln-4 and Ala-20 (Figure 1.13c; Chattopadhyay *et al.*, 1995; Tan and Frankel, 1995; van Gilst *et al.*, 1997; Legault *et al.*, 1998). NMR and CD spectroscopy analysis have determined that this region of N is disordered in solution. However, it becomes a highly structured alpha-helix with a pronounced 120° bend when in complex with its RNA target (van Gilst and von Hippel, 1997; van Gilst *et al.*, 1997; Legault *et al.*, 1998; Schärpf *et al.*, 2000). RNase footprinting studies have revealed that N binds to the 5' single-stranded region of *boxA*, and that while all 5 nucleotides within the loop of *boxB* are required for N-mediated antitermination, only the first, third, and fifth bases in the loop are directly contacted during N/*boxB* interaction (Chattopadhyay *et al*, 1995; Mogridge *et al*, 1995; Tan and Frankel, 1995; Cilley and Williamson, 1997). NMR analysis indicates that the five base pair stem of *boxB* forms a symmetric A-form helix comprising approximately one half of a full turn (Legault *et al.*, 1998). The pentaloop of *boxB* adopts a fold structurally identical to a GNRA tetraloop (N= any base; R= purine), although the G/A at position 9 in the loop is "flipped out," and stacks with A at position 8 (Figure 1.13b). This GNRA-like fold is essential for N/*boxB* interaction, and base substitutions that alter the structure of the GNRA-like pentaloop eliminate high-affinity N binding (Legault *et al.*, 1998). Base substitutions or deletion of G or A at position 9 in the *boxB* loop had little effect on high-affinity N binding, however they did reduce *boxB*/N/NusA interaction (Legault *et al.*, 1998). The identity of the base pairs in the stem likewise had no influence on N binding, provided Watson-Crick base pairs were maintained. However, the A:U closing base pair at the top of the *boxB* stem, and the sheared G6:A10 base pair in the

GNRA-like pentaloop, provide critical structural recognition factors for high-affinity N

binding (Chattopadhyay *et al.*, 1995; Legault *et al.*, 1998; Schärpf *et al.*, 2000).

The N/*boxB* binding process depends on several specific interactions between the

protein and the RNA. Five Arg and six Lys residues in the N-terminal ARM of N form a

positively charged surface on one side of the alpha-helix, allowing for electrostatic

interactions with the phosphodiester backbone of the RNA. Arg-7, 8, and 10 appear to be

the most critical Arg residues in this region for high-affinity binding (Su *et al.*, 1997;

Legault *et al.*, 1998; Schärpf *et al.*, 2000). Only nucleotides on the 5′ side of the loop and

the upper part of the stem are contacted directly by the ARM of N. Hydrogen bonding

between Gln-4 and Arg-7 with U5 and G6 in *boxB* provides evidence of why the sheared

G6:A10 base pair, a critical structural feature of GNRA tetraloops, plays such an

important role in the N/*boxB* interaction. The formation of this sheared base pair likely

positions G6 in such a manner that it can interact directly with Arg-7 of N (Gutell *et al.*,

1994; Legault *et al.*, 1998; Schärpf *et al.*, 2000). The pronounced 120° bend centered

around Arg-11 in the N *boxB* binding domain is also an important factor for high-affinity

binding, likely because it aligns the positive RNA binding face of the protein with *boxB*

RNA (Schärpf *et al.*, 2000). Trp-18 stacks with A7 on the 5′ side of the *boxB* loop

(Figure 1.13b), providing another critical feature of N required for high-affinity RNA

binding. Replacing Trp-18 with Tyr or Phe decreases the affinity of N for *boxB* by

approximately two-fold, while replacing it with any other amino acid reduces the affinity

considerably more (Su *et al.*, 1997; Legault *et al.*, 1998). Thus, the N/*boxB* interaction

relies primarily on electrostatic interactions, however hydrogen bonding and hydrophobic

stacking interactions between specific bases and amino acids play a significant role in the interaction as well.

1.7.2 The bacterial Hfq protein.

Hfq is a highly conserved bacterial Sm-like protein, which is found in approximately 30,000-60,000 copies per cell. Eukaryotic Sm and Sm-like proteins share multiple structural features, and they play a role in forming snRNPs (small nuclear ribonucleoproteins) during mRNA metabolism via interaction with U-rich RNA sequences (Branlant et al., 1982; Pillai et al., 2001). Hfq localizes primarily to the cytoplasm, and is generally associated with ribosomes (Kajitani et al., 1994). The protein was originally identified as a host factor for phage Qβ replication, and has since been recognized as a global regulator in E. coli which binds to many diverse RNA targets (de Franze Fernandez et al., 1968; Miranda et al., 1997). Hfq functions by destabilizing secondary structure in the (+) strand RNA of the phage genome (de Franze Fernandez et al., 1968, 1972; Shapiro et al., 1972). Hfq binds Qβ RNA with high affinity, and also binds poly(A) RNA and OxyS RNA, among many other RNA species (Carmichael et al, 1975; Zhang et al., 1998). The protein is implicated in influencing efficient translation of E. coli rpoS mRNA, but it also targets numerous mRNAs for degradation, possibly by increasing poly(A) adenylation of the mRNA (Muffler et al., 1996; Hajnsdorf and Régnier, 2000). Hfq also prevents OmpA translation by promoting ompA mRNA degradation through inhibition of ribosome binding to the transcript (Vytvytska et al., 2000). Hfq can promote RNA:RNA interaction between Spot42 antisense RNA and its target galK mRNA (Møller et al., 2002a), and it influences the modulation of RpoS expression in E. coli by the antisense RNAs DsrA and OxyS (Sledjeski et al., 2001;

Zhang *et al.*, 2002). This protein appears to be a multifunctional RNA chaperone, which can exert both positive and negative effects on gene expression in bacteria.

Recent X-ray crystallographic studies have determined the structure of *Staphylococcus aureus* Hfq to 1.55Å resolution, and an Hfq/RNA complex to 2.71Å resolution. The protein consists of 77 amino acids with a molecular weight of 8.9 kDa, and it forms a symmetric homohexamer with a ring-shaped "donut-like" structure, with an approximately 12 Å diameter hole in the center of the ring (Figure 1.14; Schumacher *et al.*, 2002). One face of the hexamer is highly non-polar, while the opposite side (the RNA binding side) is characterized by a basic electropositive region surrounding the hole, which is in turn surrounded by a negatively charged region (Schumacher *et al.*, 2002). Co-crystallization of Hfq with the ribo-oligonucleotide 5'-A(U)$_5$G-3' was also performed. This RNA construct was chosen because A/U-rich sequences have been shown to be high-affinity targets for Hfq binding, and 5'-A(U)$_5$G-3' is the canonical sequence recognized by Sm-like protein complexes (Kambach *et al.*, 1999; Møller *et al.*, 2002a; Schumacher *et al.*, 2002). The RNA was determined be bound to the basic face of the hexameric protein complex, within "pockets" that are formed at the interface between subunits. Binding of the RNA induces a structural change in the Hfq hexamer, causing the hole in the center of the RNA binding face to increase in diameter by several angstroms (Schumacher *et al.*, 2002). The authors propose that this opening may facilitate threading of single-stranded RNA through the hole, however this has not yet been shown to occur.

Alignment of the bound oligo-ribonucleotide target with the binding pockets of Hfq results in the extension of the RNA bases into the pockets. This interaction results in

Figure 1.14 The structure of the *S. aureus* Hfq protein. Ribbon diagram of the Hfq monomer (upper structure) and hexamer (lower structure) as determined by X-ray crystallographic studies. Individual monomers within the Hfq hexamer are shown in shades of gray. Adapted from Schumacher *et al.* (2002).
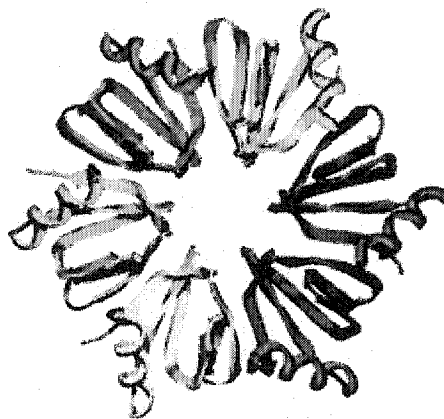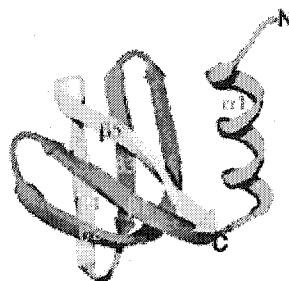
the stacking of base rings between Tyr-42 residues from adjacent subunits. Additionally, a Lys residue at position 41 interacts via both hydrogen bonding and base stacking interactions with uracil bases in the RNA. A Gln residue at position 8 can also directly contact U bases in the RNA, and together all of these amino acids play a crucial role in stabilizing the oligo-ribonucleotide within the binding pockets in the hexamer. The 5' A residue engages in similar interactions with Lys residues at position 41 and 57, which is suggested to allow discrimination of the binding pocket against the presence of C residues, explaining the observed preference of Hfq for binding to A/U-rich sequences (Zhang *et al.*, 1998, 2002; Sledjeski *et al.*, 2001; Schumacher *et al.*, 2002). Binding of Hfq to 5'-A(C)$_5$G-3' and 5'-A(G)$_6$-3' ribo-oligonucleotides and selected DNA oligonucleotides resulted in a significant loss of Hfq binding affinity, reaffirming the observation that Hfq is highly specific for binding A/U-rich RNA sequences (Schumacher *et al.*, 2002).

Based on the structure of Hfq, and the observation that Hfq can promote RNA/RNA interactions (Møller *et al.*, 2002b; Zhang *et al.*, 2002), a mechanism for Hfq/RNA binding has been proposed. Electrostatic interaction of the basic binding face of the Hfq hexamer likely aligns single-stranded RNA such that bases can insert within the binding pockets at the junction of each subunit, stabilizing the RNA on the face of the protein. This interaction may cause the RNA to wrap around a portion of the protein, and possibly through the hole in the hexamer, causing an opening of the local RNA secondary structure, facilitating subsequent intermolecular RNA:RNA interactions (Schumacher *et al.*, 2002). The finding that Hfq binding to *E. coli* OxyS untranslated regulatory RNA promotes an opening of a stem-loop in the RNA supports this model, although further

work is required to determine the exact mechanisms involved in the ability of Hfq to promote such interactions (Zhang *et al.*, 2002).

1.8 The Cpx two-component signal transduction system of *E. coli.*

The Cpx regulon was first identified by isolating mutations in the *Escherichia coli* chromosome that affected F conjugative plasmid expression and caused an inability to assemble F-pili on the surface of the cell (McEwen and Silverman 1980b). Conjugative pilus expression and transfer of the F-plasmid from donor to recipient *E. coli* cells requires the proteins encoded by the 33.3 kb *tra* operon of the F plasmid (reviewed in Frost, *et al.,* 1994). The major promoter of the *tra* operon, P_Y, is directly upregulated by the F regulatory protein, TraJ (Finnegan and Willetts 1972). Silverman *et al.,* (1993) observed that *cpxA* deletion mutants exhibited quasi-wild-type levels of F*lac* transfer. However, F*lac* transfer was decreased in some *cpxA* gain-of-function mutants, and the levels of TraJ protein and expression from a P_{traY}-*lacZ* fusion construct were also reduced, suggesting that activation of the Cpx system led to a lowered level of TraJ. Decreased levels of TraJ, therefore, most likely caused the impaired transfer ability of F in *cpxA* gain-of-function mutants.

Most *cpx* phenotypes have been associated with the cell envelope (McEwen and Silverman 1982; McEwen *et al.,* 1983), and subsequent work showed that the *cpx* regulon is controlled by a two-component signal transduction system, which senses and responds to cell envelope stress in *E. coli* (reviewed in Raivio and Silhavy, 2001). This system consists of the membrane-bound sensor kinase, CpxA, and its cognate cytoplasmic response regulator, CpxR (Figure 1.15; Weber and Silverman, 1988). CpxA localizes to the inner membrane, and contains transmembrane, cytoplasmic, and periplasmic domains

Figure 1.15 Schematic representation of the process of signal transduction in the CpxAR

two-component signal transduction pathway. "O.M." and "I.M." designate the outer

membrane and inner membrane, respectively, of the *E. coli* cell envelope. The Cpx

proteins are represented by block diagrams, and do not represent the true structures of the

proteins. The "P" in the diagram represents the transfer of a phosphate moiety from ATP

to CpxA, and then to CpxR, during the phosphotransferase signaling process. This

drawing is not to scale.
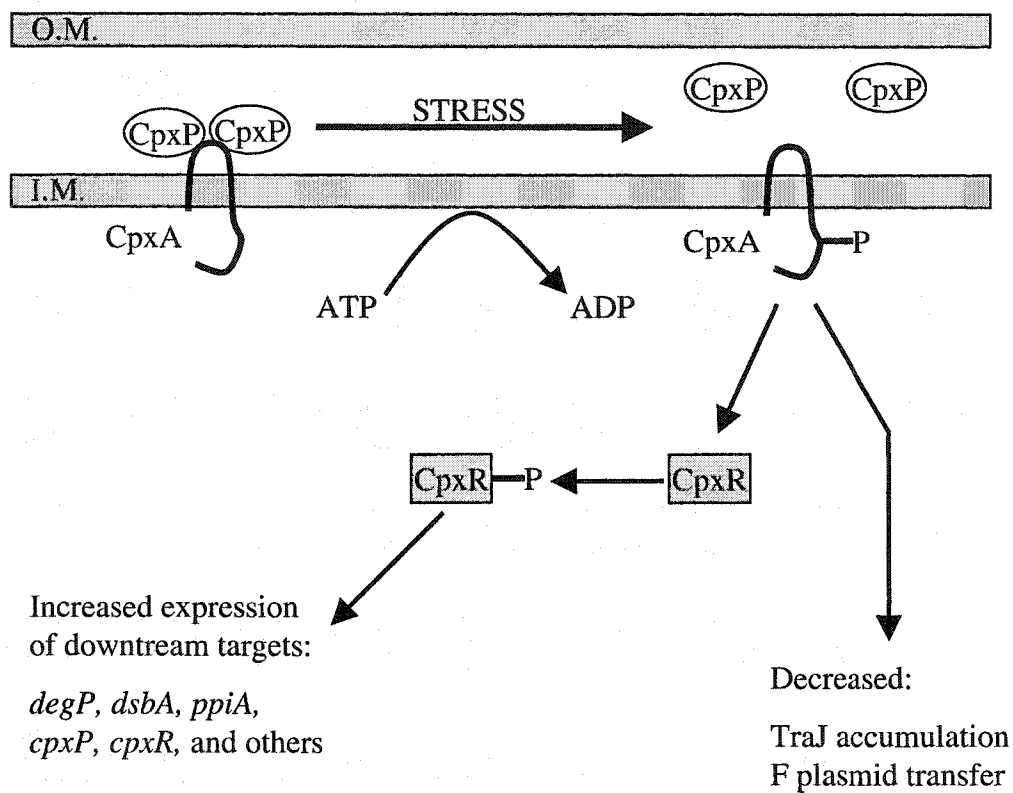
(Weber and Silverman, 1988). CpxA exhibits autokinase activity, and both kinase and phosphatase activity specific for CpxR (Raivio and Silhavy, 1997). CpxR is a cytoplasmic OmpR-like transcriptional activator (Dong *et al.*, 1993) which, when phosphorylated, binds target promoters at a consensus sequence (Figure 1.15; Pogliano *et al.*, 1997; De Wulf *et al.*, 1999). As is typical for such systems, the stress-inducing signal is transferred from CpxA to CpxR through a highly conserved phosphotransferase reaction (Hoch and Silhavy, 1995). The last component of the Cpx signal transduction pathway is a small periplasmic protein, CpxP (Figure 1.15; Danese and Silhavy, 1998). CpxP overexpression was found to suppress *cpx*-mediated gene expression, while inhibition of CpxP expression was found to have the opposite effect (Raivio *et al.*, 1999). Thus, in the absence of signaling cues, CpxP-mediated feedback inhibition is hypothesized to maintain the Cpx regulon in an "off state" via an interaction with CpxA that prevents CpxA autophosphorylation. Expression of *cpxAR* and *cpxP* is influenced by activated CpxA, demonstrating autoregulation of the *cpxAR* operon. The activity of the *cpx* regulon therefore appears to be subject to at least two levels of control (DeWulf *et al.*, 1999; Raivio *et al.*, 1999, 2000).

A variety of signals can activate the Cpx stress response, including overexpression of the outer membrane lipoprotein NlpE, (Snyder *et al.*, 1995), overexpression of misfolded P-pilus subunits (Jones *et al.*, 1997), and elevated pH (Nakayama and Watanabe, 1995), among others. Overproduction of NlpE and P-pilus subunits causes an increased level of misfolded proteins in the cell envelope, which is thought to be the main activating signal of the Cpx system (Raivio *et al.*, 2000) . Active, phosphorylated CpxR upregulates the transcription of several genes which are involved

in protein folding and degradation in the bacterial envelope (Danese *et al.*, 1995; Jones *et al.*, 1997; Dartigalongue and Raina, 1998). Examples of such Cpx-activated targets are the periplasmic protease DegP (Danese *et al.*, 1995; Pogliano *et al.*, 1997) and the periplasmic disulfide oxidase, DsbA (Danese and Silhavy, 1997; Jones *et al.*, 1997; Pogliano *et al.*, 1997).

cpxA* gain-of-function mutants were characterized by their ability to suppress the toxic effects of mislocalized and misfolded proteins in the cell envelope (Cosma *et al.*, 1995). *cpxA** mutants exhibit up to a ten-fold increase in expression of targets of the Cpx regulatory pathway (Danese *et al.*, 1995). *cpxA** mutations in the periplasmic, inner-membrane, and cytoplasmic domains have been characterized. One well-characterized class contains point or deletion mutations in the periplasmic sensing domain of the protein, which are believed to render CpxA "signal blind" (Raivio and Silhavy, 1997). The effect of this condition is constitutive activation of CpxA and thus upregulation of both the *cpxRA* operon and its downstream targets (Raivio *et al.*, 1999, 2000). A second well-characterized class of *cpxA** mutants contains point mutations in the cytoplasmic domain of CpxA. An example is *cpxA101**, which contains a single amino acid change from threonine to proline at position 253, located near the putative site for autophosphorylation (Raivio and Silhavy, 1997). This mutant retains its autokinase and kinase functions, but has lost its phosphatase activity. The result is elevated levels of active, phosphorylated CpxR, shifting the Cpx regulon to a constitutively active state (Raivio and Silhavy, 1997). *cpxA** mutants exhibit numerous and varied phenotypes, including resistance to amikacin (Rainwater and Silverman, 1990), sensitivity to elevated

temperatures (McEwen and Silverman, 1980a), and tolerance to elevated pH (Danese and Silhavy, 1998).

The *cpxA* mutation that was first shown to inhibit F transfer by Silverman and coworkers (Silverman *et al.*, 1993) was later identified as a relatively weak, constitutively activated gain-of-function mutation (Raivio and Silhavy, 1997). Chapter 6 presents evidence that the well-characterized *cpxA101** mutation, which results in strong, constitutive activation of the *cpx* regulon, results in a specific post-transcriptional reduction of the level of the F *tra* regulatory protein, TraJ.

1.9 Summary and research objectives.

The function of the FinOP system is to inhibit rapidly expression of the main activator of the F *tra* operon, the positive regulatory protein TraJ. FinP antisense RNA is susceptible to degradation by RNase E, and its intracellular concentration and its half-life are both increased by the protective action of the FinO RNA binding protein. FinO has a second function, to promote FinP/*traJ* mRNA duplex formation. By forming such a duplex, the RBS of *traJ* mRNA is blocked, preventing translation of the message and inhibiting TraJ accumulation. This function is analogous to the CopA/CopT replication control system of plasmid R1, where CopA antisense binding to CopT prevents translation of the RepA protein, which is required for replication of the plasmid. The ability of FinO to promote FinP/*traJ* mRNA duplex formation is also similar to the process of the facilitation of RNA I/RNA II duplex formation mediated by the ColE1 Rom protein. However, Rom only binds to a pre-formed kissing loop complex, while FinO binds both of its RNA targets separately. Nevertheless, FinO may, like Rom, facilitate duplex formation by stabilizing an initial kissing intermediate between its RNA

targets. The function of FinO may also be compared to the facilitation of RNA/RNA duplex formation by the *E. coli* Hfq RNA chaperone. Both proteins may facilitate RNA/RNA duplex formation via destabilization of the secondary structures present in the RNAs to which they bind. By examining various antisense RNA control systems and RNA binding proteins, one can propose that the FinOP system of F parallels many of the features of other systems. However many differences also exist between FinOP and other well-characterized systems, leading to the conclusion that FinOP is a rather unique system, whose mechanism of operation is becoming progressively better understood.

The primary goal of this thesis is to establish a better overall understanding of the regulation of F transfer control, specifically by examining different aspects of the FinOP system. The first objective was to perform a detailed analysis of the RNA binding domains of FinO, using purified native FinO derived from the F-like plasmid R6-5. FinP RNA transcribed *in vitro* was subjected to gel-shift analysis with wild-type FinO and several mutant derivatives, to determine the affinity of FinP binding by each protein. Deletions of multiple regions of FinO reveal that this protein contains two distinct FinP binding domains, one in the N-terminal region of the protein, and the second at the C-terminus. Analysis indicates that each of these domains can bind to FinP as separate entities, however high-affinity binding requires that both domains are present. Chapter 3 presents *in vitro* RNA binding studies that were used to make this determination.

The second goal of this thesis was to determine whether a specific domain of FinO was able to facilitate FinP/*traJ* mRNA duplex formation *in vitro*. Chapter 4 provides an analysis of the ability of FinO containing multiple deletion and point mutations to catalyze FinP/*traJ* mRNA duplex formation *in vitro*. Wild-type FinO was

determined to increase the rate of duplex formation by approximately sixty-fold compared to duplex formation in the absence of protein, as determined by *in vitro* gel-shift analysis and kinetic studies. The N-terminal 44 amino acids of FinO were determined to be required for this process. This region of FinO also contains double-stranded RNA unwinding ability, suggesting that the ability of FinO to unwind RNA and catalyze RNA/RNA duplex formation are linked. *In vivo* mating inhibition studies revealed that the ability of FinO to unwind double-stranded RNA and promote FinP/*traJ* mRNA duplex formation *in vitro* is also directly linked to its ability to inhibit F plasmid transfer.

The third objective was to determine the structural features of FinP and *traJ* mRNA that influence their progression into a duplex. The results of these studies are presented in Chapter 5. Multiple RNA constructs derived from FinP SL-I and *traJ* SL-Ic were synthesized *in vitro* and subjected to duplex formation assays in the presence and absence of FinO, in order to determine the association rate constants for duplex formation. The bulged nucleotides in the stems, the single-stranded loops, and the single-stranded tails of FinP SL-I and its complement in *traJ* mRNA were all found to influence duplex formation. It was determined that FinO can overcome a variety of structural changes to its RNA targets in order to facilitate RNA/RNA duplex formation. A transversion mutation in the anti-RBS in FinP, which reduced its complementarity with the RBS of *traJ* mRNA, was found to profoundly reduce the regulatory function of FinP. FinP containing this mutation was provided *in trans* at both medium and high copy number to complement a *finP*⁻ mutant F derivative. It was able to inhibit mating and TraJ accumulation, but only when supplied at high copy number, or when FinO was also

provided *in trans.* These results confirm the hypothesis that interaction between the RBS of *traJ* mRNA and the anti-RBS in FinP RNA is an important first step in promoting inhibition of *tra* operon expression.

The last goal of this thesis, presented in Chapter 6, was to determine specifically what effect a constitutive *cpxA** mutation had on F transfer. This mutation causes the CpxAR two-component signal transduction system to be turned on constitutively, mimicking constant envelope stress in the cell. Analysis of TraJ expressed from an F derivative plasmid determined that TraJ does not accumulate in such a mutant. Furthermore, the reduction of expression of TraJ was determined to be specific, and occurred at the post-transcriptional level. Preliminary analyses suggest that a cytoplasmic protein degradation pathway may be activated in *cpxA** mutants, leading to TraJ degradation.

Chapter 2: Materials and Methods

2.1 Bacterial strains, growth conditions, and transformation.

The *Escherichia coli* strains used in this study are listed in Table 2.1. The genotypes and sources of each strain are listed in the table. Standard genetic techniques were employed in construction of all strains (Silhavy *et al*, 1984). All liquid cultures were grown in trypticase soy broth (TSB; Becton Dickinson) or Luria-Bertani broth (LB; 1% Difco Tryptone, 0.5% Difco Yeast Extract, 1% NaCl), with appropriate antibiotic selection. All strains were grown at 37°C, except *cpx* mutant strains, which were grown at 30°C. Antibiotics (Sigma) were included at the following concentrations when required: ampicillin, 25 µg/mL; chloramphenicol, 50 µg/mL; kanamycin, 25 µg/mL; spectinomycin, 100 µg/mL; streptomycin, 200 µg/mL; tetracycline, 10 µg/mL; nalidixic acid, 40 µg/mL; amikacin, 3 µg/mL. Transformation of *E. coli* cells was performed using calcium chloride competent cells, unless indicated otherwise (Sambrook *et al.*, 1989).

2.2 Plasmids.

The plasmids used in this study and the relevant details and sources of each are listed in Table 2.2. Isolation of all plasmid DNA was performed using a rapid alkaline extraction technique as described (Birnboim and Doly, 1979). All clones constructed during the course of this work were sequenced using the DYEnamic ET fluorescent sequencing system according to the manufacturer's instructions (Amersham Pharmacia Biotech) to confirm that the correct DNA sequence was present in each clone. Sequence analysis was performed at the Molecular Biology Services Unit (University of Alberta) using an Applied Biosystems 373 DNA Sequencer. All restriction enzymes used for DNA cloning were purchased from Roche.

Table 2.1 *Escherichia coli* strains used in this study

Strain	Genotype or description	Reference
ED24	F⁻ *lac⁻* Spc^r	Achtman *et al.* (1971)
MC4100	F⁻ *araD139 Δ(argF-lac)U169 rpsL150*(Str^r) *relA1 flb5301 deoC1 ptsF25 rbsR*	Casadaban (1976)
XK1200	Nal^r F⁻ *lacΔU124 Δ(nadA araG gal attL)*	Moore *et al.* (1981)
TR8	MC4100 *cpxA::cam*	Raivio *et al.* (1999)
TR10	MC4100 *cpxA24**	Raivio, unpublished
TR20	MC4100 *cpxA101**	Raivio *et al.* (1999)
TR51	MC4100 *cpxR::spc*	Raivio *et al.* (1997)
TR189	MC4100 *cpxA101 zii::Tn10 λRS88[degP-lacZ]*	T. Raivio
TR981	MC4100 *cpxA101 zii::Tn10 λRS88[degP-lacZ] recA::kan*	T. Raivio
TR984	MC4100 *cpxA101 zii::Tn10 λRS88[degP-lacZ] clpP::cat ΔlonA rcs::kan*	T. Raivio
JMR201	MC4100 *degP::Tn10*	Reiss and Silhavy, unpublished
JC3272	F⁻ *lacΔx74 his trp lys* Tc^r Str^r	Achtman *et al.* (1972)
JC6255	F⁺ *trp lac* Str^s *sup⁺*	Achtman *et al.* (1972)
JCFL0	F*lac* wild-type in JC3272	Achtman *et al.* (1971)
JCFL1	F*lac traA1* in JC6255	Achtman *et al.* (1972)
JCFL2	F*lac traB2* in JC6255	Achtman *et al.* (1972)
JCFL8	F*lac traD8* in JC6255	Achtman *et al.* (1972)
JCFL14	F*lac traD14* in JC6255	Achtman *et al.* (1972)
JCFL81	F*lac traG81* in JC6255	Achtman *et al.* (1972)
JCFL90	F*lac traJ90* in JC6255	Achtman *et al.* (1972)

Table 2.2 Plasmids used in this study

Plasmid	Description	Reference
pOX38-Km	Km^r F *tra* region, Rep FIA replicon, 55 kb *Hin*dIII F fragment	Chandler and Galas (1983)
pOX38-Tc	Tc^r F *tra* region, Rep FIA replicon, 55 kb *Hin*dIII F fragment	Anthony *et al.* (1994)
pRS27	Tc^r 9 kb partial *Eco*RI F fragment in pSC101	Skurray *et al.*(1978)
pUC18	Ap^r general cloning vector, modified ColE1 replicon	Vieira and Messing (1982)
pT7-3	Ap^r general cloning vector, ColE1 replicon	Tabor and Richardson (1985)
pLT180	Ap^r pT7-3 derivative expressing wild-type FinP	Jerome (1999)
pUC180	Ap^r pUC18 derivative expressing wild-type FinP	Jerome (1999)
pUC180GGA	Ap^r pUC18 derivative expressing FinP(C16G/C17G/U18A)	This work
pLT180GGA	Ap^r pT7-3 derivative expressing FinP(C16G/C17G/U18A)	This work
pCR®4Blunt-TOPO®	General cloning vector	Invitrogen
pBAD24	Ap^r P$_{BAD}$ cloning vector	Guzman *et al.* (1995)
pBADTraJ	*traJ* coding region fused to P$_{BAD}$	This work
pBADTraM	*traM* coding region fused to P$_{BAD}$	Ryan Will, unpublished
pBADTraY	*traY* coding region fused to P$_{BAD}$	Janet Manchak, unpublished
pBR322	General cloning vector	New England Biolabs
pLD404	Ap^r NlpE in pBR322	Snyder at al.(1995)
pMC874	Km^r *lacZ$^+$* Δ*plac*	Casadaban *et al.* (1980)
pMCJ211	Km^r *traJΩlacZ* FinP$^+$ *traJ-lacZ* reporter plasmid	van Biesen and Frost (1994)
pSLF20	*finP$^-$* F derivative	Lee *et al.* (1992)
pLJ5-13	Ap^r *T7Φ10-finP* fusion in pUC19	Jerome *et al.* (1999)
pGEX-KG	IPTG-inducible GST fusion expression vector	Amersham Pharmacia Biotech
pGEX-FinO(1-186)	R6-5 wild-type *finO* in pGEX-KG	Ghetu *et al.* (1999)
pGEX-FinO(26-186)	R6-5 *finO* deletion fragment in pGEX-KG	Ghetu *et al.* (1999)
pGEX-FinO(45-186)	R6-5 *finO* deletion fragment in pGEX-KG	Ghetu *et al.* (1999)
pGEX-FinO(62-186)	R6-5 *finO* deletion fragment in pGEX-KG	Ghetu *et al.* (1999)
pGEX-FinO(1-61)	R6-5 *finO* deletion fragment in pGEX-KG	Ghetu *et al.* (1999)
pGEX-FinO(1-170)	R6-5 *finO* deletion fragment in pGEX-KG	Ghetu *et al.* (1999)

Table 2.2 continued

Plasmid	Description	Reference
pGEX-FinO(1-174)	R6-5 *finO* deletion fragment in pGEX-KG	Ghetu *et al.* (1999)
pGEX-FinO(62-170)	R6-5 *finO* deletion fragment in pGEX-KG	Ghetu *et al.* (1999)
pGEX-FinOT32A	R6-5 *finO* T32A in pGEX-KG	Ghetu *et al.* (2002)
pGEX-FinOP33A	R6-5 *finO* P33A in pGEX-KG	Ghetu *et al.* (2002)
pGEX-FinOP34A	R6-5 *finO* P34A in pGEX-KG	Ghetu *et al.* (2002)
pGEX-FinOK35A	R6-5 *finO* K35A in pGEX-KG	Ghetu *et al.* (2002)
pGEX-FinOW36A	R6-5 *finO* W36A in pGEX-KG	Ghetu *et al.* (2002)
pGEX-FinOK37A	R6-5 *finO* K37A in pGEX-KG	Ghetu *et al.* (2002)
pGEX-FinOV38A	R6-5 *finO* V38A in pGEX-KG	Ghetu *et al.* (2002)
pGEX-FinOK39A	R6-5 *finO* K39A in pGEX-KG	Ghetu *et al.* (2002)
pGEX-FinOK40A	R6-5 *finO* K40A in pGEX-KG	Ghetu *et al.* (2002)
pGEX-FinOQ41A	R6-5 *finO* Q41A in pGEX-KG	Ghetu *et al.* (2002)
pGEX-FinOK37A/V38A	R6-5 *finO* K37A/V38A in pGEX-KG	Ghetu *et al.* (2002)
pGEX-FinOK39A/K40A	R6-5 *finO* K39A/K40A in pGEX-KG	Ghetu *et al.* (2002)
pSn0104	Cm^r *finO*$^+$ pACYC184 derivative	Lee *et al.* (1992)
R100	IncFII F-like plasmid	Yoshioka *et al.* (1990)
Flac traG106	Frameshift mutation in *traG*	Achtman *et al.* (1972)

P_{BAD}-TraJ/M/Y overexpression plasmids were constructed using plasmid pRS27 (Table 2.2) as the template for PCR amplification. The *traJ* coding region of F was amplified by PCR using the upstream primer MGU8 to introduce a *Nco*I site, and the downstream primer MGU7 to introduce a *Pst*I site. Vent Polymerase (NEB) was used to generate the approximately 750 bp PCR product, which was inserted directly into the pCR®4Blunt-TOPO® cloning vector according to the manufacturer's instructions (Invitrogen). This plasmid was then digested with *Pst*I and *Nco*I, and the 750 bp *Pst*I/*Nco*I fragment was purified from a 0.8% (w/v) agarose gel using a QIAquick® Gel Extraction Kit (Qiagen) according to the manufacturer's instructions. The purified fragment was then inserted into *Pst*I/*Nco*I digested pBAD24 in-frame with P_{BAD}. pBADTraY was constructed using the same techniques, using the upstream primer LFR129 and the downstream primer LFR130 (J. Manchak, personal communication). pBADTraM was constructed using the same techniques, using the upstream primer RFE6 and the downstream primer SPE9, except the PCR product was gel purified as described above and cloned directly into appropriately digested pBAD24 (W. Will, personal communication).

The plasmid pUC180GGA (Table 2.2) was constructed to express FinP(C16G/C17G/U18A) from its own promoter in the high copy number vector pUC18. The plasmid pUC180 contains a 180 base *Eco*R1/*Hin*dIII fragment derived from F which encodes wild-type FinP, expressed from its own promoter (Jerome, 1999). This plasmid served as a template for site-directed mutagenesis of FinP using the mutagenic primers MGU53 and MGU54 (Table 2.3) and Pfu Turbo® (Stratagene) to create pUC180GGA. All procedures were performed according to the manufacturer's

Table 2.3 Primers used in this study. Base changes are underlined, and the T7 promoter sequence is in bold text.

Primer name	Primer Sequence(5′-3′)	Function
TvB14	CCTGAATAACTGCCGTCAG	PCR amplification of *traJ184*
TvB15	TCGAATTCTAATACGACTCACTATAGACGTGGTTAATGCCACG	PCR amplification of *traJ184*
JSA12	CGGTAGAGTTGCCCCTACTCCGGTTTTAG	tRNA^{ser} probe
LFR21	GAGGTTCCTATGTAT	FinP probe
MGU7	CTGCAGAATAATCAGAAAAGGT	TraJ PCR amplification
MGU8	CCATGGATCCGATGGATCGTAT	TraJ PCR amplification
RFE6	GGATCCATGGCTAAGGTGAACCTG	TraM PCR amplification
SPE9	GAATTCTTATTCATCATCATTTTTTG	TraM PCR amplification
LFR129	CGCGTCGACTAGAGTGTATTAAATGTTA	TraY PCR amplification
LFR130	GGCGGATCCATGGCAAAAGATTTGGTACACG	TraY PCR amplification
MGU53	CCATCGGATACATAGGAACCT<u>GGA</u>CACAAAGGATTCTATGGACAG	Mutagenic quick-change primer for creating FinP(C16G/C17G/U18A)
MGU54	CTGTCCATAGAATCCTTTGTG<u>TCC</u>AGGTTCCTATGTATCCGATGG	Mutagenic quick-change primer for creating FinP(C16G/C17G/U18A)
MGU5	TAATACGACTCACTATAG	Top strand of the consensus T7 RNA polymerase recognition sequence
MGU10	AAATATCGCCGATGCAGGGTCACGTGAACTCCCTGCATCGACTGTC**CTATAGTGAGTCGTATTA**	*In vitro* transcription template for SL-II 11 base loop
MGU11	AAAATCCAGCTACGTCCCAGTTCACGTGAGGGACGTAGCCGTGTC**CTATAGTGAGTCGTATTA**	*In vitro* transcription template for SL-IIcR 11 base loop
MGU12	TGTCCATAGAATCCTTTGTGAGGAGGTTCCTATGTATCCTATAGTGAGTCG**TATTA**	*In vitro* transcription template for wild-type SL-I
MGU13	TGTCGTATCCTTGGACCTCACAATCCTAAGATACTATCC**TATAGTGAGTCGTATTA**	*In vitro* transcription template for wild-type SL-IcR
MGU14	GATACATAGGAACCTCCTCACAAAGGATTCTATGGACA**CTATAGTGAGTCGTATTA**	*In vitro* transcription template for wild-type SL-Ic
MGU15	GACAGTCGATGCAGGGAGTTCACGTCTCCCTGCATCGGCGATTTT**CCTATAGTGAGTCGTATTA**	*In vitro* transcription template for wild-type SL-IIc

Table 2.3 continued

Primer name	Primer Sequence(5'-3')	Function
MGU16	AAAATCGCCGATGCAGGGAGACGTGAACTCCCTGCATCGACTGTCCTATAG TGAGTCGTATTA	*In vitro* transcription template for wild-type SL-II
MGU17	TGTCCATAGAA<u>A</u>CCTTTGTGAGGAGGTTCCTATGTATCCTATAGTGAGTCG TATTA	SL-I(A27U)
MGU18	GATACATAGGAACCTCCTCACAAAGG<u>T</u>TTCTATGGACACTATAGTGAGTCG TATTA	*In vitro* transcription template for SL-Ic(U85A)
MGU45	CATAGG<u>TTGGA</u>CCTCACAA<u>TCCTA</u>TCTATGCTATAGTGAGTCGTATTA	*In vitro* transcription template for SL-Ic(TSR)
MGU46	<u>GTATCC</u>AACCTCCTCACAAAGGAT<u>AGATAC</u>CTATAGTGAGTCGTATTA	*In vitro* transcription template for SL-Ic(BSR)
MGU41	TGTCCATAGAATCCTTTGTG<u>TCC</u>AGGTTCCTATGTATCCTATAGTGAGTCGT ATTA	*In vitro* transcription template for SL-I(C16G/C17G/U18A)
MGU28	TGTCCATAGAATCCTTT<u>CACT</u>GGAGGTTCCTATGTATCCTATAGTGAGTCG TATTA	*In vitro* transcription template for SL-I(U18A/C19G/A20U/C21G)
MGU44	TGTCCATAGAATCCT<u>AAC</u>TGAGGAGGTTCCTATGTATCCTATAGTGAGTCG TATTA	*In vitro* transcription template for SL-I(C21G/A22U/A23U)
MGU24	CATAGGAACCTCCTCACAAAGGATTCTATGCTATAGTGAGTCGTATTA	*In vitro* transcription template for SL-Ic(Δtails)
MGU22	GATACATAGGAACCTCCTCACAAAGGATTCTATGCTATAGTGAGTCGTATT A	*In vitro* transcription template for SL-Ic(Δ5'tail)
MGU20	CATAGGAACCTCCTCACAAAGGATTCTATGGACACTATAGTGAGTCGTATT A	*In vitro* transcription template for SL-Ic(Δ3'tail)
MGU23	CATAGAATCCTTTGTGAGGAGGTTCCTATGCTATAGGTAGTCGTATTA	*In vitro* transcription template for SL-I(Δtails)

instructions (Stratagene), except the plasmid was transformed into rubidium chloride competent *E. coli* DH5α to propagate the DNA (Sambrook *et al.*, 1989). The presence of the mutation was confirmed by sequencing as described above. pLT180GGA was created by inserting the 180 base *Eco*R1/*Hind*III fragment containing FinP(C16G/C17G/U18A) from pUC180GGA into similarly digested pT7-3 (Tabor and Richardson, 1985), allowing this mutant FinP antisense RNA to be expressed from its own promoter in a medium copy number plasmid. All pGEX-FinO plasmids were constructed by Dr. Alex Ghetu as described in Ghetu *et al.* (1999, 2002).

2.3 Mating assays of various *cpx* mutant strains.

Donor strains containing pOX38-Km and the recipient strain XK1200 were grown in 2 mL LB at 30°C or 37°C with appropriate antibiotic selection to an OD_{600} of 0.6-1.0, and 1 mL of each donor culture was pelleted by centrifugation and resuspended in 0.9 mL fresh LB to remove antibiotics. An aliquot of 0.1 mL of recipient cells (XK1200) was added and mating was allowed to proceed for 45 minutes at 30°C or 37°C without shaking. Mating mixtures were vortexed vigorously for 30 seconds and placed on ice to disrupt mating pairs, and 10-fold serial dilutions (1 mL) were made in ice-cold 1X phosphate buffered saline (PBS; 137 mM NaCl, 2.7 mM KCl, 4.3 mM $Na_2HPO_4 \cdot 7\ H_2O$, 1.4 mM KH_2PO_4). Ten μL of each dilution was inoculated onto selective plates to select donors and transconjugants. Donor strains were selected on LB agar plates containing 200 μg/mL streptomycin and 25 μg/mL kanamycin. Transconjugants were selected on LB agar plates containing 40 μg/mL nalidixic acid and 25 μg/mL kanamycin. Plates were incubated overnight at 30°C or 37°C and donor and transconjugant colonies were counted. The ratio of transconjugants:donors was used as a measure of efficiency of

transfer of pOX38-Km from donors to recipients. Comparing this ratio of the mutants tested to that of wild-type MC4100 then allowed comparison of relative mating efficiencies among the strains tested.

2.4 Mating assays to determine the ability of various FinO deletions and a FinP mutant to inhibit F plasmid transfer.

Donor MC4100 cells containing pOX38-Km alone, pOX38-Km and pGEX-KG, or pOX38-Km and any one of the pGEX-FinO plasmids (Table 2.2) were grown in 2 mL TSB, containing the appropriate antibiotics, at 37°C with agitation to an OD_{600} of 0.5-0.9. Expression of the various pGEX-FinO fusion proteins in the cells was confirmed by Western blot analysis as described in section 2.5 using monoclonal anti-GST antibodies (Sigma). Aliquots of cells equivalent to 0.5 OD_{600} units were collected, pelleted by centrifugation, and resuspended in 0.5 mL fresh TSB to remove the antibiotics. *E. coli* ED24 cells to be used as recipients for conjugative transfer of pOX38-Km were grown in TSB at 37°C without antibiotic selection to an OD_{600} of 0.5-0.9. One hundred μL of donor cells were mixed with 100 μl of recipient cells and 0.8 mL of fresh TSB, mixed, and incubated without shaking at 37°C for 30 minutes to allow mating to occur. The mating mixtures were then vortexed vigorously for 20 seconds and immediately placed on ice to disrupt mating pairs. Ten-fold serial dilutions of the mating mixtures were performed in 1 mL total volumes using ice-cold 1x SSC (150 mM NaCl, 15 mM Na-citrate, pH 7.0). Ten μL of each dilution was plated on the following selective media. Donor MC4100 cells containing pOX38-Km alone were selected on TSB agar plates containing 25 μg/mL kanamycin and 200μg/mL streptomycin, and donor MC4100 cells containing pOX38-Km and any of the pGEX-FinO plasmids were selected on TSB agar

plates containing 25 µg/mL each kanamycin and ampicillin, and 200 µg/mL streptomycin. All transconjugants were selected on TSB agar plates containing 25 µg/mL kanamycin and 100 µg/mL spectinomycin. All plates were incubated at 37°C overnight. Donor and transconjugant cells were then counted, and the ratio of transconjugants to donors was calculated, allowing mating efficiency to be compared with the control of conjugal transfer of pOX38-Km alone, which was set at 100% mating efficiency.

To test for the inhibitory function of mutant FinP(C16G/C17G/U18A) provided *in trans* at both high and medium copy number, the *finP⁻ Flac* plasmid pSLF20 (Lee *et al.*, 1992) was transformed into *E. coli* MC4100. The control plasmids pUC18 or pT7-3 were introduced, with or without plasmid pSn0104 (Table 2.2; Lee *et al.*, 1992) which expresses plasmid R6-5 FinO *in trans*. The test plasmids pUC180, pUC180GGA, pLT180, or pMG180GGA (Table 2.2) were also introduced into MC4100 containing pSLF20, with or without pSn0104. Mating assays were performed essentially as described above using *E. coli* ED24 as the recipient strain, to test for the ability of wild-type FinP and FinP(C16G/C17G/U18A), provided *in trans* in both medium and high copy number, to complement the *finP⁻* mutation and restore fertility inhibition to pSLF20. Donors containing pSLF20 alone were selected on Maconkey-Lactose plates (Difco) containing 200 µg/mL streptomycin. Donors containing pSLF20 and any one of the plasmids pUC18, pT7-3, pUC180, pUC180GGA, pLT180, or pMG180GGA were selected on Maconkey-Lactose plates containing 200 µg/mL streptomycin and 5.0 µg/mL ampicillin. All donor constructs containing pSn0104 were selected on Maconkey-Lactose plates to which chloramphenicol was added to a final concentration of 50 µg/mL, in addition to the other antibiotics listed above. All transconjugants were selected on L1-

spectinomycin plates (Lee *et al.*, 1992) or Maconkey-Lactose plates containing spectinomycin.

2.5 Western immunoblot analysis.

Unless otherwise indicated, cell pellets corresponding to 0.1 OD_{600} equivalents were used in immunoblot assays. Samples were boiled in SDS sample buffer (Laemmli, 1970) for 5 minutes and then centrifuged at 14,000 rpm/4°C for approximately 5 minutes. The supernatants were then electrophoresed on 15% (29:1) SDS polyacrylamide gels using the Bio-Rad Mini-Protean® system. Proteins were transferred to Immobilon-P membranes (Millipore) at 100 V for 1 hour at 4°C using transfer buffer (25 mM Tris-HCl, 192 mM glycine, 20% (v/v) methanol, 0.004% (w/v) SDS) (Towbin *et al.*, 1979). Membranes were blocked overnight at 4°C with 10% (w/v) skim milk (Difco) dissolved in TBST (50 mM Tris-HCl pH7.5, 150 mM NaCl, and 0.1% (v/v) Tween-20 (Caledon Laboratories)). Primary antibodies diluted in 10% skim milk in TBST were added to blots and incubated for 1 hour at room temperature. The following dilutions of polyclonal antisera (raised in rabbits) were used: anti-FinO, 1:50,000; anti-TraJ, 1:15,000; anti-TraM, 1:5000; anti-TraY, 1:2000. Monoclonal anti-GST antibodies (Sigma) were used at a 1:10,000 dilution. Blots were washed at room temperature 4 times for 15 minutes each time with TBST. The secondary antibody used was HRP-conjugated donkey anti-rabbit IgG (Amersham Life Sciences) at a 1:10,000 dilution. Blots were incubated for 1 hour at room temperature with the secondary antibody, and then washed as described above. Blots were developed with Renaissance Western Blot Chemiluminescence Reagent Plus (Perkin Elmer) and exposed to Kodak X-Omat R film for varying times to visualize the signals.

2.6 Stability of TraJ, TraM, and TraY expressed from pBAD overexpression vectors in various *cpx* backgrounds.

Cultures of various *E. coli cpx* mutants containing the arabinose-inducible plasmids pBADTraJ/TraM/TraY (Table 2.2) were grown at 30°C in TSB supplemented with 1.0% (w/v) glucose and appropriate antibiotics to an OD_{600} of 0.6-0.9. Pre-induction samples (0.1 OD_{600} equivalents) were collected, and these and all subsequent samples were stored at −20°C until required. Two mL of the pre-induction cultures were centrifuged and washed twice with 1 mL fresh TSB to remove antibiotics and glucose. Arabinose (0.1% (w/v)) in 2 mL fresh TSB was added to induce expression of the *tra* proteins from the P_{BAD} plasmids, and induction was carried out at 30°C for 50 minutes with agitation. The 0 time sample was collected, and the induced culture was centrifuged and washed twice with 1 mL fresh TSB to remove the arabinose. Two mL of fresh TSB containing 1.0% (w/v) glucose and 200 μg/mL rifampicin (Sigma) was added to prevent further expression from P_{BAD}. Samples were collected at 15, 30, 60, and 120 minutes post-induction, and subjected to immunoblot analysis as described in section 2.5.

2.7 Northern analysis to detect total amounts of *traJ* mRNA and FinP antisense RNA expressed in various *cpx* mutant strains.

Strains were grown in 10 mL liquid cultures (TSB) with appropriate antibiotic selection to an OD_{600} of 0.8-1.0. Samples (1.5 mL) were collected and the cells pelleted by centrifugation. Three hundred μL of lysis buffer (0.5% SDS, 10 mM Tris-HCl pH 7.5, 1 mM EDTA) was used to resuspend the cells, and then 300 μL of Tris-saturated phenol was added, and the mixtures were incubated at 65°C for 10-15 minutes with occasional 15 second periods of vortexing. The phases were separated by centrifugation at 14,000

rpm, 4°C, for 15 minutes. The aqueous phase was removed to a fresh tube, and extracted twice with an equal volume of chloroform, followed by a 2 minute spin at 14,000 rpm in a microfuge. The aqueous phase was then removed to a fresh tube, and the RNA precipitated with 3 M sodium-acetate and 1.5 volumes of 95% ethanol on dry ice for 10 minutes, followed by a 10 minute centrifugation at 14,000 rpm, 4°C. The RNA pellets were washed twice with ice-cold 70% ethanol to remove excess salt, and the RNA was dissolved in 40 μL DEPC-treated sterile Milli-Q® water. The RNA concentration was determined by A_{260} measurement in a Bio-Rad Smartspec 3000. RNA (40μg) was denatured for 5 minutes at 95°C in 2x RNA loading dye (96% (v/v) deionized formamide, 0.05% (w/v) each bromophenol blue and xylene cyanol, 20 mM EDTA). Samples were electophoresed on an 8%(29:1)/8M urea polyacrylamide gel at 250 V, and the RNA was transferred to Zeta-Probe nylon membranes (Bio-Rad) at 20 V for 1 hour at 4°C in a Bio-Rad Semi-dry transfer apparatus, and crosslinked to the membrane at 150 mJoules in a Bio-Rad GS Gene-linker. Blots to be probed for *traJ* were prehybridized at 58°C for 4 hours in: 50% (v/v) deionized formamide, 5x Denhardt's (100x Denhardt's contains 20 mg/mL each polyvinylpyrrolidone, Ficoll 400, and bovine serum albumin), 2.5x SSC (1x SSC contains 150 mM NaCl, 15 mM Na-citrate, pH 7.0), 1.5% (w/v) SDS, and 200 μg/mL each of boiled *E. coli* Strain W tRNA Type XX and sonicated calf thymus DNA (Sigma). Approximately 10 pmol of FinP RNA uniformly-labeled with $\alpha[^{32}P]$-UTP (NEN) was prepared as described in section 2.9 and added along with fresh hybridization buffer to the blots and incubated overnight at 58°C. Blots were washed at room temperature as follows: 2x SSC for 5 minutes, 2x SSC/0.1% SDS for 10 minutes, 0.5x SSC/0.1% SDS for 10 minutes. A final wash at 55°C was done in 0.1x SSC/0.1% SDS

for 5 minutes, and the blots were exposed on a Molecular Dynamics Storage Phosphor Screen. Blots were stripped at 70°C in 5mM Tris-HCl pH8, 2mM EDTA, 0.1x Denhardt's, and 0.1% SDS for 4 hours. Stripped blots were prehybridized at 37°C for 4 hours in: 2.5x SSC, 0.5% SDS, 5x Denhardt's, 90 mM Tris-HCl pH7.5, 0.9 M NaCl, 6 mM EDTA, and 200 µg/mL each boiled *E. coli* Strain W tRNA Type XX and sonicated calf thymus DNA. The tRNA^{ser}-specific oligonucleotide probe JSA12 (Table 2.3; Sandercock and Frost, 1998) and the FinP-specific probe LFR21 (Table 2.3; Jerome *et al.*, 1999) were 5' end labeled with $\gamma[^{32}P]$-ATP (NEN) and T4 polynucleotide kinase (Roche), and purified through mini Quick Spin Oligo columns (Roche) to remove unincorporated $\gamma[^{32}P]$-ATP. Approximately 10 pmol of each probe was added to the blots in fresh hybridization solution, incubation proceeded overnight at 37°C, and washing was carried out as described above. Bands corresponding to the *traJ* and FinP transcripts and tRNA^{ser} were detected and quantified using a Molecular Dynamics Phosphorimager 445 SI and ImageQuaNT™ software.

2.8 Northern analysis to determine FinP half-life in the presence of various FinO deletion proteins.

MC4100 strains containing pOX38-Km alone or with various pGEX-FinO derivative plasmids were grown with appropriate antibiotic selection in 10 mL TSB at 37°C with agitation to an OD$_{600}$ of 0.7-1.0. A 1.5 mL sample was taken at time 0, and the cells were pelleted by centrifugation and immediately frozen on dry ice until ready for processing. Rifampicin (Sigma) was added to the remaining 8.5 mL of culture to a final concentration of 200 µg/mL to prevent further rounds of transcription and the cultures were incubated at 37°C without agitation. Samples (1.5 mL) were collected at timed

intervals after rifampicin addition, pelleted, and frozen on dry ice until ready for processing. Total RNA isolation, electrophoresis, and transfer was performed as described in section 2.7. Approximately 10 pmol of the FinP-specific probe LFR21 (Table 2.2) were added to the blots in fresh hybridization buffer (section 2.7), and the blots were incubated overnight at 37°C. Blots were washed as described in section 2.7, and exposed overnight on a Molecular Dynamics Storage Phosphor Screen. Blots were then stripped and reprobed with the tRNA^{ser}-specific oligonucleotide probe JSA12 as described in section 2.7. Bands corresponding to FinP and tRNA^{ser} were detected and quantified using a Molecular Dynamics Phosphorimager 445 SI and ImageQuaNT™ software. The signal obtained from tRNA^{ser} was used to normalize the signal obtained from FinP, allowing the FinP half-life to be determined by plotting the amount of FinP remaining against the time each sample was taken after the addition of rifampicin to the culture.

2.9 *In vitro* transcription of FinP.

Approximately 2 μg of *Bam*HI linearized pLJ5-13 plasmid DNA (Table 2.2) was used as the template for T7 *in vitro* run-off transcription reactions, which were performed in a total volume of 20 μL. The presence of the *Bam*HI site resulted in the addition of 7 extra bases, 5'-(G)$_4$AUC-3', at the 3' end of FinP (Jerome and Frost, 1999). GTP, ATP, and CTP were each added to a final concentration of 0.5 mM, and UTP was added to a final concentration of 0.02 mM. One to fifty μCi of α[^{32}P]-UTP (3000 Ci/mmol; Perkin Elmer) was added for labeling. Twenty-six U of RNA Guard (Pharmacia) was added to each reaction (Pharmacia), along with 1x transcription buffer (Roche; 400 mM Tris-HCl, pH8.0, 6 mM MgCl$_2$, 10 mM DTT, 2mM spermidine). Twenty U of T7 RNA polymerase

(Roche) were added, and reactions were incubated at 37°C for approximately 2 hours. Ten U of DNase-I (RNase-Free, Roche) were added and the reactions were incubated for a further 15 minutes. One μL samples were taken for scintillation counting ("pre-cpm"). Ten μL of 2x RNA loading dye (96% deionized formamide, 0.05% each xylene cyanol and bromophenol blue, 20 mM EDTA) were added to the reactions, mixed, and then heated to 90°C for 5 minutes and immediately chilled on ice. The reactions were electrophoresed on an 8%(29:1)/8M urea polyacrylamide gel at 250 V for approximately 2 hours. Radioactive bands were then visualized using Kodak X-Omat R film, excised from the gel, crushed, and eluted overnight in 300 μL elution buffer (0.5 M ammonium acetate, 0.1 mM EDTA) at 37°C with vigorous shaking. Polyacrylamide was pelleted by centrifugation at 14,000 rpm, and the supernatants were removed and extracted once using an equal volume of a 1:1 mixture of phenol:chloroform followed by an extraction with an equal volume of chloroform. The aqueous phase was removed to a fresh tube, and the RNA was precipitated using 2 μg glycogen (Roche), 0.1 volume 3 M sodium-acetate, and 1.5 volumes of 95% ethanol on dry ice for 10 minutes, followed by centrifugation at 14,000 rpm for 10 minutes. The precipitated RNA pellet was then washed twice with ice-cold 70% ethanol to remove excess salt. RNA was dried under vacuum for no more than 2 minutes, and then dissolved in 10 μL of DEPC-treated sterile Milli-Q® water. One μL was subjected to scintillation counting ("post-cpm") and used to calculate the yield of RNA as follows:

Specific activity (S.A.)= $(\text{pre-cpm})(V_{total})/\text{pmol UTP in reaction}$

pmol RNA/μL = $(\text{post-cpm})/(\text{S.A.})(\#\text{Uridine residues in RNA molecule})$

2.10 *In vitro* transcription of *traJ184* mRNA.

The DNA template for *traJ184* mRNA transcription was generated by PCR amplification of the *traJ* gene from plasmid pRS27 (Table 2.1) using the primers TvB 14 and TvB 15 (Table 2.2). This template results in the expression of the first 184 bases of the 5′ untranslated region of *traJ* mRNA after *in vitro* transcription (Jerome and Frost, 1999). The PCR product was purified by electrophoresis on an 8%(29:1)/8 M urea polyacrylamide gel followed by excision, elution, and purification as described in section 2.9. Approximately 2 µg of the purified template was used in an *in vitro* transcription reaction. To make [^{3}H]-labeled *traJ184* mRNA, all procedures were the same as those for FinP (section 2.9), except 10 µCi of 5,6-[^{3}H]-UTP (Perkin Elmer) were included in the reactions in place of α[^{32}P]-UTP. [^{32}P]-labeled *traJ184* mRNA was used as a marker to locate the [^{3}H]-*traJ184* mRNA bands in the gel. Bands were excised from the gel and purified and quantified exactly as described for FinP in section 2.9. To make cold *traJ184* mRNA, all procedures were the same except GTP/ATP/CTP/UTP were added to the transcription reaction at a final concentration of 0.5 mM. RNA was purified as described in section 2.9 except bands were visualized by ethidium bromide staining, and RNA concentration was determined by UV absorbance at 260 nm in a Bio-Rad Smartspec 3000.

2.11 Preparation of oligonucleotide *in vitro* transcription templates and *in vitro* transcription of FinP and *traJ184 mRNA* stem-loop derivatives.

DNA oligonucleotide *in vitro* transcription templates were synthesized at the Molecular Biology Services Unit (Dept. of Biological Sciences) using an Applied Biosystems DNA/RNA 392 Synthesizer unit. The oligonucleotide template strands

(Table 2.3) were dissolved in DEPC-treated sterile Milli-Q® water, and 30 µL of formamide load dye was added. The mixture was heated to 95°C for approximately 5 minutes, cooled on ice, and then electrophoresed on a 10%(29:1)/8M urea polyacrylamide gel at 300 V for approximately 3 hours. This procedure ensured that only fully formed oligonucleotides of the correct size were purified to homogeneity. Bands were visualized by ethidium bromide staining, and then excised, crushed, eluted overnight in 300 µL elution buffer, and purified as described in section 2.9. The DNA was dried under vacuum for 5 minutes, and then dissolved in 50 µL of DEPC-treated sterile Milli-Q® water. The DNA concentration was determined by UV absorbance at 260 nm in a Bio-Rad Smartspec 3000. One and one-half pmol of the template strand were mixed with a 1.5x molar excess of the consensus T7 promoter top strand oligonucleotide MGU5 (Table 2.3), in a total volume of 50 µL containing $MgCl_2$ at a final concentration of 100 mM. The mixtures were heated to 95°C for 5 minutes and then cooled slowly to room temperature over 1 hour and 45 minutes to anneal the template oligonucleotide and MGU5 oligonucleotide. Annealed templates were used immediately, or stored at -20°C with no detectable loss of function over several weeks. A final template concentration of 300 nM was used in transcription reactions with a final volume of 20 µL. For synthesizing [^{32}P]-labeled RNAs, GTP, ATP, CTP were each added to a final concentration of 2.5 mM, and UTP was added to a final concentration of 0.1 mM, along with 10-50 µCi of α[^{32}P]-UTP (3000 Ci/mmol; Perkin Elmer). Twenty-six U of RNA Guard (Pharmacia) were added to each reaction, along with 1x transcription buffer (Roche) supplemented with 0.01% Triton X-100 (Sigma) and 0.1 mg/mL Bovine Serum Albumin (RNase-Free; Roche). Twenty U of T7 RNA polymerase (Roche) were added,

and the reactions were incubated at 37°C for approximately 2 hours. Ten U of DNaseI (RNase-Free, Roche) were added and the reactions were incubated for a further 15 minutes. One μL samples were taken for scintillation counting. Ten μL of 2x RNA loading dye were added, and the reactions were mixed, heated to 90°C for 4 minutes, and then immediately cooled on ice. The reactions were electrophoresed on 10%(29:1)/8M urea polyacrylamide gels at 250 V for approximately 2 hours. Radioactive bands were then visualized using Kodak X-Omat R film, and excised, eluted and purified as described in section 2.9. A 1 μL aliquot was subjected to scintillation counting and used to calculate the yield of RNA as described in section 2.9. To make cold RNA, all procedures were the same except GTP/ATP/CTP/UTP were added to the transcription reaction at a final concentration of 2.5 mM. RNA was purified as described above except bands were visualized by ethidium bromide staining, and the RNA was dissolved in 50 μL sterile DEPC-treated Milli-Q® water after purification. RNA concentration was determined by UV absorbance at 260 nm in a Bio-Rad Smartspec 3000. It should be noted that all of the RNAs produced using this method contain an extra G residue on their 5' ends, because the transcription start site (+1) is the last G residue in the T7 promoter sequence (Table 2.3; Milligan *et al.*, 1987; Lopez *et al.*, 1997).

2.12 Gel-shift analysis of FinO and various FinO deletion derivatives binding to FinP

Seven and one half fmol of [^{32}P]-FinP as prepared in section 2.9 were incubated with increasing amounts of FinO protein derivatives in separate reactions. The total reaction volume was 30 μL, and contained 1x TEBN buffer (50 mM Tris-HCl pH8, 1 mM EDTA, 100 mM NaCl, 2.0 mM DTT, 10% glycerol, 3.0 μg RNase-Free BSA

(Roche)) supplemented with 7.6 units of RNAguard (Pharmacia). Reactions were incubated at 4°C for 30 minutes. In competition assays, a 1000-fold molar excess of *E. coli* Strain W tRNA Type XX (Sigma) was added to the reaction and incubated for 5 minutes at 4°C prior to the addition of protein. Reactions were loaded onto continuously running 5% or 8%(29:1) polyacrylamide gels and electrophoresed at 150 V for 1 hour at 4°C. Tris-Glycine buffer (25 mM Tris-HCl, 0.19 M glycine, pH8-8.3) was used in the gel and running buffer. Gels were dried and then exposed on a Molecular Dynamics Storage Phosphor Screen for at least 10 hours. Free FinP and FinO/FinP complexes were visualized and quantified using a Molecular Dynamics Phosphorimager 445 SI and ImageQuaNT™ software. The equilibrium association constant (k_a) for FinO:FinP binding was determined from the amount of protein in a given reaction that caused 50% of the labeled FinP present to be shifted in the gel (van Biesen and Frost, 1994; Ghetu et al, 1999). The following schematic diagram represents the equilibrium binding reaction:

$$\text{Protein } [P]_o + \text{RNA } [R] \Leftrightarrow \text{RNA-protein complex } [P\text{-}R]$$

Where: $K_a = [P\text{-}R]/[P]_o[R]$

When 50% of the RNA is in an RNA-protein complex, [P-R]=[R], therefore the k_a can be calculated as:

$$K_a = 1/[P]_o$$

where $[P]_o$ is the concentration of protein (FinO or derivative) initially added to the reaction. In cases where more than one shifted band was present, all shifted bands were considered to represent a single species.

2.13 FinP/*traJ184* mRNA duplex assays

All RNAs used in these assays were diluted to their final working concentrations in sterile DEPC-treated Milli-Q® water, then heated to 90°C for 4 minutes and immediately snap-frozen in a dry-ice/ethanol bath for approximately 2 minutes. The RNAs were then thawed until they reached room temperature (approximately 30-40 minutes), and incubated at 4°C for approximately 60 minutes. The RNA was used immediately or stored at –20°C for no longer than 5 days. Seven and one half fmol (0.15 nM) of [^{32}P]-FinP were incubated with a 10-fold molar excess of [^{3}H]-*traJ184* mRNA in the presence or absence of 1 μM of wild-type FinO or one of several FinO deletion mutants. The total reaction volume was 50 μL, and contained 1x TMEB buffer (25 mM Tris-HCl pH 8, 4 mM Mg-acetate, 0.4 mM EDTA, 40 mM NaCl, 40 μg/mL BSA, 0.3 units/mL RNAguard). In some cases a 2- to 5-fold molar excess of *traJ184* mRNA was added to give measurable rates of duplex formation. Reactions containing all of the constituents except the RNAs were pre-incubated at 37°C for approximately three minutes. The premixed RNAs were added, and incubation was allowed to proceed at 37°C. Aliquots (5 μL) were removed at various times and mixed immediately with 10 μL ice-cold stop buffer (95% formamide, 10 mM EDTA, 0.05% each xylene cyanol and bromophenol blue), and kept on ice. Reactions were electrophoresed at room temperature at 150 V for 75 minutes on 8%(29:1) native polyacrylamide gels using 1x Tris-Glycine buffer in the gel and running buffer. Gels were dried and exposed on a Molecular Dynamics Storage Phosphor Screen. Free FinP and FinP/*traJ184* mRNA duplexes were visualized and quantified using a Molecular Dynamics Phosphorimager 445 SI and ImageQuaNT™ software. The apparent second-order association binding rate constant

for FinP/*traJ* mRNA duplex formation (k_{app}) was determined from plots of the log value of the % of free [^{32}P]-FinP remaining versus the time the sample was taken.

The reaction is represented as:

$$k_1 \quad FinP + traJ184 \Leftrightarrow FinP/traJ184$$
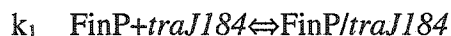
Because there was an excess of the unlabeled RNA, *traJ184*, pseudo-first-order kinetics were obtained (van Biesen *et al.*, 1993). The pseudo-first-order rate constant, k_1' can then be calculated from $t_{1/2}$, the time required (in seconds) for 50% of the labeled RNA, FinP, to form a duplex with the unlabeled RNA in excess (Persson *et al.*, 1988):

$$k_1' = \ln2/t_{1/2}$$

The second-order rate constant can then be calculated from the following:

$$k_{app} = k_1'/[traJ184]$$

In cases where more than one shifted band was present, all shifted bands were considered to represent a single species.

2.14 Duplex assays of SL-I and SL-II, and their various derivatives

All RNAs used in these assays were diluted to their final working concentrations in DEPC-treated sterile Milli-Q® water, then heated, chilled, and thawed as described in section 2.13. Thirty to sixty fmol (0.6-1.2 nM) of [^{32}P]-labeled SL-I and SL-II or their various mutant derivatives were mixed with a 10- to 50-fold molar excess of their unlabeled complementary RNAs. In reactions containing FinO, the purified protein was added to a final concentration of 1 µM (reactions containing SL-II) or 6 µM (reactions containing SL-I or SL-I mutant derivatives). The final reaction volume was 50 µL, and contained 1x TMN buffer (20 mM Tris-HCl, 10 mM Mg-acetate, 100 mM NaCl). Reactions containing all constituents except the RNAs were pre-incubated at 37°C for

approximately three minutes. The premixed RNAs were then added, and the reactions were further incubated at 37°C. Aliquots (5 μL) were removed at various times and mixed immediately with 10 μL of ice-cold stop buffer (1x TMN containing 30% glycerol, 0.05% bromophenol blue), and kept on ice. Reactions were electrophoresed at room temperature at 160 V for 65 minutes on 8%(29:1) native polyacrylamide gels using 1x Tris-Glycine buffer in the gel and running buffer. Gels were dried and exposed on a Molecular Dynamics Storage Phosphor Screen. Free RNA and RNA/RNA duplexes were visualized and quantified using a Molecular Dynamics Phosphorimager 445 SI and ImageQuaNT™ software. k_{app} values were calculated as described in section 2.13.

2.15 ß-galactosidase assays

Cultures of the various *E. coli* test strains containing either the parental control vector pMC874 or the P_{traJ}-*lacZ* reporter plasmid pMCJ211 were grown at 30°C in LB broth supplemented with the appropriate antibiotics to an OD_{600} of 0.6-1. One hundred to three hundred μL of each culture were added to Z-buffer (60 mM $Na_2HPO_4 \cdot 7H_2O$, 40 mM $NaH_2PO_4 \cdot H_2O$, 10 mM KCl, 1 mM $MgSO_4$, and 0.27% (v/v) β-mercaptoethanol) to bring the final volume to 1.0 mL. Two drops of 0.1% SDS and 4 drops of chloroform were added and the tubes were vortexed vigorously for 15 seconds. The tubes were incubated at 28°C for 5 minutes, and the reactions were initiated by the addition of 13.3 mM ONPG (Sigma) and stopped after a timed interval by the addition of 0.5 mL 1 M Na_2CO_3. Cell debris was removed by centrifugation at 14,000 rpm for four minutes. The A_{420} of each supernatant was read in a Bio-Rad Smartspec 3000, and the activity was calculated according to the equation:

Activity (MU)=1000 × [A_{420}/ (time (min.) × volume (mL) × O.D.$_{600}$] (Miller, 1972).

2.16 RNA secondary structure predictions

Secondary structure predictions and ΔG values of SL-I, SL-Ic, SL-II, and SL-IIc and their mutant derivatives were analyzed using the Mfold version 3.1 algorithm (Mathews *et al.*, 1999; Zuker *et al.*, 1999). The RNA sequences were analyzed at the Rensselaer Polytechnic Institute Mfold server (bioinfo.math.rpi.edu/~mfold) using standard settings. The secondary structure of FinP and *traJ184* mRNA were experimentally determined (van Biesen *et al.*, 1993).

2.17 R17 phage sensitivity assays

Single colonies were inoculated onto LB or TSB agar plates such that an approximately 1 cm diameter circle of cells was formed. The plates were then incubated at 37°C for approximately one hour. Five μL of R17 phage (approximately 10^9 pfu/mL) were placed into the center of the inoculated region, and the plate was allowed to incubate for at least 6 hours at 37°C. Formation of a clear plaque in the middle of the inoculum indicated sensitivity to the phage as an indirect measure of F pilus formation.

Chapter 3: Analysis of the FinP binding domains of FinO*

* Portions of this chapter were published: Ghetu, A.F., Gubbins, M.J., Oikawa, K., Kay,

C.M., Frost, L.S., and Glover, J.N.M. (1999) *Biochemistry* **38:** 14036-14044.

3.1 Introduction

RNA binding proteins play an important role in gene regulation of a variety of biological systems, and both their structures and RNA targets are highly diverse (Mattaj, 1993; Draper, 1995). Similarly, the mechanisms employed by RNA binding proteins to bind their target with high affinity covers a wide range of intermolecular interactions. Electrostatic interactions between positively charged amino acids and the negatively charged phosphodiester backbone of RNA are a common theme in RNA-protein interaction (Predki *et al.*, 1995; Schumacher *et al.*, 2002). Base-specific hydrogen bonding and hydrophobic base-stacking interactions present other methods by which such proteins can specifically bind their targets with high affinity (Legault *et al.* 1998; Schärpf *et al.*, 2000). Clearly, a diverse range and combination of mechanisms is employed to allow these proteins to bind their targets.

Control of expression of the F plasmid positive regulatory protein TraJ, and therefore control of *tra* gene expression and F-plasmid transfer, is mediated by two components comprising the FinOP system, FinP antisense RNA (Figure 3.1) and the RNA chaperone protein, FinO (Finnegan and Willetts, 1971; reviewed in Frost *et al.*, 1994). FinO is encoded by a variety of F-like plasmids (McIntyre and Dempsey, 1987; van Biesen and Frost, 1994), and it contains 186 amino acids with a molecular mass of approximately 21.2 kDa. It is basic in nature, and localizes to the cytoplasm (Figure 3.2; Yoshioka *et al.*, 1987; Sandercock and Frost, 1998). FinO is highly alpha-helical in nature, and has a unique, elongated structure (see Figure 1.8 in Chapter 1; Ghetu *et al.*, 2000). FinO binds with high affinity to both FinP and *traJ* mRNA *in vitro*, and it stabilizes FinP *in vivo* by preventing its degradation by RNase E (Figure 3.1; Lee *et al.*,

Figure 3.1 Secondary structure of FinP RNA used in this work. SL-I and SL-II are labeled above the relevant portion of the molecule. Every tenth base is numbered, starting from the 5' side of the molecule. A black line indicates the anti-RBS. The RNase E cleavage site in the single-stranded spacer region is indicated below the figure. Bases in brackets are extra bases added to the 79 base RNA molecule resulting from *in vitro* run-off T7 transcription of the template pLJ5-13 which was cut with *Bam*H1 (Materials and Methods, section 2.9).

SL-II

                              A
                           C   C
        SL-I   U   G
                        U   U
              C A²⁰   G C 60
           U   C   A U
          C   A 50G C
          C U A A   G C
            C G   G C
            C G   A U
        A   A   C G
         A U   G C
      10 G•U   U A
         G C³⁰   A U
         A U   G C⁷⁰
         U A   40 C G
         A U   U•G

FinP

5'-GAUA C G GACA G C GAUUUU(GGGGAUC)-3'

RNase E
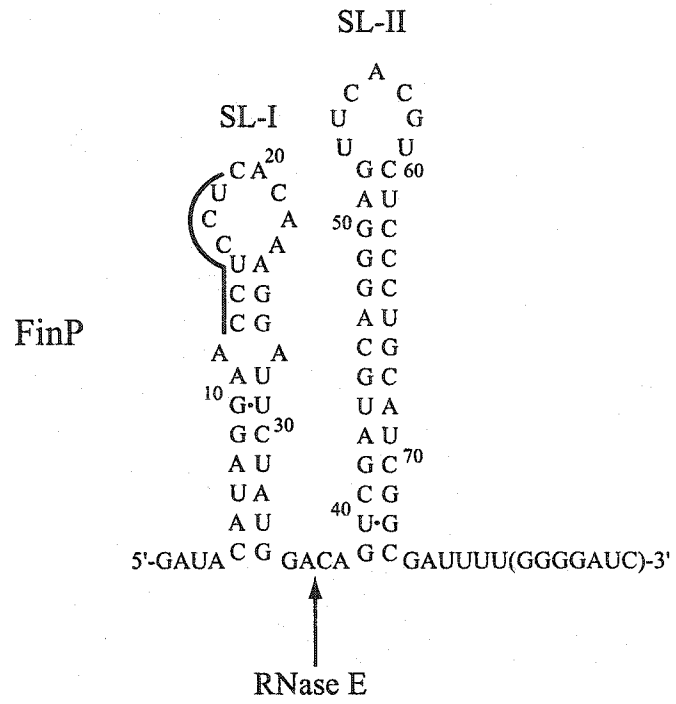
Figure 3.2a The primary amino acid sequence of plasmid R6-5 FinO. Standard single-letter amino acid notation is used. Every tenth amino acid is labeled starting from the N-terminus of the protein.

Figure 3.2b Schematic representation of the FinO deletion proteins used in this study. The top line (small text) represents full length FinO(1-186) and shows the primary amino acid sequence. The black lines below represent various FinO deletions. Each is labeled according to the amino acids contained within the protein.

a.

```
                10          20          30          40          50          60          70
MTEQKRPVLTLKRKTEGETPTRSRKTIINVTTPPKWKVKKQKLAEKAAREAELTAKKAQARQALSIYLNL

                80          90         100         110         120         130        140
PTLDEAVNTLKPWWPGLFDGDTPRLLACGIRDVLLEDVAQRNIPLSHKKLRRALKAITRSESYLCAMKAG

               150         160         170         180
ACRYDTEGYVTEHISQEEEVYAAERLDKIRRQNRIKAELQAVLDEQ
```

b.

MTEQKRPVLTLKRKTEGETPTRSRKTIINVTTPPKWKVKKQKLAEKAAREAELTAKKAQARQALSIYLNLPTLDEAVNTLKPWWPGLFDGDTPRLLACGIRDVLLEDVAQRNIPLSHKKLRRALKAITRSESYLCAMKAG ACRYDTEGYVTEHISQEEEVYAAERLDKIRRQNRIKAELQAVLDEQ

```
━━━━━━━━━━━━━━━━━━━━  FinO(1-61)

━━━━━━━━━━━━━━━━━━━━━━━━━━━━━━━━━━━━━━━━━━━━━━  FinO(1-174)

FinO(26-186)  ━━━━━━━━━━━━━━━━━━━━━━━━━━━━━━━━━━━━━━━━━━

                       FinO(62-186)  ━━━━━━━━━━━━━━━━━━━━━━━━━━

                       FinO(62-174)  ━━━━━━━━━━━━━━━━━━━━━━━

                       FinO(62-170)  ━━━━━━━━━━━━━━━━━━━━━━
```

103

1992; Sandercock and Frost, 1998; Jerome *et al.*, 1999). This protective property of FinO is one of the key functions of this protein in mediating F plasmid transfer.

Studies over the past several years have revealed insights into how FinO can selectively bind to both *traJ* mRNA and FinP antisense RNA (Jerome and Frost, 1999). Since FinP and *traJ* mRNA are complementary, their sequences differ completely from one another. This observation led to an examination of whether FinO recognizes these molecules in a structure- or sequence-dependent manner. Structurally, FinP and the complementary portion of the 5' UTR of *traJ* mRNA are essentially identical (van Biesen *et al.*, 1993). Each contains two stem loop structures, flanked on either side by short single-stranded tails and separated by a single-stranded spacer (see Figure 1.6 in Chapter 1; Figure 3.1). Studies have revealed that FinO recognizes and preferentially binds to SL-II of FinP and SL-IIc of *traJ* mRNA, and that the highest binding affinity is achieved when the 5' and 3' single-stranded tails are present (Jerome and Frost, 1999). Since FinO recognizes specific RNA structures rather than sequences, FinO derived from one plasmid can repress the transfer of other F-like plasmids, even though the sequences of the interacting RNAs can differ significantly (Willetts and Maule, 1986; Frost *et al.*, 1994).

The structural principles that underlie the ability of FinO to interact with RNA are currently unknown. To determine regions of FinO which are functionally important, a variety of FinO deletion mutants were previously expressed as GST-fusion proteins and assayed for several relevant properties, including F plasmid transfer repression, FinP binding, FinP/*traJ* mRNA duplex catalysis, and FinP protection (Sandercock and Frost, 1998). N-terminal fragments of FinO were shown to bind specifically to both FinP

antisense RNA and *traJ184* mRNA. Similarly, such N-terminal FinO fragments were able to catalyze FinP/*traJ184* mRNA duplex formation *in vitro*. However, a fragment of FinO comprising only the C-terminal portion of the protein was unable to perform either of these functions. The acidic C-terminal region of FinO was, however, shown to be important in mediating repression of F plasmid transfer and protection of FinP against degradation by RNase E *in vivo* (Sandercock and Frost, 1998).

This chapter presents an analysis of the regions of FinO that are important in allowing FinO to bind FinP antisense RNA with high affinity. The results demonstrate that FinO contains two distinct regions that each specifically bind FinP RNA. Taken together with previous results (Sandercock and Frost, 1998), the results presented in this chapter suggest that high-affinity binding of FinO to FinP requires that both RNA binding domains are present in FinO.

3.2 Results

3.2.1 Wild-type FinO(1-186) binds to FinP with high affinity.

Previous studies (van Biesen and Frost, 1994; Sandercock and Frost, 1998; Jerome and Frost, 1999) have shown that a GST:FinO fusion can bind FinP antisense RNA *in vitro* with high affinity. We sought to examine the ability of native FinO lacking a GST tag to bind FinP *in vitro*. Various plasmid R6-5 FinO derivatives (Sandercock and Frost, 1998) were cloned and purified to near homogeneity by Dr. Alexandru Ghetu, as described in Ghetu *et al.* (1999). An example of several purified proteins examined by SDS-PAGE analysis and Coomassie staining is shown in Figure 3.3. Uniformly ^{32}P-labeled FinP was produced by *in vitro* run-off T7 transcription using the plasmid

Figure 3.3 An example of the purity of the FinO deletion proteins employed in this study. Coomassie stained SDS-PAGE of a selection of the purified plasmid R6-5 FinO proteins employed in this work. All proteins were cloned, purified, and quantified by Dr. Alexandru Ghetu as described in Ghetu *et al.* (1999). The proteins are listed above each lane, and relevant molecular weight markers (kDa; lane "M") are listed to the left of the figure.
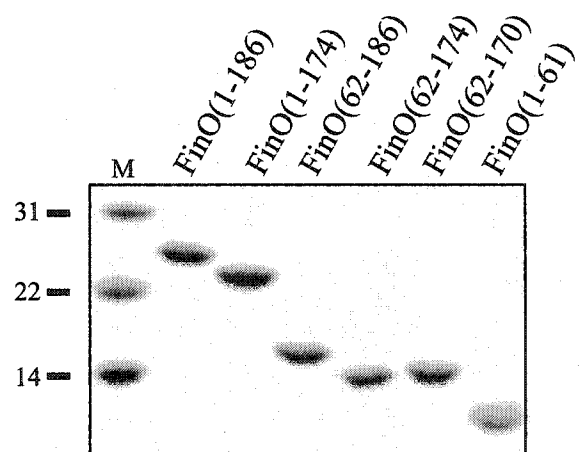
template pLJ5-13 (Jerome and Frost, 1999; Materials and Methods, section 2.9). FinP produced in this way has an extra seven bases, 5'-GGGGAUC-3', added to its 3' side due to the presence of a *Bam*H1 cleavage site in the template DNA (Figure 3.1; Materials and Methods, section 2.9). The presence of these additional bases has been shown to have no influence on the ability of FinO to bind FinP (Jerome and Frost, 1999). Purified FinO derivatives were subjected to EMSA analysis to determine their affinity for binding to *in vitro* transcribed FinP RNA.

Increasing amounts of FinO were incubated for 30 minutes at 4°C with 7.5 fmoles of uniformly ^{32}P-labeled FinP in 30μL reactions containing TEBN binding buffer (Materials and Methods, section 2.12). Free FinP and FinO/FinP complexes were then separated by electrophoresis on 5% or 8% non-denaturing polyacrylamide gels, and the equilibrium association constant (K_a) was calculated based on the concentration of protein required to retard 50% of the labeled FinP present in the reaction (Materials and Methods, section 2.12). As shown in Figure 3.4, EMSA analysis of FinO(1-186) binding to FinP in the absence of any competitor RNA resulted in the presence of four distinct bands. The K_a was determined to be 2.0×10^7 M^{-1} (Table 3.1), in good agreement with previous results examining the ability of GST:FinO to bind FinP (Sandercock and Frost, 1998; Jerome and Frost, 1999). In the presence of a 1000-fold molar excess of *E. coli* total tRNA (Figure 3.4), the K_a was reduced by approximately four-fold, to 5.1×10^6 M^{-1} (Table 3.1). This observation suggests that FinO binding to FinP was specific, although tRNA did appear to be able to compete to some extent with FinP for binding by FinO.

Figure 3.4 EMSA analysis of FinO(1-186) binding to FinP. Seven and one half fmol of uniformly labeled FinP were incubated with increasing amounts of purified FinO, indicated above each lane, in 30 µL reactions containing TEBN buffer. Parallel reactions were carried out without (No tRNA) or with (+tRNA) a non-specific competitor (a 1000-fold molar excess of *E. coli* total tRNA), as indicated above each panel (Materials and Methods, section 2.12). Reactions were incubated at 4°C for 30 minutes, then resolved by electrophoresis on a non-denaturing 8% polyacrylamide gel. Free FinP (open arrow) and FinP/FinO complexes (closed arrows) were quantified and the values were used to calculate the K_a as described in Materials and Methods (section 2.12). The K_a was determined from the concentration of FinO that caused 50% of the labeled FinP to retard in the gel.

FinO(1-186)

No tRNA | + tRNA

0 .6 1.5 3 6 13 26 0 .6 1.5 3 6 13 26 pmol protein
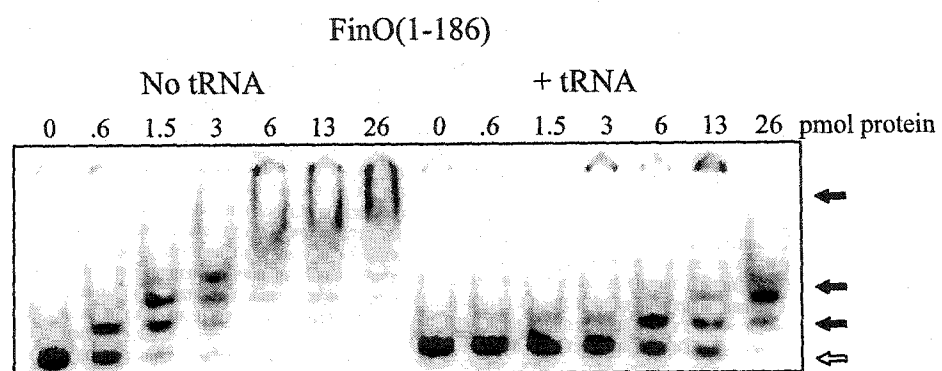
Table 3.1 Equilibrium association constants (K_a) for a variety of FinO deletion proteins binding to FinP antisense RNA. 7.5 fmoles of uniformly labeled ^{32}P-FinP were incubated with increasing concentrations of protein and the reactions subjected to EMSA analysis. K_a values were determined from the concentration of FinO that caused 50% of the labeled RNA to become retarded in the polyacrylamide gels during EMSA analysis.

FinO fragment	K_a $(M^{-1})^a$	
	no competitor[b]	+competitor[b]
FinO(1-186)	$(2.0 \pm 0.5) \times 10^7$	$(5.1 \pm 0.3) \times 10^6$
FinO(1-61)	$(2.1 \pm 0.7) \times 10^6$	$(1.4 \pm 0.1) \times 10^6$
FinO(1-174)	$(2.7 \pm 1.1) \times 10^6$	$(1.1 \pm 0.2) \times 10^6$
FinO(26-186)	$(3.2 \pm 0.5) \times 10^7$	$(7.3 \pm 1.8) \times 10^6$
FinO(62-186)	$(4.2 \pm 1.0) \times 10^6$	$(8.1 \pm 1.0) \times 10^5$
FinO(62-170)[c]	$<1 \times 10^4$	N.D.[d]
FinO(62-174)[c]	$<1 \times 10^4$	N.D.[d]

[a] K_a values determined from at least three independent EMSA experiments, ± standard deviation.

[b] Competitor was *E. coli* total tRNA in a 1000-fold molar excess.

[c] K_a was estimated because these fragments were unable to bind more than 35-40% of the RNA present in binding reactions.

[d] Not determined.

3.2.2 Deletion of C-terminal portions of FinO reduces FinO/FinP binding.

Limited proteolysis of FinO bound to its minimal RNA binding target, SL-II of FinP (Ghetu *et al.*, 1999; Jerome and Frost, 1999) suggested that regions extending between residues 23-61 and 170/174-186 might be important for RNA binding. C-terminal deletion proteins FinO(1-174) and FinO(1-61) were therefore tested via EMSA analysis to determine their affinities for FinP binding. EMSA analysis was performed as described above in section 3.2.1 and in Materials and Methods, section 2.12. EMSA experiments with FinO(1-61) revealed several retarded FinO(1-61)/FinP bands (Figure 3.5a), although these bands were less distinct than the retarded bands resulting from FinO(1-186)/FinP EMSA analysis (compare Figures 3.4 and 3.5a). The K_a for FinO(1-61) binding to FinP was determined to be 2.1×10^6 M^{-1} in the absence of any RNA competitor, and moderately reduced to 1.4×10^6 M^{-1} in the presence of a 1000-fold molar excess of *E. coli* tRNA (Table 3.1).

FinO(1-174) revealed a similar electrophoretic profile when analyzed for FinP binding via EMSA analysis, with two retarded species evident (Figure 3.5b), both of which were more diffuse than the retarded bands evident from EMSA analysis with FinO(1-186). The K_a for FinP binding by this fragment was almost identical to the K_a for FinO(1-61), 2.7×10^6 M^{-1} in the absence of any RNA competitor, and 1.1×10^6 M^{-1} in the presence of competitor (Table 3.1).

These results suggest that the region of FinO extending from Met-1 to Arg-61 comprises a region of the protein that is fully capable of binding to FinP with high affinity. However, the observation that FinO(1-61)/FinP and FinO(1-174)/FinP bands in EMSA analyses were more diffuse that the FinO(1-186)/FinP bands suggests that

Figure 3.5a Removal of portions of the C-terminus of FinO reduces the protein's ability to bind FinP. EMSA analysis of purified FinO(1-61) binding to FinP was performed as described in the legend to Figure 3.5. The amount of purified protein present in each reaction is indicated above each lane. Parallel reactions were carried out with no competitor or in the presence of a non-specific competitor, a 1000-fold molar excess of *E. coli* total tRNA, as indicated above each panel. Free FinP (open arrows) and FinP/FinO complexes (closed arrows) were quantified and the values were used to calculate the K_a as described in Materials and Methods (section 2.12).

Figure 3.5b EMSA analysis of FinO(1-174) binding to FinP. The experiment was performed as described above in the legend to Figure 3.6a.

a.

FinO(1-61)

No tRNA   + tRNA

0 4.2 9.8 42 98 210 420 0 4.2 9.8 42 98 210 420 pmol protein

b.

FinO(1-174)

No tRNA   + tRNA

0 1.5 7.5 15 30 60 75 0 1.5 7.5 15 30 60 75 pmol protein

interactions between the tested C-terminal FinO deletion proteins and FinP may be less stable than the interaction of wild-type FinO with FinP.

3.2.3 Deletion of N-terminal portions of FinO reduces FinO/FinP binding.

Since limited proteolysis of FinO bound to SL-II also revealed protection of a fragment extending from Thr-26 to the C-terminus of FinO at Gln-186 (Ghetu *et al.*, 1999), this fragment was purified and tested for its ability to bind FinP *in vitro* via EMSA analysis. Figure 3.6a demonstrates that the electrophoretic mobility profile for this FinO fragment binding to FinP was almost identical to that of FinO(1-186) (compare Figure 3.6a and Figure 3.4). Furthermore, the K_a for FinO(26-186) binding to FinP was close to that of FinO(1-186), 3.2×10^7 M^{-1} in the absence of any RNA competitor, and 7.3×10^6 M^{-1} in the presence of competing tRNA (Table 3.1). The similarity of K_a values for FinO(1-186) and FinO(26-186) suggests that the N-terminal 25 amino acids of FinO plays a very minor role in FinO/FinP binding *in vitro*. The implication from these results is that FinO(26-186) contains all of the regions required for high affinity FinP binding *in vitro*.

As discussed in section 3.2.2, FinO(1-61) exhibited an ability to bind FinP with relatively high affinity. A longer deletion of the N-terminal region extending from Met-1 to Arg-61, FinO(62-186), was therefore tested to determine whether this fragment displayed an ability to bind FinP . EMSA analysis of FinO(62-186) binding to FinP revealed the presence of two distinct shifted bands (Figure 3.6b). Examination of these bands shows that they are more diffuse than the shifted bands present in the EMSA analyses using FinO(1-186) and FinO(26-186) (compare Figure 3.6b with Figure 3.6a and Figure 3.4). FinO(62-186) has a K_a of 4.2×10^6 M^{-1} in the absence of any RNA

Figure 3.6a Removal of portions of the N-terminus of FinO reduces binding to FinP. EMSA analysis of purified FinO(26-186) binding to FinP was performed as described in the legend to Figure 3.5. The amount of purified protein present in each reaction is indicated above each lane. Parallel reactions were carried out with no competitor or in the presence of a non-specific competitor, a 1000-fold molar excess of *E. coli* total tRNA, as indicated above each panel. Free FinP (open arrows) and FinP/FinO complexes (closed arrows) were quantified and the values were used to calculate the K_a as described in Materials and Methods (section 2.12).

Figure 3.6b EMSA analysis of FinO(62-186) binding to FinP. The experiment was performed as described above in the legend to Figure 3.6a.

a.

FinO(26-186)

No tRNA   + tRNA

0   .4   1.8 3.6 7.2 14   18   0   .4   1.8 3.6 7.2 14   18   pmol protein

b.

FinO(62-186)

No tRNA   + tRNA

0   4.4   8   41   82 246 406   0   4.4   8   41   82 246 406   pmol protein
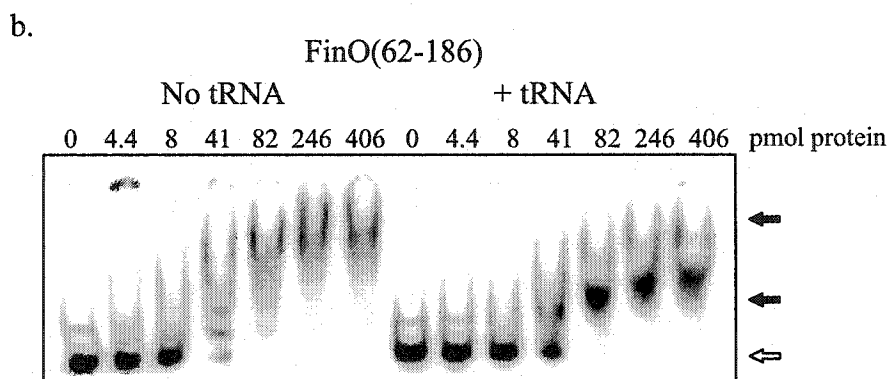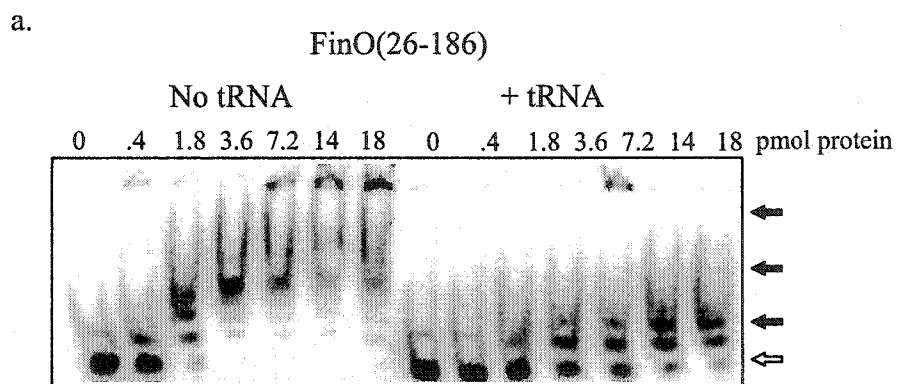
competitor, and 8.1×10^5 M^{-1} in the presence of a 1000-fold molar excess of *E. coli* tRNA (Table 3.1), which is considerably lower than the K_a values for FinO(1-186) and FinO(26-186). However, this fragment was able to bind FinP with high affinity.

3.2.4 Deletion of both N- and C-terminal portions of FinO eliminates the ability of FinO to bind FinP *in vitro*.

Limited proteolysis of wild-type FinO revealed susceptibility of the protein to trypsin digestion in the absence of FinP SL-II, resulting in the formation of FinO(62-170) and FinO(62-174) (Ghetu *et al.*, 1999). Mutant derivatives FinO(1-61), FinO(1-174), and FinO(62-186) all demonstrated an ability to bind FinP with relatively high affinity (discussed in previous sections). FinO(62-170) and FinO(62-174) were therefore examined via EMSA analysis to determine whether these deletion proteins were able to bind FinP *in vitro*. As demonstrated in Figure 3.7, FinO(62-170) was almost completely unable to bind FinP. Since less than 50% of the labeled FinP present in the binding reactions was bound by FinO(62-170), a K_a could only be estimated. The estimated K_a for both FinO(62-170) and FinO(62-174) was approximately 1.0×10^4 M^{-1} in the absence of competitor RNA (Table 3.1). EMSA analysis in the presence of *E. coli* tRNA was not performed due to the obviously low affinity of this fragment for FinP.

3.2.5 FinO binds to FinP SL-II as a monomer.

A minimal high affinity RNA target for FinO binding is FinP SL-II, including the single-stranded spacer and tail on the 5' and 3' sides of SL-II, respectively (Figure 3.1; Jerome and Frost, 1999). Whether FinO binds this minimal target as a monomer, dimer, or multimer was not known. FinO binds FinP with approximately the same affinity as a GST:FinO fusion protein *in vitro* (Sandercock and Frost, 1998; Jerome and Frost, 1999).

Figure 3.7 Removal of portions of the both the N-terminus and C-terminus of FinO eliminates the protein's ability to bind FinP. EMSA analysis of purified FinO(62-170) binding to FinP was performed as described in the legend to Figure 3.5. The amount of purified protein present in each reaction is indicated above each lane. Free FinP (open arrows) and FinP/FinO complexes (closed arrows) are indicated to the right of the figure. A lack of binding by FinO(62-170) prevented a K_a from being calculated, as described in detail in the text.

FinO(62-170)

0   24   60 120 240 360 480 600 720   pmol protein
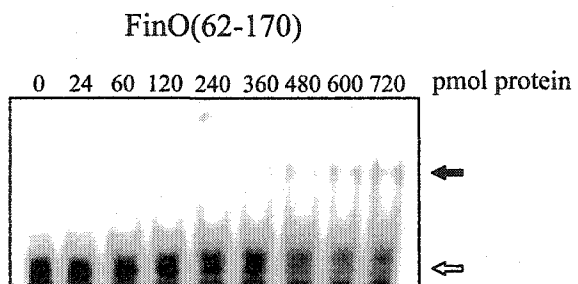
In an experiment performed by Dr. Alexandru Ghetu, purified FinO, GST:FinO, or equimolar amounts of both were incubated with ^{32}P-labeledFinP SL-II and then separated by electrophoresis on a non-denaturing polyacrylamide gel (Ghetu *et al.*, 1999). The large size difference between FinO and GST:FinO allows for clear separation of FinO/FinP and GST:FinO/FinP complexes. Since the affinity of each protein for FinP is essentially the same, one would expect a potential FinO/GST:FinO/FinP complex to migrate at an intermediate position in a non-denaturing polyacrylamide gel during EMSA analysis if FinO bound to FinP SL-II as a dimer. Figure 3.8 shows that FinO/FinP and GST:FinO/FinP complexes were easily separable during EMSA analysis. No intermediate FinO/GST:FinO/FinP complex was evident in this experiment, performed by Dr. Alexandru Ghetu, revealing that FinO binds its minimal RNA target as a monomer (Ghetu *et al.*, 1999).

3.3 Discussion

The results presented in this chapter indicate that FinO contains two distinct RNA binding regions, each of which can bind RNA independently of the other. The first region is located within the N-terminal third of the protein, between Thr-26 and Arg-61. The second region extends from Gln-62 to the far C-terminus of the protein, at Gln-186. The boundaries of the much larger C-terminal RNA binding region were not precisely delineated. However, its primary RNA contact surface is predicted to be located near a region of positively charged residues, Arg-165 to Lys-176, located in the C-terminal alpha-helical region of the protein (Figure 3.2; Ghetu *et al.*, 1999). FinP binding was shown to protect purified FinO from cleavage by trypsin at arginine residues 170 and

Figure 3.8 FinO binds to its minimal RNA target, FinP SL-II, as a monomer. Purified

FinO, GST:FinO, or an equimolar combination of both, as indicated above each lane, was

incubated with ^{32}P-labeled FinP SL-II. Protein/RNA complexes were resolved on an 8%

non-denaturing polyacrylamide gel in an EMSA assay. The locations of free SL-II, SL-

II/FinO, and SL-II/GST:FinO complexes are indicated to the right of the figure. This

experiment was performed by Dr. Alexandru Ghetu (Ghetu *et al.*, 1999).
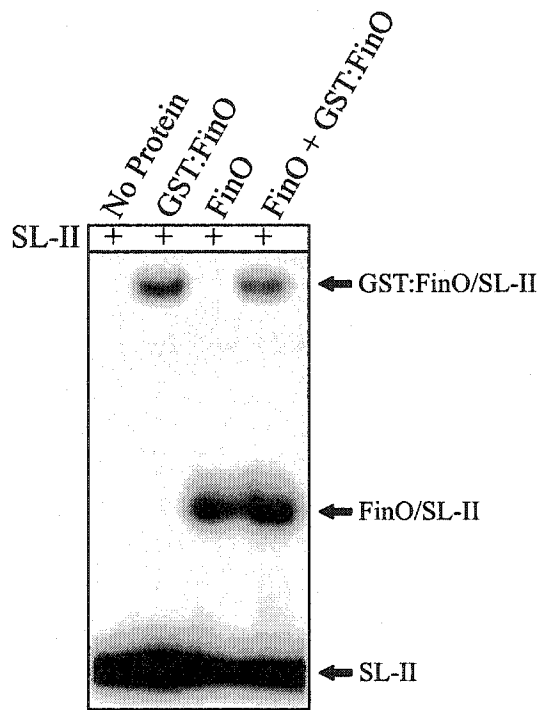
174, which suggests that FinP sterically blocks access of the protease to this region of FinO when they are in a complex (Ghetu *et al.*, 1999). Deletion of residues Ile-175 to Gln-186, coupled with deletion of the N-terminal 61 amino acids of FinO (FinO(62-174)) rendered this protein almost completely unable to interact with FinP (Figure 3.8). These results both support the notion that the region in the vicinity of Arg-165 to Lys-176 makes direct contact with FinP, as a "subdomain" of the larger C-terminal RNA binding domain of the protein, including residues 175-186. The similar CD spectra of wild-type FinO(1-186), FinO(62-174) and FinO(62-186) suggests that the lack of *in vitro* FinP binding by FinO(62-174) is not indirectly caused by a conformational change in residues 62-174 upon deletion of residues 175-186 (Ghetu *et al.*, 1999). On its own, a 37 amino acid C-terminal fragment of FinO could not efficiently bind FinP, however part of this C-terminal region of FinO was required to protect FinP from RNase E-mediated degradation (Sandercock and Frost, 1998). Coupled with the results presented here, one can predict that this C-terminal region of FinO may perform an essential function in contacting FinP antisense RNA. However, it appears that the entire 62-186 domain is needed for high affinity FinP binding *in vitro*.

EMSA analysis of FinO(1-186) and FinO(26-186) binding to FinP revealed retarded protein/RNA complexes with relatively distinct, sharp bands (Figure 3.4; Figure 3.6a). Each of these FinO fragments contains both the N- and C-terminal RNA binding regions, as defined by this work. However, the fragments which contain only one of the RNA binding regions, FinO(1-61), FinO(1-174), and FinO(62-186), form protein/RNA complexes with more diffuse bands during EMSA analysis (Figure 3.5; Figure 3.6b). Dissociation of the protein/RNA complexes during electrophoresis may be the reason for

the less well-defined bands observed with these FinO fragments. One can speculate that both of the RNA binding domains are required in order for a kinetically stable FinO/FinP complex to form *in vitro*.

RNase E cleaves FinP specifically within the four base single-stranded region located between SL-I and SL-II (Figure 3.1; Jerome *et al.*, 1999), and one of the functions of FinO *in vivo* is to protect FinP from this degradation. The C-terminal region of FinO extending from Ala-141 to Gln-186 was determined to be required for protection of FinP from RNase E-mediated degradation *in vivo* (Sandercock and Frost, 1998). High-affinity *in vitro* binding of FinP by FinO also depends on the presence of this single-stranded spacer region in FinP (Jerome *et al.*, 1999). Contact between the spacer region of FinP and the C-terminal region of FinO may occur directly, resulting in protection from RNase E-mediated cleavage of the RNA. Examination of the high resolution three-dimensional structure of FinO reveals that the length of the positively charged long N-terminal helix extending from residues Trp-36 to Tyr-67 is approximately the same as the predicted length of FinP SL-II (Ghetu *et al.*, 2000). This N-terminal alpha-helix may align itself with the stem of SL-II, promoting electrostatic interactions with the negatively charged phosphate backbone of the RNA (Ghetu *et al.*, 2000). Trp-36, a solvent exposed residue at the top of the N-terminal alpha-helix of FinO may also play a role in FinP binding. This residue may stack with unpaired bases in the loop of SL-II, similar to the interaction of a tryptophan residue in the λN transcriptional antiterminator protein with its RNA target, the GNRA-like pentaloop of the box B RNA hairpin structure of early phage λ transcripts (Legault *et al.*, 1998; Ghetu *et al.*, 2000). A large positively charged surface extends across the central domain of FinO (see Figure 1.8b in Chapter 1), which may

couple the protein with FinP via electrostatic interactions with the RNA phosphodiester backbone (Ghetu et al., 2000, 2002). All of these interactions likely align FinO with FinP in such a manner that the C-terminal region of FinO can line up with the bottom of the stem and the single-stranded regions flanking the 5' and 3' sides of SL-II. This alignment could therefore sterically inhibit RNase E-mediated cleavage of the single-stranded spacer (Sandercock and Frost, 1998; Ghetu et al., 2000). A negatively charged region is located at the bottom of FinO (see Figure 1.8b in Chapter 1; Ghetu et al, 2000). Electrostatic repulsion between this region of FinO and the phosphodiester backbone of FinP may facilitate the proper alignment of FinO with its target to promote high affinity binding. This function would be analogous to that of the acidic C-terminal alpha-helices of the ColE1 Rom homodimer, which are thought to aid in aligning the protein with its RNA target during binding (Predki et al., 1995).

Although FinO was shown to bind isolated FinP SL-II as a monomer (Ghetu et al., 1999), FinO may bind whole FinP as a multimer. EMSA analysis of FinO binding to FinP revealed multiple retarded bands, suggesting that FinO may bind FinP at more than one site. FinO binding to the 5' UTR of traJ mRNA also resulted in the presence of multiple bands during EMSA analysis (Jerome and Frost, 1999). FinP SL-I is a target for binding by FinO, although FinO has a lower affinity for this region of the RNA (Jerome and Frost, 1999; Chapter 5). It is possible that FinO can bind to both sites on FinP, resulting in multiple retarded bands during EMSA analysis. However, this phenomenon may also be the result of non-specific aggregation of FinO with FinP when the FinO concentration is increased in the binding reactions employed (Jerome and Frost, 1999).

This chapter presents clear evidence that two separate regions of FinO contact FinP antisense RNA. FinO contains no sequence or structural similarity to other known RNA binding proteins (Ghetu *et al.*, 1999, 2000), making it difficult to draw analogies between the mechanisms involved in FinO binding to RNA and those employed by other systems. Examination of the data collected to date regarding FinO/FinP interactions suggests that electrostatic interactions and stacking between a hydrophobic Trp residue and unpaired loop bases likely play a major role in FinO/FinP binding. It is still unknown at this time whether the separate binding domains function independently or as a single entity. To make this determination, high resolution mapping of a FinO/FinP complex should be undertaken. Determination of the structure of FinO bound to FinP will also answer many questions regarding the exact nature of the interactions that occur between these two molecules.

Chapter 4: Analysis of the RNA/RNA duplex catalysis activity of FinO*

*Portions of this chapter were published: Ghetu, A.F., Gubbins, M.J., Frost, L.S., and

Glover, J.N.M. (2000) *Nat. Struct. Biol.* 7(7): 565-569.

Ghetu, A.F., Arthur, D. C., Gubbins, M. J., Frost, L. S., and Glover, J.N.M. (submitted to

Mol Cell, 2002)

4.1 Introduction

Interactions between RNA molecules are a common theme in a multitude of biological systems. The ability of HIV to replicate is governed in large part by the ability of its dimeric RNA genome to form a duplex via the stem-loop structure present at its dimerization initiation site (Laughrea and Jetté, 1994; Lodmell *et al.*, 2000). Dimerization of *bicoid* mRNA, mediated by stem-loop structures in the 3' UTR (untranslated region) of the RNA, is important for proper localization of the transcript in the *Drosophila melanogaster* embryo (Wagner *et al.*, 2001). In prokaryotes, control of replication of the *E. coli* plasmids ColE1 (Tomizawa and Som, 1984; Eguchi and Tomizawa, 1991), R1 (Wagner and Simons, 1994), and F (Frost *et al.*, 1994) all involve sense-antisense RNA interactions. In many biological systems, an accessory protein is required to promote RNA duplex formation. Control of expression of the *gal* operon of *E. coli* (Møller *et al.*, 2002a), plasmid ColE1 replication control (Eguchi and Tomizawa, 1990), and HIV genome dimerization (Muriaux *et al.*, 1998; Takahashi *et al.*, 2001; Bernacchi *et al.*, 2002) all involve an accessory protein to promote RNA/RNA interaction.

TraJ expression, and thus F plasmid transfer, is controlled by the FinOP fertility inhibition system (Finnegan and Willetts, 1971; Frost *et al.*, 1994). Binding of FinP to its complementary sequence in the 5' UTR of *traJ* mRNA (Figure 4.1) is believed to sequester the RBS of *traJ* mRNA, located in SL-Ic, within a FinP/*traJ* mRNA duplex. (Mullineaux and Willetts, 1985; Koraimann *et al.*, 1996). In F-like plasmids, the plasmid-encoded FinO protein is essential for mediating the negative regulatory activity of FinP (Yoshioka *et al.*, 1987; Frost *et al.*, 1994). When supplied *in trans*, FinO

Figure 4.1 Experimentally determined secondary structures of FinP antisense RNA and *traJ184* mRNA (van Biesen *et al.*, 1993). Black lines indicate the *traJ* RBS and corresponding anti-RBS of FinP. The start codon of *traJ* is shown in italics. Only the portion of *traJ184* mRNA up to nucleotide 110 is shown for clarity. Nucleotide positions are labeled every 10 bases starting from the 5' end of each molecule.

SL-II

SL-I

FinP

```
                                    A
                                  C   C
                          U         G
                          U       U
                   C A20  G C 60
                  U   C   A U
                  C     A  50G C
                  C   A      G C
                   U A       G C
                   C G       A U
                   C G       C G
                  A   A      G C
                   A U       U A
              10 G·U         A U
                 G C30       G C 70
                 A U         C G
                 U A      40 U·G
                 A U         G C
   5'-GAUA C G GACA   GAUUUU-3'
                C G
```

traJ184 mRNA

SL-IIc

SL-Ic

SL-III

```
                               U
                             G   G
                            C     A              U G
                          A    A            G        A
                          G C60      90 U         G
                          A U          U         G
                    50 G C             U A
                       G C             C G
                       G C             C G
                       A U          U      U 100
                       C G             A U
                       G C             A   C
                       U A             G C
                       A U             A U
                    G C70           80 U A
                       C G             A U
                                       C G
```

```
         10
       A A
      U   U
      U   G
       G C
       G C
       U A
       G C
       C G   20        30
5'-G   UUAAAAUUUGAAAUUGAAAAUCGC   ACUGUC   UAUC........3'
                                    40                   110
```

from the related plasmids R6-5 (van Biesen and Frost, 1992) and R100 (Finnegan and Willetts, 1973) can repress F transfer. FinO has been determined to catalyze FinP/*traJ* mRNA duplex formation *in vitro* (van Biesen *et al.*, 1993; Sandercock and Frost, 1998; Ghetu *et al.*, 2000), and this activity is likely important *in vivo* for the control of F plasmid transfer. In combination, the FinP protection activity (Jerome *et al.*, 1999; Ghetu *et al.*, 1999) and RNA duplex catalysis activity of FinO lead to repression of F conjugative transfer by 10- to 1000-fold.

RNA unwinding is a crucial component in a wide variety of biological processes (reviewed in Tanner and Linder, 2001 and von Hippel and Delagoutte, 2001). Two fundamental mechanisms are employed in RNA unwinding. The first uses the energy gained from ATP hydrolysis to interrupt RNA base-pairing. The DExD/H-box helicases provide an example of such ATP-dependent RNA unwinding reactions (Yu and Owttrim, 2000; reviewed in Tanner and Linder, 2001 and von Hippel and Delagoutte, 2001). The second mechanism drives the equilibrium between single- and double-stranded RNA towards the single-stranded form, which occurs via specific binding of an "RNA chaperone" to the single-stranded RNA. Examples of this mechanism are the hnRNP proteins (reviewed in Herschlag, 1995; Shahied *et al.*, 2001), and the CsrA RNA binding protein of *E. coli* (Baker *et al.*, 2002).

This chapter presents evidence that FinO promotes FinP/*traJ* mRNA duplex formation at a significantly increased rate *in vitro*, relative to duplex formation in the absence of FinO. The region of FinO that mediates this catalytic activity is located within an eighteen amino acid region within the highly alpha-helical N-terminus of the protein. The same region of FinO is also known to possess ATP-independent RNA

unwinding ability. The results presented in this chapter suggest that the ability of FinO to unwind double-stranded RNA, promote RNA/RNA duplex formation, and repress F plasmid transfer are directly related.

4.2 Results

4.2.1 Wild-type R6-5 FinO increases the rate of duplex formation between FinP and *traJ184* mRNA.

Previous work has shown that a GST:FinO fusion protein could promote duplex formation between FinP and *traJ184* mRNA *in vitro*. The reaction was shown to be bimolecular, and it followed pseudo first-order kinetics (van Biesen *et al.*, 1993). The k_{app} for FinO-mediated duplex formation was increased by approximately 5-fold compared to duplex formation in the absence of FinO. We sought to examine the ability of native R6-5 FinO to promote duplex formation *in vitro* in the absence of a GST tag. EMSA analysis using *in vitro* transcribed FinP and *traJ184* mRNA was performed in the presence and absence of purified FinO. ^{32}P-labeled FinP (7.5 fmol) was mixed with a 10-fold molar excess of ^{3}H-labeled *traJ184* mRNA and incubated at 37°C. The FinP used in this study has had an extra 7 bases added to its 3' end (5'-G$_4$AUC-3') resulting from the presence of a *Bam*HI site in the *in vitro* transcription template, pLJ5-13 (see Materials and Methods, Table 2.2). The presence of these extra bases was previously shown not to affect the affinity of FinO for FinP (Jerome and Frost, 1999). Aliquots were withdrawn at timed intervals, and free and duplexed RNA were resolved by non-denaturing PAGE, allowing the k_{app} for duplex formation to be calculated based on the time required for 50% of the free FinP to become part of a FinP/*traJ184* mRNA duplex, and the

concentration of the RNA species in excess (see Materials and Methods section 2.13). As shown in Figure 4.2, FinP/*traJ184* mRNA duplex formation increased substantially in the presence of FinO. In the absence of FinO, the k_{app} was 4.9×10^5 $M^{-1}s^{-1}$, while in the presence of FinO the k_{app} increased approximately 50-fold to 2.5×10^7 $M^{-1}s^{-1}$ (Table 4.1). We attribute this much larger increase in duplex formation compared to that determined previously (van Biesen *et al.*, 1993) to the absence of a GST moiety on the FinO protein employed in this study. These results clearly reveal that FinO has the ability to enhance the rate of formation of a FinP/*traJ184* mRNA duplex *in vitro*.

4.2.2 Removal of portions of the N-terminus of FinO drastically lowers the ability of FinO to promote FinP/*traJ184* mRNA duplex formation.

In order to delimit the regions of FinO which are involved in RNA duplex catalysis, several deletions were made in the N- and C-terminal regions of the protein. EMSA analyses were employed to determine the k_{app}s for FinP/*traJ184* mRNA duplex formation as described in section 4.2.1. Removal of the N-terminal 25 amino acids (FinO(26-186)) showed that the k_{app} for FinP/*traJ184* mRNA duplex formation was 2.9×10^6 $M^{-1}s^{-1}$, approximately 11-fold lower than the k_{app} for FinO(1-186) (Figure 4.3; Table 4.1). However, removal of the N-terminal 44 amino acids of FinO (FinO(45-186)) reduced the k_{app} to 4.8×10^5 $M^{-1}s^{-1}$, essentially identical to the k_{app} for duplex formation in the absence of any protein (Figure 4.3; Table 4.1). Removal of the C-terminal 11 amino acids (FinO(1-174)) had the opposite effect on FinP/*traJ184* mRNA duplex formation. The k_{app} in this case was 4.8×10^7 $M^{-1}s^{-1}$, an increase of almost two-fold compared to duplex formation in the presence of FinO(1-186) (Figure 4.3; Table 4.1).

Figure 4.2 Comparison of FinP/*traJ184* mRNA duplex formation in the presence or absence of 1 μM wild-type FinO(1-186). Uniformly labeled ^{32}P-FinP (7.5 fmol) was mixed with a ten-fold molar excess of cold *traJ184* mRNA in 50 μL reactions containing TMEB duplex buffer and incubated at 37°C. Samples (5μL) were withdrawn at the times indicated above each lane and resolved on 8% non-denaturing polyacrylamide gels. Open arrows indicate free FinP while closed arrows indicate FinP/*traJ184* mRNA duplexes. The k_{app} for duplex formation was determined as described in Materials and Methods (section 2.13).

No Protein

0 1 2 4 6 8 10 20 30 Time (minutes)

FinO(1-186)

0 .25 .50 1 2 4 6 Time (minutes)
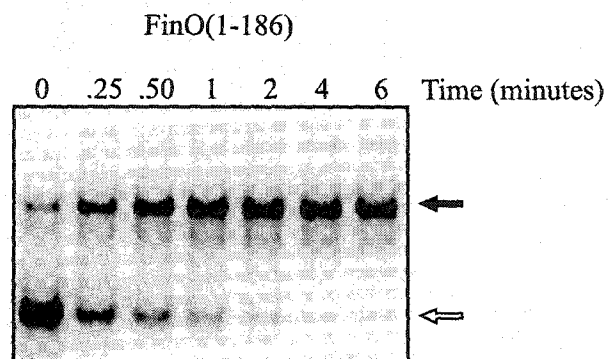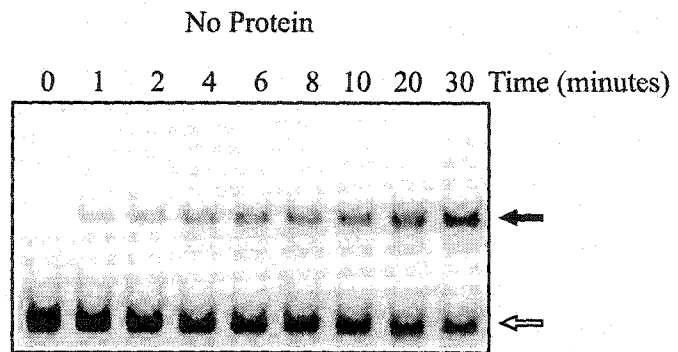
Table 4.1 Apparent association rate constants (k_{app}) for FinP/*traJ184* mRNA duplex formation in the presence of a variety of FinO proteins. k_{app} determinations were made via EMSA analysis using 7.5 fmol of uniformly-labeled FinP, and a 10-fold molar excess of cold *traJ184* mRNA. All proteins were present in reactions at a final concentration of 1 μM.

FinO protein tested	$\times 10^7\ k_{app}\ (M^{-1}s^{-1})^a$
None	0.049±0.02
FinO(1-186)	2.5±1
FinO(26-186)	0.29±0.1
FinO(45-186)	0.048±0.02
FinO(1-174)	4.8±2
FinOW36A	1.2±0.4
FinOK37A/V38A	1.5±0.7
FinOK39A/K40A	1.0±0.4

$^a k_{app}$ values are an average of at least three separate experiments, ± standard deviation.

Figure 4.3 Deletion of portions of the N- or C-terminus of FinO affects FinP/*traJ184* mRNA duplex formation. Uniformly labeled ^{32}P-FinP (7.5 fmol) was mixed with a ten-fold molar excess (FinO(26-186) and FinO(45-186)) or a five-fold molar excess (FinO(1-174)) of cold *traJ184* mRNA in 50 μL reactions containing TMEB duplex buffer and incubated at 37°C. The FinO N- and C-terminal deletion proteins indicated above each panel were present at a concentration of 1 μM. Samples (5μL) of each reaction were withdrawn at the times indicated above each lane and resolved on 8% non-denaturing polyacrylamide gels. Open arrows indicate free FinP while closed arrows indicate FinP/*traJ184* mRNA duplexes. The k_{app} for duplex formation was determined as described in Materials and Methods (section 2.13).

FinO(26-186)

0   1   2   4   6   8   10   Time (minutes)

FinO(45-186)

0   1   2   8   10   20   30   40   60   Time (minutes)

FinO(1-174)

0   .25   .50   1   2   4   6   Time (minutes)
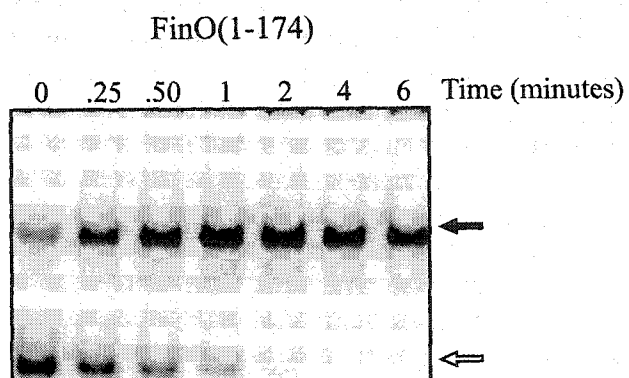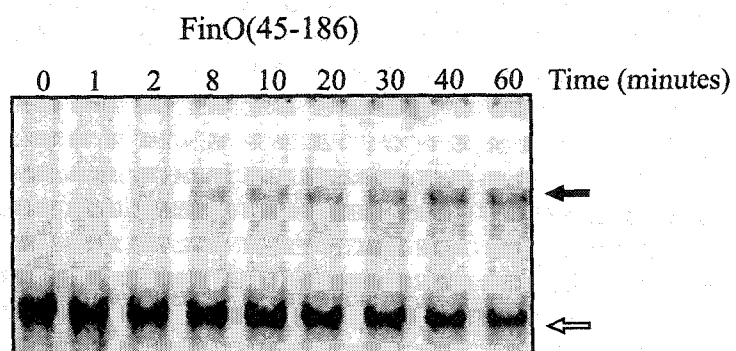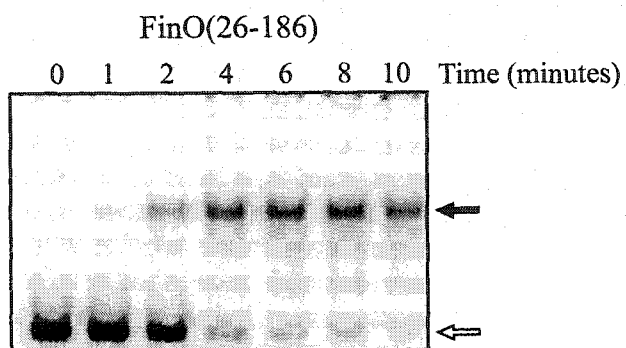
These results suggest that the N-terminal region of FinO extending from amino acids 26-44 contains the activity that is required for high efficiency FinP/*traJ184* mRNA duplex formation *in vitro*. The C-terminal 12 amino acids of FinO, which have been shown to influence FinP binding (Chapter 3; Ghetu *et al.*, 1999) appear to cause a slight increase in the rate of FinP/*traJ184* mRNA duplex formation when they are removed from FinO. The reason for this observation is unclear at this time.

FinP and the 5′ UTR of *traJ* mRNA contain stable stems and relatively small regions of single-stranded intermolecular complementarity. FinP SL-I has a stem containing 11 base pairs and a predicted free energy of unfolding of –10.1 kcal/mol. The stem of FinP SL-II contains 14 base-pairs, and a free energy of unfolding considerably higher than that of SL-I, at –28.2 kcal/mole (Figure 4.1, van Biesen *et al.*, 1993). Disruption of the stems to create more single-stranded regions available for intermolecular base pairing would aid in overcoming kinetic barriers to duplex formation imposed by the presence of the stable helices in FinP and *traJ* mRNA. EMSA analysis performed by Dr. Alexandru Ghetu revealed that FinO unwound or otherwise disrupted the structure of a double-stranded RNA molecule derived from the stem of FinP SL-II *in vitro* using an ATP-independent mechanism (Figure 4.4b; Ghetu *et al.*, submitted). It should be noted that, at this time, the ability of FinO to unwind double-stranded RNA has not yet been firmly established. FinO may in fact disrupt the secondary structure of this RNA construct without unwinding the RNA *per se*. For the sake of simplicity and clarity, this activity will be referred to as unwinding in this work.

Figure 4.4a Schematic representation of FinO double-stranded RNA unwinding experiments (Ghetu *et al.*, submitted). A double-stranded RNA construct derived from FinP SL-II ("^{32}P-up/cold down duplex") was incubated in unwinding buffer with 1μM of selected FinO mutant proteins at 37°C for 2 hours, along with a large molar excess of unlabeled "cold up strand" RNA. This allowed electrophoretic separation of the ^{32}P-up/cold down duplex from free ^{32}P-up strand RNA.

Figure 4.4b FinO possesses double-stranded RNA unwinding activity. This figure was adapted from one kindly provided by Dr. Alex Ghetu. Purified FinO and various derivatives, indicated above each lane, were tested for their ability to unwind the double-stranded RNA construct described above. Samples were resolved on 15% non-denaturing polyacrylamide gels to separate double-stranded from single-stranded RNA. Closed arrows indicate double-stranded RNA ("^{32}P-up/cold down duplex"), single-stranded ("^{32}P-up") RNA is indicated by open arrows. This experiment was performed by Dr. Alex Ghetu (Ghetu *et al.*, submitted).

a.

Excess cold up
+FinO

37°C

^{32}P

^{32}P-up/cold down RNA
duplex

cold up/cold down
RNA duplex

^{32}P

free ^{32}P-up strand

b.

No Protein
FinOT32A
FinOP33A
FinOP34A
FinOK35A
FinOW36A
FinOK37A
FinOV38A
FinOK39A
FinOK40A
FinOQ41A
FinOK42A
FinO(1-186)
FinO(45-186)
FinOK37A/V38A
FinOK39A/K40A
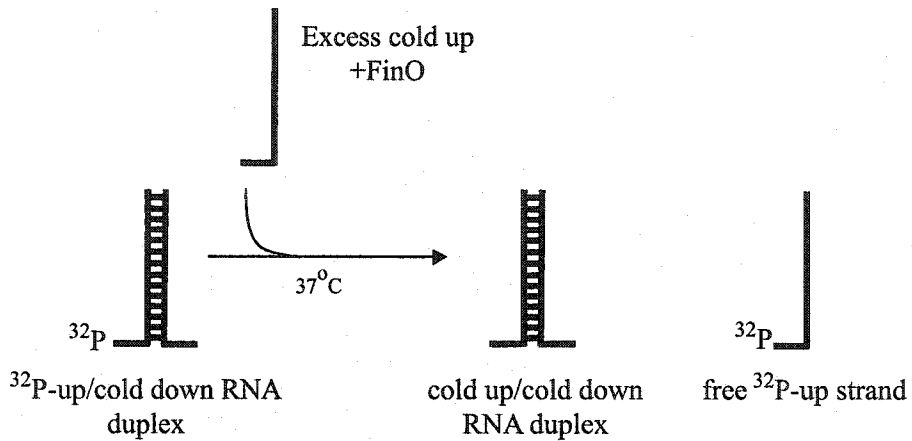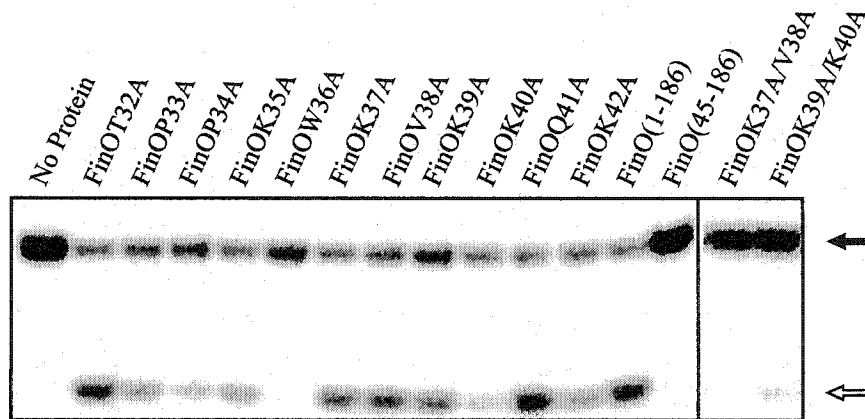
Removal of the N-terminal 25 amino acids of FinO (FinO(26-186)) decreased the RNA unwinding rate by approximately 10-fold, similar to the reduction of k_{app} for FinP/*traJ184* mRNA duplex formation mediated by this protein. Removal of the N-terminal 44 amino acids (FinO(45-186)) completely abrogated the RNA unwinding function of the protein (Figure 4.4b; Ghetu *et al.*, submitted). These results clearly illustrate that the unwinding activity of FinO resides within the N-terminal 44 amino acids of the protein. Not surprisingly, this same region appears to be responsible for catalyzing FinP/*traJ184* mRNA duplex formation, suggesting that the ability of FinO to unwind or otherwise disrupt double-stranded RNA and promote RNA/RNA duplex formation are directly linked.

4.2.3 Determining the critical amino acids of FinO involved in duplex formation.

The region of FinO that is required for both RNA unwinding and duplex formation is clearly located in the N-terminal alpha-helical region of the protein extending from Thr-26 to Ala-44. The region extending from Pro-33 to Ala-44 forms a solvent-exposed alpha helix that directly contacts its minimal RNA binding target, SL-II (Figure 4.5b; Ghetu *et al.*, 2000). Single and double alanine replacements were made in this region and tested for their ability to unwind double-stranded RNA *in vitro*. All of the RNA unwinding experiments presented in this work were performed by Dr. Alexandru Ghetu. Of the single alanine replacement mutants tested, the largest decrease in unwinding was displayed by W36A (Figure 4.4b; Ghetu *et al.*, submitted), suggesting that the hydrophobic tryptophan residue at position 36 plays a critical role in double-stranded RNA unwinding.

Figure 4.5a The primary amino acid sequence of FinO. Amino acids are represented in standard single-letter code. The region outlined in gray represents the entire solvent-exposed alpha helix extending from Trp-36 to Tyr-67. Residues that are underlined represent the region of FinO shown to influence RNA unwinding and RNA/RNA duplex formation.

Figure 4.5b The three-dimensional structure of FinO as determined by Dr. Alex Ghetu (Ghetu *et al.*, 2000). The structure represents the region extending from Trp-36 (indicated in the figure) to Gln-186 at the C-terminus. The alpha-helical region extending from Trp-36 to Leu-43 shaded in black corresponds to the underlined amino acid residues described above.

a.

```
         10          20          30          40          50          60          70
MTEQKRPVLTLKRKTEGETPTRSRKTIINVTTPPKWKVKKQKLAEKAAREAELTAKKAQARQALSIYLNL
         80          90         100         110         120         130         140
PTLDEAVNTLKPWWPGLFDGDTPRLLACGIRDVLLEDVAQRNIPLSHKKLRRALKAITRSESYLCAMKAG
        150         160         170         180
ACRYDTEGYVTEHISQEEEVYAAERLDKIRRQNRIKAELQAVLDEQ
```

b.

N

C

← Trp-36

145
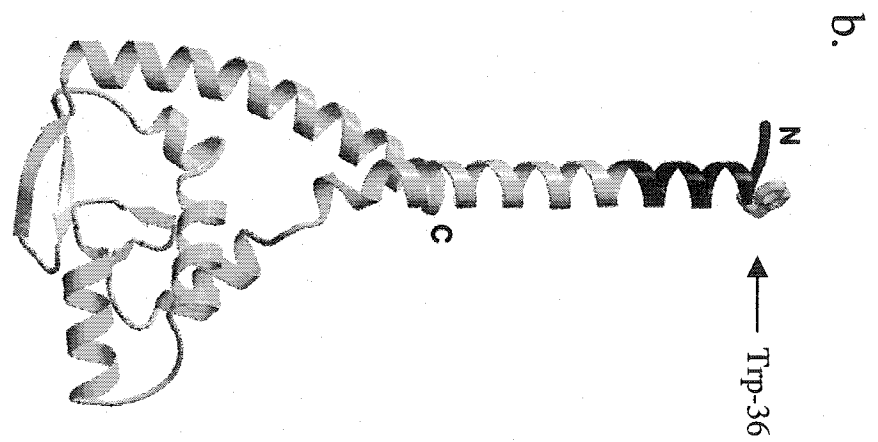
Several double alanine replacement mutants were also examined for double-stranded RNA unwinding activity, with the largest decrease in unwinding double-stranded RNA displayed by mutants K37A/V38A and K39A/K40A, which almost completely lost their unwinding functions (Figure 4.4b; Ghetu *et al.*, submitted). It is interesting to note that single alanine replacements in the region extending from K37-K40 displayed only minor decreases in RNA unwinding, but the double mutants K37A/V38A and K39A/K40A suffered a drastic loss of unwinding activity. These results suggest that this lysine-rich region plays a significant role in RNA unwinding, but the effects of these mutations *in vitro* are only evident when they are combined (Ghetu *et al.*, submitted).

To determine whether the unwinding activity of the single and double alanine replacement mutants was related to the FinP/*traJ184* mRNA duplex catalysis activity, the FinO mutants showing the most dramatic decrease in unwinding were tested via duplex formation assays as described in section 4.2.2 (Figure 4.6). As shown in Table 4.1, FinOW36A displayed a k_{app} for duplex formation of 1.2×10^7 $M^{-1}s^{-1}$, a decrease of 2.1-fold compared to wild-type FinO(1-186) (Table 4.1). The double mutants FinOK37A/V38A and K39A/K40A revealed k_{apps} of 1.5×10^7 $M^{-1}s^{-1}$ and 1.0×10^7 $M^{-1}s^{-1}$, a decrease of 1.7 and 2.5-fold, respectively, compared to wild-type FinO(1-186) (Table 4.1; Figure 4.6). These results suggest that these single and double alanine replacement mutants can promote FinP/*traJ184* mRNA duplex formation at a rate only slightly lower than wild-type FinO, even though their RNA unwinding activity is significantly impaired. It is likely that the *in vitro* RNA unwinding function of FinO is more sensitive to small mutations in the N-terminal residues tested in these assays. The duplex catalysis activity of the protein appears to depend more on the entire region extending from Thr-26 to Ala-

Figure 4.6 Comparison of FinP/*traJ184* mRNA duplex formation in the presence of FinO containing single and double alanine replacement mutations in the N-terminus of the protein. Uniformly labeled ^{32}P-FinP (7.5 fmol) of was mixed with a ten-fold molar excess of cold *traJ184* mRNA in 50 μL reactions containing TMEB duplex buffer and incubated at 37°C. The mutant FinO protein listed above each panel was present at a concentration of 1 μM. Samples were withdrawn at the times indicated above each lane and resolved on 8% non-denaturing polyacrylamide gels. Open arrows indicate free FinP while closed arrows indicate FinP/*traJ184* mRNA duplexes. The k_{app} for duplex formation was determined as described in Materials and Methods (section 2.13).

FinOW36A

| 0 | .25 | .50 | 1 | 2 | 4 | 6 | Time (minutes) |

FinO K37A/V38A

| 0 | .25 | .50 | 1 | 2 | 4 | 6 | Time (minutes) |

FinOK39A/K40A

| 0 | .25 | .50 | 1 | 2 | 4 | 6 | Time (minutes) |
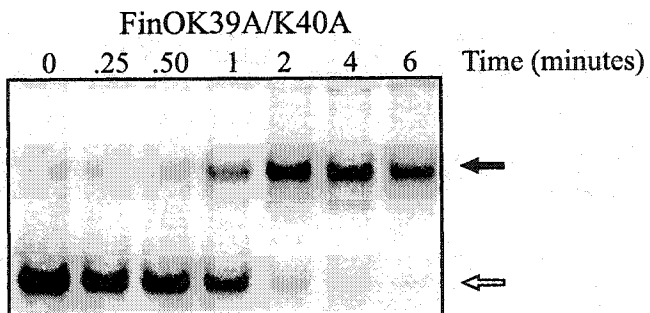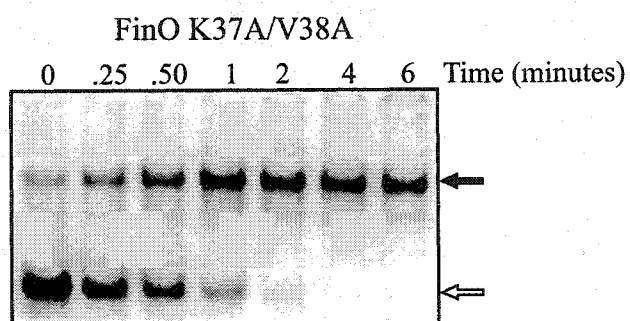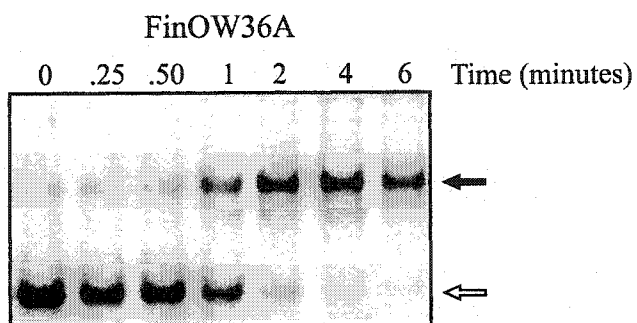
44 rather than on specific amino acids within the region. Other amino acids within this region that are less critically important for RNA unwinding can likely compensate for the loss of activity caused by alteration of the amino acids deemed to be crucial for unwinding, such as Trp-36.

4.2.4 The effect of unwinding and duplex catalysis mutations in FinO on F plasmid conjugative transfer.

The results presented thus far indicate that both the RNA unwinding and FinP/traJ184 mRNA duplex catalysis activities of FinO reside in the N-terminal region extending from Thr-26 to Ala-44. It was decided to test the effects of deletion and alanine replacement mutations of FinO on the transfer of the F-derivative plasmid pOX38-Km. FinO expressed *in trans* from the related plasmids R100 (Finnegan and Willetts, 1973) and R6-5 (van Biesen and Frost, 1992) effectively represses conjugative transfer of F. The level of repression of transfer varies from 10-1000 fold depending on which allele of *finO* is expressed by a given plasmid (Willetts and Maule, 1986). *E. coli* MC4100 cells containing pOX38-Km and one of a variety of pGEX-FinO derivative plasmids were allowed to mate with F⁻ recipient cells, and donor and transconjugant cells were selected on appropriate antibiotic media (Materials and Methods, section 2.4). This allowed the ratio of transconjugants:donors for each strain containing the pGEX-FinO plasmids to be compared to the same ratio obtained from the control strain containing pOX38-Km alone. The % mating efficiency value for pOX38-Km alone was normalized to a value of 100%, since this plasmid, like its F parent, is derepressed for transfer (Yoshioka *et al.*, 1987).

As shown in Table 4.2 and Figure 4.7, GST:FinO(1-186) provided *in trans* was fully able to repress pOX38-Km transfer, with a mating efficiency of 4.7% compared to the control of pOX38-Km alone in MC4100 (set at 100% mating efficiency). GST:FinO(26-186) displayed a reduced ability to repress pOX38-Km transfer, with a mating efficiency of 66.5%. Interestingly, the ability of GST:FinO(26-186) to repress mating varied by as much as ±33%, suggesting that the function of this mutant protein is particularly sensitive to *in vivo* conditions. As expected, GST:FinO(45-186) was unable to repress pOX38-Km transfer, consistent with its loss of ability to both unwind RNA and promote FinP/*traJ184* mRNA duplex formation (Table 4.2; Figure 4.7). Of all the single and double alanine replacement mutants tested, only GST:FinOW36A displayed a significant loss of mating repression ability, revealing a 36% mating efficiency compared to the control (Table 4.2). All of the strains were tested for pilus synthesis competency using the F-pilus specific bacteriophage R17, as an indirect measure of fertility inhibition (Materials and Methods, section 2.17). As shown in Table 4.2, sensitivity to this phage correlated perfectly with conjugative transfer ability.

4.2.5 All of the FinO mutants tested protect FinP from degradation *in vivo* and increase its half-life.

One of the *in vivo* functions of FinO is to sterically block RNase E-mediated cleavage of FinP, allowing its steady state concentration to increase until a critical concentration is reached to allow repression of *traJ* expression and subsequent inhibition of plasmid transfer (Jerome *et al.*, 1999). To ensure the reduced mating efficiency of pOX38-Km in the presence of the various pGEX-FinO mutant plasmids was not due to a reduction in the level of FinP, Northern blot analysis of FinP expressed from pOX38-Km

Table 4.2 Inhibition of pOX38-Km transfer by GST:FinO expressed *in trans* from various pGEX-FinO derivative plasmids.

GST:FinO protein expressed	% Mating Efficiency vs. pOX38-Km alone[a]	Phage R17 Sensitivity[b]
None	100	S
GST	100	S
FinO(1-186)	4.7±1	R
FinO(26-186)	66.5±33	S
FinO(45-186)	102±17.6	S
FinOT32A	3.0±0.7	R
FinOP33A	1.8±0.4	R
FinOP34A	3.4±2.8	R
FinOK35A	3.1±1.7	R
FinOW36A	36±10	R
FinOK37A	1.7±0.8	R
FinOV38A	2.1±1.1	R
FinOK39A	2.9±1.8	R
FinOK40A	2.8±1.5	R
FinOQ41A	4.8±4.3	R
FinOP34AK35A	3.3±0.6	R
FinOK37AV38A	6±1.4	R
FinOK39AK40A	1.6±0.2	R
FinOQ41AK42A	1.9±0.80	R

[a] The ratio of transconjugants:donors for each mating assay was determined, and compared to the transconjugants:donors ratio for pOX38-Km in the absence of any FinO protein, which was set as 100% mating efficiency. Values were determined from at least three separate experiments, ± standard deviation.

[b] S=sensitive, R=resistant, based on phage plaque assays as described in Materials and Methods (section 2.17).

Figure 4.7 Comparison of conjugative transfer efficiency of pOX38-Km in the absence of FinO and in the presence of various GST:FinO mutant derivative proteins expressed *in trans*. *E. coli* MC4100 strains containing the F-derivative plasmid pOX38-Km and various pGEX-FinO plasmids were allowed to mate with the recipient *E. coli* strain ED24 for 30 minutes. Donor and transconjugant cells were selected on appropriate antibiotic media as described in detail in Materials and Methods (section 2.4). The percent mating efficiency of each strain containing a pGEX-FinO plasmid was determined by comparing the ratio of transconjugants:donors for each strain to the same ratio obtained from the mating of MC4100 cells containing only pOX38-Km. The transconjugant:donor ratio of MC4100 containing pOX38-Km alone was used to set the 100% mating efficiency level because this plasmid does not encode *finO* and is derepressed for transfer. The percent mating efficiency of each strain is listed to the left of the graph, and the pGEX-FinO plasmid present in the donor cells along with pOX38-Km are listed along the bottom of the graph.

Plasmids present in donor MC4100 cells
along with pOX38-Km
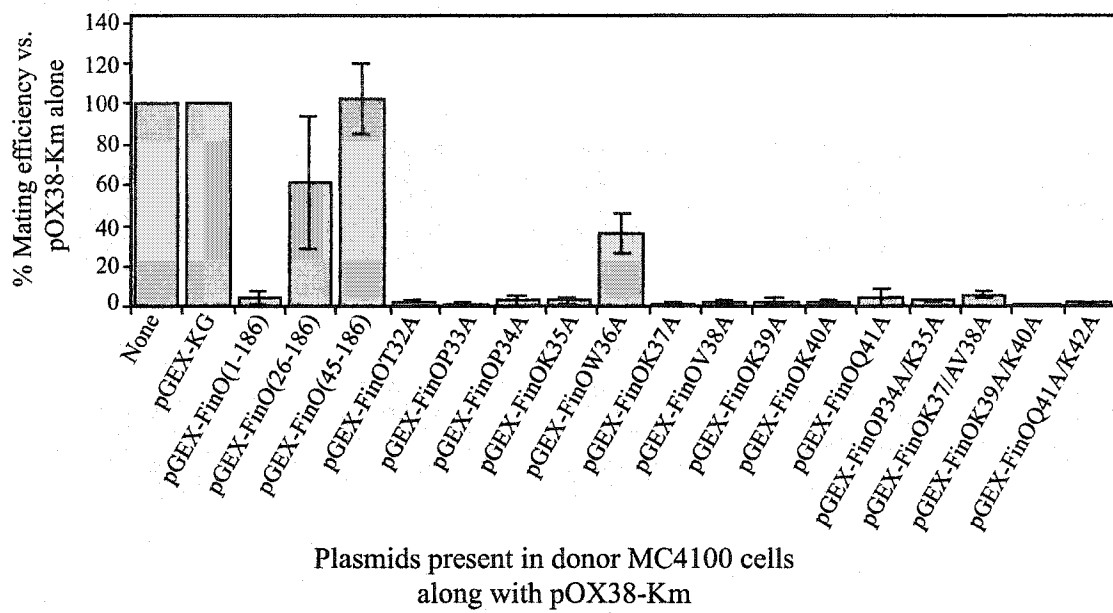
was performed. MC4100 cells containing pOX38-Km alone or pOX38-Km and one of the co-resident pGEX-FinO plasmids were grown in liquid culture to mid-log phase, at which time an initial culture sample was taken (time=0). Rifampicin was added to prevent further rounds of transcription, and samples were taken from each culture over two hours. Total cellular RNA was extracted from all of the samples, equal amounts were separated by electrophoresis on 8% denaturing polyacrylamide gels, and transferred to nylon membranes. The blots were probed with the FinP-specific probe LFR21 and the tRNA^{ser}-specific probe JSA12 (Table 2.3; Materials and Methods section 2.8). The signal obtained from FinP at each time-point was then normalized against the equivalent signal obtained from tRNA^{ser}. A plot of the normalized signal obtained from FinP against the time of sampling was then used to calculate the half-life of FinP, determined by the time required for 50% of the signal to decay (data not shown).

As shown in Figure 4.8, FinP is detectable in the absence of FinO until 60 minutes after the addition of rifampicin, and the half-life was calculated to be approximately 40 minutes, similar to the negative control containing pGEX-KG. Accurate half-lives were difficult to determine in the absence of FinO due to the small amount of FinP expressed from the low copy number pOX38-Km plasmid. Nonetheless, it is clear from the Northern blots that FinP levels decrease significantly with time. In the presence of GST:FinO(1-186), the total amount of FinP was increased considerably, and the half-life of FinP was extended to over two hours (Figure 4.8). Similar results were observed with the GST:FinOW36A, K37A/V38A, and K39A/K40A mutants. GST:FinO(26-186) and GST:FinO(45-186) showed a smaller increase in the total amount of FinP, however the half-life was still extended to over two hours. These results indicate

Figure 4.8 Both the total amount and half-life of FinP are increased in the presence of wild-type and various mutant GST:FinO fusion proteins expressed *in trans. E. coli* MC4100 cells containing no plasmid, pOX38-Km alone, or pOX38-Km and various pGEX-FinO plasmids as indicated above each panel were grown approximately to mid-log phase in liquid culture. Samples were withdrawn at the times indicated (minutes) after the addition of rifampicin to each culture to stop further rounds of transcription, and total cellular RNA was extracted as described in Materials and Methods (section 2.8). Thirty-five µg of RNA were separated by electrophoresis on denaturing (8M urea) 8% polyacrylamide gels, and subjected to Northern blot analysis as described in detail in Materials and Methods (section 2.8). The position of FinP, detected using Primer A (Materials and Methods, Table 2.3), is indicated to the right of each panel. Blots probed for FinP were stripped and reprobed using the primer JSA12 (Materials and Methods, Table 2.3) to detect the internal loading control, $tRNA^{ser}$. The position of $tRNA^{ser}$ is shown to the right of the bottom panel, a representative internal loading control blot.
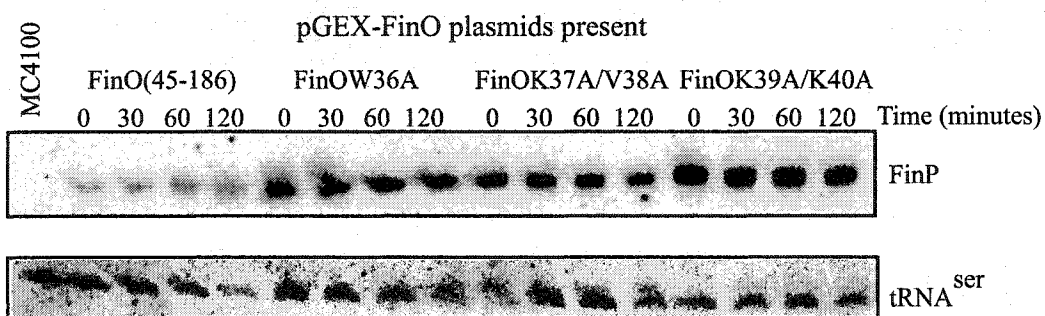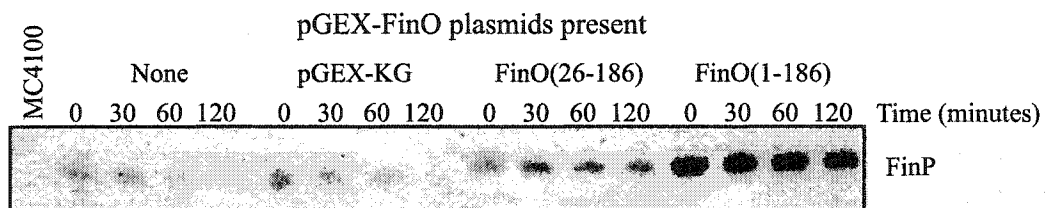
that any effects seen on conjugative transfer of pOX38-Km were not due to an inability of the GST:FinO proteins to protect FinP from RNase E-mediated degradation.

To estimate the increase in the level of FinP mediated by each GST:FinO mutant, the level of FinP expressed from pOX38-Km in each strain at time 0 was compared to the level expressed from pOX38-Km in the absence of any FinO at time 0, as determined from the normalized FinP signal obtained from the Northern blot analyses. As shown in Figure 4.9, GST:FinO(1-186) and GST:FinOW36A each resulted in an approximately 4.5-fold increase in the level of FinP. GST:FinO(26-186) and GST:FinO(45-186) mediated an approximately 1.8-fold increase in the level of FinP, while GST:FinOK37A/V38A resulted in an approximately 3-fold increase in the level of FinP (Figure 4.9). The largest increase in FinP levels was evident in the presence of GST:FinOK39A/K40A, which showed an approximately 7-fold increase (Figure 4.9). It should be noted that these values were obtained from two trials. To confirm that any differences in FinP levels were not due to differences in the level of expression of the GST-fusion proteins, Western immunoblot analysis was performed on samples obtained from the same cultures used for the Northern analyses. Cell pellets equivalent to 0.1 OD_{600} were obtained from all of the cultures immediately before the addition of rifampicin, and subjected to SDS-PAGE and immunoblot analysis. The GST:FinO fusions were detected using monoclonal anti-GST antibodies (Sigma) as described in Materials and Methods (Section 2.5). Native FinO expressed from the F-like plasmid R100 was also examined, using polyclonal anti-FinO antiserum, in order to compare the relative levels of GST:FinO expression to natural FinO expression. As shown in Figure 4.10, all of the GST:FinO proteins tested were detectable at levels comparable to the level

Figure 4.9 The relative level of FinP expressed from pOX38-Km is increased to varying

degrees in the presence of GST:FinO and several GST:FinO mutant derivatives. Levels

of FinP expressed from pOX38-Km in MC4100 cells containing various pGEX-FinO

derivative plasmids were determined as described in the legend to Figure 4.8 and in

Materials and Methods (section 2.8). The baseline level of FinP expressed in the absence

of FinO was set using the level of FinP present in cultures of MC4100 containing

pOX38-Km alone, as determined from Northern blot analysis of the initial sample of

cellular RNA extracted from cultures before the addition of rifampicin (Time 0 in Figure

4.8). This baseline level is not included in this figure. The relative level of FinP

expressed at the same time point from pOX38-Km in the presence of various pGEX-FinO

plasmids was determined by comparing the FinP signal obtained to the baseline level

obtained in the absence of FinO. The fold-increase in FinP level in each case is listed to

the left of the graph, while the pGEX-FinO plasmids present in each strain are listed on

the bottom of the figure.

pGEX-FinO plamids present in MC4100 cells
along with pOX38-Km
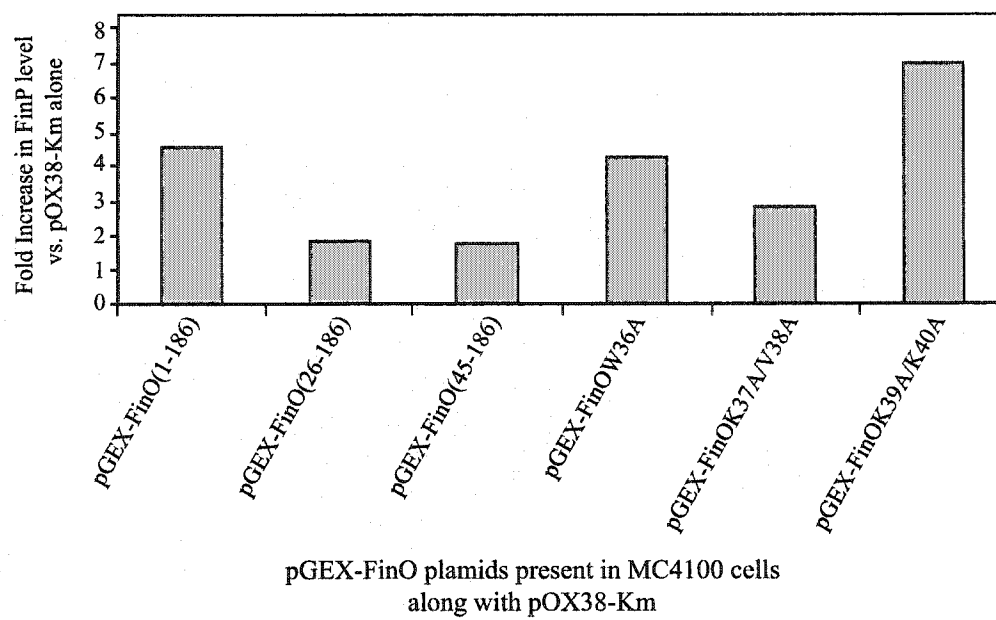
Figure 4.10 GST:FinO derivative proteins are expressed *in vivo* from various pGEX-FinO plasmids at levels similar to wild-type R100 FinO. Western immunoblot analysis was performed on MC4100 cells containing pOX38-Km and the pGEX-FinO plasmids listed above each panel. Cell pellets comprising 0.1 OD_{600} equivalents were subjected to SDS-PAGE and immunoblot analysis as described in detail in Materials and Methods (section 2.5). Monoclonal anti-GST antibodies (Sigma) were used to detect the GST:FinO fusion proteins, while polyclonal anti-FinO antiserum raised in rabbits was used to detect FinO expressed from the F-like plasmid R100. Relevant molecular weight markers (kDa) are shown on the left of the figure. The FinO band derived from R100 is shown as a reference for comparing relative protein levels only, and is not represented in the figure at its actual molecular mass of 21.2 kDa.
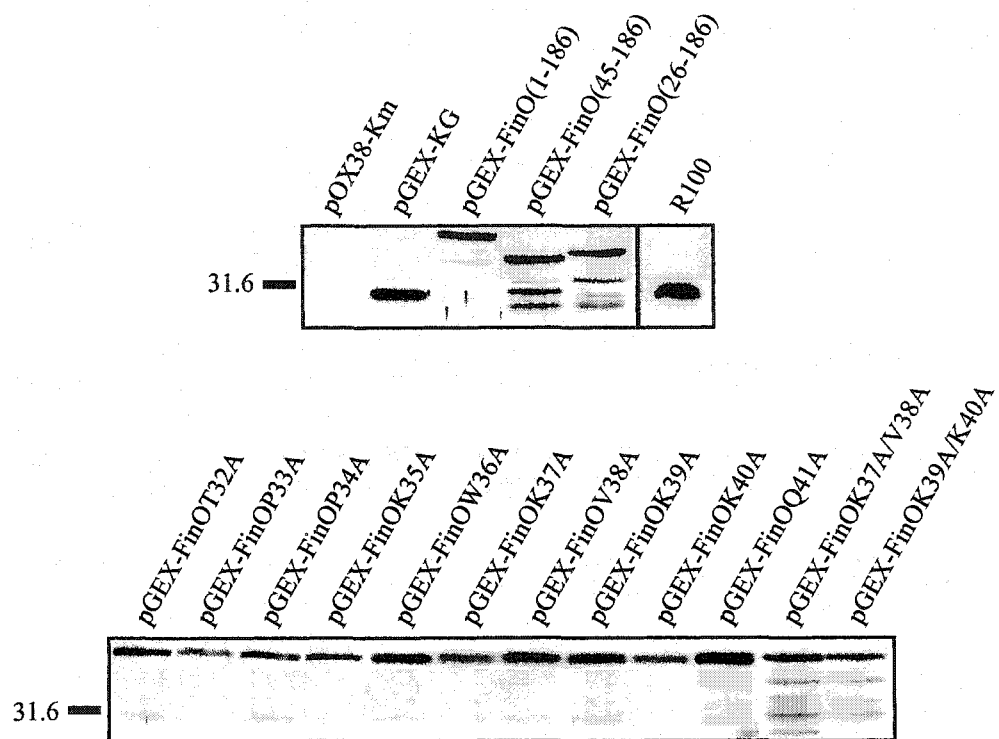
of R100 FinO, suggesting that the level of GST:FinO proteins expressed from the pGEX plasmids did not have any influence on either mating inhibition or FinP half-life. Some GST:FinO degradation products can be seen in the immunoblot (Figure 4.10), however the major protein species evident the relevant lanes is the full-length GST:FinO derivative protein. Therefore, any degradation appeared to have little or no obvious effect on the function of the proteins *in vivo*. While it is unknown at this time why these proteins cause such varied increases in the level of FinP expressed from pOX38-Km, it is clear that all of the FinO mutant proteins tested increase the half-life of FinP antisense RNA.

4.2.6 FinO-mediated double-stranded RNA unwinding, RNA/RNA duplex catalysis, and mating inhibition are correlated.

A summary of the correlation between FinO-mediated double-stranded RNA unwinding, FinP/*traJ184* mRNA duplex formation, and mating inhibition is presented in Figure 4.11. Deletion of the N-terminal 25 (FinO(26-186)) or 44 (FinO(45-186)) amino acids of FinO caused significant reductions in all three activities. The single alanine replacement mutant FinOW36A caused a severe deficit in the ability of FinO to mediate RNA unwinding, and a significant reduction in the ability of the protein to mediate fertility inhibition. However, this mutant FinO promoted FinP/*traJ184* mRNA duplex formation at a rate only slightly lower than wild-type FinO(1-186). A much weaker correlation could be made between the activities mediated by the double alanine replacement mutants FinOK37A/V38A and FinOK39A/K40A. Both of these mutants suffered a significant loss of RNA unwinding ability, however they were able to promote FinP/*traJ184* mRNA duplex formation and fertility inhibition at only slightly reduced

Figure 4.11 Comparison of FinP/*traJ184* mRNA duplex formation, RNA unwinding, and mating inhibition activities of selected FinO derivatives. The values obtained for these parameters, as previously described, were compared for each of the selected FinO derivatives, listed below the figure. Each value obtained for each FinO mutant derivative was compared to the optimum value obtained from wild-type FinO(1-186). This optimum value was set at 1, and the lowest value of 0 was set based upon each listed activity in the absence of FinO. Relative values for each parameter are listed on the left of the graph.

FinO Protein Tested
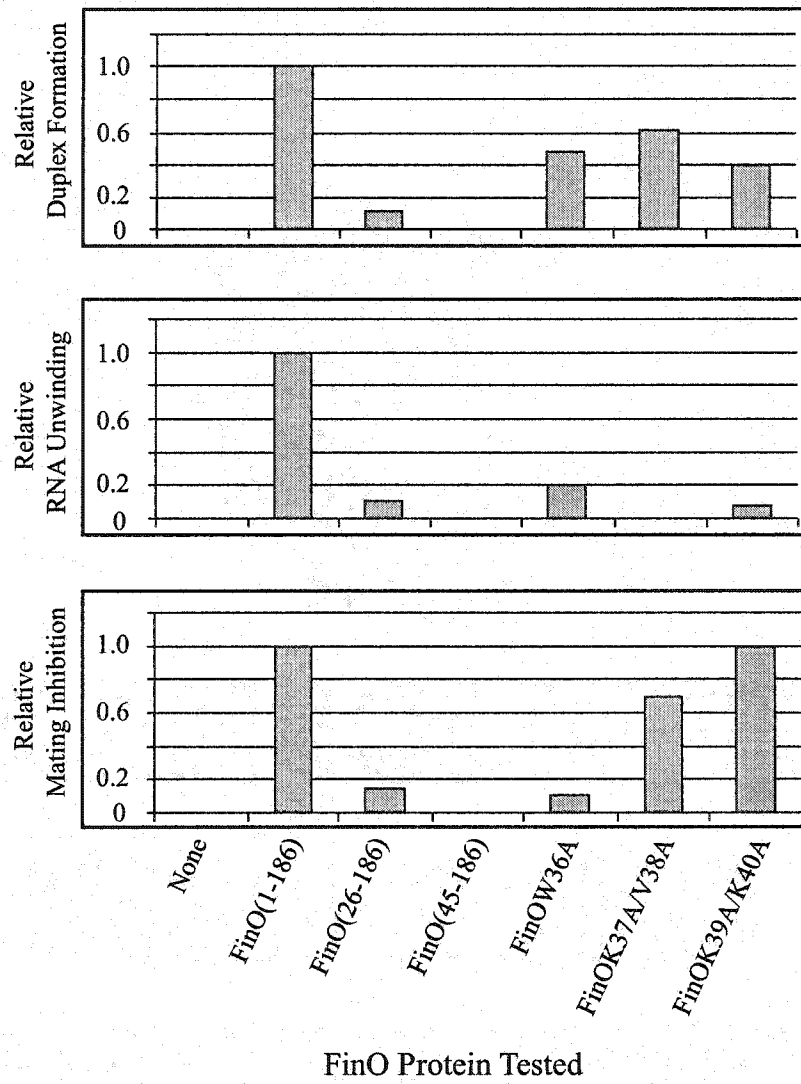
levels compared to wild-type FinO(1-186). Overall, a good correlation could be made between RNA unwinding, fertility inhibition, and RNA duplex catalysis mediated by the region of FinO extending from Thr-26 to Ala-44 in the N-terminal alpha helix of FinO. This correlation was most evident only when the entire Thr-26 to Ala-44 region of FinO was deleted, while alteration of specific amino acids within this region showed a far weaker correlation between the functional activities of the protein described above.

4.3 Discussion

This chapter confirms that the FinO protein of F-like plasmids increases the rate of RNA/RNA interactions *in vitro* between its targets, FinP antisense RNA and *traJ* mRNA. The N-terminal alpha helical region of FinO extending from Met-1 to Ala-44 appears to confer the ability of FinO to catalyze RNA/RNA duplex formation and double-stranded RNA unwinding (Ghetu *et al.*, submitted). More specifically, residues extending from Thr-26 to Ala-44 are responsible for FinP/*traJ* duplex catalysis, FinOP-mediated repression of F transfer, and ATP-independent double-stranded RNA unwinding (Ghetu *et al.*, submitted). High-resolution crystallographic studies show that the region of FinO extending from Thr-26 to Ala-44 is situated within a lysine-rich, solvent-exposed alpha-helix (Figure 4.5b; Ghetu *et al.*, 2000). It has been proposed that the long N-terminal alpha-helix of FinO aligns with the helical stem of FinP SL-II, placing this region in close proximity to the loop of the RNA (Ghetu *et al.*, 2000). Replacement of the tryptophan residue at position 36 in FinO with alanine demonstrated the importance of this residue in unwinding double-stranded RNA (Ghetu *et al.*, submitted). The potential alignment of FinO with the stem of FinP SL-II may position

Trp-36 in close proximity to the loop, which may then allow it to intercalate between base pairs in the stem to promote stem disruption or stack with unpaired bases in the loop (Ghetu et al., 2000). Substrate unwinding by ATP-dependent RNA and DNA helicases has been shown to involve the stacking of hydrophobic amino acids with unpaired bases (Kim et al., 1998; Marians, 2000; reviewed in Tanner and Linder, 2001). Further investigation will be required to determine if FinO in fact uses this mechanism during the process of double-stranded RNA unwinding.

Pro-34, Lys-35, Lys-40, and Lys-42 of FinO were shown by alanine replacement to influence RNA unwinding (Ghetu et al., submitted), however these residues did not have any significant influence on mating inhibition in vivo. Mating inhibition is affected by a variety of factors (Frost et al., 1994), including the concentration of FinO and its RNA targets, nutrient availability, and temperature, among others. Furthermore, interactions of the FinOP system in vivo occur between full length FinP and traJ mRNA, which differ in size, and likely in overall tertiary structure, compared to the in vitro RNA target employed in unwinding assays. It is not entirely surprising then, that the importance of single residues in in vitro unwinding assays was not completely reflected in the mating inhibition assays. It is clear, however, that all of the mutant FinO proteins tested were able to protect FinP antisense RNA from degradation in vivo. This observation confirms the importance of the function of FinO in increasing the steady-state level of FinP during the process of mating inhibition. Overall, the results suggest that the ability of FinO to unwind double-stranded RNA is not inextricably linked to the ability of the protein to mediate fertility inhibition, and that other factors must influence the ability of FinO to perform this function in vivo.

FinOW36A was the only single-residue alanine replacement mutant that exhibited a significantly reduced ability to both unwind double-stranded RNA and repress F transfer. The critical function of Trp-36 may be to facilitate the formation of the initial loop-loop kissing interaction between FinP and *traJ* mRNA. Its unwinding activity may act to destabilize the upper stem regions of the stem-loops in both molecules, stabilizing the kissing intermediate. This initial interaction may be sufficient to inhibit *traJ* translation (Jerome and Frost, 1999), explaining why replacing Trp-36 with alanine reduced the ability of FinO to inhibit conjugative transfer of pOX38-Km. Indeed, full duplex formation between CopA and its target, CopT, is not a requirement for inhibiting plasmid R1 replication control (Malmgren *et al.*, 1997; Kolb *et al.*, 2000a). The importance of Trp-36 in RNA unwinding and FinP/*traJ184* mRNA duplex formation was not as well correlated. While unwinding of the FinP and *traJ* mRNA stems mediated by Trp-36 may be an important initial step in duplex formation, FinO may function after this initial step to facilitate alignment of complementary single-stranded regions of FinP and *traJ* mRNA to propagate intermolecular interactions. Other amino acids in the region extending from Thr-26 to Ala-44 may be able to compensate for the loss of Trp-36 function during this process. Removal of the N-terminal 25 amino acids of FinO caused an approximately 10-fold reduction in both the rate of FinP/*traJ* mRNA duplex formation and the rate of double-stranded RNA unwinding *in vitro* (Ghetu *et al.*, submitted). These N-terminal 25 amino acids may therefore also help to partially compensate for the loss of RNA unwinding activity exhibited by FinOW36A, allowing this protein to promote FinP/*traJ* mRNA duplex formation at nearly wild-type levels. Since the structure of this portion of FinO is currently unknown (Ghetu *et al.*, 2000), it is difficult to predict what

precise function this region may have in RNA/RNA duplex formation. Overall, the data suggest that a significant loss of the unwinding ability of FinO resulting from replacement of Trp-36 with alanine may cause a less severe decrease in its ability to promote RNA/RNA duplex formation while significantly reducing FinO-mediated fertility inhibition.

The critical function of residues in the region of FinO which were shown to be responsible for RNA unwinding is probably to disrupt the intramolecular helices immediately below the loops of FinP SL-I and SL-II (SL-Ic and SL-IIc in *traJ* mRNA). Destabilization of intramolecular RNA secondary structure is a common mechanism that results in the facilitation of RNA/RNA pairing in several biological systems (Muriaux *et al.*, 1996; Kolb *et al.*, 2001a; Takahashi *et al.*, 2001; Bernacchi *et al.*, 2002). It is likely that FinP/*traJ* mRNA duplex formation depends on such disruptions to promote an opening of the secondary structure of SL-I and SL-II to create more single-stranded regions available for interstrand duplex formation.

The exact mechanism for FinO-mediated duplex formation is still not known. The results presented in this chapter provide insight and preliminary evidence of how such interactions might occur. In the next chapter, an examination of the RNA structural features of FinP and *traJ* mRNA which influence FinO-mediated duplex formation presents further evidence of how this system functions to cause such a significant level of RNA/RNA duplex formation *in vitro*, and how the system efficiently represses F transfer *in vivo*.

Chapter 5: Analysis of FinO-mediated duplex formation

5.1 Introduction

Antisense/sense RNA mechanisms for control of gene expression are common in a wide variety of organisms (reviewed in Brantl, 2002). Antisense RNA interactions are key components of plasmid replication control for the *E. coli* plasmids ColE1 (Tomizawa and Som, 1984; Eguchi *et al.*, 1991), R1 (Wagner and Simons, 1994), and F, the paradigm for pilus-mediated plasmid transfer (reviewed in Frost *et al.*, 1994). The FinOP system of F and F-like plasmids controls *tra* operon expression, and thus plasmid transfer, by regulating expression of the positive regulatory protein, TraJ (Finnegan and Willetts, 1971). The 5′ UTR (untranslated region) of *traJ* mRNA, which contains SL-Ic and SL-IIc, is perfectly complementary to SL-I and SL-II, respectively, of the antisense RNA, FinP (Figure 5.1). The *traJ* RBS (ribosome binding site) extends down the 3′ side of the loop of SL-Ic and into the top portion of the stem of SL-Ic (Figure 5.1). Binding of FinP to the 5′ UTR of *traJ* mRNA is believed to sequester the RBS within a FinP/*traJ* mRNA duplex, preventing TraJ translation (Mullineaux and Willetts, 1985).

The regulatory activity of FinP depends upon the action of the plasmid-encoded RNA binding protein, FinO (Yoshioka *et al.*, 1987). One of the functions of FinO is believed to be the promotion of FinP/*traJ* mRNA duplex formation *in vivo* to prevent translation and accumulation of TraJ. Support for this *in vivo* activity has been strengthened by the finding that FinO efficiently catalyzes FinP/*traJ* mRNA duplex formation *in vitro* (Chapter 4; van Biesen *et al.*, 1993; van Biesen and Frost, 1994; Ghetu *et al.*, 2000). FinO can bind to multiple FinP and *traJ* mRNA species and inhibit transfer of several related F-like plasmids (Finnegan and Willetts, 1973; van Biesen and Frost,

Figure 5.1 Secondary structure of FinP antisense RNA and a portion of the 5' UTR of

traJ mRNA. Only the portion of the 5' UTR of *traJ* that is complementary to FinP

antisense RNA is shown for clarity. Black lines indicate the *traJ* mRNA RBS and the

corresponding anti-RBS of FinP. The *traJ* start codon is shown in italics. The secondary

structures are based on FinP and *traJ* mRNA mapping studies as performed in van Biesen

et al., (1993).

SL-II

SL-I

FinP

```
                        A
                     C     C
                   U         G
                    U       U
       C A 20        G C 60
     U     C        A U
    C       A    50 G C
    C  U A A        G C
       U A          G C
       C G          A U
       C G          C G
    A       A       G C
      A U           U A
  10 G·U            A U
     G C 30         A U
     A U            G C 70
     U A          40 C G
     A U            U·G
5'-GAUA C G GACA G C GAUUUU-3'
```

traJ mRNA

SL-IIc

SL-Ic

```
                   U
                G     G
               C       A
              A         A
               G C 60
               A U
            50 G C
               G C
               G C
               A U
               C G
               G C 70
               U A
               A U
               G C
               C G
5'.......AAAAUCGC      ACUGUC
              40
```

```
                 U G
              G       A
           90 U         G
               U       G
                U A
                C G
                C G
              U     U 100
              A U
              A     C
              G C
              A U
           80 U A
              A U
              C G
                    C G UAUC............3'
                    110
```
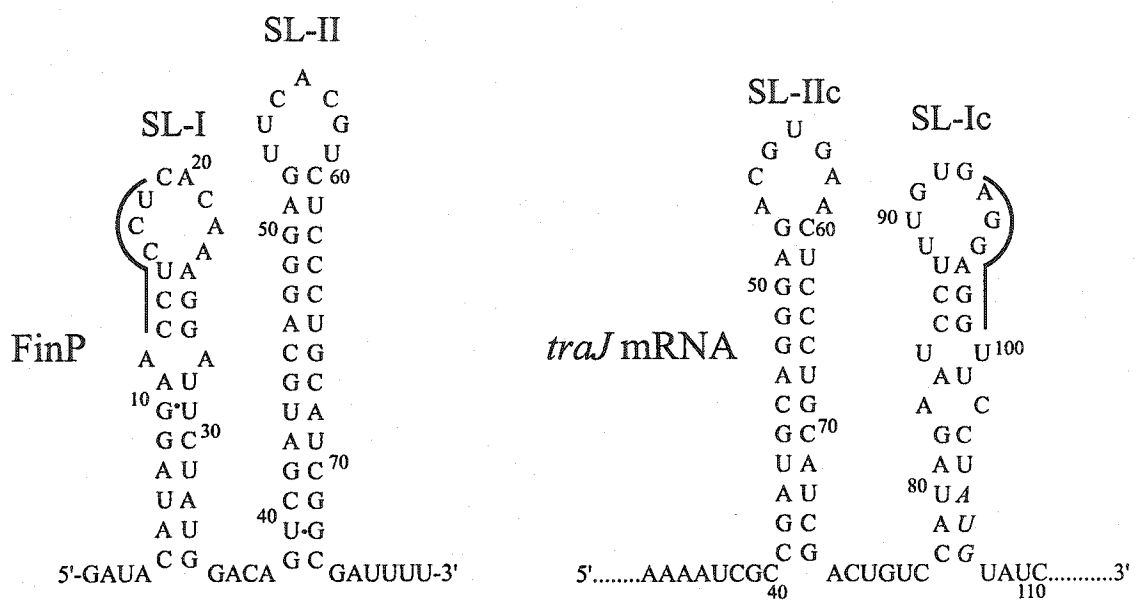
1992; Jerome and Frost, 1999). This observation suggests that FinO can also catalyze the formation of duplexes between RNAs that contain differences in their primary sequences.

Kissing interactions between loops of RNA stem-loop structures are usually the first interaction to occur during the process of RNA:RNA duplex formation (Wagner and Simons, 1994; reviewed in Brantl, 2002). F-like conjugative plasmids encode eight different alleles of FinP, with the highest variability in the loops and a high degree of conservation in the stems (Figure 5.2; Finlay *et al.*, 1986; Frost *et al.*, 1994). The loop sequences of FinP and *traJ* mRNA are therefore responsible for mediating the plasmid specificity of the F-like FinOP systems, and are thought to be the initial site of interaction between the sense and antisense RNAs (Koraimann *et al.*, 1991, 1996). Although the loop sequences of FinP in F-like plasmids vary considerably, a common motif, 5'-YUNR-3' (Y=C or U, N=any base, R=A or G), is found in many *finP* alleles, and it forms a key structural feature in the loops of several plasmid antisense RNA systems (Figure 5.2; Franch *et al.*, 1999). The secondary structure of antisense RNAs and their target RNAs is an important determining factor in their efficient transition into stable duplexes, which is critical for their regulatory role in gene expression (Tomizawa, 1984; Hjalt and Wagner, 1995; Kolb *et al.*, 2000a; reviewed in Brantl, 2002).

A preliminary examination of the structural features of FinP and *traJ* mRNA that influence FinO-mediated RNA:RNA duplex formation is presented in this chapter. Duplex analyses employing EMSAs using *in vitro* synthesized RNAs (Figure 5.3) and purified FinO reveal that multiple structural features of the interacting RNAs influence their formation into RNA:RNA duplexes.

Figure 5.2 Comparison of six different alleles of FinP encoded by F-like plasmids. The F-like plasmids from which the *finP* alleles are derived are listed on the left of the figure. The stem regions of each stem loop are underlined. The single-stranded regions at the 5' and 3' end of the RNAs, and the spacer separating SL-I and SL-II are indicated above each region in the diagram. The conserved 5'-YUNR-3' motif (Y=C or U, N=any base, R=A or G) present in Loop I or Loop II of each sequence is outlined by black boxes. This figure is adapted from Jerome and Frost (1999).

	5' tail	Loop I	Spacer	Loop II	3' tail

F   GAUACAUAGGAACCUC CUCA CAAAGGAUUCUAUGGACAGUCGAUGCAGGGAG UUCA CGUCUCCCUGCAUCGGCGAUUUU 79

ColB2 AUACAUAGGAACCUC CUCA CAAAGGAUUCUAUGGACAGUCGAUGCAGGGAG UUCA CGUCUCCCUGCAUCGGCGAUUUU 78

R1-19 ACACAUAGGAACCUC--CGUUAAGGAUUCUAUGGACAGUCGAUGCAGGGAG UUCA GACCUCCCUGCAUCGGCGAUUUU 76

R100-1 AUACAUAGGAACCUCCU CUCA AAGGAUUCUAUGGACAGUCGAUGCGGGGAGGUCGC-UCUCCCUGCAUCGGCGAUUUU 77

ColB4 ACACAUAGGAACCUC--CGUUAAGGAUUCUAUGGACAGUCGAUGCAGGGAGGU CUGA ACUCCCUGCAUCGGCGAUUUU 76

SU233 ACACAUAGGAACCUC-- CUCA AAGGAUUCUAUGGACAGUCGAUGCAGGGAGGGACAAGCUCCCUGCAUCGGCGAUUUU 76

175

Figure 5.3 *In vitro* transcribed FinP SL-I and *traJ* SL-Ic constructs employed in this work. All RNAs were transcribed and purified as outlined in Materials and Methods (section 2.11) using the oligonucleotide primer templates listed in Table 2.3. Loop and single-base stem mutations are indicated in bold text. The *traJ* mRNA start codon in the SL-Ic constructs is indicated in italics. The regions of the SL-Ic stem that were changed to remove complementarity with the corresponding regions in SL-I are outlined by black boxes. RNA secondary structure predictions were performed as outlined in Materials and Methods (section 2.16). All of the RNAs shown in this figure contain an extra G residue at their 5′ ends. This extra residue is omitted from the diagram simply for clarity.

SL-I(Δtails)

SL-I(Δ3'tail)

SL-I(Δ5'tail)

SL-I(21-23)

SL-I(18-21)

SL-I(16-18)

SL-I

SL-IcR

SL-I(A27U)

SL-Ic(BSR)

SL-Ic(TSR)

SL-Ic(U85A)

SL-Ic(Δtails)

SL-Ic(Δ3'tail)

SL-Ic(Δ5'tail)

SL-Ic
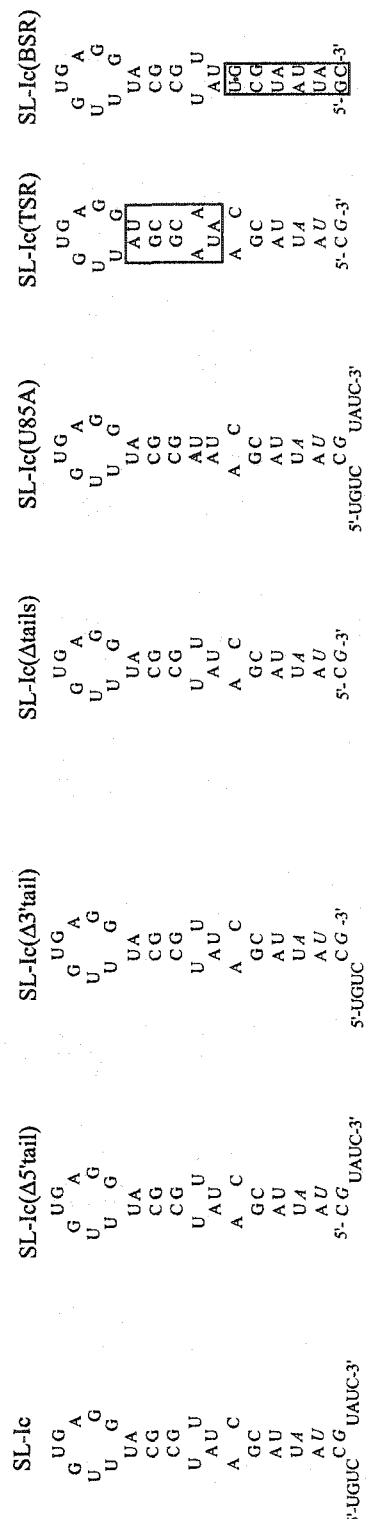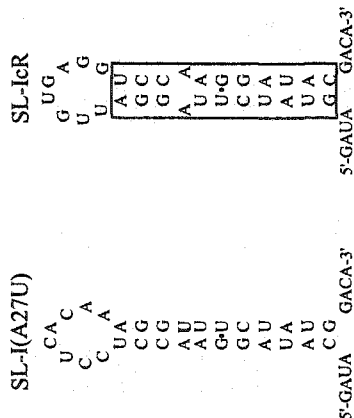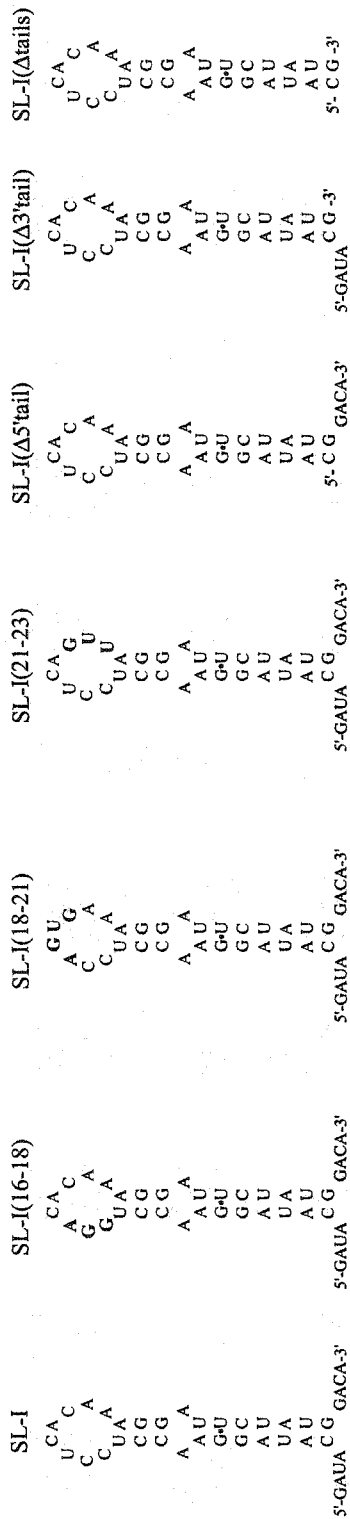
5.2 Results

5.2.1 FinP SL-I and SL-II contribute to FinP/*traJ* duplex formation.

FinO from the related F-like plasmid R6-5 has been determined to function *in vivo* to repress F transfer, and *in vitro* to both bind FinP antisense RNA and promote duplex formation between FinP and *traJ* mRNA (van Biesen *et al.*, 1993; Ghetu *et al.*, 1999; Ghetu *et al.*, 2000). In the absence of FinO, FinP/*traJ184* mRNA duplex formation occurs *in vitro* with a k_{app} of 5×10^5 $M^{-1}s^{-1}$, and in the presence of wild-type R6-5 FinO, the k_{app} increases to 2.5×10^7 $M^{-1}s^{-1}$ (Chapter 4; Ghetu *et al.*, 2000). In this chapter, a variety of RNA stem-loop constructs derived from FinP and *traJ184* mRNA were synthesized *in vitro* (Figure 5.3) and subjected to EMSA analysis to determine their apparent second-order association rate constants in the presence and absence of FinO (Materials and Methods, section 2.14). Non-denaturing polyacrylamide gels were used because previous work employing denaturing PAGE resulted in protein/RNA aggregation in the wells of the gels (van Biesen, 1994).

Analysis of FinP SL-I and FinP SL-II duplexing with *traJ184* mRNA revealed that SL-I/*traJ184* mRNA duplex formation occurs at a rate of 7.4×10^3 $M^{-1}s^{-1}$ without FinO, and a rate of 4.0×10^5 $M^{-1}s^{-1}$ in the presence of FinO (Figure 5.4a; Table 5.1). FinP SL-II duplexes with *traJ184* mRNA at a rate of 2.1×10^4 $M^{-1}s^{-1}$ in the absence of FinO, and a rate of 2.8×10^5 $M^{-1}s^{-1}$ in the presence of FinO (Figure 5.5a; Table 5.1). In the absence of FinO, a third band was evident in the SL-II/*traJ184* mRNA duplex formation assays in the absence of FinO (Figure 5.5a). This result was unexpected, however it was reproducible. The constituents of this band are unknown at this time, but may represent an alternate conformation of a complex formed between SL-II and *traJ184*

Figure 5.4a EMSA analysis of duplex formation between SL-I and *traJ184* mRNA in the presence and absence of FinO. Sixty fmol of ^{32}P-labeled SL-I were incubated with 600 fmol of unlabeled *traJ184* mRNA in a 50μl reaction containing TMN buffer, and incubated at 37°C in the presence or absence of 6μM FinO (as indicated above each panel). Samples were taken at 0, 15, 30, 60, and 120 minutes (-FinO) and at 0, 0.25, 0.5, 1, 2, 4, 6, 10, and 15 minutes (+FinO), and separated by electrophoresis on 8% non-denaturing polyacrylamide gels. Free RNA is denoted by open arrows, duplex RNA by closed arrows. The k_{app} for duplex formation was determined based upon the amount of time required for 50% of the labeled RNA to form a duplex with its unlabeled cognate binding partner, and the concentration of the unlabeled RNA species in excess, as described in Materials and Methods, sections 2.13 and 2.14.

Figure 5.4b EMSA analysis of duplex formation between SL-I and SL-Ic in the presence and absence of FinO. The legend for this figure is the same as the legend for Figure 5.4a, except in the presence of FinO, samples were taken at 0, 1, 2, 4, 6, 8, 10, and 15 minutes.

a. SL-I/*traJ184*

- FinO   + FinO

0   120   0   15   Time (minutes)

b. SL-I/SL-Ic

- FinO   + FinO

0   120 0   15   Time (minutes)
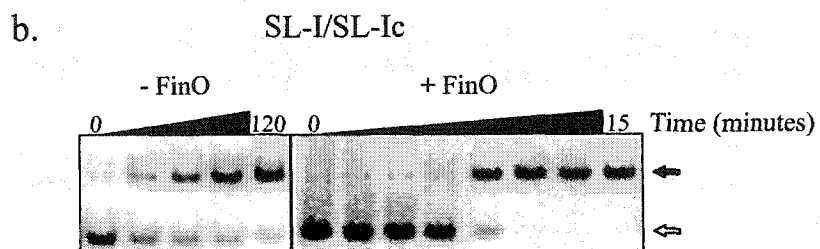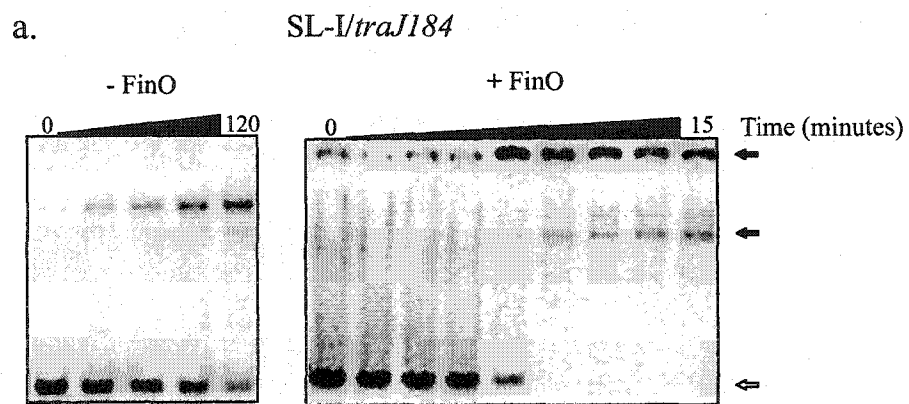
Table 5.1 k_{app} values for duplex formation of various SL-I and SL-II derivatives with their interacting RNA partners.

RNAs present	$\times 10^5 \, k_{app} \, (M^{-1}s^{-1})^{\,a}$ -FinO	Relative k_{app} $(\%)^{b}$	$\times 10^5 \, k_{app} \, (M^{-1}s^{-1})^{\,a}$ +FinO	Relative k_{app} $(\%)^{b}$
FinP/traJ184^c	4.9 ± 2	100	250 ± 100	100
SL-II/traJ184	0.21	4.3	2.8 ± 0.4	1.1
SL-II/SL-IIc	0.25 ± 0.02	5.1	0.39 ± 0.2	0.2
SL-I/traJ184	0.074 ± 0.006	1.5	4.0 ± 0.7	1.6
SL-I/SL-Ic	0.31 ± 0.07	6.3	5.3 ± 1.0	2.1

^{a} k_{app} values are an average of at least two to three independent EMSA analyses, ± standard deviation where appropriate.

^{b}Relative k_{app}=[k_{app}(variant pair)/k_{app} (FinP/traJ184 mRNA)]×100

^{c} Value was obtained from experiments performed in Chapter 4.

Figure 5.5a EMSA analysis of duplex formation between SL-II and *traJ184* mRNA in the presence and absence of FinO. Sixty fmol of ^{32}P-labeled SL-II were incubated with 600 fmol of unlabeled *traJ184* mRNA in a 50µl reaction containing TMN buffer, and incubated at 37°C in the presence or absence of 6µM FinO (as indicated above each panel). Samples were taken at 0, 15, 30, 60, and 120 minutes (-FinO) and at 0, 0.25, 0.5, 1, 2, 4, 6, 10, and 15 minutes (+FinO), and separated by electrophoresis on 8% non-denaturing polyacrylamide gels. Free RNA is denoted by open arrows, duplex RNA by closed arrows. The k_{app} for duplex formation was determined as described in detail in the legend to Figure 5.4a

Figure 5.5b EMSA analysis of duplex formation between SL-II and SL-IIc in the presence and absence of FinO. The legend for this figure is the same as the legend for Figure 5.5a.

a.   SL-II/*traJ184*

b.   SL-II/SL-IIc
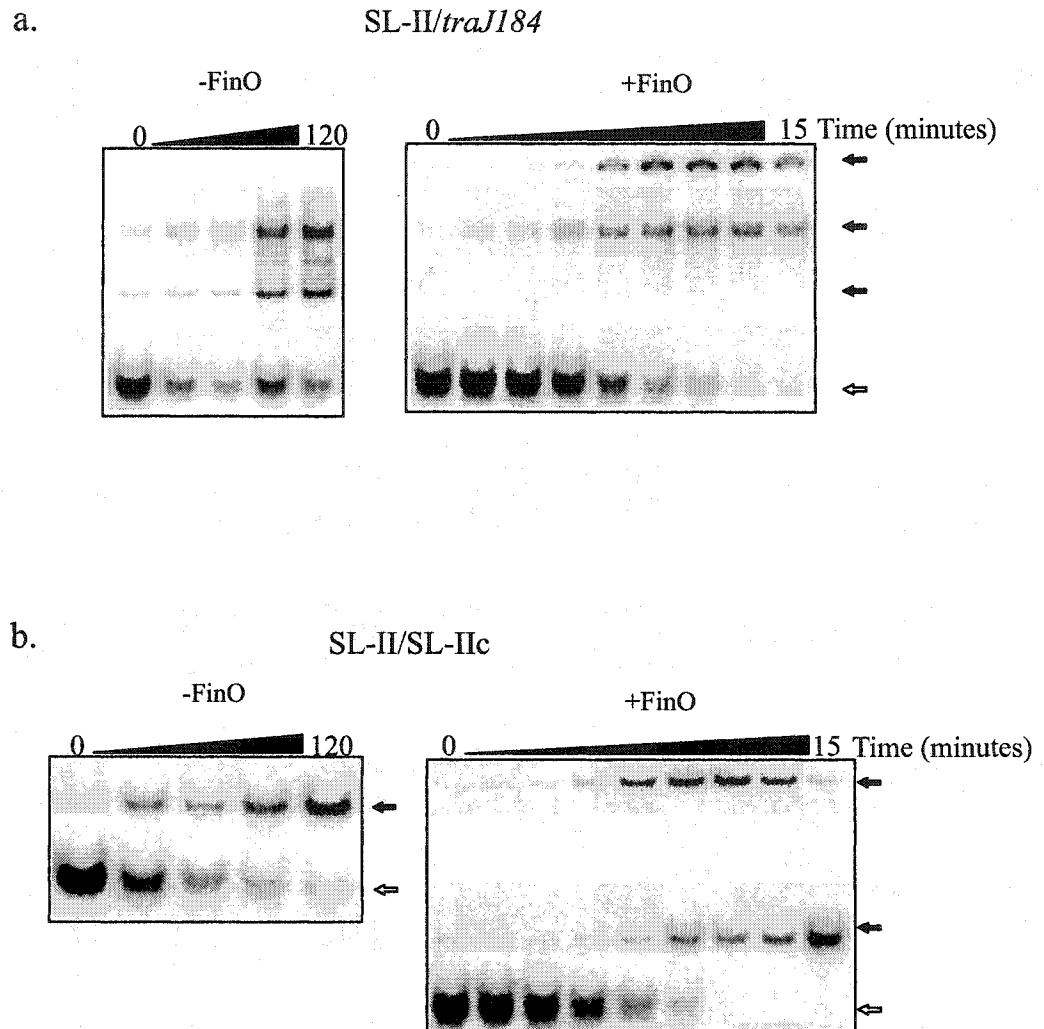
mRNA. These results suggest that FinO can catalyze the formation of a duplex between separate portions of FinP and the whole of *traJ184* mRNA, and that both FinP SL-I and SL-II contribute to the FinP/*traJ184* mRNA duplex interaction. SL-I/SL-Ic duplex formation occurred at a rate of 3.1×10^4 $M^{-1}s^{-1}$ in the absence of FinO, and 5.3×10^5 $M^{-1}s^{-1}$ in the presence of FinO (Figure 5.4b; Table 5.1). SL-II/SL-IIc duplex formation occurred at a rate of 2.5×10^4 $M^{-1}s^{-1}$ in the absence of FinO, while the rate increased to 3.9×10^4 $M^{-1}s^{-1}$ in the presence of FinO (Figure 5.5b; Table 5.1). The increase of the k_{app} for SL-II/SL-IIc duplex formation in the presence of FinO was smaller than expected. Previous experiments have shown this interaction to have a k_{app} of approximately 1.4×10^5 $M^{-1}s^{-1}$ (Ghetu *et al.*, 2002 submitted). The difference in these k_{app} values may be due to the stabilizing effect of Mg^{2+} cations in the TMN duplexing buffer employed in the duplex formation assays performed in this thesis (Materials and Methods, section 2.14).

To determine specific regions of FinP and *traJ184* mRNA which are required for duplex formation, multiple sequence and structural mutants of FinP SL-I were synthesized by *in vitro* T7 transcription. SL-I was chosen for several reasons. The anti-RBS for *traJ* mRNA is located in SL-I (Figure 5.1), which is hypothesized to make important initial contacts with the *traJ* RBS in order to prevent translation of the message *in vivo*. The loop of SL-I is also one base larger than the loop of SL-II, and while both contain the consensus 5'-YUNR-3' motif (Y=C or U, N=any base, R=A or G) which has been shown to make important structural contributions to RNA/RNA interactions (Franch *et al.*, 1999), SL-I exhibits higher conservation in the loop nucleotides than SL-II (Figure 5.2; Frost *et al.*, 1994; Jerome and Frost 1999). These observations suggest that the loop of SL-I is important in the initial interaction between FinP and *traJ* mRNA molecules and

that these interactions are most likely conserved amongst the different *finP* alleles of the

F-like plasmids. A single base pair mismatch in the stem of SL-I and two single base pair

mismatches in the stem of SL-Ic results in lower stability of these stems compared to the

more extensively base paired stems in SL-II and SL-IIc (Figure 5.1). The lower free

energy of unfolding of SL-I (ΔG=-10.1 kcal/mol) and SL-Ic (ΔG=-8.6 kcal/mol)

compared to SL-II (ΔG=-28.2 kcal/mol) and SL-IIc (ΔG=-23.3 kcal/mol) suggests that

base pairing interactions between the stems of SL-I and SL-Ic during the formation of a

stable FinP/*traJ184* mRNA duplex are more likely to occur than between the stems of

SL-II and SL-IIc (van Biesen *et al.*, 1993).

5.2.2 Contribution of the loop residues of SL-I to RNA/RNA duplex formation.

Three regions of the loop of SL-I were chosen to test for their contribution to SL-

I/SL-Ic duplex formation. All mutations were transversions that disrupted the expected

Watson-Crick base pair interactions between the loops. The predicted secondary

structures of all of these constructs are shown in Figure 5.3. One and two base

transversion mutations in these regions resulted in no noticeable alterations to duplex

formation (data not shown), therefore three and four base transversion mutations were

examined. The first region examined lies within the 5' side of the loop of SL-I, 5'-

C16G/C17G/U18A-3', which is referred to as SL-I(16-18) throughout this chapter. The

second region is located on the 3' side of the loop of SL-I, 5'-C21G/A22U/A23U-3',

which is referred to as SL-I(21-23). The last region extends across the top of the loop of

SL-I, 5'-U18A/C19G/A20U/C21G-3', which is referred to as SL-I(18-21). When

compared to SL-I/SL-Ic duplex formation under identical conditions, SL-I(16-18)/SL-Ic

duplex formation demonstrated a relative k_{app} reduced by 52% in the absence of FinO, and a relative k_{app} reduced by 55% in the presence of FinO, compared to SL-I/SL-Ic duplex formation under the same conditions (Figure 5.6; Table 5.2). SL-I(18-21)/SL-Ic duplex formation exhibited a relative k_{app} reduced by 35% in the absence of FinO, and a relative k_{app} reduced by 60% in the presence of FinO, while SL-I(21-23)/SL-Ic revealed a relative k_{app} reduced by 55% in the absence of FinO, and a relative k_{app} reduced by 51% in the presence of FinO, when compared to SL-I/SL-Ic duplex formation under the same conditions (Figure 5.6; Table 5.2). These results suggest that the level of complementarity between loop residues of SL-I and SL-Ic affects FinO-mediated duplex formation *in vitro*. The observation that the k_{app} values for duplex formation of all of the interactions tested between the SL-I loop mutants and SL-Ic were 10-19 fold higher in the presence of FinO than in the absence of FinO (Table 5.2) reveals that FinO can overcome as many as 4 mismatches in the loop-loop base pairing interaction to promote duplex formation *in vitro*.

5.2.3 The effect of SL-I loop mutations on the ability of FinP to repress mating.

As shown in the previous section, mutations in the loop of SL-I reduce the rate of FinO mediated duplex formation *in vitro*. Previous work examined the role of specific nucleotides in the loops of FinP in the F-like plasmid R1 in promoting fertility inhibition (Koraimann *et al.*, 1996). Various FinP mutants were supplied *in trans* at medium copy number from a pBR322 derivative plasmid, and tested for their ability to inhibit both *traJ* expression, as measured by β-galactosidase activity of a *traJ-lacZ* translational fusion, and R1 conjugative transfer. The results from this study suggested that a single base mutation at the top of the loop of FinP SL-I, which altered complementarity with the

Figure 5.6 Mutations in SL-I that disrupt Watson-Crick base pairing interactions between the loops decrease SL-I/SL-Ic duplex formation rates. 60 fmol of ^{32}P-labeled SL-I loop mutants (as indicated above each panel) was mixed with 600 fmol of unlabeled SL-Ic in a 50μl reaction containing TMN buffer. Reactions were incubated at 37°C in the presence and absence of 6μM FinO, as indicated below each panel. Samples were taken at 0, 15, 30, 60, and 120 minutes (-FinO) and at 0, 1, 2, 3, 4, 6, 10, and 15 minutes (+FinO), and separated by electrophoresis on 8% non-denaturing polyacrylamide gels. Free RNA is denoted by open arrows, duplex RNA by closed arrows. The k_{app} for duplex formation was determined as described in the legend to Figure 5.4a.

SL-I(16-18)/SL-Ic

SL-I(18-21)/SL-Ic

SL-I(21-23)/SL-Ic

- FinO   + FinO
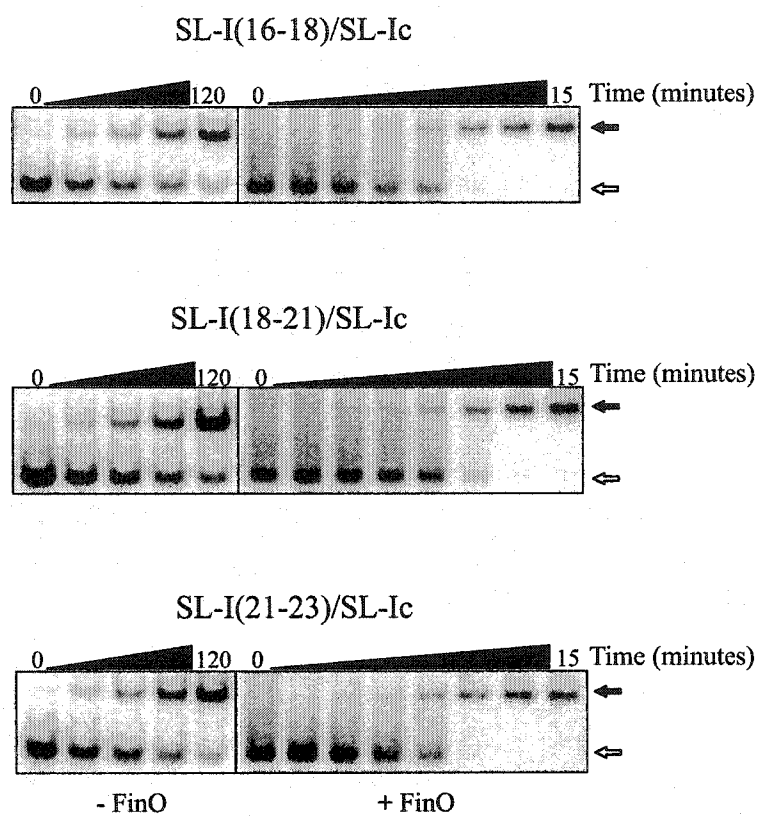
Table 5.2 k_{app} values for duplex formation of a variety of SL-I loop mutant derivatives interacting with SL-Ic tail mutant derivatives

RNAs present	$\times 10^5 k_{app}$ $(M^{-1}s^{-1})^a$ -FinO	Relative k_{app} $(\%)^b$	$\times 10^5 k_{app}$ $(M^{-1}s^{-1})^a$ +FinO	Relative k_{app} $(\%)^b$
SL-I/SL-Ic	0.31 ± 0.07	100	5.3 ± 1.0	100
SL-I(16-18)/SL-Ic	0.15	48	2.4	45
SL-I(16-18)/SL-Ic(Δtails)	< 0.01	<3	0.71 ± 0.2	13
SL-I(16-18)/SL-Ic(Δ5'tail)	N.D.^{c}	N.D.	0.94	18
SL-I(16-18)/SL-Ic(Δ3'tail)	N.D.	N.D.	1.3	25
SL-I(18-21)/SL-Ic	0.2	65	2.1	40
SL-I(18-21)/SL-Ic(Δtails)	<0.01	<3	0.89 ± 0.02	17
SL-I(18-21)/SL-Ic(Δ5'tail)	N.D.	N.D.	0.88	17
SL-I(18-21)/SL-Ic(Δ3'tail)	N.D.	N.D.	1.7	32
SL-I(21-23)/SL-Ic	0.14 ± 0.02	45	2.6 ± 0.3	49
SL-I(21-23)/SL-Ic(Δtails)	0.053	17	1.6	30

$^a k_{app}$ values are an average of at least two to three independent EMSA analyses, ± standard deviation where appropriate.

^{b}Relative k_{app}=[k_{app}(variant pair)/k_{app} (SL-I/SL-Ic)]×100

^{c}N.D. Not determined.

corresponding region in *traJ* mRNA, reduced the ability of the mutant FinP RNA to inhibit *traJ* expression in the absence of FinO. Wild-type FinP expressed under the same conditions was able to fully repress *traJ* expression. However, when FinO was supplied *in trans*, FinP containing the single base mutation at the top of the loop of SL-I was able to repress *traJ* expression at a level approaching that of wild-type FinP. Interestingly, all of the FinP loop mutants tested in that study, except for one containing a single base mutation on the 3′ side of FinP SL-I, were unable to promote fertility inhibition, in the presence or absence of FinO, when supplied *in trans* from a medium copy number plasmid (Koraimann *et al.*, 1996). It was therefore decided to test the ability of FinP(16-18) to repress TraJ expression and inhibit F transfer when supplied from both high and medium copy number plasmids, to determine whether the anti-RBS of FinP influences its function *in vivo*.

The plasmids pUC180GGA and pLT180GGA (Materials and Methods, Table 2.2) were created to express FinP(16-18) *in trans* from a high (pUC18) and medium (pT7-3) copy number plasmid, respectively. Each of these plasmids was introduced into *E. coli* MC4100, with or without plasmid pSn0104, which expresses plasmid R6-5 FinO *in trans* (Materials and Methods, Table 2.2). Their counterparts, pUC180 and pLT180, which express wild-type FinP at high and medium copy number, respectively, were tested in the same way, as were the negative control parental plasmids, pUC18 and pT7-3 (Materials and Methods, Table 2.2). The *finP⁻* F-derivative pSLF20 (Materials and Methods, Table 2.2; Lee *et al.*, 1992) was present in all strains, and expression of TraJ and pSLF20 conjugative transfer were tested in the presence of the mutant FinP molecules described above, expressed *in trans*. As shown in Figure 5.7a, when supplied at high copy number,

Figure 5.7a Wild-type FinP and FinP(16-18) expressed at high copy number inhibits TraJ accumulation. Western immunoblot analysis of MC4100 cells containing the *finP*⁻ F-derivative plasmid pSLF20, along with pUC18 or the pUC18-derived plasmids pUC180 and pUC180GGA, expressing wild-type FinP and FinP(16-18), respectively, at high copy number *in trans*. The FinP expression plasmids present in the cells are indicated above each lane. The presence of plasmid pSn0104, which expresses R6-5 FinO *in trans*, in the constructs is indicated above each lane. A negative control of MC4100 containing no plasmids is located in the far right lane. The location of TraJ and FinO (detected with polyclonal antisera as described in Materials and Methods, section 2.5) is indicated to the right of the figure, while relevant molecular weight markers (kDa) are indicated on the left. The panel labeled "loading control" is a signal obtained from crossreaction of the antisera with an unknown protein. The bottom panel is a Northern blot which shows the presence of FinP RNA expressed in the various constructs. Twenty μg of total cellular RNA, isolated from the same cultures used for the Western immunoblot, was assayed via Northern blot analysis as described in Materials and Methods (section 2.7).

Figure 5.7b FinP(16-18) expressed at medium copy number inhibits accumulation of TraJ less effectively than wild-type FinP. The legend to this figure is the same as the legend for Figure 5.7a, except wild-type FinP was expressed *in trans* from the medium copy number pT7-3 derived plasmid pLT180, while FinP(16-18) was expressed from the medium copy number pT7-3 derived plasmid pLT180GGA.

a.

	No plasmid		pUC18		pUC180		pUC180GGA		MC4100
pSn0104	−	+	−	+	−	+	−	+	−
pSLF20	+	+	+	+	+	+	+	+	−

26 — TraJ

19.6 — FinO

Loading control

FinP RNA

b.

	No plasmid		pT7-3		pLT180		pLT180GGA		MC4100
pSn0104	−	+	−	+	−	+	−	+	−
pSLF20	+	+	+	+	+	+	+	+	−

26 — TraJ

19.6 — FinO

Loading control

FinP RNA
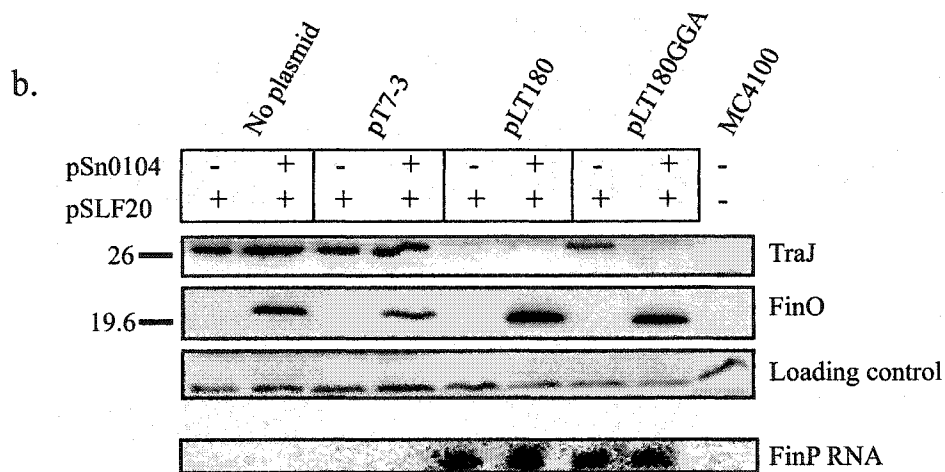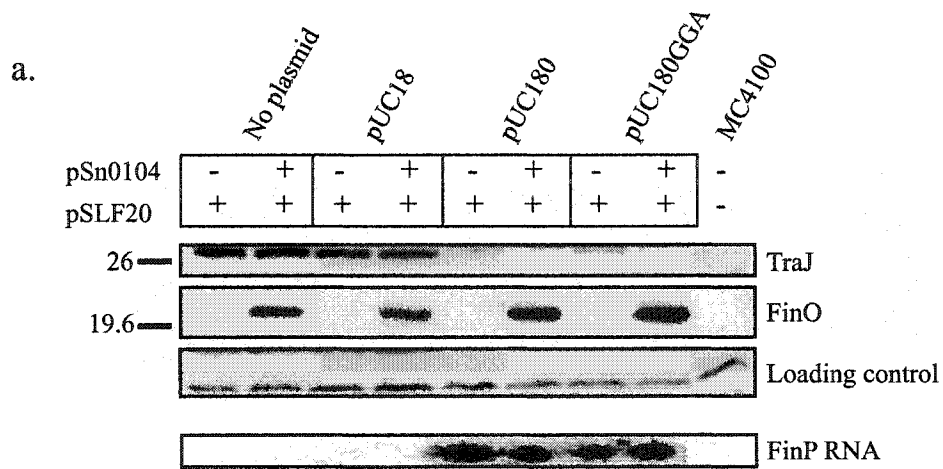
both wild-type FinP (pUC180) and FinP(16-18) (pUC180GGA) were able to almost completely repress accumulation of TraJ, in both the presence and absence of FinO, as determined by Western immunoblot analysis. In the absence of FinO, a small amount of TraJ was detectable in the presence of plasmid pUC180GGA (Figure 5.7a). Similarly, each FinP variant was able to repress pSLF20 mating regardless of whether FinO was present, although the presence of FinO did significantly increase the effectiveness of mating inhibition. FinP(16-18) repressed mating inhibition with an approximately 850-fold lower efficiency in the absence of FinO, and an approximately 70-fold reduced efficiency in the presence of FinO, compared to wild-type FinP (Table 5.3). When supplied at medium copy number, wild-type FinP (pLT180) fully repressed TraJ accumulation in both the presence and absence of FinO, while FinP(16-18) (pLT180GGA) was able to significantly repress TraJ accumulation only in the presence of FinO (Figure 5.7b). Mating inhibition assays (Table 5.3) revealed that FinP(16-18) was able to repress mating with an efficiency reduced by approximately 100-fold compared to wild-type FinP in the absence of FinO, and an efficiency reduced by approximately 150-fold compared to wild-type FinP in the presence of FinO. As in the case of FinP and FinP(16-18) expressed at a high copy number discussed above, the presence of FinO significantly enhanced mating repression mediated by both FinP molecules expressed *in trans* at a medium copy number. These results confirm previous observations that the ability of FinP to inhibit F mating is dependent upon gene dosage (Koraimann *et al.*, 1996). They also confirm the results from the *in vitro* duplex formation assays described in the previous section, which showed that FinO can overcome multiple base mutations in FinP SL-I and promote SL-I/SL-Ic duplex

Table 5.3 Inhibition of pSLF20 conjugative transfer by FinP expressed *in trans* from medium and high copy number plasmids.

FinP expressing plasmid present along with pSLF20 in MC4100 donor cells	FinP expressed	% Mating Efficiency vs. pSLF20 alone[a]	
		No FinO	+FinO[b]
None	None	100	100
High copy number			
pUC18	None	100	100
pUC180	Wild-type FinP	0.02	0.008
pUC180GGA	FinP(16-18)	17	0.53
Medium copy number			
pT7-3	None	100	100
pLT180	Wild-type FinP	0.71	0.05
pLT180GGA	FinP(16-18)	70	7.3

[a] The ratio of transconjugants:donors for each mating assay was determined, and compared to the transconjugants:donors ratio for pSLF20, which was set as 100% mating efficiency. Values were determined from two separate experiments (performed in duplicate) and averaged.

[b] FinO was provided *in trans* by the plasmid pSn0104, expressing wild-type plasmid R6-5 FinO.

formation *in vitro* when complete loop:loop complementarity is absent. *In vivo*, it also appears that FinO can compensate for sub-optimal loop-loop basecomplementarity and promote fertility inhibition, but only when a FinP loop mutant is supplied at an elevated copy number.

5.2.4 The effect of stem mutations on SL-I /SL-Ic duplex formation.

The bulged A12:A27 base pair mismatch in SL-I and the corresponding U85:U100 mismatch in SL-Ic (Figure 5.1) were examined for their contribution to duplex formation. SL-I(A27U) (ΔG=-14.3 kcal/mol) and SL-Ic(U85A) (ΔG=-12.1 kcal/mol) were made to increase the free energy and stability of the stems while maintaining full intermolecular complementarity between the stems of the two RNAs. SL-I(A27U)/SL-Ic(U85A) duplex formation in the absence of FinO demonstrated a relative k_{app} reduced by 32% compared to SL-I/SL-Ic duplex formation (Figure 5.8; Table 5.4). In the presence of FinO, the relative k_{app} for duplex formation was reduced by 74%. These results suggest that the overall stability of the stem regions of SL-I and SL-Ic influences their transition into a stable duplex.

To create more drastic mutations affecting stem complementarity and to provide insight into the direction of progression of duplex formation, SL-Ic(TSR) and SL-Ic(BSR) were constructed. SL-Ic(TSR) has had 5 base pairs in the stem immediately below the loop reversed in orientation to make them non-complementary to the corresponding region in SL-I (Figure 5.3). SL-Ic(BSR) has had the 6 base pairs at the bottom of the stem reversed in the same fashion (Figure 5.3). The single-stranded tail regions were not included in these constructs, to ensure that only the effects on intermolecular stem:stem interactions were examined. SL-I/SL-Ic(TSR) duplex formation

Figure 5.8 Mutations in the stem regions of SL-I and SL-Ic decrease duplex formation rates. Sixty fmol of ^{32}P-labeled SL-I stem variants and 600 fmol of unlabeled SL-Ic stem variants were incubated at 37°C in 50 μL reactions containing TMN buffer, with or without 6μM FinO as indicated below each panel. The RNA constructs present in each reaction are listed above each panel. In reactions without FinO, samples were taken at 0, 15, 30, 60, and 120 minutes. In reactions containing FinO, samples were taken at 0, 1, 2, 3, 4, 6, 10, and 15 minutes (SL-I(A27U)/SL-Ic(U85A)) and at 0, 1, 2, 5, 10, 15, 30, and 60 minutes (SL-I/SL-Ic(TSR) and SL-I/SL-Ic(BSR)). Free RNA is denoted by open arrows, duplex RNA by closed arrows. EMSA analysis was performed as described in the legend to Figure 5.6, and k_{app} determinations were performed as described in the legend to Figure 5.4a.

SL-I(A27U)/SL-Ic(U85A)

SL-I/SL-Ic(TSR)

SL-I/SL-Ic(BSR)

- FinO   + FinO
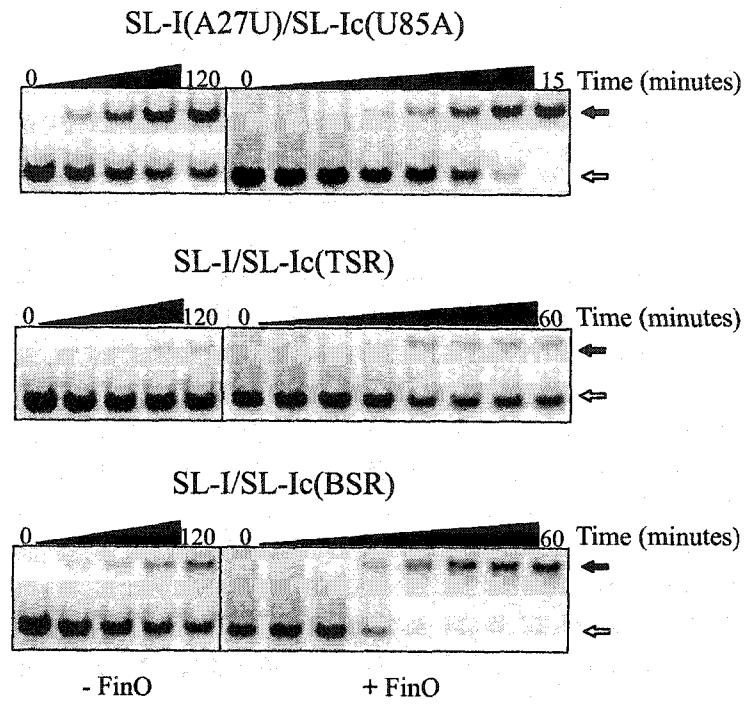
Table 5.4 k_{app} values for duplex formation between various SL-I and SL-Ic stem and tail mutant derivatives.

RNAs present	$\times 10^5\ k_{app}(\mathrm{M^{-1}s^{-1}})^a$ -FinO	Relative $k_{app}\ (\%)^b$	$\times 10^5\ k_{app}\ (\mathrm{M^{-1}s^{-1}})^a$ +FinO	Relative $k_{app}\ (\%)^b$
SL-I/SL-Ic	0.31 ± 0.07	100	5.3 ± 1.0	100
SL-I(A27U)/SL-Ic(U85A)	0.21 ± 0.03	68	1.4	26
SL-I/SL-IcR	0	0	0	0
SL-I/SL-Ic(TSR)	0	0	0	0
SL-I/SL-Ic(BSR)	0.051	16	1.8 ± 0.2	34
SL-I/SL-Ic(Δtails)	0.1 ± 0.03	32	1.5	28
SL-I/SL-Ic($\Delta 5'$tail)	0.16 ± 0.02	52	2.3 ± 0.3	43
SL-I/SL-Ic($\Delta 3'$tail)	0.14 ± 0.06	45	3.1 ± 0.2	58
SL-I(Δtails)/SL-Ic(Δtails)	0.09 ± 0.05	30	1.0	19

$^a k_{app}$ values are an average of at least two to three independent EMSA analyses, $\pm$ standard deviation where appropriate.

^{b}Relative k_{app}=[k_{app}(variant pair)/k_{app} (SL-I/SL-Ic)]$\times$100

in both the presence and absence of FinO was minimal, and a k_{app} could not be calculated in either case because less than 20% of the ^{32}P-labeled free RNA in the reactions was converted to a duplex (Figure 5.8). SL-I/SL-Ic(BSR) duplex formation in the absence of FinO revealed a relative k_{app} reduced by 84% compared to SL-I/SL-Ic duplex formation (Figure 5.8; Table 5.4). In the presence of FinO, the relative k_{app} for SL-I/SL-Ic(BSR) duplex formation was lowered by 66% compared to the k_{app} for SL-I/SL-Ic duplex formation (Figure 5.8; Table 5.4). These results suggest that full duplex formation between SL-I and SL-Ic can proceed only if intermolecular complementarity extends from the loop through the top of the stem. The virtually identical k_{app} values for SL-I/SL-Ic(Δtails) and SL-I/SL-Ic(BSR) duplex formation also suggests that a region of non-complementarity at the bottom of the stem has no significant effect on the ability of FinO to promote duplex formation between these constructs *in vitro*.

5.2.5 Detection of SL-I/SL-Ic kissing complexes.

Since kissing between loop regions is the first interaction in most antisense/sense RNA pairing reactions, it was decided to determine whether a SL-I/SL-Ic kissing dimer could form and be detected by EMSA analysis. SL-IcR was created such that the loop region was completely complementary to SL-I, but the stems and tails shared no complementarity (Figure 5.3). These constructs were subjected to duplex analysis in the same way as all of the other RNA constructs (Materials and Methods, section 2.14). In both the presence and absence of FinO, no stable kissing intermediate could be detected (Figure 5.9), even after extended periods of incubation. These results suggest that a stable kissing intermediate is not detectable by EMSA analysis or that any initial kissing complex that forms between SL-I and SL-Ic is transient and unstable. These results also

Figure 5.9 SL-I/SL-Ic kissing intermediates are not detectable by EMSA analysis.

EMSA analysis to detect a kissing intermediate between SL-I and SL-IcR, an RNA

construct containing a loop that is complementary to the loop of SL-I, but whose stems

share no complementarity (Figure 5.3). Sixty fmol of ^{32}P-labeled SL-I were incubated at

37°C in TMN buffer with 600 fmol of unlabeled SL-IcR, in the presence and absence of 6

μM FinO, as indicated below each panel. Samples were taken at 0, 60, and 120 minutes,

and separated by electrophoresis on 8% non-denaturing polyacrylamide gels, as described

in detail in the legend to Figure 5.4a. The open arrow denotes free RNA.

SL-I/SL-IcR

0   60 120   0   60 120   Time (minutes)

- FinO   + FinO
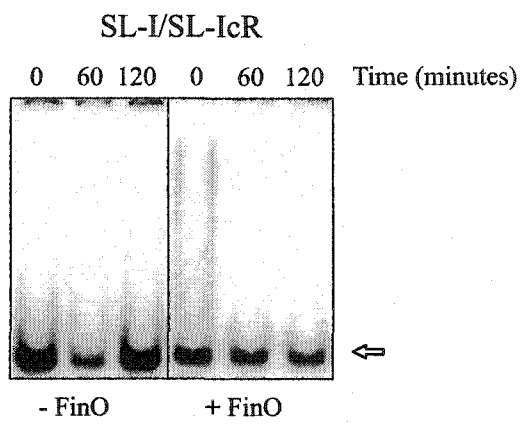
confirm the observations resulting from the SL-I/SL-Ic(TSR) duplexing experiments described in the previous section, suggesting that formation of a stable SL-I/SL-Ic duplex requires complementarity in both the loops and as much as half of the stem region immediately below the loops of both RNA molecules.

5.2.6 Contribution of the single-stranded tail regions of SL-I to RNA/RNA duplex formation.

Since the single-stranded tails of FinP SL-I and SL-II have been shown to influence the ability of FinO to bind FinP with high affinity (Jerome and Frost, 1999), the contribution of these regions to duplex formation *in vitro* was tested. SL-I/SL-Ic(Δtails) duplex formation showed a relative k_{app} reduced by 68% in the absence of FinO, and relative k_{app} reduced by 72% in the presence of FinO, compared to SL-I/SL-Ic duplex formation under identical conditions (Figure 5.10; Table 5.4). SL-I/SL-Ic(Δ5'tail) and SL-I/SL-Ic(Δ3'tail) duplex formation demonstrated relative k_{app} values reduced by 48% and 55%, respectively, in the absence of FinO, compared to SL-I/SL-Ic duplex formation under the same conditions (Figure 5.10; Table 5.4). In the presence of FinO, SL-I/SL-Ic(Δ5'tail) duplex formation exhibited a relative k_{app} reduced by 57%, while SL-I/SL-Ic(Δ3'tail) demonstrated a relative k_{app} reduced by 42% (Table 5.4). When SL-I(Δtails) was analyzed for duplex formation with SL-Ic(Δtails), the relative k_{app} was reduced by 70% in the absence of FinO, and by 81% in the presence of FinO, compared to SL-I/SL-Ic duplexing under identical conditions (Figure 5.10; Table 5.4). These results suggest that the presence of both the 5' and 3' single-stranded tails flanking SL-I and SL-Ic make important contributions to the formation of the RNA/RNA duplex *in vitro*.

Figure 5.10 Removal of the single-stranded tails of SL-I and SL-Ic reduces the rate of duplex formation. Sixty fmol of ^{32}P-labeled SL-I variants were incubated with 600 fmol of unlabeled SL-Ic single-stranded tail deletion variants in several combinations, as indicated above each panel. Analyses were performed in the presence and absence of 6μM FinO, as indicated below the panels. Samples were taken at 0, 15, 30, 60, and 120 minutes (-FinO) and 0, 1, 2, 4, 6, 8, 10, and 15 minutes (+FinO), and subjected to EMSA analysis as described in detail in the legend to Figure 5.4a. Closed arrows denote duplex RNA, while open arrows indicate free RNA. k_{app} determinations were performed as described in the legend to Figure 5.4a.

SL-I/SL-Ic(Δtails)

SL-I/SL-Ic(Δ5'tail)

SL-I/SL-Ic(Δ3'tail)

SL-I(Δtails)/SL-Ic(Δtails)

- FinO   + FinO
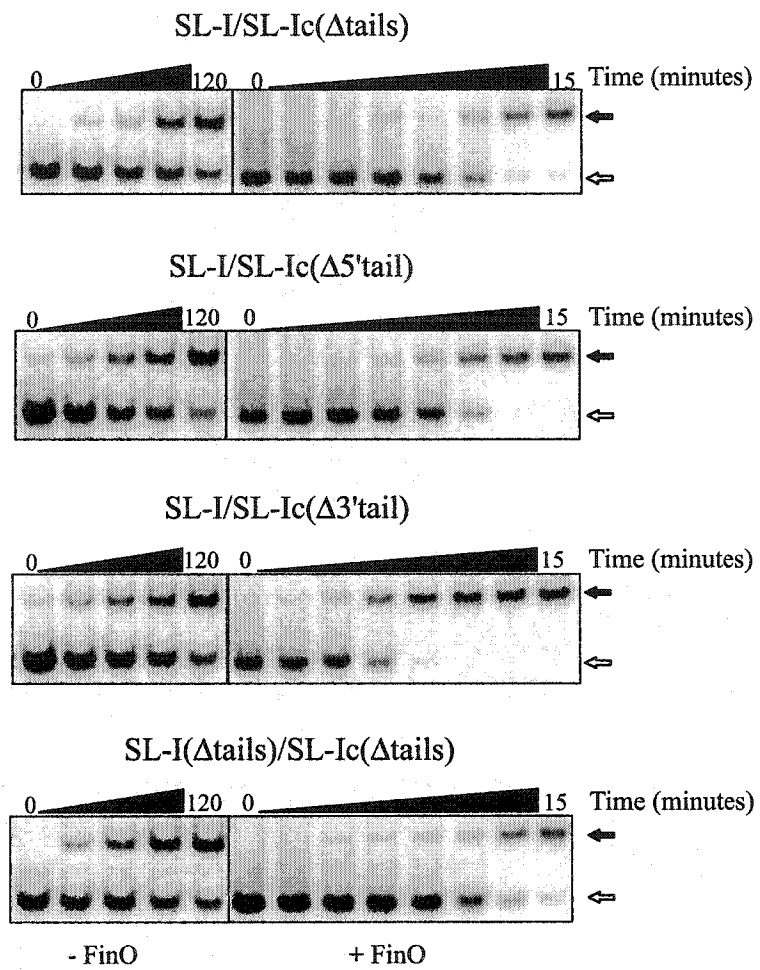
5.2.7 FinO binds SL-I with relatively high affinity.

In order to ensure that any decreases in k_{app} were the result of alterations in the structure of the interacting RNAs and not due to an inability of FinO to bind them, EMSA analysis was performed to determine the K_a for FinO binding to SL-I and SL-I(Δtails). As shown in Figure 5.11, FinO was able to bind to both RNA molecules, with a K_a of approximately 8.6×10^6 M^{-1} for binding SL-I, and 3.5×10^6 M^{-1} for binding SL-I(Δtails). These K_a values are higher than those reported in a previous study, which may be attributable to the fact that this study employed FinO lacking a glutathione S-transferase (GST) tag, while the previous study employed a GST:FinO fusion protein (Jerome and Frost, 1999). Regardless, our results indicate that the reduction in k_{app} values observed for duplex formation between the various SL-I and SL-Ic mutant derivatives lacking single-stranded tails was not the result of an inability of FinO to bind to the RNA molecules present in the duplex assays.

5.2.8 The effect of combined loop and single-stranded tail mutations on SL-I/SL-Ic duplex formation.

Since mutations in the loops of SL-I and the removal of complementary single-stranded tails both had moderate effects on RNA/RNA duplex formation rates, combinations of such mutations were tested (Figure 5.12). SL-I(16-18)/SL-Ic(Δtails) and SL-I(18-21)/SL-Ic(Δtails) duplex formation in the absence of FinO both demonstrated k_{app} values which were reduced by more than an estimated 30-fold compared to SL-I/SL-Ic duplex formation. The rate of duplex formation in both cases was too low for accurate quantification (Figure 5.12a). In the presence of FinO, the relative k_{app} for SL-I(16-18)/SL-Ic(Δtails) and SL-I(18-21)/SL-Ic(Δtails) were each reduced by 87%, substantially

Figure 5.11 FinO binds FinP SL-I and SL-I(Δtails) with high affinity. Six fmol of ^{32}P-labeled RNA (listed above each panel) were incubated at 4°C with increasing concentrations of FinO (0, 0.038, 0.076, 0.19, 0.38, 0.76, and 1.9 μM) in 20 μl reactions containing TMEB binding buffer. Reactions were subjected to EMSA analysis on an 8% non-denaturing polyacrylamide gel. Open arrows denote free RNA, and closed arrows denote FinO/RNA complexes. The K_a for FinO binding was determined from the concentration of FinO that caused 50% of the labeled RNA to shift in the gel, as described in Materials and Methods, section 2.12.

SL-I   SL-I(Δtails)

0 _____ 1.9   0 _____ 1.9 μM FinO
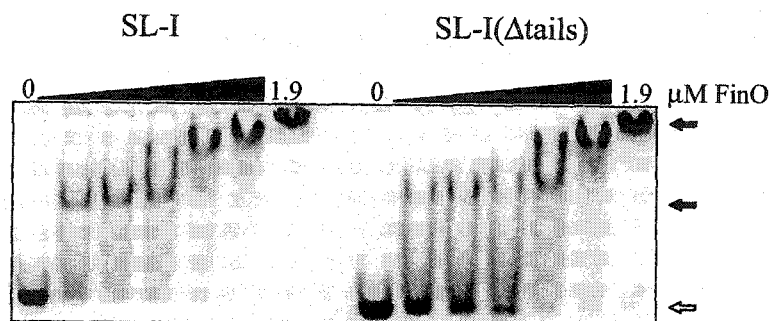
Figure 5.12a Loop mutations which interrupt loop:loop base pairing combined with removal of the single-stranded tails reduces the rate of SL-I/SL-Ic duplex formation. Sixty fmol of each ^{32}P-labeled SL-I loop variant, as indicated above each panel, were incubated with 600 fmol of unlabeled SL-Ic(Δtails) in 50 µL reactions containing TMN buffer. The presence or absence of 6µM FinO in the reactions is indicated below each panel. Samples were withdrawn at 0, 15, 30, 60, and 120 minutes (-FinO), and 0, 1, 2, 4, 6, 8, 10, and 15 minutes (+FinO) and subjected to EMSA analysis as described in the legend to Figure 5.4a. Free RNA is denoted by open arrows, duplex RNA by closed arrows. k_{app} determinations were performed as described in detail in the legend to Figure 5.4a.

Figure 5.12b Combined loop and single-stranded tail mutations lower the rate of SL-I/SL-Ic duplex formation. Sixty fmol of ^{32}P-labeled SL-I(16-18) or SL-I(18-21) were incubated with 600 fmol of unlabeled SL-Ic(Δ3'tail) or SL-I(Δ5'tail) in 50 µL reactions containing TMN buffer in the presence of 6µM FinO. The RNA species present in each reaction is indicated above each panel. Samples were taken at 0, 1, 2, 4, 6, 8, 10, and 15 minutes, and subjected to EMSA analysis as described in the legend to Figure 5.4a. Free RNA is denoted by open arrows, duplex RNA by closed arrows. k_{app} determinations were performed as described in detail in the legends to Figure 5.4a.

a. SL-I(16-18)/SL-Ic(Δtails)

Time (minutes)

SL-I(18-21)/SL-Ic(Δtails)

Time (minutes)

SL-I(21-23)/SL-Ic(Δtails)

Time (minutes)

- FinO   + FinO

b. SL-I(16-18)

Duplexing with:

SL-Ic(Δ3'tail)   SL-Ic(Δ5'tail)

Time (minutes)

+ FinO   + FinO

SL-I(18-21)

Duplexing with:

SL-Ic(Δ3'tail)   SL-Ic(Δ5'tail)

Time (minutes)

+ FinO   + FinO
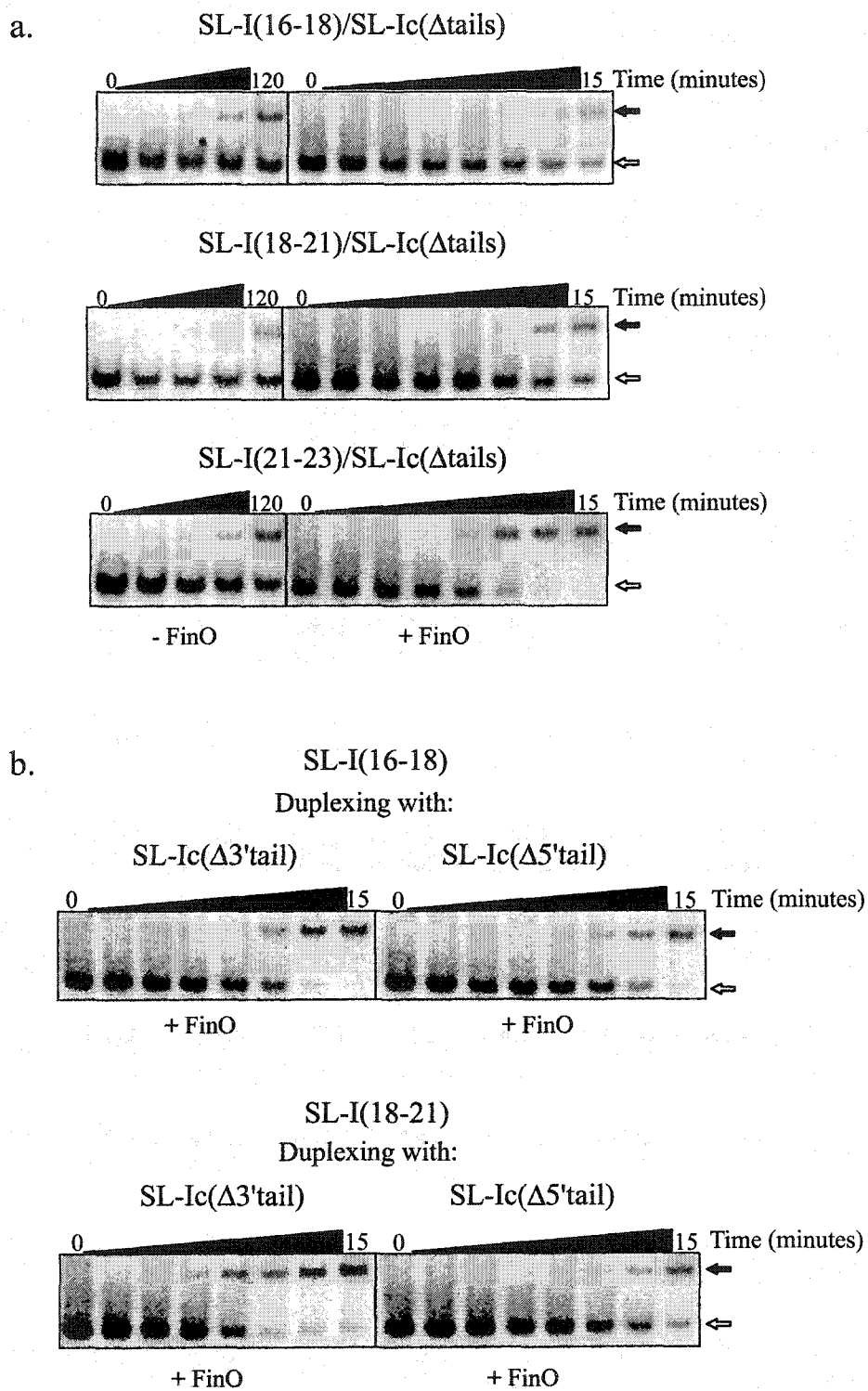
lower than the k_{app} for SL-I/SL-Ic duplex formation under identical conditions (Figure 5.12a; Table 5.2). To determine whether the 5′ or 3′ single-stranded tail of SL-Ic was more important for FinO-mediated duplex formation, k_{app} values for SL-I(16-18)/SL-Ic(Δ5′tail), SL-I(16-18)/SL-Ic(Δ3′tail), SL-I(18-21)/SL-Ic(Δ5′tail), and SL-I(18-21)/SL-Ic(Δ3′tail) duplex formation were determined (Figure 5.12b; Table 5.2). In the presence of FinO, the relative k_{app} for SL-I(16-18)/SL-Ic(Δ5′tail) duplex formation was lowered by 82%, while the relative k_{app} for SL-I(16-18)/SL-Ic(Δ3′tail) duplex formation was reduced by 75%, compared to SL-I/SL-Ic duplex formation under the same conditions (Table 5.2). In the presence of FinO, the relative k_{app} for SL-I(18-21)/SL-Ic(Δ5′tail) duplex formation was reduced by 83% compared to SL-I/SL-Ic duplex formation, while the relative k_{app} for SL-I(18-21)/SL-Ic(Δ3′tail) was reduced by 68% (Table 5.2). Duplex assays without FinO were not performed for these RNA constructs, because the rates of duplex formation were too low to accurately quantify. The relative k_{app} for SL-I(21-23)/SL-Ic(Δtails) duplex formation was reduced by 55% in the absence of FinO, compared to SL-I/SL-Ic duplex formation, while in the presence of FinO, SL-I(21-23)/SL-Ic(Δtails) duplex formation was lowered by 51% (Figure 5.12a; Table 5.2). The reduction of these k_{app} values was less dramatic than those determined for the other combinatorial SL-I/SL-Ic loop and single-stranded tail mutant pairs tested, leading to the conclusion that the loop nucleotides C21-A23 in the 3′ portion of SL-I make a smaller contribution to duplex formation *in vitro* than those extending from C16-C21. In the presence of FinO, all of the combinatorial mutant pairs described above demonstrated k_{app} values 11-60 fold higher than in the absence of FinO (Table5.2), which suggests that

FinO can overcome a significant loss of single-stranded regions in SL-I and SL-Ic and promote RNA/RNA duplex formation *in vitro*.

5.3 Discussion

This chapter describes the structural features of FinP antisense RNA and *traJ* mRNA which influence FinO-mediated duplex formation. A common theme amongst antisense-sense interactions is the mediation of an initial interaction between single-stranded complementary loops of the RNA molecules (Tomizawa 1984; Persson *et al.*, 1988; Asano and Mizobuchi., 1998, 2000; reviewed in Brantl, 2002). Three-base transversion mutations that disrupted expected Watson-Crick base pairing were made in FinP SL-I on the 5' and 3' sides of the loop, while a four-base transversion was made across the top of the loop. In each case, the k_{app} for duplex formation decreased by a moderate amount, in both the presence and absence of FinO. In the plasmid ColIb-P9, single-base mutations in multiple loop regions which altered canonical loop-loop base pairing between Inc RNA and RepZ mRNA significantly decreased their *in vivo* function and impaired RNA/RNA duplex formation *in vitro* (Asano and Mizobuchi., 1998). However, Kolb *et al.* (2000a) demonstrated that a single base mutation on the 3' side of the loop of the CopA antisense RNA of plasmid R1, which disrupted potential loop-loop base pairing, had only a minor effect on the ability of this RNA to form a duplex with its target, CopT RNA. These findings demonstrate that while loop-loop interactions are a common theme and required for antisense/sense RNA pairing, the importance of complementarity between the loop nucleotides, and the regions of loops which influence pairing, vary between different systems.

The F-like plasmid R1 shares a FinOP system very similar to the F plasmid. Single-base mutations in the top portions of the loops of FinP SL-I or SL-II that altered potential loop-loop base interactions inhibited FinO-mediated repression of conjugative transfer of R1. However, FinO-mediated repression of *traJ* expression, as measured by β-galactosidase assays of a *traJ-lacZ* translational fusion reporter construct, appeared to occur at or near wild-type levels under the same conditions (Koraimann *et al.*, 1996). When single base transversions were made in SL-I and SL-II simultaneously, FinO-mediated repression of both *traJ* expression and conjugative plasmid transfer were significantly reduced. Interestingly, a single-base transversion mutation made in the 3′ portion of the loop of SL-I had no negative effect whatsoever on FinO-mediated inhibition of *traJ* expression or plasmid transfer. These results suggest that the interaction of plasmid R1 FinP and *traJ* mRNA *in vivo* relies more on the bases located at the top of the loops rather than those situated on the 3′ side (Koraimann *et al.*, 1996). As shown in this chapter, a three-base transversion mutation which altered the anti-RBS of FinP (FinP(16-18)) was able to prevent TraJ accumulation and F plasmid transfer when supplied *in trans* at high copy number, regardless of whether FinO was present. When supplied at medium copy number, this mutant FinP was able to efficiently inhibit F plasmid transfer and TraJ accumulation only when FinO was also supplied *in trans*. These results suggest that the initial interaction between the RBS of *traJ* mRNA and the anti-RBS of FinP is critical for the process of fertility inhibition. However, it does appear as though sub-optimal loop-loop pairing between these regions of SL-I and SL-Ic can be tolerated *in vivo*, provided an elevated amount of the mutant FinP is present, and FinO is freely available in the cells. These results also confirm that FinP-mediated inhibition of F

and F-like plasmid transfer is highly gene-dosage dependent (Koraimann *et al.*, 1991, 1996).

A common structural motif in prokaryotic antisense RNA systems is the 5'-YUNR-3' loop motif, which is thought to provide optimal alignment of bases in the 3' side of the loop with those in a complementary RNA (Franch *et al.*, 1999). Mutations in the YUNR motif of *hok* RNA of the plasmid R1 *hok/sok* post-segregational killing system greatly reduced Sok antisense RNA/*hok* mRNA duplex formation *in vitro*, even though complementarity between the interacting RNAs was maintained (Franch *et al.*, 1999). Two of the three multiple loop mutations in FinP SL-I performed in the present study altered the YUNR motif and significantly disrupted complementary Watson-Crick base-pairing interactions, but led to only moderate decreases in duplex formation rates. These results suggest that while loop-loop pairing between FinP and *traJ* mRNA is important, the sequence, and possibly the structure, of the loops may play a smaller role than in other systems. This notion is supported by the *in vivo* mating inhibition data which revealed that a three-base transversion in the anti-RBS domain of the loop of FinP SL-I did not completely abolish the ability of this mutant FinP to repress F mating when it was supplied at elevated levels, provided FinO was also supplied *in trans*.

The presence of short single-stranded tails flanking both the 5' and 3' sides of SL-I were shown to influence the ability of SL-I to duplex with SL-Ic *in vitro*. Removal of the 3' tail or 5' tail of SL-Ic caused a moderate reduction in its ability to form a duplex with SL-I. However, removal of both single-stranded tails from SL-I and SL-Ic led to a decrease in FinO-catalyzed duplex formation which was more significant than any of the loop mutations that were tested, suggesting that single-stranded regions in FinP and *traJ*

mRNA play an important role in duplex formation. The importance of complementary single-stranded regions in FinP and *traJ* mRNA is illustrated by the observation that FinO-mediated SL-I/SL-Ic and SL-II/SL-IIc duplex formation rates were reduced significantly compared to FinP/*traJ* mRNA duplex formation. RNA I/RNA II interaction in ColE1 replication control (Tomizawa, 1984) as well as the CopA/CopT interaction of plasmid R1 (Persson *et al.*, 1990a; Kolb *et al.*, 2000b) rely on pairing between complementary single-stranded regions for full activity, demonstrating the importance of such regions on antisense-sense RNA pairing.

The contribution of both the single-stranded tails and the single-stranded loops of SL-I and SL-Ic to their formation of a duplex became most evident when such mutations were combined. Mutations at the top of the loop and the 5′ side of the loop of SL-I which reduced complementarity with the loop of SL-Ic and altered the YUNR motif led to the most drastic reductions in k_{app} when combined with removal of both single-stranded tails or the 5′ single-stranded tail of SL-Ic. Removal of the 3′ single-stranded tail of SL-Ic led to a more modest decrease in k_{app} when duplexing with these SL-I loop mutants. A three base transversion mutation on the 3′ side of the loop of SL-I (SL-I(21-23)) led to a less dramatic decrease in k_{app} when duplexing with an SL-Ic variant missing its single-stranded tails, suggesting that bases on the 3′ side of this loop play a smaller role in duplex formation. Interestingly, this mutation maintained the wild-type YUNR motif in the loop of SL-I (Figure 5.3). These results are consistent with the finding that bases in the 3′ portion of the loop of FinP SL-I play an apparently minor role in repression of plasmid R1 conjugative transfer (Koraimann *et al.*, 1996). In all cases, the presence of FinO led to higher k_{app} values for duplex formation, demonstrating its ability to promote

duplex formation *in vitro* between RNAs with sub-optimal complementarity in multiple regions. Considering the short length of complementary single-stranded regions in FinP and *traJ* mRNA, and the importance of such regions to duplex formation in other systems (Persson *et al.*, 1990a; Kolb *et al.*, 2000a), the requirement for complementarity in both the loop and single-stranded tail regions of these RNAs is not unexpected.

The presence of bulged nucleotides and mismatched bases in the stems of interacting RNAs is critical for antisense/sense RNA interactions both *in vitro* and *in vivo* for several plasmids. These regions are thought to allow breathing of the stems immediately below the loops in order to allow for rapid progression of a stable duplex (Siemering *et al.*, 1993; Hjalt and Wagner, 1995; Kolb *et al.*, 2001a). Both SL-I and SL-Ic contain a purine:purine mismatch at the fourth base pair below the loop, immediately preceded by two stable G:C base pairs. SL-Ic has an additional mismatched A:C base pair in the middle of the stem (Figure 5.1). In both cases, these mismatches lower the stability of the stems. When the purine:purine mismatches in SL-I and SL-Ic were altered to A:U base pairs in both molecules, maintaining their intermolecular complementarity, the k_{app} for FinO-mediated duplex formation decreased significantly compared to duplexing between wild-type SL-I and SL-Ic. These results indicate that, as in similar systems, the presence of bulges in the stems of SL-I and SL-Ic influences progression of the duplex from the loop through the stem regions. The results presented in this chapter have shown that when the first 5 base pairs below the stem of SL-Ic are rendered non-complementary to the equivalent region in SL-I duplex formation was drastically decreased. However, when these regions are complementary, but the last 6 base pairs at the bottom of the stem were non-complementary, duplex formation occurred at an appreciable rate. When

complementarity between the stems was completely eliminated, but the loops of SL-I and SL-Ic remained fully complementary, no higher order structure could be detected by EMSA analysis. The SL-I constructs tested in this case should theoretically be able to form a "kissing" intermediate (Takahashi *et al.*, 2000). The inability to detect such an intermediate suggests that such a complex is very unstable and breaks apart quickly unless initial loop-loop pairing can progress through the stems to form a more stable duplexing intermediate. Alternatively, a stable kissing intermediate may be formed, but may only be detectable using more sensitive means, such as NMR analysis (D'Souza *et al.*, 2001). These results demonstrate that providing that at least 5 base pairs of the stem immediately below the loop are complementary between SL-I and SL-Ic, rapid duplex formation can occur.

FinO has been shown to exhibit duplex RNA unwinding activity, which, along with its RNA-RNA duplex catalysis activity, has been localized to a lysine-rich region within the N-terminal 44 amino acids of the protein (Chapter 4; Ghetu *et al.*, submitted). The highest affinity binding sites of FinO are SL-II of FinP, and SL-IIc of *traJ* mRNA although SL-I is also a target for binding by FinO (Figure 5.11; Jerome and Frost, 1999). Binding of FinO to both of these regions may serve to destabilize the secondary structure of the stems. It is clear from the results presented in this chapter that the amount of single-stranded complementarity between FinP and *traJ184* mRNA is a critical factor influencing FinO-mediated duplex formation. FinO may promote duplex formation by a multi-step mechanism, which functions to progressively increase the amount of complementary single-stranded regions between FinP and *traJ* mRNA. A detailed model addressing such a mechanism is presented in Chapter 7.

An interesting feature that emerges from this work is that *in vivo*, minor changes to the RNA components of the FinOP system can cause significant changes to its function, although *in vitro*, major structural changes to the RNAs are tolerated during duplex formation. *In vivo*, the function of the FinOP system is influenced by multiple factors that are not present *in vitro*. The concentration of FinO, FinP, and *traJ* mRNA is variable *in vivo*, and influenced significantly by growth conditions. The interaction between FinP, FinO, and *traJ* mRNA occurs concurrently with transcription of the *tra* operon, which is in turn influenced by a variety of other factors (Frost *et al.*, 1994). It is likely that a delicate balance of factors influences the ability of FinO to promote the formation of a FinP/*traJ* mRNA duplex *in vivo* in order to inhibit transcription of the *tra* operon. *In vitro*, conditions are optimized to allow for duplex formation between the interacting RNAs, providing an environment much different from that found *in vivo*.

Chapter 6: TraJ is destabilized in a *cpxA101** background*

6.1 Introduction

The ability of bacteria to sense and respond to environmental changes is a hallmark of their highly adaptive nature. Changes in oxygen availability, pH, salt concentration, and nutrient availability, among many other factors, require alterations in gene expression to adapt to changing conditions. The cell envelope provides a means by which bacteria can sense environmental changes and transmit signals to the cytoplasm to initiate phenotypic alterations in order to adapt to changing conditions. Two-component signal transduction systems are commonly used by bacteria to provide a pathway for transmitting such signals (reviewed in Hoch and Silhavy, 1995). These systems have been implicated in such diverse activities as sensing oxygen and phosphate concentration (Strohmeier *et al.*, 1998; Ellison and McCleary, 2000) and envelope stress (Cosma *et al.*, 1995) to mediating the expression of genes required for vancomycin resistance (Ulijasz *et al.*, 2000). Generally, such systems employ a membrane-associated sensor kinase which transfers a phosphate group to a cytoplasmic response regulator, which in turn can inhibit or stimulate expression of genes at the transcriptional level (Raivio and Silhavy, 1997; reviewed in Hoch and Silhavy, 1995 and Raivio and Silhavy, 2001),

Mutations in the *E. coli* chromosome that affected F conjugative plasmid expression and caused an inability to assemble F-pili on the surface of the cell allowed the identification of the Cpx two-component signal transduction system (McEwen and Silverman 1980c). F plasmid transfer requires the elaboration of an extracytoplasmic pilus in order for donor/recipient contact to occur. Expression of the *tra* genes from the major *tra* promoter, P_Y, requires the F-encoded positive regulatory protein TraJ, and leads to the expression of all of the genes required for pilus elaboration. Multiple host-encoded

factors also influence *tra* operon expression, including ArcA, which is part of a two-component signal transduction system which responds to the redox state of the cell (see Figure 1.4 in Chapter 1; Finnegan and Willetts 1972; reviewed in Frost *et al.*, 1994; Strohmaier *et al.*, 1998). *E. coli cpxA* deletion mutants were shown to exhibit quasi-wild-type levels of F*lac* transfer. Conversely, transfer of F*lac*, as well as expression of TraJ, was significantly inhibited in other *cpxA* mutants, termed *cpxA** gain-of-function mutants (Silverman *et al.*, 1993). This inhibition of transfer was therefore attributed to a direct reduction in the intracellular concentration of TraJ, mediated by activation of the Cpx regulon (Silverman *et al.*, 1993).

The *cpx* regulon was determined to be controlled by a two-component signal transduction system, which senses and responds to cell envelope stress in *E. coli* (reviewed in Raivio and Silhavy, 2001). The vast majority of *cpx* phenotypes have been associated with the cell envelope (McEwen and Silverman 1982; McEwen *et al.*, 1983). The membrane-bound sensor kinase, CpxA, and its cognate cytoplasmic response regulator, CpxR function to transmit signals generated in the periplasm to the cytoplasm, in response to cell envelope perturbations, using a conserved phosphotransferase mechanism (see Figure 1.15 in Chapter 1; Weber and Silverman, 1988; Raivio and Silhavy, 1997). The *cpxRA* operon is normally maintained in an off state in the absence of inducing cues, and it appears to be subject to two levels of control (Raivio *et al.*, 1999, 2000).

Multiple targets of the Cpx regulon are upregulated at the transcriptional level in response to activating signals, although most are involved in degradation and refolding of misfolded proteins in the cell envelope (Danese *et al.*, 1995; Danese and Silhavy, 1997;

Pogliano *et al.*, 1997; Dartigalongue and Raina, 1998). An increased level of misfolded proteins in the cell envelope is thought to be the primary activating signal of the Cpx system (Raivio *et al.*, 2000), although a wide variety of signals can activate the Cpx stress response (Nakayama and Watanabe, 1995; Snyder *et al.*, 1995; Jones *et al.*, 1997). A class of *cpx* mutants, termed *cpx**, has been characterized according to their ability to suppress toxicity imparted by misfolded proteins in the periplasm (Cosma *et al.*, 1995). All *cpx** mutations have been localized to the CpxA sensor kinase, and analyses have determined that such *cpxA** mutants lead to constitutive activation of the Cpx regulon and subsequent upregulation of downstream targets of the operon (Cosma *et al.*, 1995; Danese *et al.*, 1995; Raivio and Silhavy, 1997; Raivio *et al.*, 1999, 2000).

Inhibition of F transfer by a *cpxA** mutation was first identified by Silverman *et al.* (1993), and it was suggested that such a mutation altered the protein to a "signal-on" state via alteration of the periplasmic sensing domain of the protein. A well-characterized *cpxA** mutation, termed *cpxA101**, alters the autophosphorylation domain of CpxA, causing a constitutively activated gain-of-function mutation in the protein (Raivio and Silhavy, 1997). Constitutive expression of the Cpx regulon in *cpxA** mutants has thus been hypothesized to lead to the reduction of the accumulation of the F TraJ protein originally observed (Silverman *et al.*, 1993). This observation has been confirmed in this chapter by determining that F transfer and expression of several F *tra* regulatory proteins are significantly lowered in a well-defined *cpxA** mutant background. This chapter presents evidence that the reduction of the level of TraJ in this mutant is specific, and occurs via a post-transcriptional mechanism.

6.2 Results

6.2.1 F-encoded proteins TraJ, TraM, and TraY are not detectable in the *cpxA101** background.

In order to determine the effect of the *cpxA101** mutation on several *tra* regulatory proteins, Western immunoblot analysis of *tra* proteins expressed from the F plasmid derivative pOX38-Km in various Cpx regulon mutants was performed. Cell pellets equivalent to O.1 OD_{600} units were subjected to SDS-PAGE and immunoblot analysis using polyclonal antisera specific for TraJ, TraM, and TraY (Materials and Methods, section 2.6). As expected, TraJ was not detectable in the *cpxA101** strain TR189 (Figure 6.1). Since TraJ is a positive activator of P_Y and indirectly of P_{traM}, immunoblot analysis was performed to determine whether a lack of TraJ expression had an effect on TraY or TraM levels (Figure 6.1). TraY and TraM proteins were also undetectable in the *cpxA101** background. In the *cpxR*⁻ strain TR51 and *cpxA*⁻ strain TR8, the levels of TraJ, TraM and TraY were close to wild-type, although TraM levels were slightly more reduced in the *cpxA*⁻ background (Figure 6.1). Similar results were obtained for a *cpxA24** mutant which carries a "signal blind" mutation in the periplasmic domain of CpxA (data not shown).

6.2.2 Transfer efficiency of pOX38-Km decreases in the *cpxA101** background.

The observed lack of expression of TraJ, TraM, and TraY prompted an investigation into the effect of several *cpx* mutations on pOX38-Km transfer. Mating assays were performed to test the ability of pOX38-Km to transfer into an F⁻ recipient strain, XK1200, from a variety of *cpx* mutant strains. The *cpxA*⁻ and *cpxR*⁻ donor strains were nearly as proficient for pOX38-Km transfer as the wild-type MC4100 donor,

Figure 6.1 F-encoded proteins TraJ, TraM, and TraY are not detectable in a *cpxA101**

background. Immunoblot analysis was performed using polyclonal antisera directed

against TraJ, TraM, and TraY (Materials and Methods section 2.5). Lanes 1 and 2: *E. coli*

MC4100 with (+) or without (-) pOX38-Km. Lanes 3-5: *cpxA⁻* (TR8), *cpxR⁻* (TR51), and

cpxA101* (TR189) strains containing pOX38-Km. Positions of TraJ, TraM, and TraY are

indicated on the right, and relevant molecular weight markers (kDa) are shown on the

left. The loading control indicated at the bottom of the figure is obtained from a protein

that non-specifically crossreacts with the antiserum.
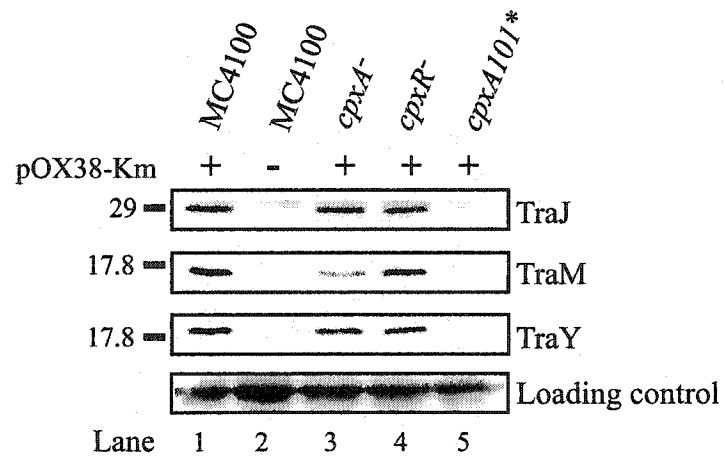
whereas in the *cpxA101** donor strain, transfer was reduced by over 600-fold (Table 6.1).

Since the periplasmic protease DegP is a member of the Cpx regulon (Danese *et al.*, 1995; Pogliano *et al.*, 1997), the effect of a *degP* mutation on pOX38-Km transfer was also examined (Table 6.1). Conjugative transfer from the *degP* donor strain JMR201 was reduced by approximately two-fold, while immunoblot analysis of the levels of TraJ and TraM expressed from pOX38-Km in the *degP* mutant revealed that both proteins were expressed at or near wild-type levels (Figure 6.2, compare lanes 1 and 3). The *degP* mutation therefore had only a small effect on pOX38-Km transfer. These results suggest that DegP has no direct influence on the level of TraJ or TraM expression or on expression of the F *tra* operon.

6.2.3 Induction of cell envelope stress reduces TraJ expression and F plasmid transfer.

Overproduction of the outer membrane lipoprotein NlpE is known to activate the Cpx pathway (Snyder *et al.*, 1995). In order to determine whether the effects of the *cpxA101** mutation were physiologically relevant, the effect of NlpE overproduction on TraJ and TraM levels expressed from pOX38-Km, and on conjugative transfer of the plasmid, was tested. Immunoblot analysis revealed that TraJ and TraM levels were significantly reduced when NlpE was overexpressed in a wild-type background, but to a lesser extent than the reduction in TraJ and TraM levels evident in the *cpxA101** background (Figure 6.2, compare lanes 1, 2, and 5). Similarly, pOX38-Km transfer was reduced but not abolished when NlpE was overexpressed (Table 6.1), suggesting that the levels of TraJ and TraM were sufficient to allow for a reduced level of plasmid transfer to occur, and that NlpE overexpression does not affect TraJ expression or plasmid transfer

Table 6.1 Efficiency of pOX38-Km transfer from a variety of donor strains.

Donor strain/plasmids	Transconjugants per 100 Donors	Mating efficiency[a] (% vs. wild-type)
MC4100/pOX38-Km	43	100
TR8 (*cpxA⁻*)/pOX38-Km	36	84
TR51 (*cpxR⁻*)/pOX38-Km	42	97
TR189 (*cpxA101**)/pOX38-Km	0.06	0.15
JMR201 (*degP⁻*)/pOX38-Km	21	49
MC4100/pOX38-Km/pBR322	28	65
MC4100/pOX38-Km/pLD404	12	28

[a] Ratio of transconjugants:donors in each strain divided by the transconjugants:donors ratio of F transfer from a wild-type MC4100 background, which was set as 100% mating efficiency.

Figure 6.2 Cell envelope stress induced by NlpE overexpression reduces TraJ and TraM levels. Immunoblot analysis was performed using polyclonal antisera directed against TraJ and TraM (Materials and Methods section 2.5). Lanes 1-3: wild-type (MC4100), *cpxA101** (TR189), and *degP* (JMR201) *E. coli* containing pOX38-Km. Lanes 4 and 5: *E. coli* MC4100 containing pOX38-Km and the control vector, pBR322, or pLD404, expressing NlpE. Positions of TraJ and TraM are indicated on the right, and the relevant molecular weight marker (kDa) is shown on the left.
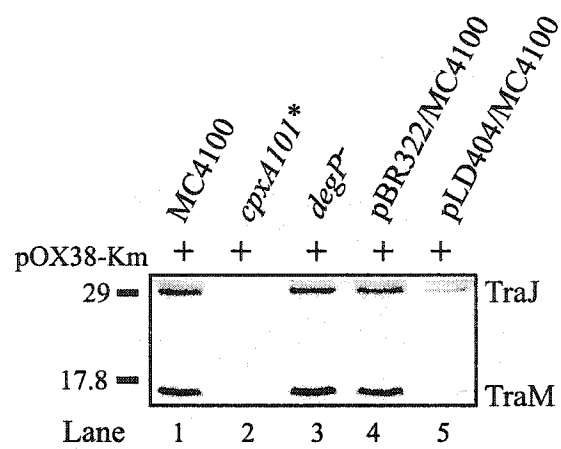
as significantly as constitutive activation of the Cpx regulon induced by the *cpxA101** mutation.

6.2.4 *traJ* transcription is only slightly reduced in various *cpx* backgrounds.

To determine whether the lack of TraJ in the constitutively activated *cpxA** background was caused by transcriptional or post-transcriptional events, Northern blot analysis was performed to detect whether the *traJ* transcript was expressed from pOX38-Km in the *cpxA101** strain. Total RNA was extracted from the appropriate strains, and separated by electrophoresis on denaturing (8M urea) polyacrylamide gels, then transferred to nylon membranes. Probing for *traJ* mRNA was performed using uniformly ^{32}P-labeled FinP antisense RNA (Materials and Methods, section 2.7). The *traJ* transcript was detectable in this strain, and its level was reduced by approximately three-fold compared to the wild-type (Figure 6.3a and 6.3b). Northern analysis to detect the *traJ* transcript in the *cpxR⁻* strain TR51 (Figure 6.3a) indicated that the *traJ* transcript was expressed at a level similar to that expressed in MC4100. However, more of the *traJ* transcript was detectable in the *cpxA⁻* strain, TR8, than in any of the other strains tested. This observation may be the result of increased stability of the transcript in TR8, since the level of expression from a P$_{traJ}$-*lacZ* reporter plasmid was very similar in all three *cpx* strains tested (see below).

β-galactosidase assays of several *cpx* mutant strains containing the P$_{traJ}$-*lacZ* reporter plasmid pMCJ211 (van Biesen and Frost, 1994) were employed to test P$_{traJ}$ activity in these backgrounds (Figure 6.4). Compared to the wild-type strain MC4100, P$_{traJ}$ activity was reduced by approximately two-fold in both the *cpxA⁻* and *cpxR⁻* strains, and approximately three-fold in the *cpxA101** strain. Both inactivation (*cpxA⁻/R⁻*) and

Figure 6.3a Northern analysis reveals that *traJ* and FinP transcripts are expressed in both wild-type and *cpxA101** *E. coli*. Total cellular RNA was extracted as described in Materials and Methods (section 2.7). Thirt-five µg of RNA were separated by electrophoresis on denaturing (8M urea) 8% polyacrylamide gels, and subjected to Northern blot analysis as described in detail in Materials and Methods (section 2.7). The position of FinP, detected using Primer A (Table 2.3), and the position of *traJ* mRNA, detected using uniformly labeled FinP are indicated to the right of the panel. Lanes 1 and 2: *E. coli* MC4100 without (-) or with (+) pOX38-Km. Lanes 2-4: pOX38-Km in *cpxA101** (TR189), *cpxR⁻* (TR51), and *cpxA⁻* (TR8) strains.

Figure 6.3b Northern analysis to show a direct comparison of *traJ* mRNA levels in wild-type and *cpxA101** backgrounds. Blots were probed for *traJ* mRNA as described above, then stripped and reprobed using the primer JSA12 (Materials and Methods, Table 2.3) to detect the internal loading control, tRNA^{ser}. Lanes 1 and 2: MC4100 without (-) and with (+) pOX38-Km. Lanes 3 and 4: *cpxA101** (TR189) without (-) and with (+) pOX38-Km. The position of the *traJ* transcript and the loading control, tRNA^{ser}, are shown on the right of the panel.

a.

	MC4100	MC4100	cpxA101*	cpxR⁻	cpxA⁻
pOX38-Km	−	+	+	+	+

traJ

FinP

Lane 1 2 3 4 5

b.

	MC4100	cpxA101*
pOX38-Km	− +	− +

traJ

tRNA^{ser}

Lane 1 2   3 4
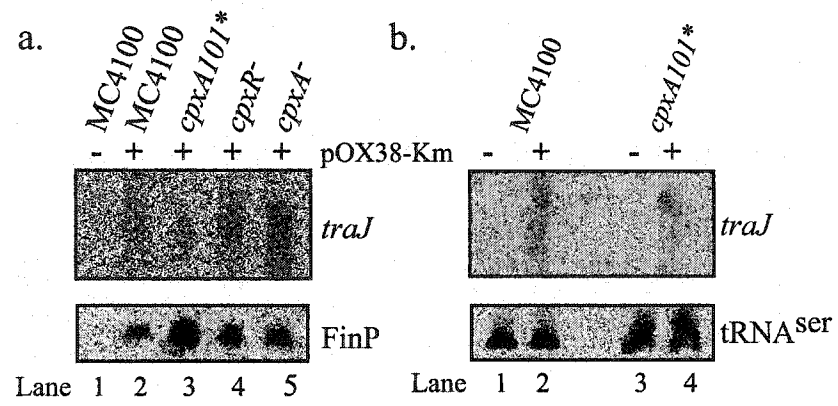
Figure 6.4 P_{traJ} activity is reduced in several *cpx* mutants. β-galactosidase assays (Materials and Methods section 2.15) were performed on culture samples as indicated. Lane 1: MC4100; Lane 2: *cpxA⁻* (TR8); Lane 3: *cpxR⁻* (TR51); and Lane 4: *cpxA101** (TR20). All strains contained the P_{traJ}-*lacZ* reporter plasmid pMCJ211. Assays with the parental control plasmid resulted in insignificant levels of β-galactosidase activity and are not included. The β-galactosidase activity (Miller Units) obtained for each culture is listed on the left of the graph.
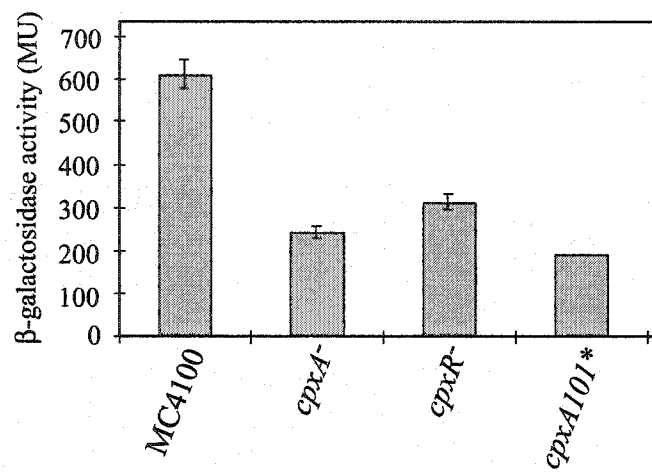
constitutive activation (*cpxA101**) of the Cpx pathway appeared to have only a minor inhibitory effect on *traJ* transcription. Taken together, the β-galactosidase assays and Northern blot analyses suggest that the reduction of TraJ expression in the *cpxA101** background was due to a post-transcriptional event. These results also suggest that general mRNA stability may vary in the *cpx* mutants, although the reason for this observation remains unclear at this time.

6.2.5 An apparent increase in FinP expression in the *cpxA101** strain does not affect TraJ accumulation.

Since expression of FinP antisense RNA is known to affect F *tra* operon expression (Lee *et al.*, 1992; Torreblanca *et al.*, 1999), the level of FinP was examined in several *cpx* mutants. Northern analysis of FinP antisense RNA expressed from pOX38-Km in wild-type, *cpxA⁻*, *cpxR⁻*, and *cpxA101** strains revealed a wild-type level of FinP in the *cpxA⁻* and *cpxR⁻* strains, and an apparently elevated FinP level in the *cpxA101** strain (Figure 6.3a). In order to determine whether FinP expression in a *cpxA101** background affected TraJ and TraM expression, immunoblot analysis of the *finP⁻* mutant F-derivative plasmid, pSLF20, was performed, using polyclonal anti-TraJ and anti-TraM antisera. TraJ was not detectable in the *cpxA101** strain, TR20, carrying pSLF20 (Figure 6.5). TR20 was used instead of TR189 to allow for selection of TR20 cells containing pSLF20, which is an F*lac* plasmid. A small amount of TraM was detected from pSLF20 and pOX38-Km in TR20, although TraM was not detectable in TR189 carrying pOX38-Km (see Figure 6.1). This may be due to small phenotypic differences between the two strains. Regardless, the amount of TraM expressed from pSLF20 in TR20 was not increased compared to the amount of TraM expressed from pOX38-Km in the same

Figure 6.5 Deletion of FinP does not rescue TraJ or TraM expression in a *cpxA101**
strain. Immunoblot analysis using polyclonal antiserum to detect TraJ and TraM
expressed from pOX38-Km and the *finP‾* F derivative plasmid pSLF20 in MC4100 and
cpxA101* (TR20) strains, as indicated above the figure. The presence (+) or absence (-)
of each plasmid (shown on the left of the figure) is indicated above each lane. The
position of TraJ and TraM are indicated on the right, and the position of the relevant
molecular weight markers (kDa) is shown on the left. The lower panel is a loading
control obtained from an unknown protein that crossreacts with the antiserum employed.
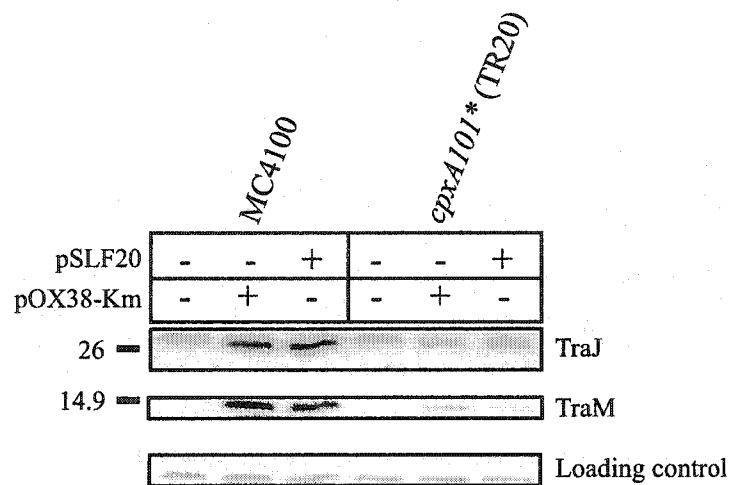
strain. Overall, these results indicate that the level of FinP in a *cpxA** strain did not affect expression of TraJ or TraM.

6.2.6 Stability of F *tra* regulatory proteins expressed from a foreign promoter is reduced in a *cpxA101** background.

Since the *traJ* transcript but not the TraJ protein was detectable in the *cpxA101** mutant, the fate of TraJ expressed from a foreign promoter was tested in order to further separate transcriptional from post-transcriptional effects. The entire coding region of *traJ* was cloned into the pBAD24 expression vector, creating pBADTraJ (Materials and Methods, Table 2.2). Wild-type *in vivo* activity of TraJ expressed from this plasmid was confirmed by a mating assay which showed that TraJ expressed from this vector was able to complement conjugative transfer of the *traJ* Flac plasmid, JCFL90, *in trans* (Table 6.2). TraJ expression from the pBADTraJ over-expression vector was induced with arabinose for 50 minutes. After induction, rifampicin and glucose were added to prevent further rounds of transcription, and culture samples were collected at various times over a two-hour period. Bacterial lysates were subjected to SDS-PAGE and immunoblot analysis to determine TraJ levels at each time point. TraJ was stable in the wild-type strain MC4100 over the duration of the experiment (Figure 6.6a, compare lanes 0 through 120). However, in the *cpxA101** strain, TraJ levels began to decrease at 15 minutes after the addition of rifampicin, and steadily decreased with time. By 120 minutes post-induction, TraJ levels decreased by approximately 75% (Figure 6.6a, compare lanes 0 and 120). Similar results were observed with a *cpxA24** mutant (data not shown). The stability of TraM expressed from the pBADTraM overexpression vector was assessed in the same manner (Figure 6.6b and 6.6c). The level of TraM was significantly reduced in

Table 6.2 TraJ expressed *in trans* from pBADTraJ complements the *traJ* F'*lac* plasmid JCFL90 and restores conjugative plasmid transfer.

Plasmids/Donor strain	% Mating Efficiency vs. pOX38-Km alone[a]
pOX38-Km/MC4100	100
JCFL90/MC4100	0.1
JCFL90/pBAD24/MC4100	0.08
JCFL90/pBADTraJ/MC4100 (Uninduced)[b]	16
JCFL90/pBADTraJ/MC4100 (Induced)[b]	130

[a] The ratio of transconjugants:donors for each mating assay was determined, and compared to the transconjugants:donors ratio for pOX38-Km, which was set as 100% mating efficiency.

[b] Induction of pBADTraJ expression was achieved by adding 0.1% (w/v) arabinose to the mating mixture.

Figure 6.6a Stability of TraJ expressed from a foreign promoter in a *cpxA101** strain. Immunoblot analysis using polyclonal antiserum to detect TraJ expressed from the pBADTraJ overexpression vector. Lane 1: TraJ expressed from pOX38-Km in MC4100. Lane 2: TraJ expressed from pBADTraJ under repressed conditions (i.e. in the presence of glucose). Lanes 3-7: TraJ expressed from pBADTraJ after induction by arabinose and subsequent inhibition of further rounds of transcription by the addition of glucose and rifampicin. The number above each lane indicates the time (minutes) each sample was taken after the addition of rifampicin and glucose. The host strains tested are shown on the right, and the relevant molecular weight marker (kDa) is shown on the left. The loading control indicated at the bottom of the figure is obtained from a protein that non-specifically crossreacts with the antiserum.

Figure 6.6b and 6.6c Stability of TraM and TraY, respectively, expressed from the pBADTraM and pBADTraY overexpression vectors. All procedures were the same as described above.

a. TraJ

pOX38-Km | Repressed | 0 | 15 | 30 | 60 | 120

29 — MC4100 (wt)

29 — TR189 (*cpxA101**)

b. TraM

pOX38-Km | Repressed | 0 | 15 | 30 | 60 | 120

17.8 — MC4100 (wt)

17.8 — TR189 (*cpxA101**)

c. TraY

pOX38-Km | Repressed | 0 | 15 | 30 | 60 | 120

17.8 — MC4100 (wt)

17.8 — TR189 (*cpxA101**)

Loading control

Lane 1 2 3 4 5 6 7
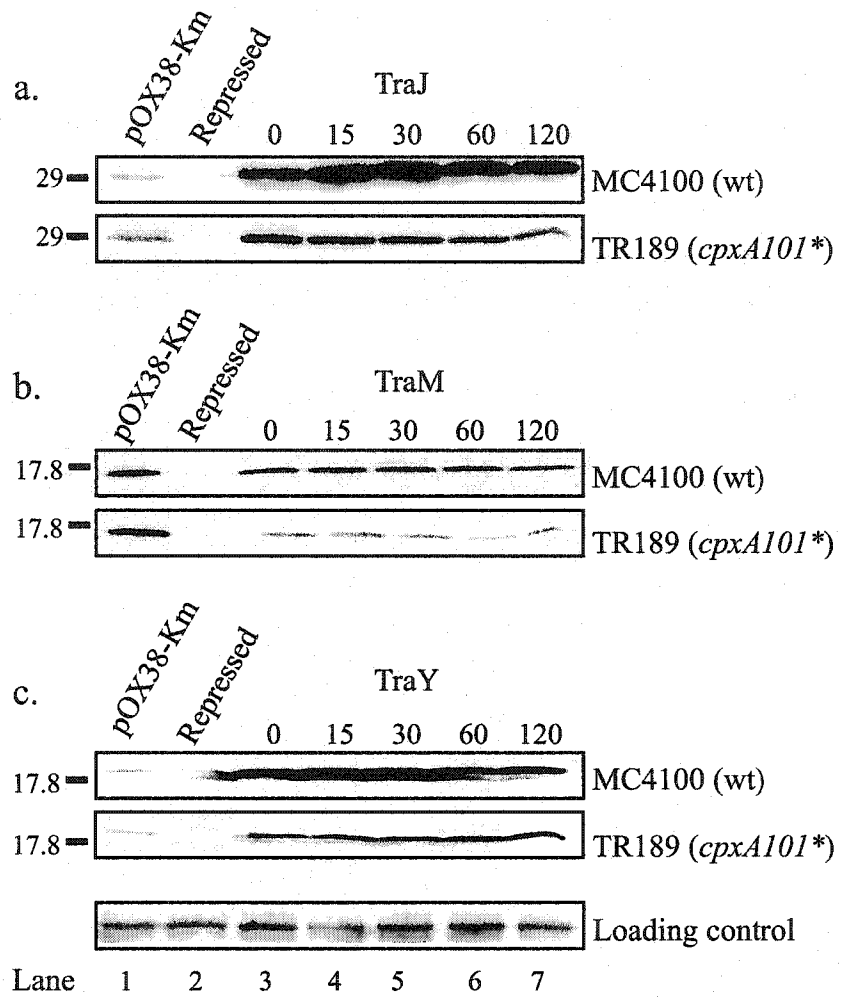
the *cpxA101** strain, but TraM was stable over time (Figure 6.6b, compare lanes 0 through 120). The stability of TraY, expressed from the pBADTraY expression plasmid, was also examined (Figure 6.6c). The level of TraY was slightly reduced in the *cpxA101** strain compared to the wild-type strain, but TraY was stable over time in both strains (Figure 6.6c, compare lanes 0 and 120). Examination of the stability of an unrelated protein, glutathione-S-transferase, revealed that it was stable in both the wild-type and *cpxA101** backgrounds (Figure 6.7). Together, these data suggest that the decreased level of TraJ in the *cpxA101** strain was a specific phenomenon.

6.2.7 Effect of *recA* and *clpP lonA* mutations on TraJ expression in the *cpxA101** strain.

Preliminary microarray analysis revealed that the expression of several *E. coli* proteases, including *recA*, was upregulated in *cpxA101* E. coli* carrying pOX38-Km (I. Lau, and T. Locke, unpublished observations). Deletion of several proteases in the *cpxA101** strain was performed to determine whether they were involved in degradation of TraJ. Immunoblot analysis of *tra* proteins expressed from the F-derivative plasmid pOX38-Tc in *cpxA101* recA* and *cpxA101* clpP lonA* backgrounds showed that TraJ was undetectable (Figure 6.8, Lanes 4 and 5). These results suggest that none of these proteases was directly involved in reducing TraJ levels expressed from F in the *cpxA101** strain.

6.2.8 Mutations in selected F membrane-associated proteins do not rescue TraJ or TraM expression in a *cpxA101** mutant.

A number of F *tra* proteins localize to the inner membrane, and therefore may be affected by the Cpx regulon under conditions of stress, which could potentially lead to

Figure 6.7 Glutathione S-transferase is stable in both wild-type and *cpxA101* E. coli*

strains. Immunoblot analysis was performed using monoclonal anti-GST antibodies, as

described in Materials and Methods, section 2.5. Lane 1: MC4100 containing no plasmid.

Lane 2: GST expressed from pGEX-KG under repressed conditions. Lanes 3-7: GST

expressed from pGEX-KG after induction by IPTG and subsequent inhibition of further

rounds of transcription by the addition of glucose and rifampicin. The number above each

lane indicates the time (minutes) each sample was taken after the addition of rifampicin

and glucose. The host strains tested are shown on the right, and the relevant molecular

weight marker (kDa) is shown on the left. The loading control indicated at the bottom of

the figure is obtained from a protein that non-specifically crossreacts with the antiserum.
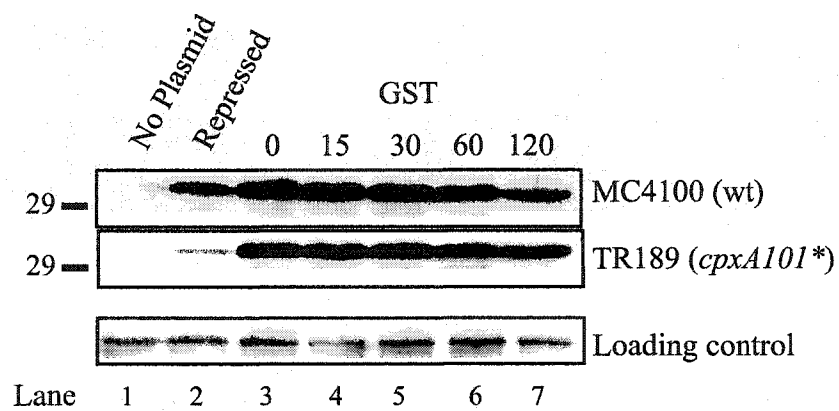
Figure 6.8 *recA* and *clpP lonA* mutations do not rescue TraJ expression in the *cpxA101**

mutant. Immunoblot analysis was performed using polyclonal antiserum directed against

TraJ, as described in Materials and Methods, section 2.5. Lanes 1 and 2: *E coli* MC4100

without (-) or with (+) pOX38-Km. Lanes 3-5: pOX38-Tc in *cpxA101** (TR189),

cpxA101* recA (TR981) and *cpxA101* clpP lonA* (TR984) strains. The position of TraJ

is indicated on the right, and the position of the relevant molecular weight marker (kDa)

is shown on the left. The loading control indicated at the bottom of the figure is obtained

from a protein that non-specifically crossreacts with the antiserum.
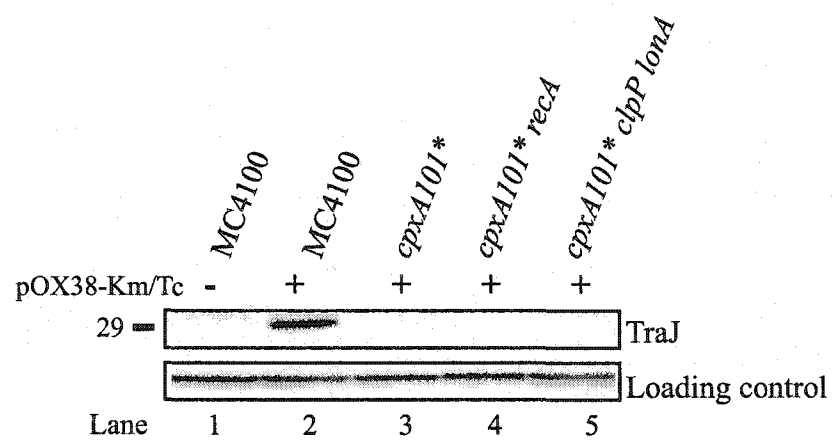
loss of TraJ expression and F plasmid transfer. Immunoblot analysis using polyclonal anti-TraJ and anti-TraM antisera was performed on *E. coli* strains carrying F*lac* plasmids with mutations in *traA, traB, traD,* and *traG,* all of which encode proteins that localize to the inner membrane (Frost *et al.,* 1994). The rationale behind this experiment was to determine whether signals from the Cpx regulon were transferred via F membrane proteins to result in reduction of TraJ stability. In a wild-type MC4100 background, TraJ and TraM were expressed at near wild-type levels from these mutant F*lac* plasmids, while in a *cpxA101** background, TraJ and TraM were undetectable by immunoblot analysis (Figure 6.9). These results suggest that the reduction of F transfer and TraJ expression observed in the *cpxA101** background was specific to TraJ, and was not influenced by any potential secondary effects of constitutive activation of the Cpx regulon on *tra* proteins that localize to the cell envelope. Similarly, the reduction of TraJ expression was not mediated by a signal from the periplasm conducted through one of the selected inner membrane F transfer proteins. While TraA, TraB, TraD, and TraG can be ruled out at this time, other F membrane-associated proteins, as well as *tra* proteins that are not associated with the membrane, remain to be tested for their involvement in reduction of TraJ stability mediated by the Cpx regulon.

6.3 Discussion

As noted by Silverman *et al.* (1993), *cpxA** gain-of-function *E. coli* exhibit reduced levels of F plasmid transfer, and a significant decrease in P_Y activity and the level of the P_Y positive regulator protein, TraJ. The results presented in this chapter reveal that the decreased level of TraJ in the *cpxA101** mutant resulted from a specific

Figure 6.9a Expression of TraJ and TraM from various F*lac* mutants in wild-type MC4100. Immunoblot analysis using polyclonal antisera was performed as described in Materials and Methods, section 2.5, to detect TraJ and TraM expressed from various F*lac* plasmids in MC4100. Lane 1: positive control of pOX38-Km in MC4100. Lane 2: negative control of MC4100 containing no plasmid. Lanes 3-8: MC4100 containing the F*lac* derivative indicated above each lane. The location of TraJ and TraM is shown on the right of the figure, and the relevant molecular weight markers (kDa) are shown on the left. The loading control indicated at the bottom of the figure is obtained from a protein that non-specifically crossreacts with the antiserum.
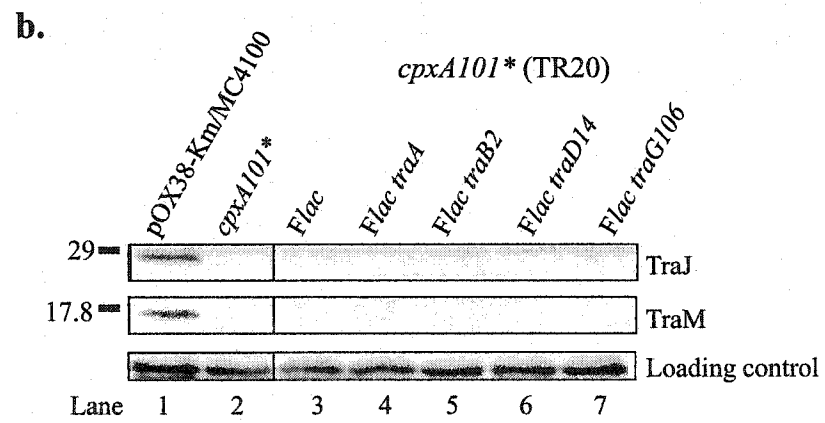
Figure 6.9b Expression of TraJ and TraM from various F*lac* mutants in a *cpxA101** host, strain TR20. Immunoblot analysis was performed as described above. Lane 1: positive control of pOX38-Km in MC4100. Lane 2: negative control of the *cpxA101** strain TR20 containing no plasmid. The rest of the figure is labeled as described in the legend for Figure 6.11a. TR20 containing F*lac traD8* was not examined, because the plasmid would not transfer into this strain after numerous attempts.

a.

MC4100

pOX38-Km/MC4100, MC4100, Flac, Flac traA, Flac traB2, Flac traD8, Flac traD14, Flac traG106

29								TraJ
17.8								TraM
								Loading control
Lane	1	2	3	4	5	6	7	8

b.

cpxA101* (TR20)

pOX38-Km/MC4100, *cpxA101**, Flac, Flac traA, Flac traB2, Flac traD14, Flac traG106

29							TraJ
17.8							TraM
							Loading control
Lane	1	2	3	4	5	6	7
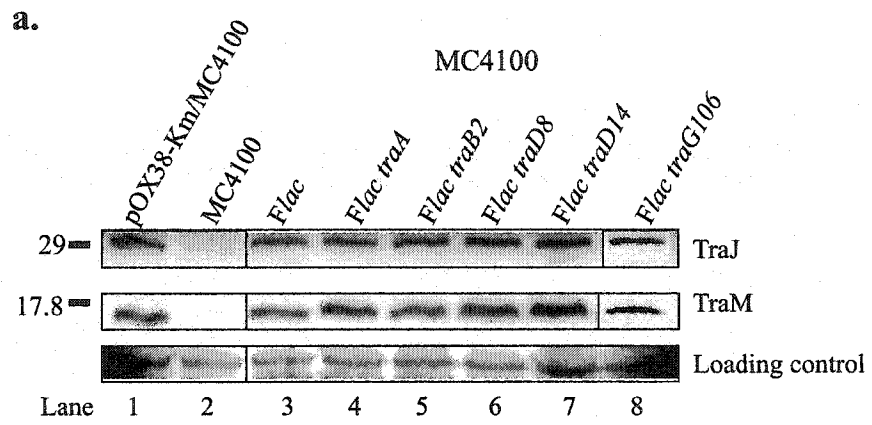
post-transcriptional event. Not only was F TraJ undetectable in a *cpxA101** strain, but TraJ expressed from a foreign promoter in this mutant was not stable. This result is somewhat unexpected, considering that the typical targets of the activated Cpx regulon are subject to regulation at the level of transcription (Danese *et al.*, 1995; Danese and Silhavy, 1997; Raivio *et al.*, 2000). It is also unexpected because the activated Cpx pathway is known to typically affect folding and stability of envelope proteins (reviewed in Raivio *et al.*, 2000), although evidence for the influence of the Cpx regulon on the function and stability of the cytoplasmic enzyme, acetohydroxyacid synthase I, exists (Sutton *et al.*, 1982). However, the specific post-transcriptional reduction of the cytoplasmic regulatory protein, TraJ, appears to be unique.

A fully functional Cpx regulon is not required for the expression of *tra* proteins and F plasmid transfer. Both *cpxA⁻* and *cpxR⁻* mutants displayed nearly wild-type levels of pOX38-Km transfer, and normal expression of the F *tra* regulatory proteins TraJ, TraM, and TraY. Conversely, constitutive activation of the Cpx sensor kinase, CpxA, in a *cpxA101** mutant (Raivio and Silhavy, 1997) drastically reduced F transfer. Activation of the wild-type Cpx pathway induced by overproduction of the outer membrane lipoprotein NlpE (Snyder *et al.*, 1995) also resulted in decreased F plasmid transfer and TraJ and TraM expression. While the effect of overproduction of NlpE on F transfer was not as severe as constitutive activation of the Cpx pathway in the *cpxA101** strain, the results support the notion that activation of the wild-type CpxAR pathway by envelope stress downregulates TraJ expression and F transfer. Interestingly, the *cpxR⁻* mutant (TR51) containing pOX38-Km became essentially non-viable when the NlpE-overexpression plasmid pLD404 was introduced into this strain (data not shown). This observation

suggests that overexpression of NlpE induces envelope stress in *E. coli* which cannot be effectively combated in the absence of a functional Cpx pathway.

Examples of negative regulation of Cpx regulon targets include downregulation of the expression of genes for motility (Dean *et al.*, 1984; Macnab, 1996; Kundu *et al.*, 1997) and chemotaxis (Kundu *et al.*, 1997) by active, phosphorylated CpxR. Expression of mRNA from the *motABcheAW* operon and swarming ability were shown to be reduced in a *cpxA** strain in a CpxR-dependent manner. Phosphorylated CpxR was also shown to bind to its consensus recognition sequence found in the promoter region of the *motABcheAW* operon (De Wulf *et al.*, 1999). However, these authors did not demonstrate whether this phenomenon was a function of the wild-type Cpx pathway. The lack of accumulation of the TraJ protein in a *cpxA101** background provides evidence of another pathway that is downregulated by constitutive Cpx regulon expression. Further, this chapter reveals that overproduction of NlpE, a known inducer of the wild-type Cpx pathway (Snyder *et al.*, 1995), has the same effect on F transfer as constitutive activation of the Cpx pathway by a *cpxA** mutation. Examination of the promoter region of *traJ* (Frost *et al.*, 1994) indicates that no consensus CpxR binding site is present (Pogliano *et al.*, 1997), supporting the idea that TraJ reduction in a *cpxA101** background is not controlled via transcriptional regulation.

TraJ expressed from pOX38-Km in a wild-type strain was found to be stable well into stationary phase, and detectable in significant amounts in cultures grown for up to twenty-four hours (Frost and Manchak, 1998). However, the *traJ* transcript is short-lived and found in only very low abundance (Lee *et al.*, 1992). These observations suggest that a low, basal level of *traJ* mRNA is sufficient to allow for enough stable TraJ to

accumulate and exert positive activation on P_Y. Examination of *traJ* promoter strength via β-galactosidase assays revealed that P_{traJ} activity was reduced by only two- to three-fold in *cpxA⁻*, *cpxR⁻*, and *cpxA101** backgrounds. Similarly, the level of *traJ* mRNA expressed from pOX38-Km was reduced by approximately three-fold in a *cpxA101** background, although in *cpxA⁻* and *cpxR⁻* strains, *traJ* mRNA was found at a level very close to that expressed from pOX38-Km in wild-type MC4100. However, TraJ levels were observed to be vastly different in these strains, with TraJ being detectable in both *cpxA⁻* and *cpxR⁻* backgrounds at nearly wild-type levels, but completely absent in a *cpxA101** strain. F transfer levels were also quite different, with the *cpxA101** strain exhibiting severely reduced pOX38-Km transfer while *cpxA⁻* and *cpxR⁻* strains showed only moderately reduced levels of plasmid transfer. These results suggest that the decreased P_{traJ} transcription exhibited by all of the *cpx* mutants tested was not responsible for the lack of detectable TraJ and reduced F transfer in the *cpxA101** strain. Although minor transcriptional effects caused by the *cpxA101** mutation cannot be ruled out, overall the data support a post-transcriptional level of control of TraJ in the *cpxA101** mutant.

Examination of F TraJ, TraM, and TraY expressed from P_{BAD} clearly demonstrated that TraJ was unstable in the *cpxA101** strain compared to the wild-type, MC4100. Interestingly, expression of all three proteins occurred at a lower level in the *cpxA101** strain than in the wild-type strain. These results suggest that a general reduction of expression from P_{BAD}, or general mRNA instability, may occur in the *cpxA101** strain. Alternatively, a reduction of the copy number of the P_{BAD} overexpression vectors in the *cpxA101** strain may also lead to lower levels of expressed

proteins although no obvious difference in plasmid levels was evident (data not shown). The reduction of the level of TraM expressed from P_{BAD} was markedly greater than the reduction of TraJ and TraY levels expressed from the same promoter. Several factors might influence TraM expression which could account for this difference, such as alterations in local superhelical density or translational efficiency (Silverman et al., 1991b).

Expression of FinP antisense RNA, part of the FinOP fertility inhibition system (see Figure 1.4 in Chapter 1; reviewed in Frost et al., 1994) is known to affect F traJ expression (Koraimann and Hogenauer, 1989; Lee et al., 1992), and is influenced by host-encoded factors such as Dam methylation and ribonuclease E degradation of FinP (Torreblanca et al., 1999). No detectable increase in TraJ expression from the finP⁻ plasmid pSLF20 occurred in the cpxA101* mutant strain (Figure 6.7), suggesting that the decreased TraJ level in a cpxA101* background is not influenced by FinP transcription. Recent microarray data (unpublished results) revealed that rne, which encodes ribonuclease E, was downregulated in a cpxA101* strain which could account for the increase in FinP expression.

Since TraJ is a cytoplasmic protein (Frost et al., 1994), the observed lack of accumulation of TraJ is most likely not directly attributable to the periplasmic protein folding and degradation pathways typically involved in response to cell envelope stress (Danese et al., 1995; Danese and Silhavy, 1997). Constitutive expression of the Cpx regulon by the cpxA101* mutant may simply mimic the induction of cell envelope stress, resulting in a reduction of expression of F tra regulatory proteins. The finding that NlpE overexpression in a wild-type background caused reduced TraJ and TraM levels supports

this idea. However, overexpression of NlpE did not cause as significant a reduction of TraJ and TraM expression or F conjugation as the *cpxA101** mutation did. These findings suggest that NlpE overexpression is not as potent an activator of the pathway that leads to a lack of TraJ accumulation as constitutive activation of CpxA. The possibility exists that a cytoplasmic protein degradation pathway is triggered by the Cpx regulon when envelope stress is induced and/or when the Cpx regulon is constitutively activated in a *cpxA101** mutant. The observation that F *traA*, *traB*, *traD*, and *traG* mutations do not rescue TraJ or TraM expression in the *cpxA101** background suggests that the Cpx regulon-mediated reduction of expression of TraJ does not occur via interactions between these F cell-envelope associated proteins and components of the Cpx regulon. While evidence for a specific pathway that leads to TraJ destabilization has not yet been obtained, work is progressing in this direction.

Preliminary microarray analysis revealed that several proteases, including RecA (Little *et al.,* 1980) and ClpP (Maurizi *et al.,* 1990), were upregulated in the *cpxA101** strain carrying pOX38-Km. The observation that filamentous growth, characteristic of cells experiencing induction of the SOS response, occurs in *cpxA** mutants (Pogliano *et al.,* 1998), coupled with our evidence of increased *recA* transcription in *cpxA101** carrying pOX38-Km, prompted an examination of the potential involvement of RecA in destabilizing TraJ. Examination of TraJ expressed from F-derivative plasmid pOX38-Tc in a *cpxA101** *recA* mutant background revealed that TraJ was not detectable, suggesting that the RecA proteolytic pathway was not involved in destabilizing TraJ. The stability of λ prophages in TR189 as well as other varied *cpx* mutants (Raivio and Silhavy, 1997) also suggests that the SOS pathway is not active in *cpxA** mutants. Similarly, a *cpxA101**

clpP lonA strain carrying pOX38-Tc exhibited undetectable levels of TraJ, implying that the ClpP and LonA proteases were not involved in the reduction of TraJ expression in the *cpxA101** mutant. Continued examination of the mechanisms involved in reducing F plasmid transfer in *cpxA** mutants should provide insight into new physiological roles for the Cpx envelope stress response.

Chapter 7: General Discussion and Conclusions

7.1 Mechanisms of FinO/RNA binding.

The ability of FinO to bind FinP is a crucial factor in allowing the FinOP fertility inhibition system to promote inhibition of expression of the F *tra* genes (Lee *et al.*, 1992; reviewed in Frost *et al.*, 1994; Firth *et al.*, 1996; Jerome and Frost, 1999). FinO recognizes multiple features in its primary RNA binding target, FinP. SL-II, which contains a stable, perfectly base-paired A-form helix, is a minimal target for FinO binding, and the presence of single-stranded tails flanking the stem increases the affinity of FinO for this RNA (Jerome and Frost, 1999). SL-I, which is shorter than SL-II and contains several mismatched base pairs, is also a target for FinO binding, but at a lower affinity (Chapter 5; Jerome and Frost, 1999). FinO also recognizes and binds the same structural features of the 5′ UTR of *traJ* mRNA, whose sequence differs completely (i.e. it is complementary to FinP) from FinP RNA (Jerome and Frost, 1999). To date, all evidence indicates that FinO recognizes RNA in a structure-dependent manner, with little or no sequence specificity. The primary target of FinO appears to be double-stranded stretches of RNA flanked by single-stranded regions (Jerome and Frost, 1999). FinO also appears to have the ability to bind multiple RNA targets. FinO can bind ColE1 RNA I with relatively high affinity (Jerome *et al.*, 1999), and tRNA can also compete with FinP, albeit at a low efficiency, for binding by FinO (Sandercock and Frost, 1998; Ghetu *et al.*, 1999). First appearances suggest that, at least *in vitro*, FinO exhibits fairly moderate specificity for multiple RNA targets.

How, then, does FinO bind to FinP antisense RNA and *traJ* mRNA with high specificity? FinP SL-II comprises a rho-independent transcription terminator, and many RNAs containing similar structural features are likely present in *E. coli*. The specificity

of FinO/FinP and FinO/*traJ* mRNA interactions therefore likely depends on several factors. When examining the secondary structure of RNAs "on paper," one often tends to think of their structures in only two dimensions, and to consider separate parts of the secondary structure as individual units. However, RNA molecules, including those of very small sizes, fold into complicated structures in three dimensions, providing a multitude of possible tertiary structural conformations that can be specifically recognized by RNA binding proteins (Draper, 1995; reviewed in Caprara and Nilsen, 2000). The folding of FinP and *traJ* mRNA in solution likely forms structures that present specific three-dimensional targets for FinO to bind. This factor, coupled with several features of FinO (discussed below), likely provide the properties that allow FinO to bind both RNAs with high specificity amongst the many RNAs that likely share similar secondary structures in *E. coli*. One cannot rule out the possibility that a protein cofactor also aids in allowing FinO to bind FinP and *traJ* mRNA *in vivo*, however no evidence has been collected to suggest that this may be the case.

The results presented in Chapter 3, and those presented in previous studies, reveal that FinO contains two distinct and separable RNA binding domains (Sandercock and Frost, 1998; Ghetu *et al.*, 1999). Each domain can bind to FinP alone, however the highest binding affinity was observed when both domains were present in the wild-type protein. The region of FinO containing the distal C-terminal 45 amino acids has been implicated in protecting FinP from RNase E-mediated degradation (Sandercock and Frost, 1998; Jerome and Frost, 1999). Proper alignment of the tertiary structure of FinP with this domain of FinO likely results in direct RNA/protein contact, leading to steric hindrance of RNase E degradation (Ghetu *et al.*, 2002). The requirement of both RNA

binding domains of FinO for high affinity RNA binding suggests that the N-terminal binding domain of FinO may aid in aligning the C-terminal protection domain of the protein with the single-stranded spacer between FinP SL-I and SL-II. One can speculate that a "lock and key" type of mechanism ensures the specificity of binding between FinO and FinP. Many RNA-protein interactions involve induced fit mechanisms, requiring structural changes to the RNA, the protein, or both moieties (Long and Crothers, 1999; reviewed in Weeks, 1997, Williamson, 2000, and Leulliot and Varani, 2001), and such processes may be involved in FinO/RNA interactions. Dynamic structural changes in FinO, FinP, or both may help to ensure that the specificity of this interaction is high (Ghetu *et al.*, 2002).

An examination of the high-resolution crystal structure of FinO provides clues as to how FinO binds to FinP. The similar length of the N-terminal alpha-helix of FinO and the stem of SL-II suggests that an alignment between these regions may occur (Ghetu *et al.*, 2000, 2002). The basic nature of the solvent-exposed N-terminal alpha-helix of FinO suggests that electrostatic interactions may occur with the phosphodiester backbone of SL-II once these regions have aligned. Previous studies proposed that a tryptophan residue, Trp-36, located at the distal end of the N-terminal alpha-helix of FinO may be brought into close proximity to the loop and upper stem region of FinP SL-II when these molecules interact (Ghetu *et al.*, 2000). The placement of Trp-36 in this region may allow for base-stacking interactions to occur with unpaired bases in the loop of SL-II, providing another specific interaction used by FinO to bind to FinP with high affinity (Ghetu *et al.*, 2000, 2002). Such interactions have been determined to occur between other protein/RNA pairs. Stacking of extended RNA bases with tyrosine side chains in

the RNA binding pockets of the *S. aureus* hexameric RNA binding protein Hfq plays a critical role in the interaction of this protein with RNA (Schumacher *et al.*, 2002). More recent studies indicate that the distal portion of the N-terminal region of FinO may in fact contact the 5′ single-stranded tail flanking SL-II (Ghetu *et al.*, 2002). However, these studies have not ruled out the possibility that dynamic interactions of both FinO and FinP SL-II may occur, and that Trp-36 may in fact still contact the loop and upper stem of SL-II. It has been suggested that the single-stranded tails of FinP may wrap around the globular central region of FinO, directly contacting the protein on the side opposite of the basic binding face of the protein (Ghetu *et al.*, 2002). High-resolution structural studies of FinO bound to FinP will likely be required to definitively answer the question of how FinO aligns with FinP during the binding process.

A highly basic, positively charged face is present on one side of FinO (Ghetu *et al.*, 2000). This face probably directly contacts FinP via electrostatic interactions with the phosphodiester backbone of the RNA, providing yet another intermolecular interaction that may increase the affinity of FinO for FinP (Ghetu *et al.*, 2000, 2002). A positively charged highly basic face is also present on one side of the Hfq hexamer, and ribo-oligonucleotide targets are bound, in part, by this face of the protein complex (Schumacher *et al.*, 2002). Both proteins may therefore use a similar mechanism to align and bind their RNA targets. From the data collected to date, it is clear that a variety of different interactions must occur to allow FinO to bind RNA with high affinity. The binding of FinO to FinP likely accomplishes two different results which both contribute to its *in vivo* function. First, an alignment of the C-terminal protection domain of FinO with the RNase E recognition/cleavage site in the single-stranded spacer between SL-I

and SL-II of FinP probably sterically inhibits RNase E cleavage. Second, when FinP and *traJ* mRNA are bound by separate FinO molecules, they may become optimally aligned to promote their formation into a kissing complex, leading to subsequent duplex formation. Both functions may be promoted by dynamic structural changes to the protein or the RNA (reviewed in Williamson, 2000 and Leulliot and Varani, 2001) once they have formed a complex (Ghetu *et al.*, 2002).

7.2 FinO-mediated RNA/RNA duplex formation.

A single region of FinO was determined to possess the ability to catalyze FinP/*traJ* mRNA duplex formation *in vitro*. The same N-terminal region of FinO which is responsible for catalyzing FinP/*traJ* mRNA duplex formation has also been shown to possess the ability to unwind double-stranded RNA (Ghetu *et al.*, 2002 submitted). This region extends from Thr-26 to Ala-44 in the N-terminal alpha-helix of FinO. The critical function of residues in this region of FinO is probably to disrupt the intramolecular helices in the stems of FinP SL-I and SL-II (SL-Ic and SL-IIc in *traJ* mRNA), immediately below the loops. Destabilization of intramolecular secondary structure of the helices of the stem-loop structures of the CopA antisense RNA and its target RNA, CopT, of plasmid R1 are critical for their function *in vivo* (Hjalt and Wagner, 1995; Kolb *et al.*, 2001a). Progression of an initial unstable kissing complex to a stable four-stranded CopA/CopT junction is dependent upon helix destabilization caused by bulged, mismatched base pairs located in the upper stems near the loops of the RNAs (Kolb *et al.*, 2001a, 2001b). Similarities between this system and the FinOP system make it tempting to speculate that RNA helix destabilization is a highly conserved mechanism that is essential for FinO-mediated RNA/RNA duplex formation.

The observation that most of the double-stranded RNA unwinding and duplex catalysis FinO mutants tested in this work could still bind FinP (Ghetu *et al.*, 2002 submitted) and protect it from degradation *in vivo* confirms previous work that has determined that the protection of FinP from RNase E degradation is a critical function of FinO (Jerome and Frost, 1999). Overall, the results presented in this thesis suggest that the ability of FinO to unwind double-stranded RNA, promote RNA/RNA duplex formation, and protect FinP from degradation are all linked to its *in vivo* function. These results reaffirm the supposition that FinO is a multifunctional protein, and that all of its functions appear to work in concert to promote fertility inhibition of F-like plasmids.

While progress has been made in determining the features of FinO required to bind FinP (Sandercock and Frost, 1998; Ghetu *et al.*, 1999, 2000, 2002) and the structural features of the RNA targets recognized by FinO (Jerome and Frost, 1999), the features of the RNA molecules required for efficient FinO-mediated duplex formation have not been as well characterized. The results presented in Chapter 5 suggest that several features of the interacting RNAs contribute to their formation into a duplex. Loop-loop base-pairing is a key initial interaction during the formation of sense-antisense RNA duplexes (reviewed in Brantl, 2002). Transversion mutations in the loop of SL-I that reduced its intermolecular complementarity with SL-Ic led to a moderate reduction in their ability to form a duplex *in vivo*, in both the presence and absence of FinO. Likewise, removal of the single-stranded tails flanking SL-I and SL-Ic led to a moderate reduction in the k_{app} for duplex formation. However, when both mutations were combined, a significant reduction in duplex formation was evident, suggesting that the amount of complementary single-stranded regions in each RNA has a profound influence on the ability of these

RNAs to form a duplex *in vitro*. Other antisense/sense RNA duplexing interactions also rely on the intermolecular pairing of single-stranded regions in each RNA, such as the pairing of RNA I and RNA II in the ColE1 replication control system (Tomizawa, 1984) and CopA/CopT pairing in plasmid R1 replication control (Persson *et al.*, 1990a; Kolb *et al.*, 2001b). Single-stranded regions of complementary RNAs allow for nucleation of duplex formation, prompting progressive duplex formation through more stable regions of secondary structure. Clearly, such interactions must be conserved across a variety of antisense/sense RNA plasmid replication control systems.

The intramolecular stability of the stems, as well as the level of their intermolecular complementarity, had a major influence on the ability of SL-I and SL-Ic to form a duplex *in vitro*. Increasing the intramolecular stability of the stems led to a reduction of FinO-mediated duplex formation, as did reducing the level of intermolecular complementarity between the stem regions of each RNA. These results indicate that base-pairing interactions between the stems of SL-I and SL-Ic are critical for the progression of an initial loop-loop interaction to a duplex. They also support the hypothesis that unwinding/destabilization of the RNA stems by FinO is a key function of the protein in promoting duplex formation. The finding that a kissing complex between SL-I and SL-Ic variants that had no intermolecular stem complementarity, but whose loops were fully complementary, could not be detected *in vitro* reaffirms the necessity for duplex formation to proceed through the stems after an initial loop-loop pairing interaction occurs. This requirement has also been well documented in the CopA/CopT pairing mechanism employed during replication control of plasmid R1 (Malmgren *et al.*, 1997; Kolb *et al.*, 2001a, 2001b). On the other hand, a stable kissing duplex may form,

but EMSA conditions may not be amenable to the detection of such a species. Further *in vitro* studies on kissing interactions between the loops of SL-I/SL-Ic and SL-II/SL-IIc will need to be performed in order to determine whether a stable kissing complex is formed between FinP and *traJ* mRNA. Optimization of EMSA conditions or alternative methods of detecting a kissing complex will need to be addressed to answer this question.

The finding that FinO could promote duplex formation between RNAs with significantly altered complementarity highlights the important role of the protein in mediating duplex formation. In all of the *in vitro* duplex analyses performed during the course of this work, FinO was able to increase the k_{app} for duplex formation between the interacting RNAs by ten- to fifty-fold. Several antisense RNA systems employ an accessory protein in order to promote RNA duplex formation, each using a different mechanism. The Rom protein of ColE1 binds to and stabilizes the initial RNA complex resulting from interaction between RNA I and RNA II, driving the reaction towards full duplex formation (Eguchi and Tomizawa, 1990). The *E. coli* Hfq protein is thought to form a nucleoprotein complex with Spot42 antisense RNA and its target *galK* mRNA, cooperatively facilitating RNA/RNA pairing. Hfq can improve the efficiency of this pairing interaction by more than 150-fold *in vitro* (Møller *et al.*, 2002b). Other RNA/RNA pairing interactions are influenced by an accessory protein. The NCp7 nucleocapsid protein of HIV-1 has been shown to facilitate dimerization between the stem-loops of the dimerization initiation site of the HIV-1 RNA genome by converting an initial unstable RNA loop-loop complex to a stable dimer (Muriaux *et al.*, 1996; Takahashi *et al.*, 2001). More recently, NCp7 was also shown to transiently melt the secondary structure of portions of the stems of HIV TAR RNA and its DNA complement,

cTAR (Bernacchi *et al.*, 2002). Based upon its similarities to such systems, previous work done on the FinOP system, and the results presented in this work, it appears that FinO may use similar mechanisms to promote FinP/*traJ* mRNA duplex formation. A refined model for FinO-mediated FinP/*traJ* mRNA duplex formation and subsequent fertility inhibition is presented in section 7.4.

7.3 The role of the Cpx regulon in F transfer inhibition.

The involvement of the Cpx two-component signal transduction system in influencing F plasmid transfer has been well established (McEwen and Silverman 1980; Silverman *et al.*, 1993). As confirmed in Chapter 6, constitutive activation of the sensor kinase, CpxA, by a *cpxA101** mutation led to a loss of TraJ accumulation. Expression of F TraM and TraY was also reduced in this mutant background, which suggests that a lack of accumulation of TraJ directly reduced expression from P_Y. The analyses presented in this thesis indicate that this phenomenon was caused by a specific post-transcriptional reduction of the level of TraJ. All evidence to date suggests that a pathway is turned on in the constitutively activated *cpxA101** mutant examined in this thesis. Preliminary evidence suggests that this pathway leads to degradation of TraJ by a cytoplasmic protease (discussed further in section 7.5).

P-pilus expression in uropathogenic *E. coli* is affected by the activity of the Cpx regulon (Hung *et al.*, 2001). The necessity for a functional Cpx regulon to correctly assemble P-pili is hypothesized to reflect the requirement of the bacterium to sense and respond to envelope stress caused by physiological changes induced by the host response to infection (Hung *et al.*, 2001). While correct folding and translocation of F pilin subunits to the inner membrane and assembly of the conjugative pilus are requirements

for F transfer (Sowa *et al.*, 1983; Frost *et al.*, 1994; Majdalani and Ippen-Ihler, 1996), a fully functional Cpx regulon was determined not to be a requirement for this process. Conversely, activation of the Cpx system negatively regulates F transfer and piliation. From a physiological standpoint, prevention of piliation and F transfer is desirable during times of actual or perceived stress, since this process requires a considerable investment in energy and metabolic resources and extensive alteration of the cell envelope (Frost *et al.*, 1994; Firth *et al.*, 1996; Wilkins and Frost, 2001)

The Cpx system typically regulates an increase in transcription of its downstream targets (reviewed in Raivio and Silhavy, 2001). However, negative regulation of flagellum expression and motility in *E. coli* has also been demonstrated (Macnab, 1996; Kundu *et al.*, 1997). Interestingly, both pilus and flagellum expression involve the elaboration of extracytoplasmic filamentous protein appendages. It is tempting to speculate that although the downregulation of expression of both moieties by constitutive activation of the Cpx regulon occurs by separate mechanisms, they may be related. Processes such as F-pilus and flagellum assembly, which require the secretion of protein subunits through the cell envelope (Sowa *et al.*, 1983; Macnab, 1996), may be shut down when cell envelope stress is detected by the Cpx pathway in *E. coli*. Since F is derepressed for transfer, Cpx-mediated reduction of TraJ may have developed as a mechanism to inhibit plasmid transfer. In the absence of such a control circuit, one can speculate that transfer would occur under adverse environmental conditions, increasing the likelihood of cellular damage and mortality via increased infection by F-specific phages and possible disruption of the integrity of the cell envelope.

A second two-component signal transduction pathway that influences *tra* operon expression is the ArcAB (SfrAB) system, which senses and responds to changes in the aerobic state of the cell (Beutin *et al.*, 1981, Silverman *et al.*, 1991a). The response regulator, ArcA, binds directly to a consensus sequence in the P_Y region of the R1 plasmid *tra* operon, directly stimulating transcription from this promoter in a TraJ-dependent manner (Strohmaier *et al.*, 1998). Similarities between the F and R1 *tra* regions and their overall control circuits suggest that the ArcAB system may function in the same manner in both plasmids (Strohmaier *et al.*, 1998). It is interesting to note that two distinct signal transduction systems act to influence *tra* operon expression in *E. coli*. Each acts via a separate mechanism, and one mediates inhibition while the other mediates upregulation of *tra* operon expression. However, a common link connects both the CpxAR and ArcAB systems: each displays an influence or dependence on TraJ. This observation suggests that these control circuits could possibly have evolved similar mechanisms for controlling *tra* gene expression via a common mediator. From a control perspective, the most efficient way to influence *tra* gene expression is to alter expression from P_Y, either directly, in the case of ArcAB, or indirectly, in the case of CpxAR. Regardless of the mechanism employed, it is obvious that two-component signal transduction systems play a critical role in influencing F and F-like plasmid transfer. These systems serve to directly connect the "decision" to transfer the plasmid with environmental cues that influence cellular health and growth.

7.4 A refined model of FinP/*traJ* mRNA duplex formation and fertility inhibition.

Synthesizing the results presented in this thesis with the work that has been performed on the FinOP system over the past decade has allowed an updated model for

fertility inhibition to be developed. F-like plasmids that are naturally repressed by a functional FinOP system generally depend on transient derepression of the *tra* genes to express the genes needed for plasmid transfer (reviewed in Frost *et al.*, 1994; Lu and Frost, unpublished observations). After transfer, FinP levels are low, due to its expression from a weak promoter and the fact that it is rapidly degraded by RNase E (Lee *et al.*, 1992; Jerome and Frost, 1999). However TraJ is expressed from a stronger promoter, allowing TraJ to accumulate and stimulate transcription from P_Y (Mullineaux and Willetts, 1985). After several generations, FinO likely accumulates to a level sufficient to protect FinP from RNase E-mediated degradation, allowing its steady-state level to increase. FinO accomplishes this protection by specifically binding to FinP, sterically inhibiting RNase E access to FinP via the placement of its C-terminal alpha-helical domain near the cleavage site located between SL-I and SL-II (Sandercock and Frost 1998; Jerome *et al*, 1999). At the same time, FinO can begin to promote the formation of a FinP/*traJ* mRNA duplex, inhibiting accumulation of TraJ and thus expression of the *tra* genes from P_Y. Unfortunately, little is currently known about the control of expression of FinO. It may be transcribed from its own promoter, or it may be transcribed from an upstream promoter in the *tra* operon such as P_{traD} (Frost *et al.*, 1994). It is unlikely that FinO is transcribed from P_Y, because inhibition of expression from P_Y would also inhibit FinO expression. Since FinP and TraJ expression occur independently of P_Y expression, it is more likely that the third component of this regulatory circuit, FinO, would also be independent of P_Y expression. This model of FinOP function therefore assumes that FinO is expressed independently of P_Y control.

FinO may function to promote FinP/*traJ* mRNA duplex formation using several mechanisms (shown schematically in Figure 7.1). Since FinO binds to both FinP and *traJ* mRNA (Jerome and Frost, 1999), these RNAs may be brought into close proximity, allowing for initial loop-loop kissing interactions to occur between SL-I/SL-Ic and SL-II/SL-IIc. It is possible that protein:protein interactions may occur between FinO molecules bound to each RNA, helping to stabilize the loop-loop interaction (Ghetu *et al.*, 2000), however there is no current evidence to support this hypothesis. Likewise, multiple FinO molecules may bind to each RNA, however further experiments would be required to make this determination. The importance of complementarity between the RBS in the loop of SL-Ic of *traJ* mRNA and the anti-RBS in the loop of SL-I of FinP was illustrated in Chapter 5. Direct evidence was provided that definitively showed that interaction between the RBS of FinP and the anti-RBS of *traJ* mRNA is required for the *in vivo* regulatory function of F FinP. Formation of a kissing complex between these loops likely suffices to inhibit TraJ translation by sequestering the *traJ* RBS in the intermolecular duplex (Koraimann *et al.*, 1991, 1996). FinO may act to stabilize this initial kissing interaction, akin to the function of the ColE1 Rom protein (Tomizawa, 1990b; Eguchi and Tomizawa, 1991). Support for this hypothesis is provided by the observation that *in vitro*, FinO can bind to a pre-formed duplex of FinP and *traJ184* mRNA (van Biesen and Frost, 1994). However, the *in vitro* EMSA analyses employed in duplex formation assays do not show a supershifted species that one would expect to observe if FinO bound to a nascent FinP/*traJ* mRNA duplex (van Biesen and Frost, 1994; Sandercock and Frost, 1998). Thus, it is more likely that once the RNA/RNA duplex has progressed to an initial stable form, FinO detaches and begins another cycle

Figure 7.1 Proposed model for the FinO-mediated catalysis of FinP/*traJ* mRNA duplex formation. In the first panel (outlined by a rectangle) preformed complexes of FinP/FinO and *traJ* mRNA/FinO are shown, as is FinO alone. Stem-loops I and II of FinP, and stem-loops Ic, IIc, and III of the 5' UTR of *traJ* mRNA, are labeled appropriately. The RBS of *traJ* mRNA and the anti-RBS of FinP RNA, in SL-Ic and SL-I respectively, are indicated by black lines. SL-III of *traJ* mRNA is only included in the first panel, and is not shown in subsequent portions of the diagram for clarity. Two separate pathways are shown, each indicated by "A" or "B." The first step is the same in both pathways, with FinO binding to both FinP and *traJ* mRNA. Individual steps in each pathway are labeled alpha-numerically, and described as follows. A1: FinO immediately disrupts the secondary structure of both RNAs, increasing the amount of single-stranded RNA available for intermolecular basepairing. A2: Kissing between the loops and duplex formation between extended single-stranded regions occurs simultaneously, creating a stable extended kissing complex. A3: "Zipping up" of FinP and *traJ* mRNA occurs rapidly, creating a full duplex that is degraded by RNase III. B1: FinP/FinO and *traJ* mRNA/FinO complexes are brought into close proximity, and loop-loop kissing proceeds. B2: FinO unwinds the stems in both RNAs, creating more extensive single-stranded regions. B3: Extended single-stranded regions in both molecules begin to base-pair, creating an extended kissing duplex. B4: "Zipping up" of FinP and *traJ* mRNA occurs rapidly, creating a full duplex that is degraded by RNase III. Diagram is not to scale, and is not intended to reflect the undoubtedly complex steps involved in the process of duplex formation. Only the key steps in the process are shown in an abbreviated form.

Full FinP/traJ mRNA duplex is degraded by RNase III.
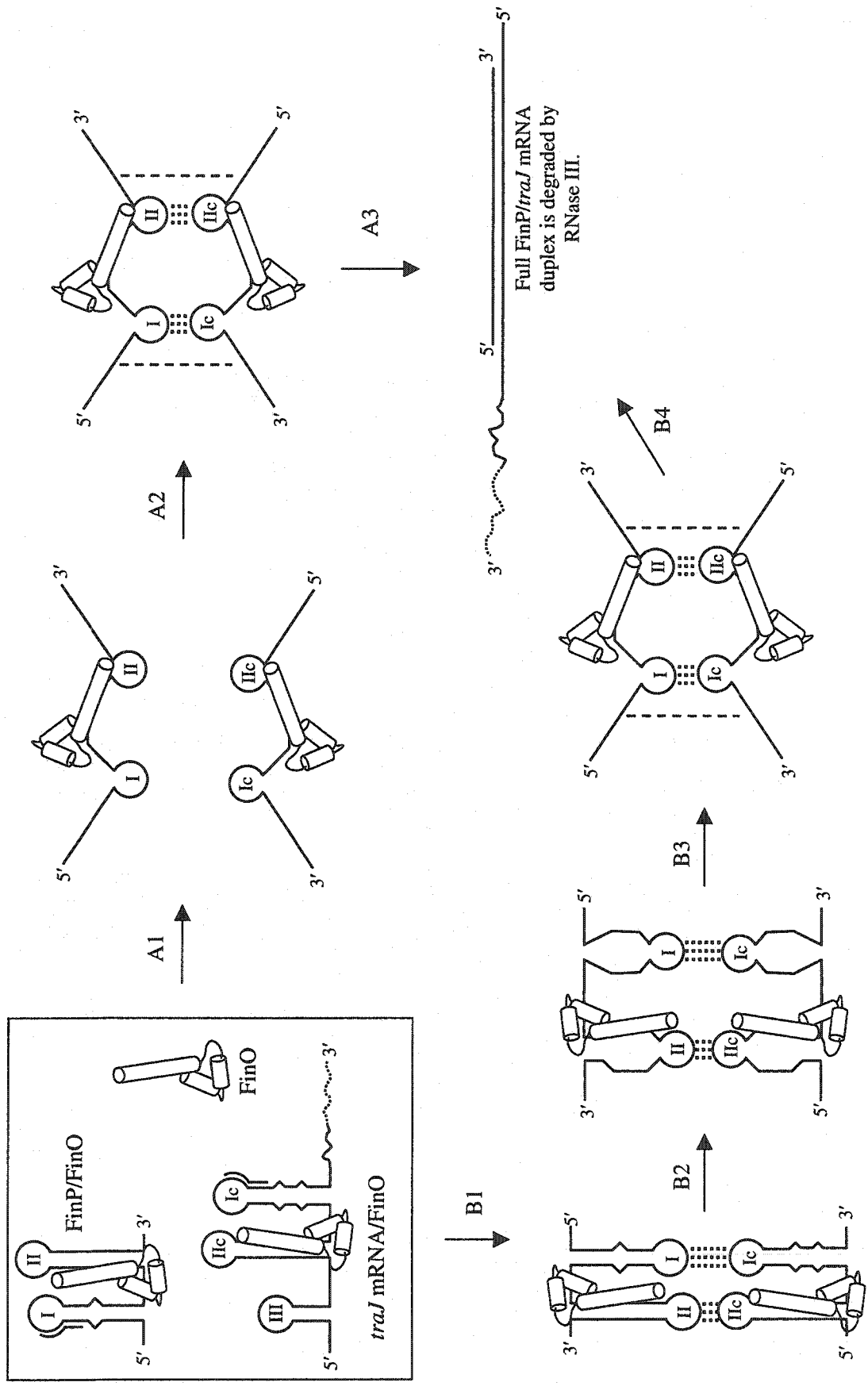
of duplex catalysis with more FinP and *traJ* RNAs. However, it is possible that a nucleoprotein complex forms that remains stable *in vivo*. The question of whether FinO remains attached to the RNA duplex remains to be established experimentally.

Once the initial kissing interaction has occurred, FinO may begin to destabilize the stems immediately below the loops, via the unwinding activity possessed by Trp-36 and other important residues in the region extending from Thr-26 to Ala-44 in the protein's alpha-helical N-terminus. The mismatched base pairs in the stems of SL-I and SL-Ic, which are important for RNA/RNA duplex formation *in vitro*, inherently destabilize these stem regions. Indeed, *traJ* mRNA is efficiently translated, even though the RBS is partially sequestered within the upper stem of SL-Ic, and the start codon is located within the lower portion of the same stem (van Biesen *et al.*, 1993). This observation suggests that SL-Ic is at least partially destabilized under normal circumstances, to allow for ribosome loading and subsequent translation of the message. In contrast, the RBS and start codon of *repA* in the plasmid R1 CopT transcript are sequestered within a very stable stem loop. Ribosome loading and translation of *repA* depends on an opening of this stem-loop, mediated by translational coupling with the *tap* gene immediately upstream (Persson *et al.*, 1990a; Blomberg *et al.*, 1992). Considering the higher free energy of unfolding of SL-II and SL-IIc, these stem-loops likely form a kinetic barrier to full duplex formation unless they can be unwound or otherwise disrupted. These observations all suggest that the initial destabilization of FinP and *traJ* mRNA by FinO is more critical for SL-II and SL-IIc than for SL-I and SL-Ic during duplex formation and mating repression.

Once unwinding of the stems progresses, a more extensive region of intermolecular single-stranded complementarity can form, allowing duplex formation to progress rapidly. The presence of complementary single-stranded regions in interacting RNAs has been shown to be critical in ColE1 RNAI/RNAII replication control (Tomizawa, 1984), as well as CopA/CopT mediated inhibition of plasmid R1 replication (Persson *et al.*, 1990a; Kolb *et al.*, 2000b). Alternatively, FinO may induce extended regions of single-stranded RNA via its unwinding activity immediately upon binding to its RNA targets. An example of this type of interaction is the *E. coli* RNA binding protein CsrA, which has been shown to cause a partial opening of a stem-loop structure present on the *glgCAP* mRNA upon binding (Baker *et al.*, 2002). While this interaction does not promote RNA/RNA duplex formation, it does provide an example of an RNA binding protein that can alter RNA secondary structure during regulation of gene expression (Baker *et al.*, 2002). Once a critical level of single-stranded complementarity between FinP antisense RNA and *traJ* mRNA is reached, rapid duplex formation between the RNAs may occur. This model would explain why significant mutations in the loop of SL-I only cause major deficits in duplex formation *in vitro* when combined with removal of the single-stranded tails. The *E. coli* Hfq chaperone has been shown to cause an opening of a stable stem-loop structure present in the untranslated regulatory RNA OxyS, and this destabilization is believed to promote the formation of a duplex between OxyS and its target, *rpoS* mRNA (Zhang *et al.*, 2002). Thus FinO, and other proteins that promote RNA/RNA pairing, such as Hfq, appear to employ a conserved mechanism to catalyze these interactions: disruption of inherently stable RNA secondary structure.

Regardless of the exact mechanism of duplex formation, the end result of the formation of the FinP/*traJ* mRNA duplex is the sequestration of the *traJ* RBS, leading to a lack of translation of the message and no accumulation of TraJ. As well, this RNA/RNA duplex becomes a target for RNase III-mediated degradation, similar to the RNase III-mediated degradation of the CopA/CopT duplex formed during inhibition of plasmid R1 replication (Blomberg *et al.*, 1990). Since the formation of a full CopA/CopT duplex is not required for inhibition of RepA synthesis (Wagner *et al.*, 1992; Malmgren *et al.*, 1997), degradation of the duplex is unimportant for control. This may also be the case for the FinOP system. The initial kissing interaction is likely sufficient to mediate inhibition of TraJ translation, and degradation of the duplex may serve simply to clear the accumulating duplexed RNA from the cell (Wagner *et al.*, 1992). However, degradation of the FinP/*traJ* mRNA duplex would also serve to decrease the potential for accumulation of TraJ, as a secondary effect of duplex formation.

7.5 Future work.

The past decade has seen a wealth of information collected that has aided in the determination of the mechanisms employed by the FinOP system to repress the transfer of F and F-like plasmids. However, a considerable amount of information is still required to understand all of the detailed mechanisms involved. Experiments using gelFRET analysis coupled with site-specific crosslinking of FinO to its minimal binding target have shown that structural changes may occur to both the protein and the RNA when they come into contact. These studies also indicate that FinO may directly contact FinP in different regions than those which were previously predicted (Ghetu *et al.*, 2000, 2002). Obtaining the crystal structure of FinO bound to FinP (and/or the 5' UTR of *traJ* mRNA)

will aid in determining exactly what contacts are made between specific amino acids of FinO and specific bases of the bound RNAs. NMR analysis of such a complex may also provide information regarding potential structural changes in the RNA/protein complex when it forms (Long and Crothers, 1999; Wilkinson *et al.*, 2000). Such analyses would aid in determining how FinO destabilizes the secondary structure of the stems in its RNA targets when it binds to them, and whether this activity is important for catalyzing duplex formation.

Duplex formation of several antisense/sense RNA interactions have been exquisitely analyzed in minute detail (Tomizawa, 1990; Kolb *et al.*, 2000a, 2001b). In order to understand the complete mechanism of FinP/*traJ* mRNA duplex formation, similar studies will need to be performed on this system. High resolution mapping of duplexes formed between FinP and *traJ* mRNA can be performed using Pb^{2+} and RNase mapping techniques to determine the structure of intermediates formed during duplex formation (Kolb *et al.*, 2001b). Similar analyses could also be used to determine whether FinO stays bound to a FinP/*traJ* mRNA duplex once it has formed, or if it simply detaches from the duplex once a stable RNA/RNA intermediate has been established. Protein-protein crosslinking could also be performed *in vitro*, in conjunction with structural analysis of FinP/*traJ* mRNA duplexes, to determine whether the flexible N-terminal regions of adjacent FinO molecules interact to stabilize the nascent RNA duplex.

The kinetics of duplex formation could also be analyzed in real-time, using methods such as surface plasmon resonance (Nordgren *et al.*, 2001), in order to more accurately determine the kinetics of the RNA/RNA interaction. Structural mapping of FinP/*traJ* mRNA duplex formation using peroxynitrous acid could also provide valuable

data regarding the step-by-step pathway involved in duplex formation. This reagent is ideally suited to analyzing structural changes during RNA/RNA interactions that occur on a short timescale (seconds to minutes), and would be well suited to sensitive analysis of the kinetics of FinP/*traJ* mRNA duplex formation (Chaulk and MacMillan, 2000). Such analyses will allow a more precise determination of which regions of each RNA come into contact with each other, in what order, and at what rate.

The analysis of the regions of FinP SL-I and *traJ* mRNA SL-Ic involved in duplex formation presented in this thesis merely scratches the surface of the potential interactions involved. Multiple mutational analyses of the loops, stems, and single-stranded regions of SL-I/SL-Ic and SL-II/SL-IIc remain to be performed. Interactions between both sets of complementary stem-loops undoubtedly contribute to rapid duplex formation, and therefore all of these regions need to be analyzed for their roles in this process. Further *in vitro* studies on duplex formation, via the methods employed in this thesis and other methods described in the previous section, should be undertaken to aid in delineating the regions of FinP and *traJ* mRNA which are most important for duplex formation. At this point, high-resolution *in vitro* structural analyses will be required to further elucidate the detailed, and likely complicated, interactions that occur between FinO, FinP, and *traJ* mRNA during duplex formation.

In vivo studies likewise need to be expanded and analyzed in detail. Mutations in multiple regions of FinP have been analyzed for their *in vivo* function in inhibiting F and R1 conjugative transfer (Chapter 5; Koraimann *et al.*, 1991, 1996). However, an exhaustive analysis has yet to be performed, and all of the studies to date have employed FinP expressed at medium or high copy number. A base-by-base mutational analysis of

FinP should be performed in order to determine what specific nucleotides might be critical for its function *in vivo*. It is possible that single, specific bases may mediate important functions of FinP. For example, *fisP305*, containing a single C30:U mutation in SL-I of FinP, is bound by FinO and duplexes with *traJ* mRNA at wild-type levels, but cannot inhibit F mating (Frost *et al.*, 1989; van Biesen, 1994; Jerome *et al.*, 1999). Also, such *in vivo* analyses should be performed using FinP expressed from a low or single copy number plasmid, to more closely approximate what occurs with a "natural" F plasmid.

Interaction of an RNA binding protein with a specific region of secondary structure on an mRNA can influence translation of the message. For example, in *E. coli.*, translation of the *glgCAP* mRNA is inhibited by the binding of the protein CsrA to a stem-loop immediately upstream of the start codon, which inhibits ribosome loading (Baker *et al.*, 2002). *traJ* mRNA is a target for FinO binding *in vitro*, but TraJ is efficiently translated in the presence of FinO (Chapter 5; Jerome and Frost, 1999). These observations suggest that if FinO does bind to the 5' UTR of *traJ* mRNA *in vivo*, it has no influence on translation of the message. As mentioned in a previous section, TraJ is efficiently translated despite the fact that the RBS and start codon are partially sequestered within SL-I, probably because SL-I is relatively unstable and can "breathe." Is it possible that the secondary structure of the 5' UTR influences translation of the message, as another level of control of *tra* operon expression? Folding of SL-Ic, SL-IIc, and SL-III in the 5' UTR of *traJ* mRNA may influence the efficiency of translation of the message, and access of ribosomes to the RBS in SL-Ic may depend on correct folding of these regions. *In vitro* "toeprint" analysis and cell-free *in vitro* translation assays could be

undertaken with various mutant *traJ* mRNAs, to determine whether the secondary structure of the 5′ UTR influences TraJ translation (Kolb *et al.*, 2001a; Baker *et al.*, 2002). This type of analysis would aid in determining whether another level of control influences TraJ, and thus *tra* operon, expression.

While we have furthered the understanding of the role of the Cpx system in controlling F transfer, much work remains to be done to fully understand how this system exerts post-transcriptional control of TraJ accumulation. Microarray analyses have been undertaken to identify potential regulatory genes that are upregulated in a constitutively active *cpxA101** mutant. Data has been collected that indicates multiple proteases are upregulated in this mutant, suggesting one or more cytoplasmic proteases may be involved in post-translational degradation of TraJ. As determined in Chapter 6, ClpP and LonA proteases have been ruled out in this process. However, current work in our lab strongly suggests that the cytoplasmic protease ClpY and its associated chaperone ClpQ (reviewed in Gottesman, 1996) are responsible for the lack of TraJ accumulation in a *cpxA101** mutant. Continued mutational analysis of proteases that are upregulated in such mutants should allow the definitive identification of a pathway involved in the post-transcriptional (or post-translational) regulation of TraJ accumulation. Analysis of *tra* expression of a naturally repressed (*finO*[+]) F-like plasmid in *cpxA101** mutant *E. coli* should also be undertaken, because the presence of a functional FinOP regulatory circuit may alter the cellular regulatory pathways that are affected by Cpx and other two-component signal transduction systems (Strohmaier *et al.*, 1998). Similarly, the role of other well-defined *cpxA** mutants in inhibiting TraJ accumulation should be examined, to determine whether a similar pathway functions in all of these mutants.

Chapter 8: References

Achtman, M., Willetts, N., and Clark, A.J. (1971) Beginning a genetic analysis of conjugational transfer determined by the F factor in *Escherichia coli* by isolation and characterization of transfer-deficient mutants. *J Bacteriol* **106**: 529-538.

Achtman, M., Willetts, N., and Clark, A.J. (1972) Conjugational complementation analysis of transfer-deficient mutants of F*lac* in *Escherichia coli. J Bacteriol* **110**: 831-842.

Anthony, K.G., Sherburne, C., Sherburne, R., and Frost, L.S. (1994) The role of the pilus in recipient cell recognition during bacterial conjugation mediated by F-like plasmids. *Mol Microbiol* **13**: 939-953.

Asano, K., and Mizobuchi, K. (1998) An RNA pseudoknot as the molecular switch for translation of the *repZ* gene encoding the replication initiator of IncIα plasmid ColIb-P9. *J Biol Chem* **273**: 11815-11825.

Asano, K., and Mizobuchi, K. (2000) Structural analysis of late intermediate complex formed between plasmid ColIb-P9 Inc RNA and its target RNA. How does a single antisense RNA repress translation of two genes at different rates? *J Biol Chem* **275**: 1269-1274.

Baker, C.S., Morozov, I., Suzuki, K., Romeo, T., and Babitzke, P. (2002) CsrA regulates glycogen biosynthesis by preventing translation of *glgC* in *Escherichia coli. Mol Microbiol* **44**: 1599-1610.

Banner,D.W., Kokkinidis,M., and Tsernoglou,D. (1987) Structure of the ColE1 *rop* protein at 1.7 Å resolution. *J Mol Biol* **196**: 657-675.

Bernacchi, S., Stoylov, S., Piemont, E., Ficheux, D., Roques, B.P., Darlix, J.L., and Mely, Y. (2002) HIV-1 nucleocapsid protein activates transient melting of least stable parts of the secondary structure of TAR and its complementary sequence. *J Mol Biol* **317**: 385-399.

Beutin, L., Manning, P.A., Achtman,M., and Willetts, N. (1981) *sfrA* and *sfrB* products of *Escherichia coli* K-12 are transcriptional control factors. *J Bacteriol* **145**: 840-844.

Birnboim, H.C., and Doly, J. (1979) A rapid alkaline extraction procedure for screening recombinant plasmid DNA. *Nucleic Acids Res* **7**: 1513-1523.

Blomberg, P., Wagner, E.G., and Nordström, K. (1990) Control of replication of plasmid R1: the duplex between the antisense RNA, CopA, and its target, CopT, is processed specifically *in vivo* and *in vitro* by RNase III. *EMBO J* **9**: 2331-2340.

Blomberg, P., Nordström, K., and Wagner, E.G.H. (1992) Replication control of plasmid R1: RepA synthesis is regulated by CopA RNA through inhibition of leader peptide translation. *EMBO J* **11**: 2675-2683.

Branlant, C., Krol, A., Ebel, J.P., Lazar, E., Haendler, B., and Jacob, M. (1982) U2 RNA shares a structural domain with U1, U4, and U5 RNAs. *EMBO J* **1**: 1259-1265.

Brantl, S., and Wagner, E.G.H. (1994) Antisense RNA-mediated transcriptional attenuation occurs faster than stable antisense/target RNA pairing: an *in vitro* study of plasmid pIP501. *EMBO J* **13**: 3599-3607.

Brantl, S. (2002) Antisense-RNA regulation and RNA interference. *Biochim Biophys Acta* **1575**: 15-25.

Brinton, C.C., Gemski, P., and Carnahan, J. (1964) A new type of bacterial pilus genetically controlled by the fertility factor of *Escherichia coli* K12 and its role in chromosome transfer. *Proc Natl Acad Sci USA* **52**: 776-783.

Camacho, E.M., and Casadesús, J. (2002) Conjugal transfer of the virulence plasmid of *Salmonella enterica* is regulated by the leucine-responsive regulatory protein and DNA adenine methylation. *Mol Microbiol* **44**: 1589-1598.

Caprara, M.G., and Nilsen, T.W. (2000) RNA: versatility in form and function. *Nat Struct Biol* **7**: 831-833.

Carey, J., Cameron, V., de Haseth, P.L., and Uhlenbeck, O.C. (1983) Sequence-specific interaction of R17 coat protein with its ribonucleic acid binding site. *Biochemistry* **22**: 2601-2610.

Carmichael, G.G., Weber, K., Niveleau, A., and Wahba, A.J. (1975) The host factor required for RNA phage Qβ RNA replication *in vitro*. Intracellular location, quantitation, and purification by polyadenylate-cellulose chromatography. *J Biol Chem* **250**: 3607-3612.

Casadaban, M.J. (1976) Transposition and fusion of the *lac* genes to selected promoters in *Escherichia coli* using bacteriophage lambda and Mu. *J Mol Biol* **104:** 541-555.

Case, C.C., Roels, S.M., Jensen, P.D., Lee, J., Kleckner, N., and Simons, R.W. (1989) The unusual stability of the *IS10* anti-sense RNA is critical for its function and is determined by the structure of its stem-domain. *EMBO J* **8:** 4297-4305.

Chandler, M., and Galas, D.J. (1983) Cointegrate formation mediated by Tn9. II. Activity of *IS1* is modulated by external DNA sequences. *J Mol Biol* **170:** 61-91.

Chang, K.Y., and Tinoco, I., Jr. (1997) The structure of an RNA "kissing" hairpin complex of the HIV TAR hairpin loop and its complement. *J Mol Biol* **269:** 52-66.

Chattopadhyay, S., Garcia-Mena, J., DeVito, J., Wolska, K., and Das, A. (1995) Bipartite function of a small RNA hairpin in transcription antitermination in bacteriophage lambda. *Proc Natl Acad Sci USA* **92:** 4061-4065.

Chaulk, S.G., and MacMillan, A.M. (2000) Characterization of the *Tetrahymena* ribozyme folding pathway using the kinetic footprinting reagent peroxynitrous acid. *Biochemistry* **39:** 2-8.

Cheah, K.C., and Skurray, R. (1986) The F plasmid carries an *IS3* insertion within *finO*. *J Gen Microbiol* **132 (12):** 3269-3275.

Cilley, C.D., and Williamson, J.R. (1997) Analysis of bacteriophage N protein and peptide binding to *boxB* RNA using polyacrylamide gel coelectrophoresis (PACE). *RNA* **3:** 57-67.

Conrad, S.E., and Campbell, J.L. (1979) Role of plasmid-coded RNA and ribonuclease III in plasmid DNA replication. *Cell* **18:** 61-71.

Cosma, C.L., Danese, P.N., Carlson, J.H., Silhavy, T.J., and Snyder, W.B. (1995) Mutational activation of the Cpx signal transduction pathway of *Escherichia coli* suppresses the toxicity conferred by certain envelope-associated stresses. *Mol Microbiol* **18:** 491-505.

D'Souza, V., Melamed, J., Habib, D., Pullen, K., Wallace, K., and Summers, M.F. (2001) Identification of a high affinity nucleocapsid protein binding element within the Moloney

murine leukemia virus Psi-RNA packaging signal: implications for genome recognition. *J Mol Biol* **314:** 217-232.

Danese, P.N., Snyder, W.B., Cosma, C.L., Davis, L.J., and Silhavy, T.J. (1995) The Cpx two-component signal transduction pathway of *Escherichia coli* regulates transcription of the gene specifying the stress-inducible periplasmic protease, DegP. *Genes Dev* **9:** 387-398.

Danese, P.N., and Silhavy, T.J. (1997) The σ^E and the Cpx signal transduction systems control the synthesis of periplasmic protein-folding enzymes in *Escherichia coli Genes Dev* **11:** 1183-1193.

Danese, P.N., and Silhavy, T.J. (1998) Targeting and assembly of periplasmic and outer-membrane proteins in *Escherichia coli. Annu Rev Genet* **32:** 59-94.

Danese, P.N., and Silhavy, T.J. (1998) CpxP, a stress-combative member of the Cpx regulon. *J Bacteriol* **180:** 831-839.

Dartigalongue, C., and Raina, S. (1998) A new heat-shock gene, *ppiD*, encodes a peptidyl-prolyl isomerase required for folding of outer membrane proteins in *Escherichia coli. EMBO J* **17:** 3968-3980.

Das, A. (1993) Control of transcription termination by RNA-binding proteins. *Annu Rev Biochem* **62:** 893-930.

Datta, N. (1975) Epidemiology and classification of plasmids. In *Microbiology-1974*. Washington, D.C.: American Society for Microbiology Press, pp. 9-15.

Davison, J. (1999) Genetic exchange between bacteria in the environment. *Plasmid* **42:** 73-91.

Dayie, K.T., Brodsky, A.S., and Williamson, J.R. (2002) Base flexibility in HIV-2 TAR RNA mapped by solution ^{15}N,^{13}C NMR relaxation. *J Mol Biol* **317:** 263-278.

De Wulf, P., Kwon, O., and Lin, E.C. (1999) The CpxRA signal transduction system of *Escherichia coli*: growth- related autoactivation and control of unanticipated target operons. *J Bacteriol* **181:** 6772-6778.

De Wulf, P., and Lin, E.C. (2000) Cpx two-component signal transduction in *Escherichia coli*: excessive CpxR-P levels underlie CpxA* phenotypes. *J Bacteriol* **182:** 1423-1426.

De Wulf, P., Akerley, B.J., and Lin, E.C. (2000) Presence of the Cpx system in bacteria. *Microbiology* **146(2):** 247-248.

Dean, G.E., Macnab, R.M., Stader, J., Matsumura, P., and Burks, C. (1984) Gene sequence and predicted amino acid sequence of the *motA* protein, a membrane-associated protein required for flagellar rotation in *Escherichia coli*. *J Bacteriol* **159:** 991-999.

DeJong, E.S., Marzluff, W.F., and Nikonowicz ,E.P. (2002) NMR structure and dynamics of the RNA-binding site for the histone mRNA stem-loop binding protein. *RNA* **8:** 83-96.

Di Laurenzio, L., Frost, L.S., and Paranchych, W. (1992) The TraM protein of the conjugative plasmid F binds to the origin of transfer of the F and ColE1 plasmids. *Mol Microbiol* **6:** 2951-2959.

Disque-Kochem, C., and Dreiseikelmann, B. (1997) The cytoplasmic DNA-binding protein TraM binds to the inner membrane protein TraD *in vitro*. *J Bacteriol* **179:** 6133-6137.

Doelling, J.H., and Franklin, N.C. (1989) Effects of all single base substitutions in the loop of *boxB* on antitermination of transcription by bacteriophage lambda's N protein. *Nucleic Acids Res* **17:** 5565-5577.

Dong, J., Iuchi, S., Kwan, H.S., Lu, Z., and Lin, E.C. (1993) The deduced amino-acid sequence of the cloned *cpxR* gene suggests the protein is the cognate regulator for the membrane sensor, CpxA, in a two-component signal transduction system of *Escherichia coli*. *Gene* **136:** 227-230.

Draper, D.E. (1995) Protein-RNA recognition. *Annu Rev Biochem.* **64:** 593-620.

Eguchi, Y., and Tomizawa, J. (1990) Complex formed by complementary RNA stem-loops and its stabilization by a protein: function of ColE1 Rom protein. *Cell* **60:** 199-209.

Eguchi, Y., and Tomizawa, J. (1991) Complexes formed by complementary RNA stem-loops. Their formations, structures and interaction with ColE1 Rom protein. *J Mol Biol* **220:** 831-842.

Eguchi, Y., Itoh, T., and Tomizawa, J. (1991) Antisense RNA. *Annu Rev Biochem* **60:** 631-652.

Ellison, D.W., and McCleary, W.R. (2000) The unphosphorylated receiver domain of PhoB silences the activity of its output domain. *J Bacteriol* **182:** 6592-6597.

Fekete, R.A., and Frost, L.S. (2002) Characterizing the DNA contacts and cooperative binding of F plasmid TraM to its cognate sites at *oriT*. *J Biol Chem* **277:** 16705-16711.

Finlay, B.B., Frost, L.S., Paranchych, W., and Willetts, N.S. (1986) Nucleotide sequences of five IncF plasmid *finP* alleles. *J Bacteriol* **167:** 754-757.

Finnegan, D., and Willetts, N. (1972) The nature of the transfer inhibitor of several F-like plasmids. *Mol Gen Genet* **119:** 57-66.

Finnegan, D., and Willetts, N. (1973) The site of action of the F transfer inhibitor. *Mol Gen Genet* **127:** 307-316.

Finnegan, D.J., and Willetts, N.S. (1971) Two classes of F*lac* mutants insensitive to transfer inhibition by an F-like R factor. *Mol Gen Genet* **111:** 256-264.

Firth, N., Ippen-Ihler, K., and Skurray,R.A. (1996) Structure and function of the F factor and mechanism of conjugation. In *Escherichia coli and Salmonella*. Neidhardt, F.C., Curtiss III, R., Ingraham, J.L., Lin, E.C.C., Low, K.B., Magasanik, B., Reznikoff, W.S., Riley, M., Schaechter, M., and Umbarger, H.E. (eds.). Washington, D.C.: American Society for Microbiology Press, pp. 2377-2401.

Franch, T., Petersen, M., Wagner, E.G.H., Jacobsen, J.P., and Gerdes, K. (1999) Antisense RNA regulation in prokaryotes: rapid RNA/RNA interaction facilitated by a general U-turn loop structure. *J Mol Biol* **294:** 1115-1125.

Franklin, N.C. (1985a) Conservation of genome form but not sequence in the transcription antitermination determinants of bacteriophages lambda, phi 21 and P22. *J Mol Biol* **181:** 75-84.

Franklin, N.C. (1985b) "N" transcription antitermination proteins of bacteriophages lambda, phi 21 and P22. *J Mol Biol* **181:** 85-91.

Franze de Fernandez, M.T., Eoyang, L., and August, J.T. (1968) Factor fraction required for the synthesis of bacteriophage Qß-RNA. *Nature* **219:** 588-590.

Franze de Fernandez, M.T., Hayward, W.S., and August, J.T. (1972) Bacterial proteins required for replication of phage Q ribonucleic acid. Pruification and properties of host factor I, a ribonucleic acid-binding protein. *J Biol Chem* **247:** 824-831.

Friedman, D.I., and Court, D.L. (1995) Transcription antitermination: the lambda paradigm updated. *Mol Microbiol* **18:** 191-200.

Frost, L., Lee, S., Yanchar, N., and Paranchych, W. (1989) *finP* and *fisO* mutations in FinP anti-sense RNA suggest a model for FinOP action in the repression of bacterial conjugation by the F*lac* plasmid JCFL0. *Mol Gen Genet* **218:** 152-160.

Frost, L.S., Ippen-Ihler, K., and Skurray, R.A. (1994) Analysis of the sequence and gene products of the transfer region of the F sex factor. *Microbiol Rev* **58:** 162-210.

Frost, L.S., and Manchak, J. (1998) F-phenocopies: characterization of expression of the F transfer region in stationary phase. *Microbiology* **144 (9):** 2579-2587.

Gaudin, H.M., and Silverman, P.M. (1993) Contributions of promoter context and structure to regulated expression of the F plasmid *traY* promoter in *Escherichia coli* K-12. *Mol Microbiol* **8:** 335-342.

Ghetu, A.F., Gubbins, M.J., Oikawa, K., Kay, C.M., Frost, L.S., and Glover, J.N.M. (1999) The FinO repressor of bacterial conjugation contains two RNA binding regions. *Biochemistry* **38:** 14036-14044.

Ghetu, A.F., Gubbins, M.J., Frost, L.S., and Glover, J.N.M. (2000) Crystal structure of the bacterial conjugation repressor *finO*. *Nat Struct Biol* **7:** 565-569.

Ghetu, A.F., Arthur, D.C., Kerppola, T.K., and Glover, J.N.M. (2002) Probing FinO-FinP RNA interactions by site-directed protein-RNA crosslinking and gelFRET. *RNA* **8:** 816-823.

Gottesman, S., Clark, W.P., and Maurizi, M.R. (1990) The ATP-dependent Clp protease of *Escherichia coli*. Sequence of *clpA* and identification of a Clp-specific substrate *J Biol Chem* **265:** 7886-7893.

Gottesman, S. (1996) Proteases and their targets in *Escherichia coli*. *Annu Rev Genet* **30:** 465-506.

Grahn, E., Moss, T., Helgstrand, C., Fridborg, K., Sundaram, M., Tars, K., Lago, H., Stonehouse, N.J., Davis, D.R., Stockley, P.G., and Liljas, L. (2001) Structural basis of pyrimidine specificity in the MS2 RNA hairpin-coat-protein complex. *RNA* **7:** 1616-1627.

Greenblatt, J., Nodwell, J.R., and Mason, S.W. (1993) Transcriptional antitermination. *Nature* **364 :** 401-406.

Gregorian, R.S., Jr., and Crothers, D.M. (1995) Determinants of RNA hairpin loop-loop complex stability. *J Mol Biol* **248:** 968-984.

Gubbins, M.J., Lau, I., Will. W.R., Manchak, J.M., Raivio, T.L., and Frost, L.S. (2002) The positive regulator, TraJ, of the *Escherichia coli* F plasmid is unstable in a *cpxA*** background. *J. Bacteriol* **184:** 5781-5788.

Gutell, R.R., Larsen, N., and Woese, C.R. (1994) Lessons from an evolving rRNA: 16S and 23S rRNA structures from a comparative perspective. *Microbiol Rev* **58:** 10-26.

Guzman, L.M., Belin, D., Carson, M.J., and Beckwith, J. (1995) Tight regulation, modulation, and high-level expression by vectors containing the arabinose P_{BAD} promoter. *J Bacteriol* **177:** 4121-4130.

Hajnsdorf, E., and Régnier, P. (2000) Host factor Hfq of *Escherichia coli* stimulates elongation of poly(A) tails by poly(A) polymerase I. *Proc Natl Acad Sci USA* **97:** 1501-1505.

Harwood, C.R., and Meynell, E. (1975) Cyclic AMP and the production of sex pili by *E. coli* K-12 carrying derepressed sex factors. *Nature* **254:** 628-660.

Hayes, W. (1953) Observations on a transmissable agent determining sexual differentiation in *Bacterium coli*. *J Gen Microbiol* **8:** 72-88.

Heaphy, S., Finch, J.T., Gait, M.J., Karn, J., and Singh, M. (1991) Human immunodeficiency virus type 1 regulator of virion expression, rev, forms nucleoprotein filaments after binding to a purine-rich "bubble" located within the rev-responsive region of viral mRNAs. *Proc Natl Acad Sci USA* **88:** 7366-7370.

Herschlag, D. (1995) RNA chaperones and the RNA folding problem. *J Biol Chem* **270:** 20871-20874.

Hjalt, T., and Wagner, E.G.H. (1992) The effect of loop size in antisense and target RNAs on the efficiency of antisense RNA control. *Nucleic Acids Res* **20:** 6723-6732.

Hjalt, T.A., and Wagner, E.G.H. (1995) Bulged-out nucleotides in an antisense RNA are required for rapid target RNA binding *in vitro* and inhibition *in vivo*. *Nucleic Acids Res* **23:** 580-587.

Hoch, J.A., and Silhavy, T.J. (1995) *Two-component signal transduction.* Hoch, J.A., Silhavy, T.J. (eds.). Washington, DC: American Society for Microbiology Press.

Howard, M.T., Nelson, W.C., and Matson, S.W. (1995) Stepwise assembly of a relaxosome at the F plasmid origin of transfer. *J Biol Chem* **270:** 28381-28386.

Hung, D.L., Raivio, T.L., Jones, C.H., Silhavy, T.J., and Hultgren, S.J. (2001) Cpx signaling pathway monitors biogenesis and affects assembly and expression of P pili. *EMBO J* **20:** 1508-1518.

Ihler, G., and Rupp, W.D. (1969) Strand-specific transfer of donor DNA during conjugation in *E. coli*. *Proc Natl Acad Sci USA* **63:** 138-143.

Ippen-Ihler, K., and Skurray, R. (1993) Genetic organization of transfer-related determinants on the sex factor F and related plasmids. In *Bacterial Conjugation*. Clewell, D. (ed.). New York: Plenum Press, pp. 23-52.

Itoh, T., and Tomizawa, J. (1980) Formation of an RNA primer for initiation of replication of ColE1 DNA by ribonuclease H. *Proc Natl Acad Sci USA* **77:** 2450-2454.

Jerome, L.J., van Biesen, T., and Frost, L.S. (1999) Degradation of FinP antisense RNA from F-like plasmids: the RNA-binding protein, FinO, protects FinP from ribonuclease E. *J Mol Biol* **285:** 1457-1473.

Jerome, L.J., and Frost, L.S. (1999) *In vitro* analysis of the interaction between the FinO protein and FinP antisense RNA of F-like conjugative plasmids. *J Biol Chem* **274:** 10356-10362.

Jones, C.H., Danese, P.N., Pinkner, J.S., Silhavy, T.J., and Hultgren, S.J. (1997) The chaperone-assisted membrane release and folding pathway is sensed by two signal transduction systems. *EMBO J* **16:** 6394-6406.

Kajitani, M., Kato, A., Wada, A., Inokuchi, Y., and Ishihama, A. (1994) Regulation of the *Escherichia coli hfq* gene encoding the host factor for phage Qß. *J Bacteriol* **176:** 531-534.

Kambach, C., Walke, S., and Nagai, K. (1999) Structure and assembly of the spliceosomal small nuclear ribonucleoprotein particles. *Curr Opin Struct Biol* **9:** 222-230.

Kim, J.L., Morgenstern, K.A., Griffith, J.P., Dwyer, M.D., Thomson, J.A., Murcko, M.A., Lin, C., and Caron, P.R. (1998) Hepatitis C virus NS3 RNA helicase domain with a bound oligonucleotide: the crystal structure provides insights into the mode of unwinding. *Structure* **6:** 89-100.

Kingsman, A., and Willetts, N. (1978) The requirements for conjugal DNA synthesis in the donor strain during F*lac* transfer. *J Mol Biol* **122:** 287-300.

Klimke, W.A., and Frost, L.S. (1998) Genetic analysis of the role of the transfer gene, *traN*, of the F and R100-1 plasmids in mating pair stabilization during conjugation. *J Bacteriol* **180:** 4036-4043.

Kolb, F.A., Engdahl, H.M., Slagter-Jager, J.G., Ehresmann, B., Ehresmann, C., Westhof, E., Wagner, E.G., and Romby, P. (2000a) Progression of a loop-loop complex to a four-way junction is crucial for the activity of a regulatory antisense RNA. *EMBO J* **19:** 5905-5915.

Kolb, F.A., Malmgren, C., Westhof, E., Ehresmann, C., Ehresmann, B., Wagner, E.G., and Romby, P. (2000b) An unusual structure formed by antisense-target RNA binding involves an extended kissing complex with a four-way junction and a side-by-side helical alignment. *RNA* **6:** 311-324.

Kolb, F.A., Westhof, E., Ehresmann, C., Ehresmann, B., Wagner, E.G.H., and Romby, P. (2001a) Bulged residues promote the progression of a loop-loop interaction to a stable and inhibitory antisense-target RNA complex. *Nucleic Acids Res* **29**: 3145-3153.

Kolb, F.A., Westhof, E., Ehresmann, B., Ehresmann, C., Wagner, E.G.H., and Romby, P. (2001b) Four-way junctions in antisense RNA-mRNA complexes involved in plasmid replication control: a common theme? *J Mol Biol* **309**: 605-614.

Koraimann, G., and Högenauer, G. (1989) A stable core region of the *tra* operon mRNA of plasmid R1-19. *Nucleic Acids Res* **17**: 1283-1298.

Koraimann, G., Koraimann, C., Koronakis, V., Schlager, S., and Högenauer, G. (1991) Repression and derepression of conjugation of plasmid R1 by wild-type and mutated *finP* antisense RNA. *Mol.Microbiol.* **5**: 77-87.

Koraimann ,G., Teferle, K., Markolin, G., Woger, W., and Högenauer, G. (1996) The FinOP repressor system of plasmid R1: analysis of the antisense RNA control of *traJ* expression and conjugative DNA transfer. *Mol Microbiol* **21**: 811-821.

Kumar, S., and Srivastava, S. (1983) Cyclic AMP and its receptor protein are required for expression of transfer genes of conjugative plasmid F in *Escherichia coli*. *Mol Gen Genet* **190**: 27-34.

Kundu, T.K., Kusano, S., and Ishihama, A. (1997) Promoter selectivity of *Escherichia coli* RNA polymerase σ^F holoenzyme involved in transcription of flagellar and chemotaxis genes. *J Bacteriol* **179**: 4264-4269.

Lacatena, R.M., and Cesareni, G. (1981) Base pairing of RNA I with its complementary sequence in the primer precursor inhibits ColE1 replication. *Nature* **294**: 623-626.

Laemmli, U.K. (1970) Cleavage of structural proteins during the assembly of the head of bacteriophage T4. *Nature* **227**: 680-685.

Laughrea, M., and Jetté,L. (1994) A 19-nucleotide sequence upstream of the 5′ major splice donor is part of the dimerization domain of human immunodeficiency virus 1 genomic RNA. *Biochemistry* **33**: 13464-13474.

Lazinski, D., Grzadzielska, E., and Das, A. (1989) Sequence-specific recognition of RNA hairpins by bacteriophage antiterminators requires a conserved arginine-rich motif. *Cell* **59**: 207-218.

Lederberg, J., and Tatum, E.L. (1946) Gene recombination in *Escherichia coli. Nature* **158**: 558-558.

Lederberg, J., Cavalli, L.J., and Lederberg, E.M. (1952) Sex compatibility in *Escherichia coli. Genetics* **37**: 720-730.

Lee, A.J., and Crothers, D.M. (1998) The solution structure of an RNA loop-loop complex: the ColE1 inverted loop sequence. *Structure* **6**: 993-1005.

Lee, S.H., Frost, L.S., and Paranchych, W. (1992) FinOP repression of the F plasmid involves extension of the half-life of FinP antisense RNA by FinO. *Mol Gen Genet* **235**: 131-139.

Legault, P., Li, J., Mogridge, J., Kay, L.E., and Greenblatt, J. (1998) NMR structure of the bacteriophage lambda N peptide/*boxB* RNA complex: recognition of a GNRA fold by an arginine-rich motif. *Cell* **93**: 289-299.

Leulliot, N., and Varani, G. (2001) Current topics in RNA-protein recognition: control of specificity and biological function through induced fit and conformational capture. *Biochemistry* **40**: 7947-7956.

Lin-Chao, S., and Cohen, S.N. (1991) The rate of processing and degradation of antisense RNA I regulates the replication of ColE1-type plasmids *in vivo. Cell* **65**: 1233-1242.

Little, J.W., Edmiston, S.H., Pacelli, L.Z., and Mount, D.W. (1980) Cleavage of the *Escherichia coli lexA* protein by the *recA* protease. *Proc Natl Acad Sci USA* **77**: 3225-3229.

Lodmell, J.S., Ehresmann, C., Ehresmann, B., and Marquet, R. (2000) Convergence of natural and artificial evolution on an RNA loop-loop interaction: the HIV-1 dimerization initiation site. *RNA* **6**: 1267-1276.

Long, K.S., and Crothers, D.M. (1999) Characterization of the solution conformations of unbound and Tat peptide-bound forms of HIV-1 TAR RNA. *Biochemistry* **38**: 10059-10069.

Lopez, P.J., Guillerez, J., Sousa, R., and Dreyfus, M. (1997) The low processivity of T7 RNA polymerase over the initially transcribed sequence can limit productive initiation *in vivo*. *J Mol Biol* **269:** 41-51.

Lowary, P.T., and Uhlenbeck, O.C. (1987) An RNA mutation that increases the affinity of an RNA-protein interaction. *Nucleic Acids Res* **15:** 10483-10493.

Luo, Y., Gao, Q., and Deonier, R.C. (1994) Mutational and physical analysis of F plasmid *traY* protein binding to *oriT*. *Mol Microbiol* **11:** 459-469.

Lynch, A.S., and Lin, E.C. (1996) Transcriptional control mediated by the ArcA two-component response regulator protein of *Escherichia coli*: characterization of DNA binding at target promoters. *J Bacteriol* **178:** 6238-6249.

Macnab, R.B. (1996) Flagella and motility. In *Escherichia coli and Salmonella: cellular and molecular biology*. Neidhardt, F.C., Curtiss III, R., Ingraham, J.L., Lin, E.C.C., Low, K.B., Magasanik, B., Reznikoff, W.S., Riley, M., Schaechter, M., and Umbarger, H.E. (eds.). Washington, D.C.: American Society for Microbiology Press, pp. 123-145.

Majdalani, N., and Ippen-Ihler, K. (1996) Membrane insertion of the F-pilin subunit is Sec independent but requires leader peptidase B and the proton motive force. *J Bacteriol* **178** : 3742-3747.

Majdalani, N., Moore, D., Maneewannakul, S., and Ippen-Ihler, K. (1996) Role of the propilin leader peptide in the maturation of F pilin. *J Bacteriol* **178:** 3748-3754.

Majdalani, N., Cunning, C., Sledjeski, D., Elliott, T., and Gottesman, S. (1998) DsrA RNA regulates translation of RpoS message by an anti-antisense mechanism, independent of its action as an antisilencer of transcription. *Proc Natl Acad Sci USA* **95:** 12462-12467.

Malmgren, C., Engdahl, H.M., Romby, P., and Wagner, E.G.H. (1996) An antisense/target RNA duplex or a strong intramolecular RNA structure 5' of a translation initiation signal blocks ribosome binding: the case of plasmid R1. *RNA* **2:** 1022-1032.

Malmgren, C., Wagner, E.G.H., Ehresmann, C., Ehresmann, B., and Romby, P. (1997) Antisense RNA control of plasmid R1 replication. The dominant product of the antisense RNA-mRNA binding is not a full RNA duplex. *J Biol Chem* **272:** 12508-12512.

Manning, P.A., Morelli, G., and Achtman, M. (1981) *traG* protein of the F sex factor of *Escherichia coli* K-12 and its role in conjugation. *Proc Natl Acad Sci USA* **78:** 7487-7491.

Marians, K.J. (2000) Crawling and wiggling on DNA: structural insights to the mechanism of DNA unwinding by helicases. *Structure Fold Des* **8:** R227-R235.

Marino, J.P., Gregorian, R.S., Jr., Csankovszki, G., and Crothers, D.M. (1995) Bent helix formation between RNA hairpins with complementary loops. *Science* **268:** 1448-1454.

Marmur, J., Rownd, R., Falkow, S., Baron, L.S., Schildkraut, C., and Doty, P. (1961) The nature of intergenic episomal infection. *Proc Natl Acad Sci USA* **47:** 972-979.

Masai H., Kaziro, Y., and Arai, K. (1983) Definition of *oriR*, the minimum DNA segment essential for initiation of R1 plasmid replication *in vitro*. *Proc Natl Acad Sci USA* **80:** 6814-6818.

Masukata, H., and Tomizawa, J. (1986) Control of primer formation for ColE1 plasmid replication: conformational change of the primer transcript. *Cell* **44:** 125-136.

Mathews, D.H., Sabina, J., Zuker, M., and Turner, D.H. (1999) Expanded sequence dependence of thermodynamic parameters improves prediction of RNA secondary structure. *J Mol Biol* **288:** 911-940.

Matson, S.W., Nelson, W.C., and Morton, B.S. (1993) Characterization of the reaction product of the *oriT* nicking reaction catalyzed by *Escherichia coli* DNA helicase I. *J Bacteriol* **175:** 2599-2606.

Mattaj, I.W. (1993) RNA recognition: a family matter? *Cell* **73:** 837-840.

Maurizi, M.R., Clark, W.P., Kim, S.H., and Gottesman, S. (1990) ClpP represents a unique family of serine proteases. *J Biol Chem* **265:** 12546-12552.

Mazodier, P., and Davies, J. (1991) Gene transfer between distantly related bacteria. *Annu Rev Genet* **25:** 147-171.

McEwen, J., and Silverman, P. (1980a) Mutations in genes *cpxA* and *cpxB* of *Escherichia coli* K-12 cause a defect in isoleucine and valine syntheses. *J Bacteriol* **144:** 68-73.

McEwen, J., and Silverman, P. (1980b) Chromosomal mutations of *Escherichia coli* that alter expression of conjugative plasmid functions. *Proc Natl Acad Sci USA* **77:** 513-517.

McEwen, J., and Silverman, P. (1980c) Genetic analysis of *Escherichia coli* K-12 chromosomal mutants defective in expression of F-plasmid functions: identification of genes *cpxA* and *cpxB. J Bacteriol* **144:** 60-67.

McEwen, J., and Silverman, P.M. (1982) Mutations in genes *cpxA* and *cpxB* alter the protein composition of *Escherichia coli* inner and outer membranes. *J Bacteriol* **151:** 1553-1559.

McEwen, J., Sambucetti, L., and Silverman, P.M. (1983) Synthesis of outer membrane proteins in *cpxA cpxB* mutants of *Escherichia coli* K-12. *J Bacteriol* **154:** 375-382.

McIntire, S.A., and Dempsey, W.B. (1987) Fertility inhibition gene of plasmid R100. *Nucleic Acids Res* **15:** 2029-2042.

Miller, J. (1972) *Experiments in Molecular Genetics* Cold Spring Harbor, New York: Cold Spring Harbor Laboratory Press, pp. 201-205.

Milligan, J.F., Groebe, D.R., Witherell, G.W., and Uhlenbeck, O.C. (1987) Oligoribonucleotide synthesis using T7 RNA polymerase and synthetic DNA templates. *Nucleic Acids Res* **15:** 8783-8798.

Miranda, G., Schuppli, D., Barrera, I., Hausherr, C., Sogo, J.M., and Weber, H. (1997) Recognition of bacteriophage Qβ plus strand RNA as a template by Qβ replicase: role of RNA interactions mediated by ribosomal proteins S1 and host factor. *J Mol Biol* **267:** 1089-1103.

Mogridge, J., Mah, T.F., and Greenblatt, J. (1995) A protein-RNA interaction network facilitates the template-independent cooperative assembly on RNA polymerase of a stable antitermination complex containing the lambda N protein. *Genes Dev* **9:** 2831-2845.

Mogridge, J., Legault, P., Li, J., Van Oene, M.D., Kay, L.E., and Greenblatt, J. (1998) Independent ligand-induced folding of the RNA-binding domain and two functionally distinct antitermination regions in the phage lambda N protein. *Mol Cell* **1:** 265-275.

Møller, T., Franch, T., Udesen, C., Gerdes, K., and Valentin-Hansen, P. (2002a) Spot42 RNA mediates discoordinate expression of the *E. coli* galactose operon. *Genes Dev* **16:** 1696-1706.

Møller, T., Franch, T., Hojrup, P., Keene, D.R., Bächinger, H.P., Brennan, R.G., and Valentin-Hansen, P. (2002b) Hfq: a bacterial Sm-like protein that mediates RNA-RNA interaction. *Mol Cell* **9:** 23-30.

Muffler, A., Fischer, D., and Hengge-Aronis, R. (1996) The RNA-binding protein HF-I, known as a host factor for phage Qß RNA replication, is essential for *rpoS* translation in *Escherichia coli. Genes Dev* **10:** 1143-1151.

Mullineaux, P., and Willetts, N. (1985) Promoters in the transfer region of plasmid F. *Basic Life Sci* **30:** 605-614.

Muriaux, D., De Rocquigny, H., Roques, B.P., and Paoletti, J. (1996) NCp7 activates HIV-1Lai RNA dimerization by converting a transient loop-loop complex into a stable dimer. *J Biol Chem* **271:** 33686-33692.

Nakayama, S., and Watanabe, H. (1995) Involvement of *cpxA*, a sensor of a two-component regulatory system, in the pH-dependent regulation of expression of *Shigella sonnei virF* gene. *J Bacteriol* **177:** 5062-5069.

Nelson, W.C., Morton, B.S., Lahue, E.E., and Matson, S.W. (1993) Characterization of the *Escherichia coli* F factor *traY* gene product and its binding sites. *J Bacteriol* **175:** 2221-2228.

Nelson, W.C., Howard, M.T., Sherman, J.A., and Matson, S.W. (1995) The *traY* gene product and integration host factor stimulate *Escherichia coli* DNA helicase I-catalyzed nicking at the F plasmid *oriT. J Biol Chem* **270:** 28374-28380.

Nodwell, J.R., and Greenblatt, J. (1991) The *nut* site of bacteriophage lambda is made of RNA and is bound by transcription antitermination factors on the surface of RNA polymerase. *Genes Dev* **5:** 2141-2151.

Nordgren, S., Slagter-Jäger, J.G., and Wagner, E.G.H. (2001) Real time kinetic studies of the interaction between folded antisense and target RNAs using surface plasmon resonance. *J Mol Biol* **310:** 1125-1134.

Nordström, K., Molin, S., and Light, J. (1984) Control of replication of bacterial plasmids: genetics, molecular biology, and physiology of the plasmid R1 system. *Plasmid* 12: 71-90.

Novotny, C.P., and Fives-Taylor, P. (1974) Retraction of F pili. *J Bacteriol* 117: 1306-1311.

Ohman, M., and Wagner, E.G.H. (1989) Secondary structure analysis of the RepA mRNA leader transcript involved in control of replication of plasmid R1. *Nucleic Acids Res* 17: 2557-2579.

Paranchych, W., Finlay, B.B., and Frost, L.S. (1986) Studies on the regulation of IncF plasmid operon expression. In *Antibiotic Resistance Genes: Ecology, Transfer, and Expression*. Levy, S.B., and Novick, R.P. (eds.). New York: Cold Spring Harbor Laboratory Press, pp. 117-129.

Penfold, S.S., Usher, K., and Frost, L.S. (1994) The nature of the *traK4* mutation in the F sex factor of *Escherichia coli. J Bacteriol* 176: 1924-1931.

Penfold, S.S., Simon, J., and Frost, L.S. (1996) Regulation of the expression of the *traM* gene of the F sex factor of *Escherichia coli. Mol Microbiol* 20: 549-558.

Persson, C., Wagner, E.G.H., and Nordström, K. (1988) Control of replication of plasmid R1: kinetics of *in vitro* interaction between the antisense RNA, CopA, and its target, CopT. *EMBO J* 7: 3279-3288.

Persson, C., Wagner, E.G.H., and Nordström, K. (1990a) Control of replication of plasmid R1: formation of an initial transient complex is rate-limiting for antisense RNA-target RNA pairing. *EMBO J* 9: 3777-3785.

Persson, C., Wagner, E.G.H., and Nordström, K. (1990b) Control of replication of plasmid R1: structures and sequences of the antisense RNA, CopA, required for its binding to the target RNA, CopT. *EMBO J* 9: 3767-3775.

Pillai, R.S., Will, C.L., Lührmann,R ., Schumperli, D., and Müller, B. (2001) Purified U7 snRNPs lack the Sm proteins D1 and D2 but contain Lsm10, a new 14 kDa Sm D1-like protein. *EMBO J* 20: 5470-5479.

Pogliano, J., Lynch, A.S., Belin, D., Lin, E.C., and Beckwith, J. (1997) Regulation of *Escherichia coli* cell envelope proteins involved in protein folding and degradation by the Cpx two-component system. *Genes Dev* **11:** 1169-1182.

Pogliano, J., Dong, J.M., De Wulf, P., Furlong, D., Boyd, D., Losick, R., Pogliano, K., and Lin, E.C. (1998) Aberrant cell division and random FtsZ ring positioning in *Escherichia coli cpxA** mutants. *J Bacteriol* **180:** 3486-3490.

Predki, P.F., Nayak, L.M., Gottlieb, M.B., and Regan, L. (1995) Dissecting RNA-protein interactions: RNA-RNA recognition by Rop. *Cell* **80:** 41-50.

Rainwater, S., and Silverman, P.M. (1990) The Cpx proteins of *Escherichia coli* K-12: evidence that *cpxA*, *ecfB*, *ssd*, and *eup* mutations all identify the same gene. *J Bacteriol* **172:** 2456-2461.

Raivio, T.L., and Silhavy, T.J. (1997) Transduction of envelope stress in *Escherichia coli* by the Cpx two-component system. *J Bacteriol* **179:** 7724-7733.

Raivio, T.L., Popkin, D.L., and Silhavy, T.J. (1999) The Cpx envelope stress response is controlled by amplification and feedback inhibition. *J Bacteriol* **181:** 5263-5272.

Raivio, T.L., and Silhavy, T.J. (1999) The sigmaE and Cpx regulatory pathways: overlapping but distinct envelope stress responses. *Curr Opin Microbiol* **2:** 159-165.

Raivio, T.L., Laird, M.W., Joly, J.C., and Silhavy, T.J. (2000) Tethering of CpxP to the inner membrane prevents spheroplast induction of the *cpx* envelope stress response. *Mol Microbiol* **37:** 1186-1197.

Raivio, T.L., and Silhavy, T.J. (2001) Periplasmic stress and *ecf* sigma factors *Annu Rev Microbiol* **55:** 591-624.

Rees, W.A., Weitzel, S.E., Yager, T.D., Das, A., and von Hippel, P.H. (1996) Bacteriophage lambda N protein alone can induce transcription antitermination *in vitro*. *Proc Natl Acad Sci USA* **93:** 342-346.

Sambrook, J.,Fritsch, E.F., and Maniatis, T. (1989) *Molecular cloning: a laboratory manual.* Cold Spring Harbor, NY: Cold Spring Harbor Laboratory Press.

Sandercock, J.R., and Frost, L.S. (1998) Analysis of the major domains of the F fertility inhibition protein, FinO. *Mol Gen Gene.* **259:** 622-629.

Schärpf, M., Sticht, H., Schweimer, K., Boehm, M., Hoffmann, S., and Rosch, P. (2000) Antitermination in bacteriophage lambda. The structure of the N36 peptide-*boxB* RNA complex. *Eur J Biochem* **267:** 2397-2408.

Schumacher, M.A., Pearson, R.F., Møller, T., Valentin-Hansen, P., and Brennan, R.G. (2002) Structures of the pleiotropic translational regulator Hfq and an Hfq-RNA complex: a bacterial Sm-like protein. *EMBO J* **21:** 3546-3556.

Shahied, L., Braswell, E.H., LeStourgeon, W.M., and Krezel, A.M. (2001) An antiparallel four-helix bundle orients the high-affinity RNA binding sites in hnRNP C: a mechanism for RNA chaperonin activity. *J Mol Biol* **305:** 817-828.

Shapiro, L., Franze de Fernandez, M.T., and August,J .T. (1968) Resolution of two factors required in the Qβ-RNA polymerase reaction. *Nature* **220:** 478-480.

Siemering, K.R., Praszkier, J., and Pittard, A.J. (1993) Interaction between the antisense and target RNAs involved in the regulation of IncB plasmid replication. *J Bacteriol* **175:** 2895-2906.

Silhavy, T.J., Berman, M.L., and Enquist, L.W. (1984) *Experiments with Gene Fusions* New York: Cold Spring Harbor Laboratory Press.

Silverman, P., Nat, K., McEwen, J., and Birchman, R. (1980) Selection of *Escherichia coli* K-12 chromosomal mutants that prevent expression of F-plasmid functions. *J Bacteriol* **143:** 1519-1523.

Silverman, P.M., Wickersham, E., and Harris, R. (1991a) Regulation of the F plasmid *traY* promoter in *Escherichia coli* by host and plasmid factors. *J Mol Biol* **218:** 119-128.

Silverman, P.M., Wickersham, E., Rainwater, S., and Harris,R. (1991b) Regulation of the F plasmid *traY* promoter in *Escherichia coli* K12 as a function of sequence context. *J Mol Biol* **220:** 271-279.

Silverman, P.M., Rother, S., and Gaudin, H. (1991c) Arc and Sfr functions of the *Escherichia coli* K-12 *arcA* gene product are genetically and physiologically separable. *J Bacteriol* **173:** 5648-5652.

Silverman, P.M., Tran, L., Harris, R., and Gaudin, H.M. (1993) Accumulation of the F plasmid TraJ protein in *cpx* mutants of *Escherichia coli*. *J Bacteriol* **175**: 921-925.

Skurray, R.A., Nagaishi, H., and Clark, A.J. (1978) Construction and *Bam*HI analysis of chimeric plasmids containing *Eco*RI DNA fragments of the F sex factor. *Plasmid* **1**: 174-186.

Sledjeski, D.D., Whitman, C., and Zhang, A. (2001) Hfq is necessary for regulation by the untranslated RNA DsrA. *J Bacteriol* **183**: 1997-2005.

Snyder, W.B., Davis, L.J., Danese, P.N., Cosma, C.L., and Silhavy, T.J. (1995) Overproduction of NlpE, a new outer membrane lipoprotein, suppresses the toxicity of periplasmic LacZ by activation of the Cpx signal transduction pathway. *J Bacteriol* **177**: 4216-4223.

Sowa, B.A., Moore, D., and Ippen-Ihler, K. (1983) Physiology of F-pilin synthesis and utilization. *J Bacteriol* **153**: 962-968.

Steitz, T.A. (1993) Similarities and differences between RNA and DNA recognition by proteins. In *The RNA World*. Gesteland, R.F., Atkins,J.F. (eds.). New York: Cold Spring Harbor Laboratory Press, pp. 219-237.

Stockwell, D.T., and Dempsey, W.B. (1997) The *finM* promoter and the *traM* promoter are the principal promoters of the *traM* gene of the antibiotic resistance plasmid R100. *Mol Microbiol* **26**: 455-467.

Stougaard, P., Molin, S., and Nordström, K. (1981) RNAs involved in copy-number control and incompatibility of plasmid R1. *Proc Natl Acad Sci USA* **78**: 6008-6012.

Strohmaier, H., Noiges, R., Kotschan, S., Sawers, G., Högenauer, G., Zechner, E.L., and Koraimann, G. (1998) Signal transduction and bacterial conjugation: characterization of the role of ArcA in regulating conjugative transfer of the resistance plasmid R1. *J Mol Biol* **277**: 309-316.

Su, L., Radek, J.T., Hallenga, K., Hermanto, P., Chan, G., Labeots, L.A., and Weiss, M.A. (1997) RNA recognition by a bent alpha-helix regulates transcriptional antitermination in phage lambda. *Biochemistry* **36**: 12722-12732.

Sukupolvi, S., and O'Connor, C.D. (1990) TraT lipoprotein, a plasmid-specified mediator of interactions between gram-negative bacteria and their environment. *Microbiol Rev* **54:** 331-341.

Sutton, A., Newman, T., McEwen, J., Silverman, P.M., and Freundlich, M. (1982) Mutations in genes *cpxA* and *cpxB* of *Escherichia coli* K-12 cause a defect in acetohydroxyacid synthase I function *in vivo*. *J Bacteriol* **151:** 976-982.

Tabor, S., and Richardson, C.C. (1985) A bacteriophage T7 RNA polymerase/promoter system for controlled exclusive expression of specific genes. *Proc Natl Acad Sci USA* **82:** 1074-1078.

Takahashi, K., Baba, S., Koyanagi, Y., Yamamoto, N., Takaku, H., and Kawai, G. (2001) Two basic regions of NCp7 are sufficient for conformational conversion of HIV-1 dimerization initiation site from kissing-loop dimer to extended-duplex dimer. *J Biol Chem* **276:** 31274-31278.

Takahashi, K.I., Baba, S., Chattopadhyay, P., Koyanagi, Y., Yamamoto, N., Takaku, H., and Kawai, G. (2000) Structural requirement for the two-step dimerization of human immunodeficiency virus type 1 genome. *RNA* **6:** 96-102.

Takeda, Y., Ohlendorf, D.H., Anderson, W.F., and Matthews, B.W. (1983) DNA-binding proteins. *Science* **221:** 1020-1026.

Tamm, J., and Polisky, B. (1985) Characterization of the ColE1 primer-RNA I complex: analysis of a domain of ColE1 RNA I necessary for its interaction with primer RNA. *Proc Natl Acad Sci USA* **82:** 2257-2261.

Tan, R., and Frankel, A.D. (1994) Costabilization of peptide and RNA structure in an HIV Rev peptide-RRE complex. *Biochemistry* **33:** 14579-14585.

Tan, R., and Frankel, A.D. (1995) Structural variety of arginine-rich RNA-binding peptides. *Proc Natl Acad Sci USA* **92:** 5282-5286.

Tanner, N.K., and Linder, P. (2001) DExD/H box RNA helicases: from generic motors to specific dissociation functions. *Mol Cell* **8:** 251-262.

Tomizawa, J., and Itoh, T. (1981) Plasmid ColE1 incompatibility determined by interaction of RNA I with primer transcript. *Proc Natl Acad Sci USA* **78:** 6096-6100.

Tomizawa, J., Itoh, T., Selzer, G., and Som, T. (1981) Inhibition of ColE1 RNA primer formation by a plasmid-specified small RNA. *Proc Natl Acad Sci USA* **78:** 1421-1425.

Tomizawa, J., and Som, T. (1984) Control of ColE1 plasmid replication: enhancement of binding of RNA I to the primer transcript by the Rom protein. *Cell* **38:** 871-878.

Tomizawa, J. (1984) Control of ColE1 plasmid replication: the process of binding of RNA I to the primer transcript. *Cell* **38:** 861-870.

Tomizawa, J. (1985) Control of ColE1 plasmid replication: initial interaction of RNA I and the primer transcript is reversible. *Cell* **40:** 527-535.

Tomizawa, J. (1986) Control of ColE1 plasmid replication: binding of RNA I to RNA II and inhibition of primer formation. *Cell* **47:** 89-97.

Tomizawa, J. (1990a) Control of ColE1 plasmid replication. Interaction of Rom protein with an unstable complex formed by RNA I and RNA II. *J Mol Biol* **212:** 695-708.

Tomizawa, J. (1990b) Control of ColE1 plasmid replication. Intermediates in the binding of RNA I and RNA II. *J Mol Biol* **212:** 683-694.

Torreblanca, J., Marques, S., and Casadesús, J. (1999) Synthesis of FinP RNA by plasmids F and pSLT is regulated by DNA adenine methylation. *Genetics* **152:** 31-45.

Towbin, H., Staehelin, T., and Gordon, J. (1979) Electrophoretic transfer of proteins from polyacrylamide gels to nitrocellulose sheets: procedure and some applications. *Proc Natl Acad Sci USA* **76:** 4350-4354.

Traxler, B.A., and Minkley, E.G., Jr. (1988) Evidence that DNA helicase I and *oriT* site-specific nicking are both functions of the F TraI protein. *J Mol Biol* **204:** 205-209.

Tsai, M.M., Fu, Y.H., and Deonier, R.C. (1990) Intrinsic bends and integration host factor binding at F plasmid *oriT*. *J Bacteriol* **172:** 4603-4609.

Ulijasz, A.T., Kay, B.K., and Weisblum, B. (2000) Peptide analogues of the VanS catalytic center inhibit VanR binding to its cognate promoter. *Biochemistry* **39:** 11417-11424.

van Biesen, T., and Frost, L.S. (1992) Differential levels of fertility inhibition among F-like plasmids are related to the cellular concentration of *finO* mRNA. *Mol Microbiol* **6:** 771-780.

van Biesen, T., Soderbom, F., Wagner, E.G.H., and Frost, L.S. (1993) Structural and functional analyses of the FinP antisense RNA regulatory system of the F conjugative plasmid. *Mol Microbiol* **10:** 35-43.

van Biesen, T., and Frost, L.S. (1994) The FinO protein of IncF plasmids binds FinP antisense RNA and its target, *traJ* mRNA, and promotes duplex formation. *Mol Microbiol* **14:** 427-436.

van Biesen, T. (1994) FinOP Fertility Inhibition System. Ph.D. Thesis, University of Alberta, Edmonton Alberta.

Van Gilst, M.R., and von Hippel, P.H. (1997) Assembly of the N-dependent antitermination complex of phage lambda: NusA and RNA bind independently to different unfolded domains of the N protein. *J Mol Biol* **274:** 160-173.

Van Gilst, M.R., Rees, W.A., Das, A., and von Hippel, P.H. (1997) Complexes of N antitermination protein of phage lambda with specific and nonspecific RNA target sites on the nascent transcript. *Biochemistry* **36:** 1514-1524.

Vieira, J., and Messing, J. (1982) The pUC plasmids, an M13mp7-derived system for insertion mutagenesis and sequencing with synthetic universal primers. *Gene* **19:** 259-268.

von Hippel, P.H., and Delagoutte, E. (2001) A general model for nucleic acid helicases and their "coupling" within macromolecular machines. *Cell* **104:** 177-190.

Vytvytska, O., Moll, I., Kaberdin, V.R., von Gabain, A., and Blasi, U. (2000) Hfq (HF1) stimulates *ompA* mRNA decay by interfering with ribosome binding. *Genes Dev* **14:** 1109-1118.

Wagner, C., Palacios, I., Jaeger, L., St. Johnston, D., Ehresmann, B., Ehresmann, C., and Brunel, C. (2001) Dimerization of the 3' UTR of *bicoid* mRNA involves a two-step mechanism. *J Mol Biol* **313:** 511-524.

Wagner, E.G.H., von Heijne, J., and Nordström, K. (1987) Control of replication of plasmid R1: translation of the 7k reading frame in the RepA mRNA leader region counteracts the interaction between CopA RNA and CopT RNA. *EMBO J* **6**: 515-522.

Wagner, E.G.H., Blomberg, P., and Nordström, K. (1992) Replication control in plasmid R1: duplex formation between the antisense RNA, CopA, and its target, CopT, is not required for inhibition of RepA synthesis. *EMBO J* **11**: 1195-1203.

Wagner, E.G.H., and Simons, R.W. (1994) Antisense RNA control in bacteria, phages, and plasmids. *Annu Rev Microbiol* **48**: 713-742.

Wagner, E.G.H., and Nordström, K. (1986) Structural analysis of an RNA molecule involved in replication control of plasmid R1. *Nucleic Acids Res* **14**: 2523-2538.

Wagner, E.G.H., and Brantl, S. (1998) Kissing and RNA stability in antisense control of plasmid replication. *Trends Biochem Sci* **23**: 451-454.

Watanabe, H. (1966) Infectious drug resistance in enteric bacteria. *New England Journal of Medicine* **275**: 888.

Watanabe, T. (1963) Infective heredity of multiple drug resistance in bacteria. *Bacteriological Reviews* **27**: 87-115.

Weber, R.F., and Silverman, P.M. (1988) The *cpx* proteins of *Escherichia coli* K12. Structure of the *cpxA* polypeptide as an inner membrane component. *J Mol Biol* **203**: 467-478.

Weeks, K.M. (1997) Protein-facilitated RNA folding. *Curr Opin Struct Biol* **7**: 336-342.

Whalen, W., Ghosh, B., and Das, A. (1988) NusA protein is necessary and sufficient *in vitro* for phage lambda N gene product to suppress a *rho*-independent terminator placed downstream of *nutL*. *Proc Natl Acad Sci USA* **85**: 2494-2498.

Whalen, W.A., and Das, A. (1990) Action of an RNA site at a distance: role of the *nut* genetic signal in transcription antitermination by phage-lambda N gene product. *New Biol* **2**: 975-991.

Wilkins, B.M., and Frost, L.S. (2001) Mechanisms of gene exchange between bacteria. In *Molecular Medical Microbiology*. Sussman,M. (ed.). London: Academic Press, pp. 355-400.

Wilkinson, T.A., Botuyan, M.V., Kaplan, B.E., Rossi, J.J., and Chen, Y. (2000) Arginine side-chain dynamics in the HIV-1 *rev*-RRE complex. *J Mol Biol* **303**: 515-529.

Willetts, N. (1977) The transcriptional control of fertility in F-like plasmids. *J Mol Biol* **112**: 141-148.

Willetts, N., and Maule, J. (1986) Specificities of IncF plasmid conjugation genes. *Genet Res* **47**: 1-11.

Willetts, N.S., and Finnegan, D.J. (1970) Characteristics of *E. coli* K12 strains carrying both an F prime and an R factor *Genet.Res.* **16**: 113-122.

Williams, A.S., and Marzluff, W.F. (1995) The sequence of the stem and flanking sequences at the 3' end of histone mRNA are critical determinants for the binding of the stem-loop binding protein. *Nucleic Acids Res* **23**: 654-662.

Williamson, J.R. (2000) Induced fit in RNA-protein recognition. *Nat Struct Biol* **7**: 834-837.

Wu, R., Wang, X., Womble, D.D., and Rownd, R.H. (1992) Expression of the *repA1* gene of IncFII plasmid NR1 is translationally coupled to expression of an overlapping leader peptide. *J Bacteriol* **174**: 7620-7628.

Yoshioka, Y., Ohtsubo, H., and Ohtsubo, E. (1987) Repressor gene *finO* in plasmids R100 and F: constitutive transfer of plasmid F is caused by insertion of *IS3* into F *finO*. *J Bacteriol* **169**: 619-623.

Yoshioka, Y., Fujita, Y., and Ohtsubo, E. (1990) Nucleotide sequence of the promoter-distal region of the *tra* operon of plasmid R100, including *traI* (DNA helicase I) and *traD* genes. *J Mol Biol* **214**: 39-53.

Yu, E., and Owttrim, G.W. (2000) Characterization of the cold stress-induced cyanobacterial DEAD-box protein CrhC as an RNA helicase. *Nucleic Acids Res* **28**: 3926-3934.

Zacharias, M., and Hagerman, P.J. (1995) The bend in RNA created by the trans-activation response element bulge of human immunodeficiency virus is straightened by arginine and by Tat-derived peptide. *Proc Natl Acad Sci USA* **92:** 6052-6056.

Zanier, K., Luyten, I., Crombie, C., Muller, B., Schumperli, D., Linge, J.P., Nilges, M., and Sattler, M. (2002) Structure of the histone mRNA hairpin required for cell cycle regulation of histone gene expression. *RNA* **8:** 29-46.

Zechner, E.L., de la Cruz, F., Eisenbrandt, R., Grahn, A.M., Koraimann, G., Lanka, E., Muth, G., Pansegrau,W., Thomas, C.M., Wilkins, B.M., and Zatyka, M. (2000) Conjugative-DNA transfer processes. In *The Horizontal Gene Pool: Bacterial Plasmids and Gene Spread.* Thomas, C.M. (ed.). Amsterdam: Harwood Academic Press, pp. 87-174.

Zhang, A., Altuvia, S., Tiwari, A., Argaman, L., Hengge-Aronis, R., and Storz, G. (1998) The OxyS regulatory RNA represses *rpoS* translation and binds the Hfq (HF-I) protein. *EMBO J* **17:** 6061-6068.

Zhang, A., Wassarman, K.M., Ortega, J., Steven, A.C., and Storz, G. (2002) The Sm-like Hfq protein increases OxyS RNA interaction with target mRNAs. *Mol Cell* **9:** 11-22.

Zhou, Y., Mah, T.F., Yu, Y.T., Mogridge, J., Olson, E.R., Greenblatt, J., and Friedman, D.I. (2001) Interactions of an Arg-rich region of transcription elongation protein NusA with NUT RNA: implications for the order of assembly of the lambda N antitermination complex *in vivo. J Mol Biol* **310:** 33-49.

Zuker, M., Mathews, D.H., and Turner, D.H. (1999) Algorithms and thermodynamics for RNA secondary structure prediction: a practical guide. In *RNA Biotechemistry and Biotechnology.* Barciszewski, J., and Clark, B.F.C. (eds.). Dordrecht, the Netherlands: Kluwer Academic Publishers, pp. 11-43.